



UNIVERSITÀ DEGLI STUDI DI PAVIA
DOTTORATO IN SCIENZE CHIMICHE
E FARMACEUTICHE
XXIX CICLO

Coordinatore: Chiar.mo Prof. Mauro Freccero

***Innovative Macromolecular Systems for
Organic Photovoltaic Applications***

Tutore

Chiar.mo Prof. DARIO PASINI

Cotutore

Dott. GABRIELE BIANCHI

Tesi di Dottorato di

ANDREA NITTI

a.a. 2015- 2016

*Dedicato a mio padre con
amore infinito*

TABLE OF CONTENTS

CHAPTER 1: Introduction

1.1	<i>Abbreviations</i>	1
1.2	<i>Introduction to Organic Photovoltaic</i>	2
1.3	<i>Conjugated Organic Donor Polymers: design and synthesis</i>	8
1.4	<i>Synthesis of scalable monomers by Direct Arylation for photovoltaic applications</i>	16
1.5	<i>References</i>	29

CHAPTER 2: Motivation Section

2.1	<i>Donor-Acceptor Conjugated Copolymers Incorporating Tetrafluoro-Benzene as The π-Electron Deficient Unit</i>	34
2.2	<i>Conjugated Thiophene-Fused Isatin Dyes Through Intramolecular Direct Arylation</i>	36
2.3	<i>One Pot Direct Arylation and Cross-Aldol Condensation For the Rapid Construction of π-Extended Thiophene and Furan-Based Scaffolds</i>	37
2.4	<i>Anthradithiophene-Based and Dihydrobenzodithiophene-Based Monomer for the Synthesis of Innovative Polymers for Photovoltaic Applications</i>	39
2.5	<i>References</i>	42

CHAPTER 3: Discussion of Results and Conclusions

3.1	<i>Donor-Acceptor Conjugated Copolymers Incorporating Tetrafluoro-Benzene as The π-Electron Deficient Unit</i>	46
3.2	<i>Conjugated Thiophene-Fused Isatin Dyes Through Intramolecular Direct Arylation</i>	56
3.3	<i>One Pot Direct Arylation and Cross-Aldol Condensation For the Rapid Construction of π-Extended Thiophene and Furan-Based Scaffolds</i>	67
3.4	<i>Anthradithiophene-Based and Dihydrobenzodithiophene-Based Monomer for the Synthesis of Innovative Polymers for Photovoltaic Applications</i>	75
3.5	<i>References</i>	86

CHAPTER 4: Experimental Section

4.1	<i>General Experimental</i>	91
4.2	<i>Synthesis of new Compounds</i>	93
4.3	<i>References</i>	111

CHAPTER 5: Appendix

	<i>Donor-Acceptor Conjugated Copolymers Incorporating Tetrafluoro-Benzene as The π-Electron Deficient Unit</i>	112
	<i>Conjugated Thiophene-Fused Isatin Dyes Through Intramolecular Direct Arylation</i>	127
	<i>One Pot Direct Arylation and Cross-Aldol Condensation For the Rapid Construction of π-Extended Thiophene and Furan-Based Scaffolds</i>	159
	<i>Anthradithiophene-Based and Dihydrobenzodithiophene-Based Monomer for the Synthesis of Innovative Polymers for Photovoltaic Applications</i>	193

Introduction

1.1 ABBREVIATIONS

BHJ	Bulk Heterojunction
BT	2,1,3-Benzothiadiazole
BTI	dithieno[3,2- <i>c</i> :2',3'- <i>e</i>]azepine-4,6-dione
CPDT	4H-cyclopenta[1,2- <i>b</i> :5,4- <i>b'</i>]dithiophene
Cz	Carbazole
D-A	Donor-Acceptor
DBrBT	4,7-dibromo-2,1,3-benzothiadiazole
DEDOTBT	4,7-bis(3,4-ethylenedioxythiophene-2-yl)-2,1,3-benzothiadiazole
DHTBT	4,7-bis(4-hexylthiophen-2-yl)-2,1,3-benzothiadiazole
DMAc	<i>N,N</i> -dimethylacetamide
DMF	<i>N,N</i> -dimethylformamide
DTBDT	Dithienobenzodithiophene
DTBT	4,7-di(thiophen-2-yl)-2,1,3-benzothiadiazole
EDOT	3,4-ethylenedioxythiophene
F	Fluorene
HOMO	Highest occupied molecular orbital
HT	3-hexylthiophene
ICBA	Indenyl-[C ₆₀]-bisadduct
ITO	Tin-doped indium oxide
JHONPHOS	(2-Biphenyl)di-tert-butylphosphine
LUMO	Lowest unoccupied molecular orbital
MDMO-PPV	Poly[2-methoxy-5-(3,7-dimethyloctyloxy)-1,4-phenylene-vinylene]
NDT	Naphto[2,1- <i>b</i> :3,4- <i>b'</i>]dithiophene
NMP	<i>N</i> -methyl-2-pyrrolidone
ODMB	<i>o</i> -dimethylbenzene
OPV	Organic Photovoltaics
P3HT	Poly(3-hexylthiophene)
PC ₆₁ BM	[6,6]-phenyl-C61-butyric acid methyl ester
PC ₇₁ BM	phenyl-[C71]-butyric acid methyl ester
PCE	Power conversion efficiency
PDT	2-pyridone dithiophene
PEDOT:PSS	Poly(3,4-ethylenedioxythiophene)-poly(styrenesulfonate)
PivOH	2,2-dimethylpropionic acid (Pivalic acid)
PPV	Poly(1,4-phenylene-vinylene)
PSC	Polymer Solar Cell
T	Thiophene
TDPT	Thieno[2',3',:5,6]pyrido[3,4- <i>g</i>]thieno[2,2- <i>c</i>]isoquinoline-5,11-dione
TFA	Trifluoroacetic acid
TPTBL	Thiophene-phenylene-thiophene fused bilactam
TTe	Thieno[3,4- <i>b</i>]thiophene
Tz	Thiazole

1.2 INTRODUCTION TO ORGANIC PHOTOVOLTAICS

Since the beginning of history, the human energy demand has been constantly increasing, together with the growth of living standards. From the birth of industrialization, fossil fuels (coal, oil and natural gas) have been the most used sources to meet this need. With a world population of about 7.4 billion of people in 2016 and a prediction of increment to 8-11 billion by the middle of this century,¹ it is clear that the global energy policies must aim towards a gradual increase in energy consumption from alternative sources respect to fossil fuels (nuclear, hydroelectric and renewable energy), that in addition to being limited, produce large amounts of carbon dioxide known to be damaging to the planetary ecosystem.

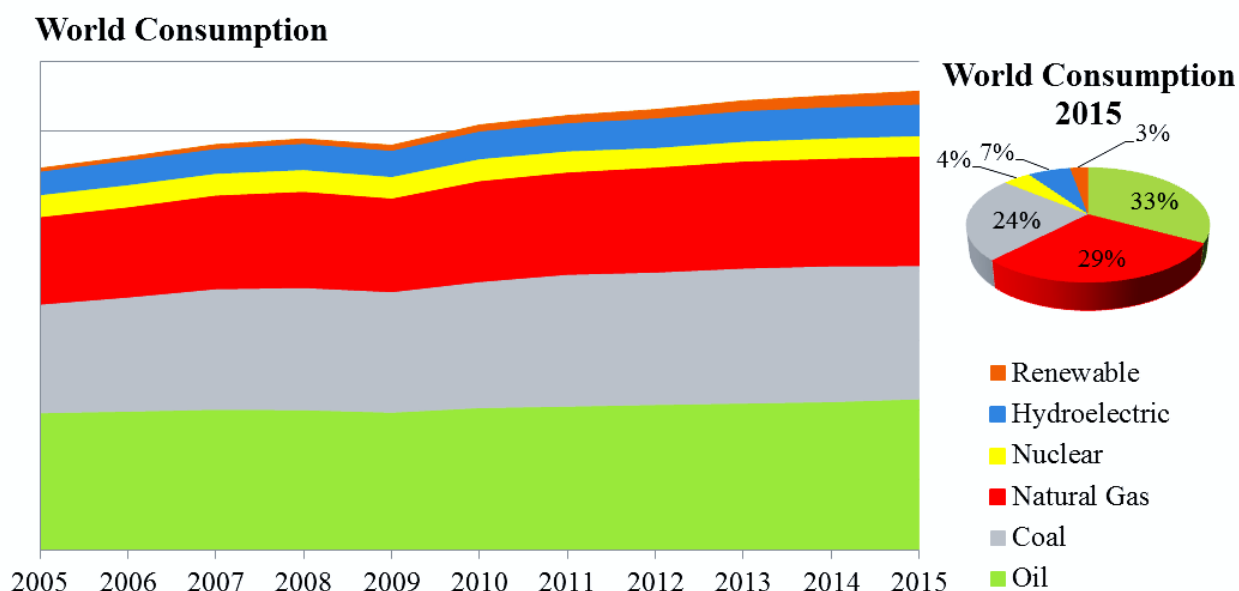


Figure 1. Left: global trend of energy consumption from 2005 to 2015. In 2015 an increase of world energy consumption by 0.1% has been recorded compared to 2014. Right: 2015 world primary energy consumption. In 2015, fossil fuels holds 85.9% of global demand. Of alternative energy sources, only renewable shows an important growth trend compared to nuclear and hydroelectric which remain almost unchanged in the years.

The World Energy Agency data, over the past years, confirm a trend towards renewable

energies (Figure 1).²

Fossil fuels have the largest percentage of energy consumption, but from 2005 to 2015, the global consumption of energy from alternative sources is constantly growing. Unlike of the nuclear and hydroelectric energies, for which consumption is virtually unchanged during the years, an increase of annual consumption from the other renewable energy sources is observed. Solar energy holds the strongest growth rate in last 5 years (Figure 2) compared to other renewable sources (in 2015 was reported a growing consumption vs 2014 of +32.2% for solar, +17.4% for wind and +5.3% for geothermal & other).

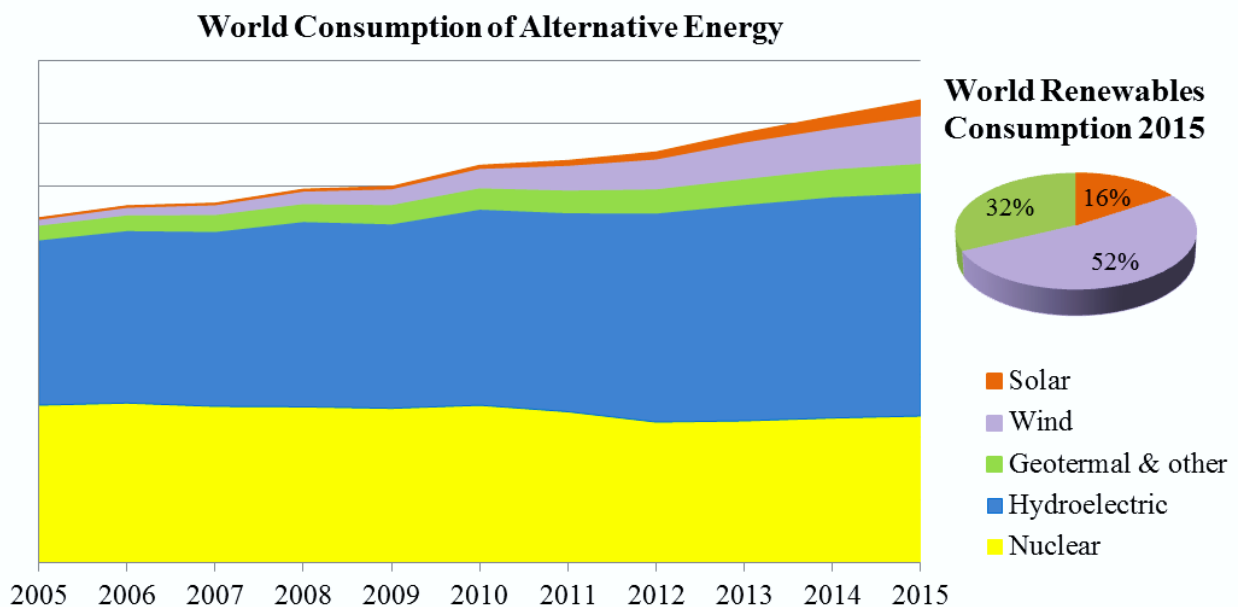


Figure 2. Left: global trend of alternative energy consumption from 2005 to 2015.

In 2015 has been recorded an increase of world energy consumption from alternative energies by +0.1% compared to 2014. Right: world renewables energy consumption 2015. In 2015, solar holds 15.7% of global demand while wind and geothermal holds respectively 52.2% and 32.1%.

Favorable world politics and a not optimal level of technology are some of the reasons that make the photovoltaic business very active both in selling massive technology and in investment for the development of innovative technologies in terms of PCE and costs.³ The de-

velopment of a new technology which could reach efficiencies of 20% with low production and disposal costs, two of the key limiting factors in current silicon-based technologies, will be probably the final push towards a widely spread use of solar energy as the alternative energy of choice.

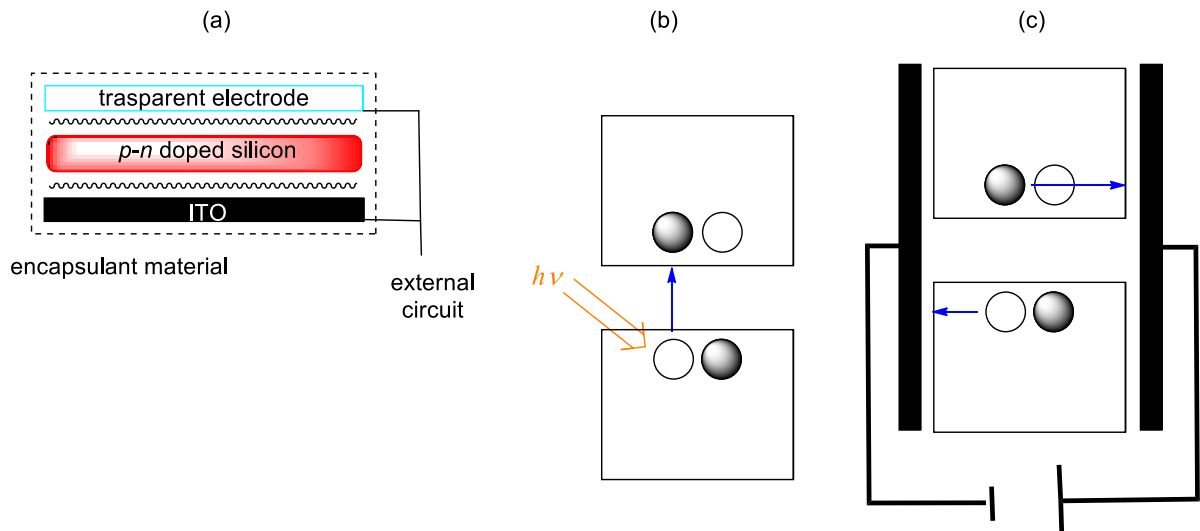


Figure 3. Scheme of a typical silicon-based solar cell and fundamental mechanism of light-harvesting.

Commercially-available solar cells are devices constituted by light absorbing inorganic materials (crystalline or amorphous silicon doped so to generate a $p-n$ junction) interposed between two electrodes, one of which is transparent to radiation in the visible region (Figure 3a). The physical principle behind light-harvesting is the photoelectric effect, the current generation when a metal is irradiated by light.⁴ When an electromagnetic radiation hits the silicon-based light absorptive material with a $h\nu$ energy, to promote an electronic transition from the valence band to the conduction band (Figure 3b), the excited electrons acquire mobility and become negative charge carriers. At the same time the electron leaves a "hole" in the starting level. The electron mobility is responsible for the conduction of current between the two electrodes (Figure 3c). The silicon is then doped to produce a downward (p -doped) or upward (n -doped) shift of the valence and conduction bands of the semiconductor.⁵

The best PCE performances achieved for this technology on a commercial scale are up to

21%. The disadvantages of this technology are the high costs of production and disposal of the photovoltaic modules. The production cost of the single cell was calculated to be the 33% of the total price, to which the subsequent costs of production of the modules, inverters, design, employers, maintenance, and not least the disposal at end of life (around 20 years) need to be added.⁶

It is possible to build solar cells using different materials and architectures from the silicon-based solar cells. The fundamental constituent elements in a solar cell are represented by a light absorptive material which creates charge carriers, and by a pair of electrodes, one of which is transparent, to which the charge carriers need to be channeled.

There is currently great activity in order to be able to manufacture scalable organic photovoltaic devices. Because silicon doesn't absorb sunlight strongly, silicon cells contain a relatively thick layer of silicon, which must be supported on a rigid glass. In contrast, emerging photovoltaic cells are made from inexpensive materials, including organic polymers, small molecules, and various types of inorganic compounds. And unlike silicon cells, the emerging ones can be fabricated on flexible supports via inexpensive solution-phase techniques common in plastics manufacturing, such as high-speed roll-to-roll printing. Despite the considerable progress achieved compared to the first OPVs cells produced from Tang *et al.*⁷, however, none of these emerging technologies has made its full trajectory to the market.⁸

It is well known that organic molecules that contain extended π -conjugated systems (typically materials composed of condensed aromatic polycyclic hydrocarbons, such as pentaenes, organic dyes such as phthalocyanines or conjugated polymers such as polyacetylenes, polyphenylenevinylenes or polythiophenes) are capable of absorbing photons in the visible region. Differently from inorganic semiconductor materials, in the organic active layer the photoabsorption generates excited states (excitons) through the electrons transfer from HOMO to LUMO levels.⁹ However, this excited state does not necessarily lead to the formation of charge carriers (electrons and holes). In order for an exciton to dissociate, it must reach the

interface with another material with different electronic affinity, able to extract the electron from the excited molecule and thus creating the hole-electron pair. An OPV device is based on the combined use of an electron acceptor compound and an electron donor compound. The fundamental mechanism of operation by which light energy is converted into electrical energy in these devices occur in 4 elementary steps illustrated in Figure 4.

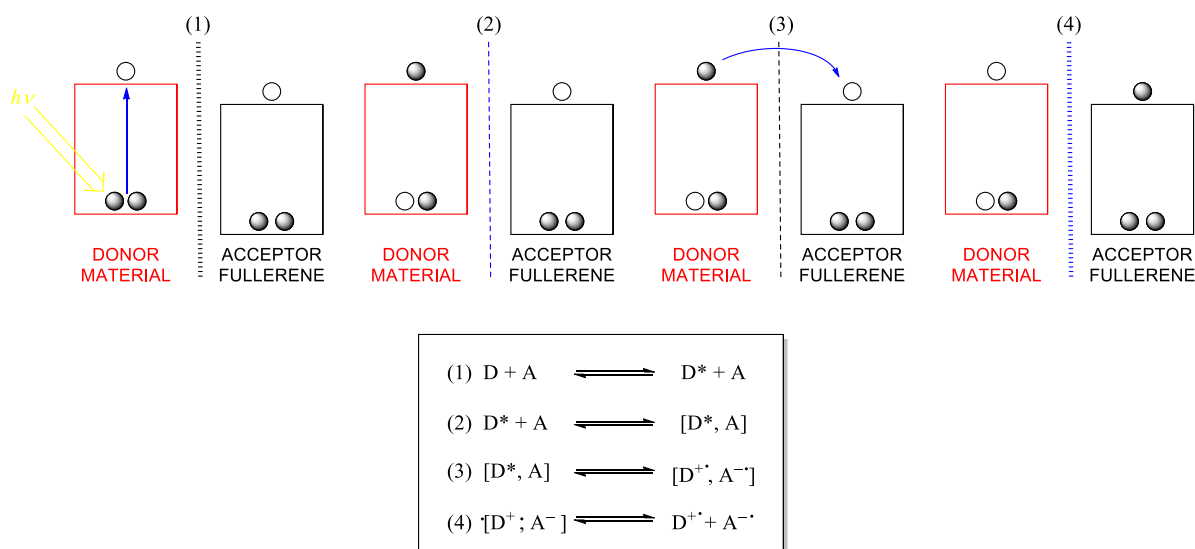


Figure 4. Elementary process occurring in OPV devices. (1) Photoabsorption with formation of excitons; (2) diffusion of excitons toward the interface with fullerene; (3) dissociation with hole/electron pair formation; (4) migration toward electrodes.

Photoabsorption of the donor material promote the formation of an exciton. Exciton diffusion from the donor polymer to the interface with the fullerene acceptor compound follows, and by exciton dissociation electron charge carriers (–) in the acceptor material and hole (+) in the donor material are formed, which migrate to the electrodes with electricity generation in the external circuit.

Among all types of emerging OPV devices, polymer solar cells with BHJ architecture probably offer the best growth prospects due to the potential advantages including low cost, low toxicity, light weight and fast/cheap manufacturing.¹⁰⁻¹³ The success of these devices has

been emphasized by the rapid increase of the PCE from below 1% to over 10% in the past of 20 years.

In a complete BHJ solar cell, the active layer is sandwiched between a transparent anode (typically ITO) and a metal cathode (Figure 5). Additionally, a thin layer of PEDOT:PSS is generally applied between the ITO and the active layer to improve the electrical contacts.¹⁴ For commercial applications the encapsulation of cells is required to increase its stability and lifetime and protecting itself against oxygen and moisture that are considered the main cause of degradation.¹⁵⁻¹⁷ In these devices the photoactive material is composed from an organic π -conjugated polymer (polymer donor) blended with a fullerenes derivative as the acceptor compound.¹⁸ The interpenetrated network of the BHJ architecture offers several advantages: (1) it minimizes the diffusion distance of excitons migrating to the donor polymer/fullerene interface; (2) it maximizes the donor polymer/fullerene interfacial area; (3) it offers charge transport pathways to facilitate the charge collection at the electrodes.

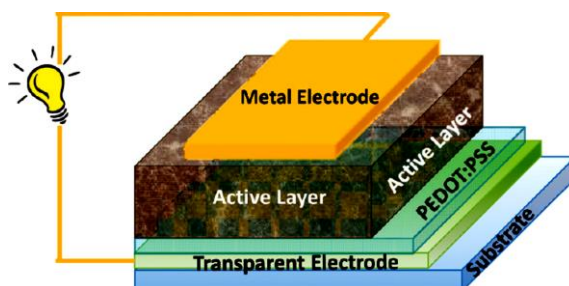


Figure 5. Architecture of Bulk Heterojunction solar cell.

Fullerenes are currently considered ideal acceptor compounds for several reasons. First, they have an energetically deep-lying LUMO,¹⁹ which endows the molecule with a very high electron affinity relative to the numerous potential organic donors. Second, the triply degenerate LUMO of C_{60} allows to the molecule to be reversibly reduced with up to six electrons, thus illustrating its ability to stabilize negative charge. Third, a number of conjugated polymer–fullerene blends are known to exhibit ultrafast photoinduced charge transfer (ca. 45 fs), with a back transfer that is orders of magnitude slower.²⁰ Last, C_{60} has been shown to have a

very high electron mobility of up to $1 \text{ cm}^2 \text{ V}^{-1} \text{ s}^{-1}$ in field-effect transistors (FETs).²¹ These fundamental properties, coupled with the ability of soluble fullerene derivatives to pack effectively in crystalline structures conducive to charge transport,²² have made fullerenes the most important acceptor materials for BHJ solar cells.

The poor solubility of buckminsterfullerene (C_{60}) in common organic solvents limited its direct use, so that soluble fullerene derivatives PC_{61}BM and PC_{71}BM have been used as a standard acceptor compounds in PCS-BHJ (figure 6).

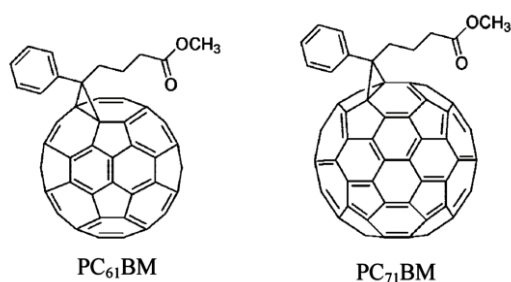


Figure 6. PC₆₁BM and PC₇₁BM compounds used as acceptor compound in OPV-BHJ devices.

Because the acceptor compound is a constant in the BHJ cells, increasing efficiency is related to the properties of donor polymers. Starting from early work on organic conducting polymers conducted by McDiarmid, Heeger and Shirakawa, who received the 2000 Nobel Prize in Chemistry for this discovery,²³ many scientists have investigated stable aromatic conjugated polymers and a large amount of literature is available.²⁴

1.3 CONJUGATED ORGANIC DONOR POLYMERS: DESIGN AND SYNTHESIS

From an industrial point of view, PCS with BHJ architecture should exhibit power conversion energy of around 10% on large modules using affordable components. This value of PCE is the fundamental goal for the ultimate legitimation and large scale commercialization of this technology. As previously mentioned, an increasing efficiency is predominantly related

to the properties of donor polymers.

Over the years a number of theoretical²⁵⁻²⁷ and semi-empirical²⁸ models have been formulated to predict the properties of conjugated polymers. The electronic and structural properties that an ideal donor polymer must satisfy are:

1. a broad absorption spectrum and a red-shifted absorption maximum, meaning a relatively low energy gap (E_g). A λ_{\max} of 800 nm, corresponding to an energy gap of around 1.5 eV, is considered optimal (Figure 7);

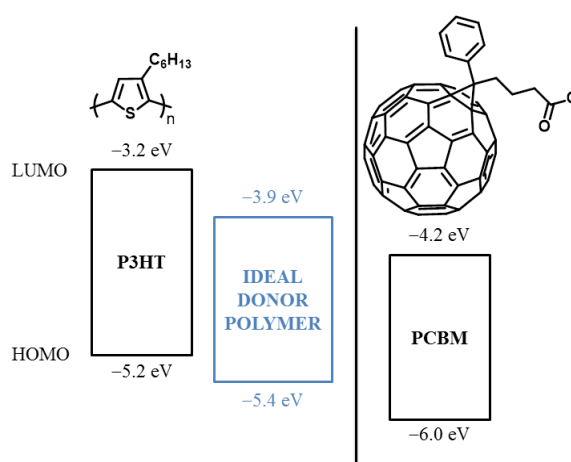


Figure 7. Optimal E_g calculated for ideal donor polymer using fullerene as acceptor compared with the “workhorse” of BHJ donor polymers, P3HT.

2. suitable energy level offsets to the acceptor (about 0.3 eV) to provide the driving force for an efficient exciton dissociation into charge-separated pairs at the donor/acceptor interface;
3. HOMO energy level lower than -5.3 eV (with conventional fullerene acceptors) to increase the open circuit voltage (V_{oc}) and to get a good stability toward oxidation;
4. an extended π -electrons delocalization to favor charge carrier separation and transport. The hole mobility should be in the range 10^{-4} to 10^{-3} $\text{cm}^2 \cdot \text{V}^{-1} \cdot \text{s}^{-1}$, balanced with the electron mobility in the fullerene acceptor;
5. good mixing properties with the acceptor to form a suited phase segregated bicontinu-

ous nanomorphology. In particular, the morphology is determined by several factors like: (a) film processing conditions, (b) molar ratio of the polymer and the fullerene, (c) the nature of the solvent, (d) the thermal post-deposition treatments, (e) adequate ink viscosity required for roll-to-roll printing techniques.

In summary, only those conjugated polymers that are able to combine good transport, optical and mechanical properties together with processability and environmental stability have chances to be utilized toward the large scale production of photovoltaic devices.

A large number of conjugated polymers have been proposed in the literature. There are relatively few synthetic methods allowing an efficient preparation of such alternating copolymers; most of these polymers are obtained *via* the well-known Suzuki, Stille and DHA cross-coupling polymerization reactions.

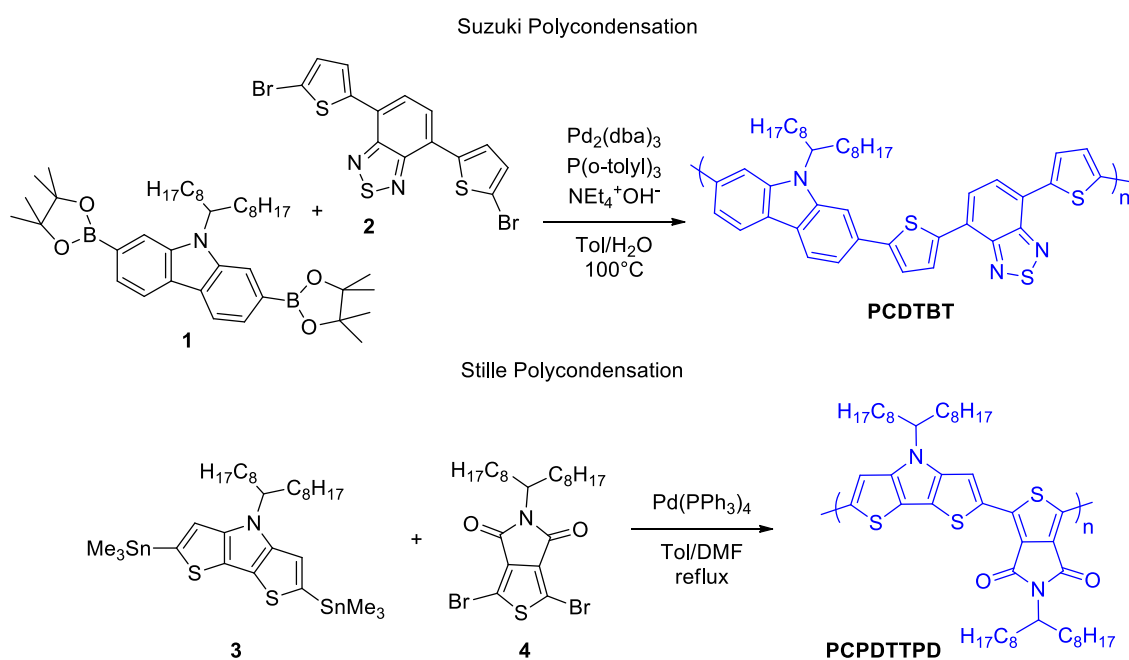


Figure 8. Selected example of Suzuki and Stille polycondensation protocol.

Suzuki polycondensation was first used by Schlüter *et al.*²⁹ to prepare poly(*p*-phenylene)s. A typically Suzuki polycondensation are performed using organoboron reagent in presence of aryl coreagent having bromides, iodides or triflates as leaving groups and Pd(0) as catalyst, generally Pd[P(*p*-tolyl)₃]₄ or Pd(PPh₃)₄, in alkaline conditions (figure 8).

The boron-containing byproducts can be separated from the reaction mixture, a much needed feature especially in large-scale production. Additionally, several boronic acids are commercially available and environmentally friendly. The Suzuki–Miyaura reaction suffers from a few key drawbacks, the first of which is the requirement for basic conditions. A number of monomers may be unstable in basic conditions, thus rendering this methodology impractical for these applications, or requiring more complex protection–deprotection strategies. Also, the Suzuki–Miyaura reaction requires a two-phase system; thus, polymers that rapidly decrease in solubility as molecular weight increases may form precipitates, resulting in very low molecular weights or very high polydispersities.

On the other end, following the pioneering work of Yu *et al.*³⁰, Stille polycondensations are widely applied to the synthesis of a wide variety of conjugated polymers for OPVs with high molecular weights. A typically Stille polycondensation protocol use organotin reagent and aryl halides or pseudohalides (example triflates) in presence of Pd(0) catalyst, generally Pd(PPh₃)₄ or more air-stable Pd₂(dba)₃, and ligands such as tri(*o*-methoxyphenyl)phosphine, PPh₃ and tri(2-furyl)phosphine (figure 8). The major advantages of Stille polycondensation are the tolerance of many functional groups and the mild reaction conditions. The organotin monomers can be conveniently prepared, and they are far less sensitive to oxygen and moisture than many other organometallic compounds. However, purification of many tin compounds is difficult because of their instability under silica gel column chromatography.

The preparation of organotin or organoboron monomers used for Stille or Suzuki coupling require multistep reactions and tedious purifications. Additionally, Stille coupling requires the use of very toxic reagents as well as generating toxic byproducts. In fact, some important classes of heteroaryl organotin or organoboron reagents are not readily accessible and may even be too unstable to undergo the coupling processes.

In recent years, direct arylation of non-preactivated arenes with aryl halides or pseudohalides has attracted much attention and worldwide interest.³¹ DHA reactions would be one of

the most ideal routes toward π -conjugated polymers due to their indisputable advantages of synthetic simplicity and atom economy, avoiding troublesome and toxic (hetero)aryl organometallic intermediates (figure 9).

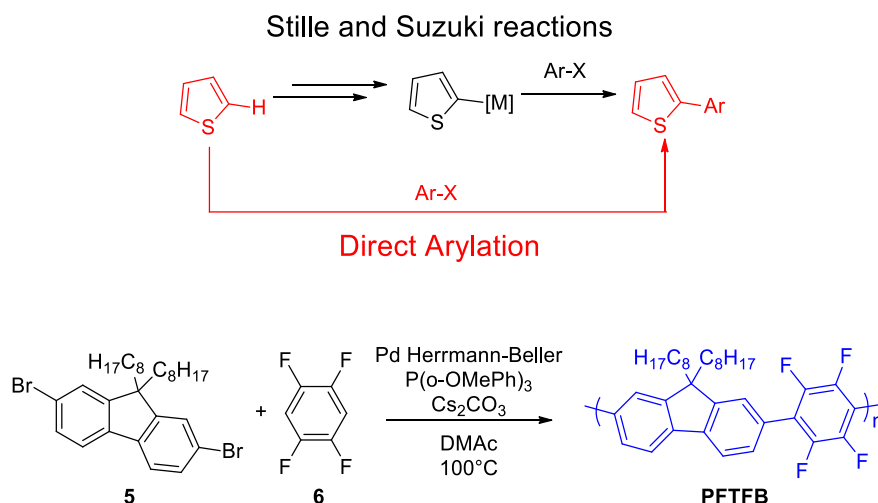


Figure 9. General scheme of Direct arylation reactions with selected example of DHAP.

In most polymerization examples, $\text{Pd}(\text{OAc})_2$ is used as the palladium source, but the stable Herrmann–Beller catalyst is also widely used. Catalytic addition of pivalic acid can aid the C–H activation. Phosphine ligands are not essential to achieve high molecular weight materials. Several electron-rich monomers and electron-deficient monomers have been used for DHA polymerization, however the poor selectivity of the C–H bond in direct arylation could be a serious limitation, resulting in the formation of branched and/or cross-linked polymer structures that affect solubility and optoelectronic properties of polymers.

A typical conjugated donor polymer used in PSC is illustrated in Figure 10.³² Generally, a conjugated polymer can be divided into 3 constituting components: the conjugated backbone, the side chains and the substituents.

Side chains play a crucial role in improving the molecular weight, solubility, processability of conjugated polymers over to adjust intermolecular interactions to form the desired morphology. However, they can also hinder π - π stacking between chains, which could interfere

with the light absorption and charge transport. On the other hand, substituents (such as F and CN) are generally used in order to tweak the physical properties of conjugated polymers.

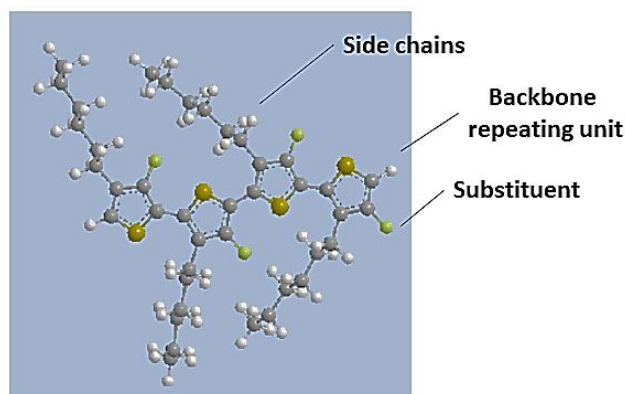


Figure 10. Illustration of a typical conjugated polymer for PSC.

The conjugated backbone is the most important component because most of the PSC-related physical properties of the conjugated polymer depend from it. Hundreds of different backbones have been reported so far; however, the design of polymer backbones has been quite empirical. Therefore, the rational design of repeating units into conjugated backbone is of utmost importance in the further development of polymer solar cells. All reported conjugated backbones for PSC can be classified in base on the constitution of the repeating unit in homopolymers and D–A polymers.

Homopolymers were the first class of processable polymers developed for OPVs, consisting in repeating units of a single aromatic ring or fused aromatics.³³ The electronic and optical properties of these polymers are determined by the electronic properties of the single repetitive unit as well as from degree of polymerization and from the interference of steric hindrance between these repeating units. The degree of polymerization and then the length of polymeric backbones have important impact on the band gap of polymers and their planarity, with negative influences on absorption of the light and the morphology of active layer. On the other end, the steric hindrance can cause the loss of the desired coplanarity, impacting negatively on light absorption, band gap, and on the morphology of active layer, decreasing

the crystallinity of the polymer.

The most studied homopolymers are regioregular P3HT and PPV derivatives, especially MDMO-PPV (shown in Figure 11). PCEs of around 5-6% for *rr*P3HT and around 2-3% for PPVs have been reported, after thorough optimization.

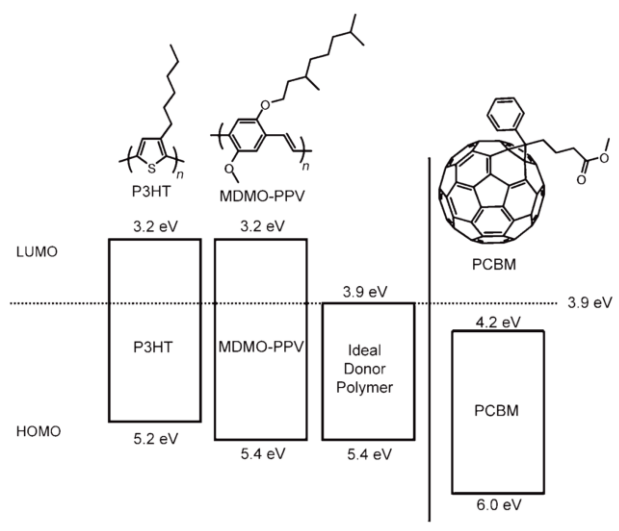


Figure 11. Band gap of P3HT and MDMO-PPV polymers compared to ideal donor polymer.

The need to obtain highly conducting polymers with tunable electronic and optical properties (HOMO/LUMO levels and E_g), not achievable with homopolymers, pushed towards the use of push-pull architectures, proposed theoretically for the first time in 1993 by Wynberg *et al.*³⁴, and well demonstrated by Tour *et al.*³⁵ through the synthesis of a copolymer between 3,4-aminothiophene and 3,4-nitrothiophene with a band gap of 1.0 eV.

A typical D–A polymeric frameworks, in which an electron-rich units are followed by electron-poor units, offers tremendous advantages respect to strategy that make use of homopolymeric frameworks. First, the internal charge transfer (ICT) intrinsic with the D–A frameworks leads to a more pronounced double bond character between repeating units (figure 12a). Therefore, the conjugated backbone adopts a more planar configuration to facilitate the π -electrons delocalization along the conjugated backbone, leading to a polymers with smaller band gap. Second, the possibility of tuning of HOMO/LUMO levels and band gap of the pol-

ymers simply combining different donor and acceptor components into the monomeric unit (figure 12b).

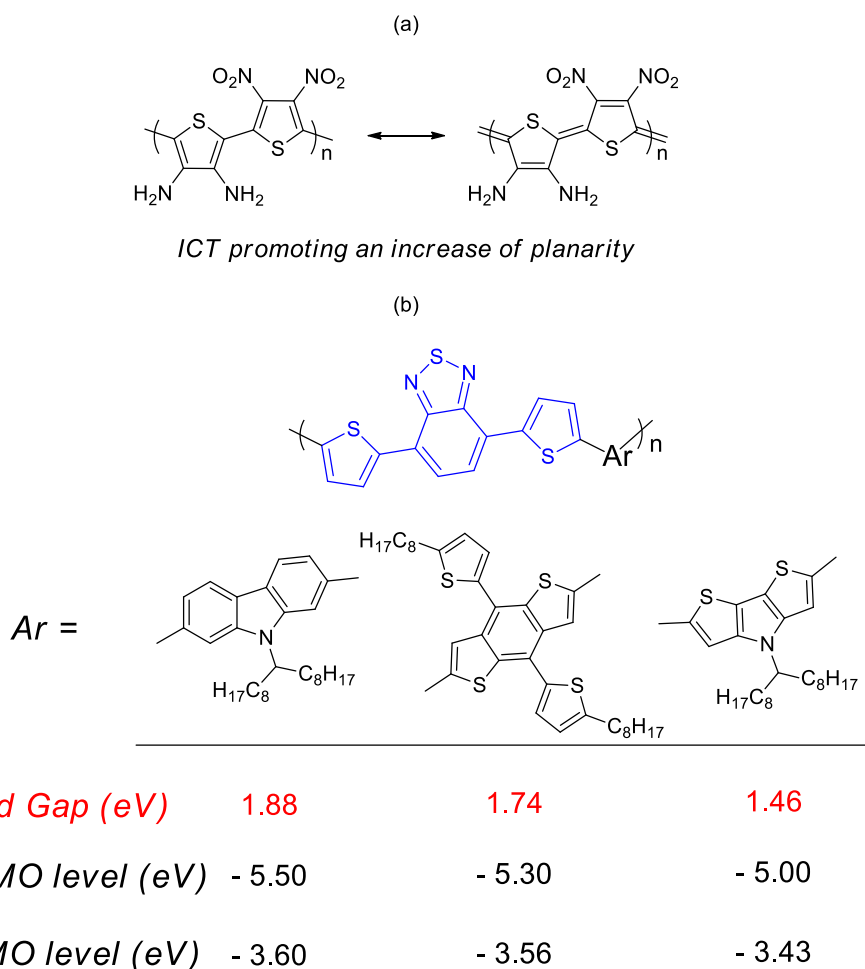


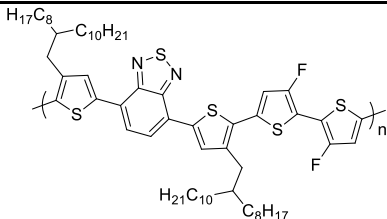
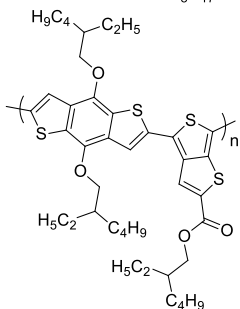
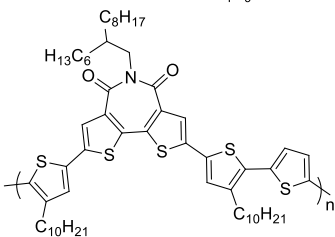
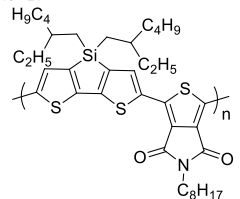
Figure 12. D-A concept for tuning of polymeric frameworks with D–A architecture.

This feature offers a tremendous advantage because it is possible to modify independently the HOMO level, the LUMO level and the band gap of the polymers by modifying independently the HOMO-LUMO levels of donor components while keeping constant the acceptor component or *vice versa*. In addition, the charge mobility, molecular interaction, and stability of a conjugated polymer can be optimized by appropriate backbone design.

The application of this strategy has allowed a significant improvement of the efficiencies compared to the efficiency of P3HT-based solar cells, up to overcoming the critical threshold of commercialization (around 10%), currently certified to 11.5%.⁵¹ (see Table 1). The use of this

concept evidences once more the fundamental roles of the rational design of cheap and scalable donor and acceptor units constituting monomeric frameworks for the achieving of best performance of cell.

Table 1. Polymers used in top performance solar cells

Polymers	Method of Polymerization	Ease of Synthesis	PCE (%)
	Stille	Low	11.5
	Stille	Low	9.4
	Stille	Low	8.5
	Stille	Medium	7.8

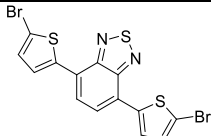
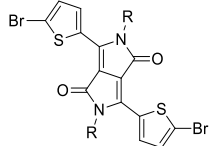
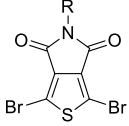
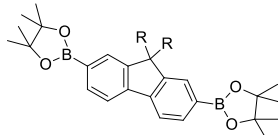
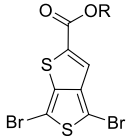
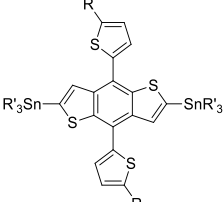
1.4 SYNTHESIS OF SCALABLE MONOMERS BY DIRECT ARYLATION FOR PHOTOVOLTAIC APPLICATIONS

This paragraph is partially based on the following publication:

Andrea Nitti, Riccardo Po, Gabriele Bianchi and Dario Pasini, *Molecules* **2017**, 22, 21-36.

The synthetic accessibility of the monomers is a key element for the scalability of the resultant donor polymer because a significant percentage of the final cost of the devices is due to the cost of monomers.³⁶ During the last couple of years several high-efficiency polymers have been made commercially available but only on the 0,1–1 g scale.

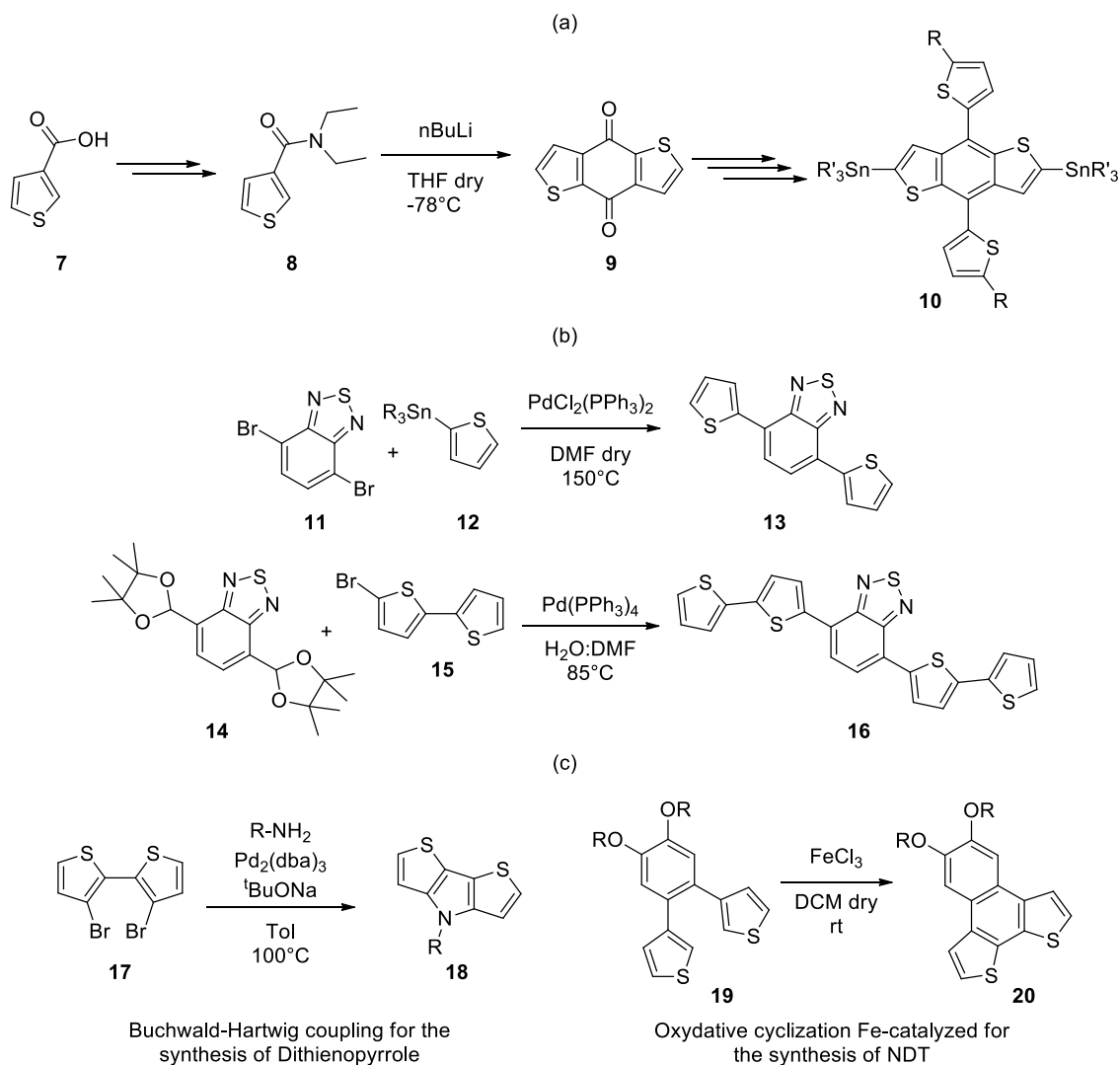
Table 2. Number of synthetic steps for the preparations of selected monomers

Monomer	Type of monomers	Number of synthetic step	Yield [%]
	ACCEPTOR	3	48
	ACCEPTOR	3	36
	ACCEPTOR	4	55
	DONOR	3	75
	DONOR	7	20
	DONOR	7	9

According to a recent analysis,³⁷ based on published laboratory-scale synthetic procedures, the cost *per* gram of the polymers increases linearly with the number of synthetic steps required for the preparation of the monomers. Only simple synthetic sequences, requiring less than six steps, do not affect significantly the final cost of a device. Considering a linear synthetic route for the monomers, the total amount of synthetic steps required to obtain D–A polymers is equal to sum of synthetic steps required by donor and acceptor monomers, plus one.

Table 2 summarizes the minimum number of steps required for the preparation of most popular monomers for highly-efficient monomers. The threshold of the “six steps” is never fulfilled for those combinations.

Scheme 1. Typically crucial step in the synthesis of monomers



The number of synthetic steps is not the only requirement in order to obtain scalable monomers and polymers. The minimization of work-up procedures (ruling out the need for flash chromatography purifications), and of solvents and reagents consumption are essential to achieve low cost materials. No exotic reactions, making use of expensive reagents and giving low yields, must be used in the synthetic route.

The crucial step in the synthesis of the monomers is the formation of the carbon frame-

work, generally utilizing reactions between an intermediate organometallic species and its electrophilic partner. The synthesis of these organometallic species generally leads to an increment of the number of steps. A typically example of this strategy is the α -lithiation of *N,N*-diethyl-3-carboxythiophene for the reaction with itself to give DTBDT framework³⁸ (Scheme 1a) or lithium-halogen exchange for the synthesis of silafluorene.³⁹

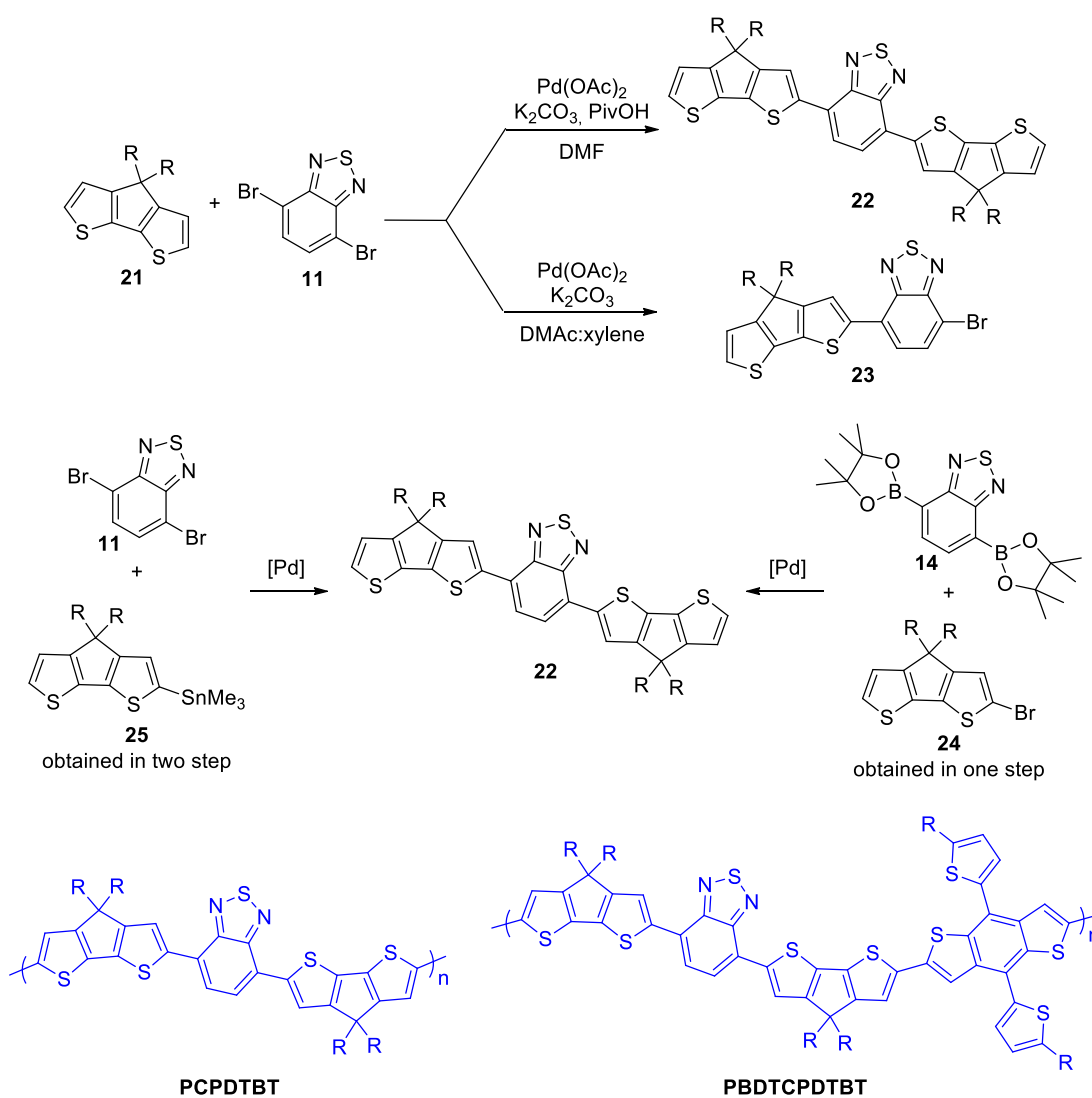
Cross-coupling methodologies, as Stille and Suzuki protocols, may use commercial available organotin and organoboron species for the achievement of target molecules (Scheme 1b).^{40, 41} However, the formation of inorganic or organometallic byproducts with intrinsic toxicity, especially for the trialkyltin derivatives used in the Stille protocols, require the use of flash-chromatography as the purification method. Furthermore, similarly to Grignard or organolithium compounds, when Stille and Suzuki reactions require pre-activation of the halide-intermediate and organotin or organoboron species are not commercially available, the synthetic advantage is lost.

Transition-metal-catalyzed methodologies that do not make use of organometallic reagents such as Buchwald-Hartwig cross coupling⁴² or Cu-⁴³ and Fe-catalyzed⁴⁴ oxidative couplings have shown great potential in the construction of the carbon frameworks of high-efficiency monomers (scheme 1c).

DHA reactions are attracting increasing attention as a Pd-catalyzed cross-coupling methodology, since no pre-activation of the starting monomers with organometallic reagents is required; they are regioselective, efficient and flash-chromatography purifications can be avoided. Direct arylation has been efficiently applied to the coupling of a number of different arene and heteroarene systems.⁴⁵ In particular thiophene-based compounds with electron-rich and electron-deficient substituents have shown high reactivity due to the small activation energy in the “concerted metalation-deprotonation”, the fundamental step of the catalytic cycle.³¹ These aspects make the DHA reaction an important tool for the construction of new and efficient π -conjugated thiophene-based compounds.

In this section, we will highlight recent examples of use of DHA reactions for the construction of π -extended monomers, in order to establish a link between the current use of this relatively recent synthetic protocol, and the development of novel scalable monomers for OPV-BHJ low-cost polymers. We will divide literature approaches into two categories: (1) intermolecular DHA and (2) intramolecular DHA.

Scheme 2. DHA reaction between CPDT and BT compounds and their selected polymers



2,1,3-Benzothiadiazole and its derivatives are an important class of high-performance dyes that in recent years have been widely explored for optoelectronic applications because of their unique electrical and optical properties as well as their exceptional stability. BT deriva-

tives are generally synthesized through Stille or Suzuki coupling reactions using different organometallic reagent and DBrBT. It is not thus surprising that much of the literature on DHA reactions is focused on the synthesis of BT derivatives.

M. Horie *et al.*⁴⁶ reported an interesting DHA reaction between DBrBT **11** (scheme 2) and alkylated CPDT **21** for the construction of a monomeric unit to incorporate in several polymers with high hole mobility and PCE around 5-6% such as PCPDTBT or PBDTCPDTBT.⁴⁶⁻⁴⁸

The synthesis of oligomeric monomer **22**, shown in scheme 2, was achieved with a 40% yield using Pd(OAc)₂ as catalyst in presence of K₂CO₃ as base, PivOH as additive and DMF. The same author reported the synthesis of **22** *via* Suzuki coupling (60% yield) using commercial 2,1,3-Benzothiadiazole-4,7-bis(boronic acid pinacol ester) **14** and mono-brominated CPDT **24**, this last compound obtained after bromination reaction with NBS. The synthesis of **22** could be achieved with Stille protocol⁴⁹ but, in analogy with the Suzuki protocol, the synthesis of starting material **25** was needed. The procedure highlights a greater synthetic sustainability of DHA compared to Suzuki and Stille reaction in terms of reduction of synthetic steps, reaction time and cost of reaction in spite of a yield decrease.

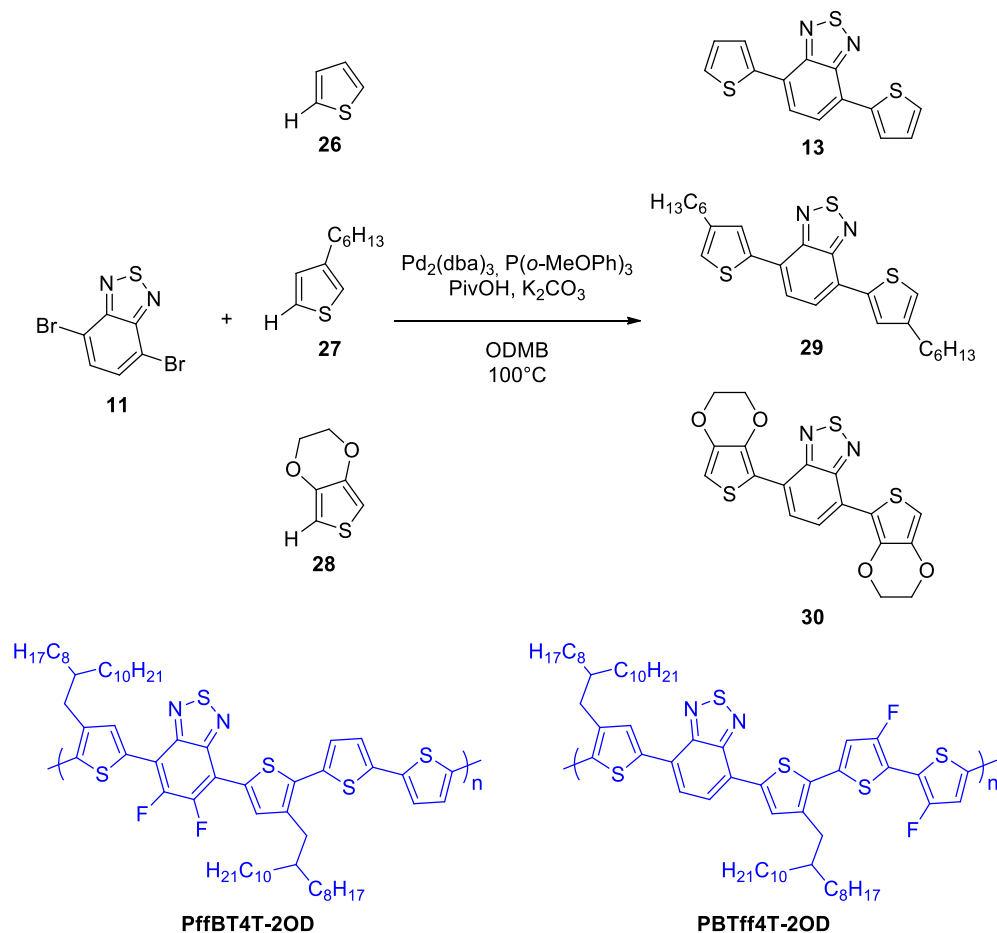
M. Wang *et al.*⁵⁰ reported the synthesis of a series DTBT monomers **13** (DTBT), **29** (DHTBT) and **30** (DEDOTBT) with a Pd₂(dba)₃-catalyzed DHA protocol using commercial **11**, **26**, **27** and **28** (Scheme 3). DTBTs are one of the most important building blocks in conjugated polymers for high-performance optoelectronic devices, the current record of PCE achieved to date (11,5% with PBTff4T-2OD) was obtained from a polymer having as a acceptor DTBT unit.⁵¹

The reaction shows modest efficiencies (compounds **13**, **29** and **30** was obtained respectively with yields of 67%, 76% and 43%.) when compared with the efficiencies obtained with Stille and Suzuki protocols (yield >90%),⁵² due to the inevitable formation of byproducts.

The authors reported, even in optimized conditions, the formation of insoluble and par-

tially insoluble purple byproducts (oligomers and polymers) when **13** was reacted with **26** and **28**.

Scheme 3. Synthesis of DTBTs and its high-efficiency polymers



The formation of these higher molecular weight byproducts was explained with a greater reaction rate of **13** and the **TBrBT** intermediate towards aryl bromide species (**11** and **TBrBT** intermediate) with respect to the reaction rate involving bare thiophene **26** (Figure 13a).

The increase in the Brønsted acidity of the remaining α -H on the thiophene ring of **TBrBT** intermediate and **13** compared to bare thiophene **26** (figure 13a, red bonds) is likely the cause of their greater reactivity of C5–H bond toward the intermolecular DHA reaction (Figure 13a, blue bonds).

The reaction between **11** with symmetric **28** showed lower yields of **30** (43%) due to formation of a high molecular weight byproducts in analogy to the precedent case, while the reaction with asymmetric **27** showed good yields of **29** with a suppressed formation of by-

products (figure 13b). The authors ascribe the improvement in the yield of **29** to the suppression of byproducts formation, due to the different reactivity of the 2- and 5-position C-H bonds on **27**. In fact C5–H bond on **27** (Figure 11b, blue bond) is more reactive toward DHA reactions than C2–H bond on **27** and C5–H bond on **HTBrBT** intermediate (Figure 13b, red bonds).

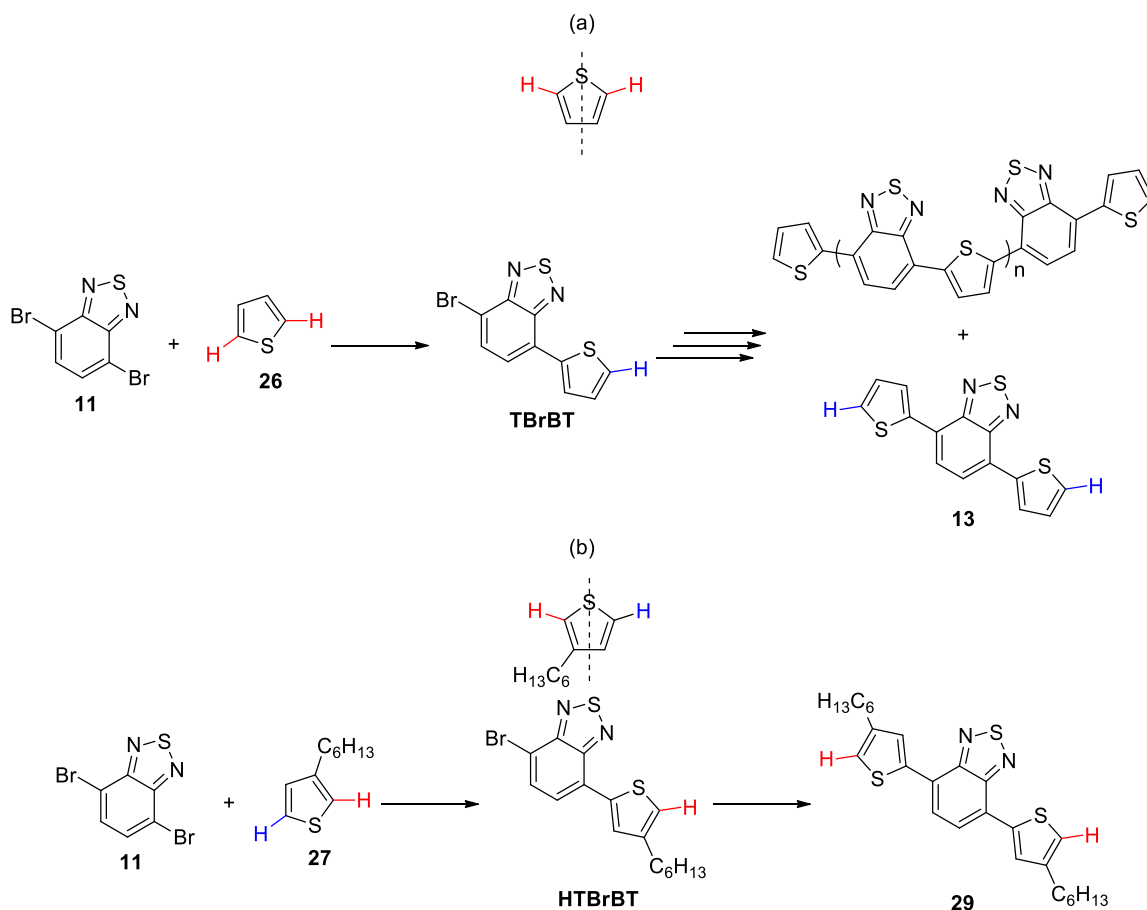


Figure 13. Possible reaction pathways and side reactions. Blue C–H bonds are more reactive in intermolecular DHA reaction than red C–H bonds.

These examples showed an important limitation to the use of intermolecular DHA protocols when symmetric compounds (such as **21**, **26** and **28**) are used. In all cases in which precursors with a plane of symmetry are used (synthesis of **22**, **13** and **30**), both α -H position on thiophene rings are equally reactive toward DHA reaction, and intermediates with α -H more reactive than its precursor are formed with the consequent formation of oligomeric byproduct

and reduction of the yield. In case in which precursor does not present a plane of symmetry (synthesis of **29**), when the α -H are unsymmetrically reactive towards the DHA reaction, an intermediate with α -H less reactive than its precursor is formed with important benefit to the yield of reaction. In general the intermolecular DHA reaction work well if the intermediate species have a less reactive α -H than its precursor, otherwise the intermolecular DHA reaction will show a decrement of yield due to the formation of a byproduct.

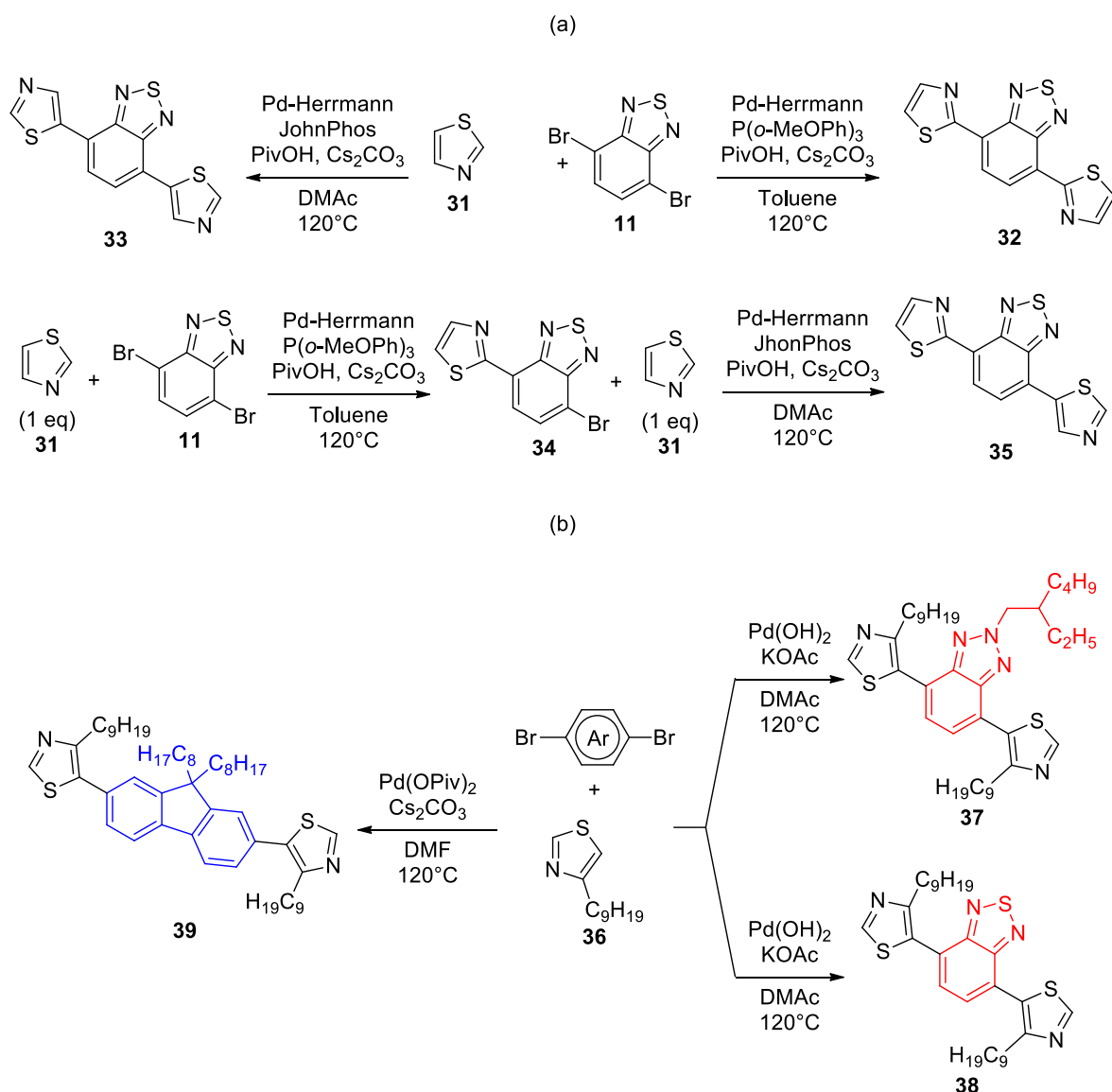
These considerations have further confirmation in the work of N. Leclerc *et al.*⁵³ on intermolecular DHA between **11** and commercial thiazole **31** to give monomers **32** and **33** respectively with Tz unit linked with its C2 position and C5 position with high regioselectivity (scheme 4a).

The thiazole unit has non-equivalent C2–H and C5–H positions that can be activated differently toward DHA using different reaction conditions. This asymmetric reactivity of two α -H position promote the formation of intermediate species **34**, possessing an α -H less reactive than Tz precursor toward DHA reaction conditions and avoiding the formation of byproduct with high molecular weight. In this article the authors obtained highly regioselective C2-C2 products **32** (**32/33** ratio 99:1, 79% yield) using an apolar solvent (toluene) and Pd-Herrmann catalyst with smaller ligand tris(*o*-methoxyphenyl)phosphine, whereas the use a polar solvent (DMAc) and Pd-Herrmann catalyst with bulkier ligand JHONPHOS have led highly regioselective C5-C5 products **33** (**32/33** ratio 1:99, 75% yield). In both cases the authors did not observe any polycondensation byproducts indicating good control over DHA reaction. The author yet reported the synthesis of C2:C5 monomer **35** starting from isolated compound **34**.

J. You *et al.*⁵⁴ obtained monomer **37** (62% yield) and **38** (77% yield), which presented electron-poor arene unit (BT unit and BTZ unit), using Pd(OH)₂ as catalyst in DMAc, while for monomer **39** (72% yield), which present electron-rich arene unit (F unit **5**), was used Pd(OPiv)₂ as catalyst in DMF. With these monomers the authors reported their homopoly-

mers obtained with DHAP methodologies.

Scheme 4. Synthesis of Tz-based monomers *via* DHA reaction

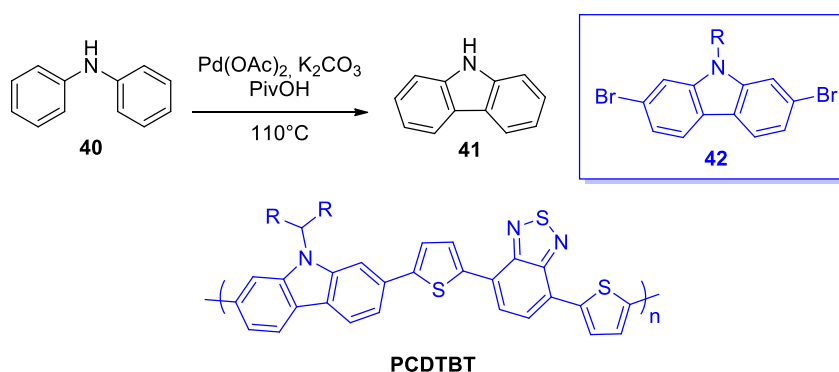


In contrast to intermolecular DHA, the intramolecular DHA has been used for the construction of novel monomer frameworks due to reliability and possibility of standardization of the process. The protocols developed for these reactions are generally conducted without the use of expensive phosphines and using $\text{Pd}(\text{OAc})_2$ as the catalyst for its stable catalytic working conditions even without use of an inert atmosphere. The presence of the nucleophile and electrophile moieties in the same molecule, placed at the right distance and with the right orientation, is essential for an efficient DHA reaction but introduces the problem of the synthesis of the precursor. For this reason, the synthesis results to be advantageous, only in cases in

which the precursor is obtained with simple reactions and in a few steps. In next examples we report the most important cases to use of intramolecular DHA for construction of novel monomers selected from the recent literature.

K. Fagnou *et al.*⁵⁵ reported an interesting carbazole synthesis using mild and scalable intramolecular oxidative DHA reaction shown in scheme 5.

Scheme 5. Intramolecular DHA reaction for the synthesis of carbazole monomers

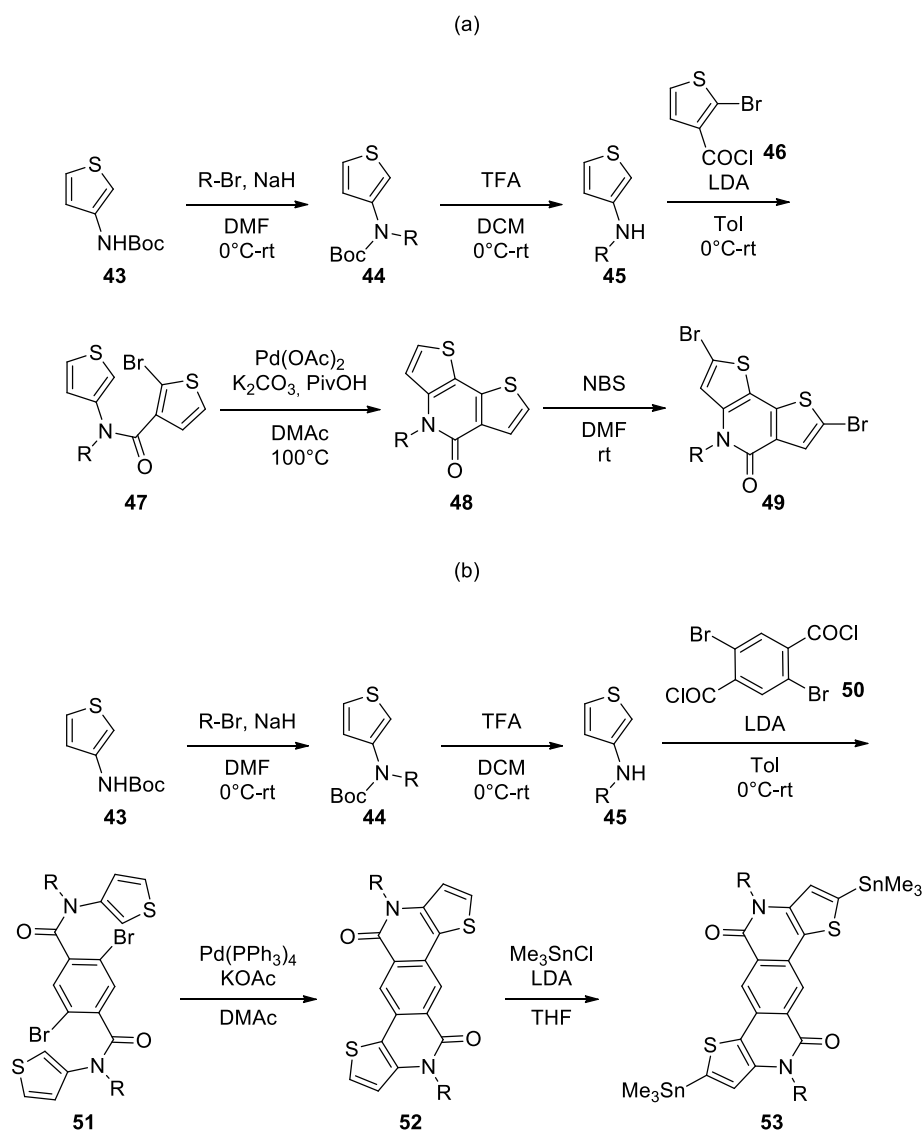


Carbazole monomers have received much interest in the optoelectronic field due to interesting HOMO energy levels, very close to the ideal HOMO level. Carbazole scaffold **41** was obtained with 95% yield and without formation of byproduct starting from diphenylamine **40** in presence of Pd(OAc)₂ as catalyst, K₂CO₃ as base and PivOH as co-solvent to form **41** in air (O₂ acts as oxidant reagent). In this case the synthetic route developed provides the use of cheap precursor **40**, scalable high-efficiency, mild reaction condition, and it avoids flash-chromatography purification. The synthesis of carbazole-based polymerizable monomer **42** is achieved after other 2 synthetic steps of bromination and *N*-alkylation.

Luping Yu *et al.*⁵⁶ reported an interesting synthesis of PDT monomers using Pd(OAc)₂-catalyzed intramolecular DHA reaction as crucial step of the synthesis (scheme 6a). The authors achieved the PDT synthesis in 5 step *via* alkylation of Boc-protected 3-aminothiophene **43** (89% yield) followed by deprotection of resulting alkylated amine **44** with TFA.

The deprotected amine **45** was directly reacted with thiophene **46** to afford precyclized intermediate **47** in 58% yield after 3 steps.

Scheme 6. Synthesis of PDT and TPTI monomers



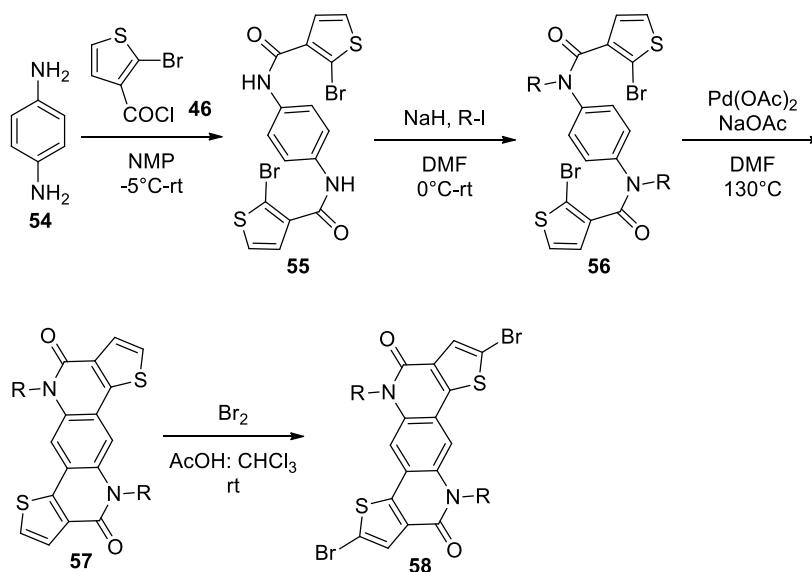
This compound was finally cyclized through an intramolecular DHA to give the PDT framework (compound **48**) and then brominated, using NBS, to obtain monomer **49**. The same authors reported the synthesis of TPTI framework using analogue synthetic route to the synthesis of PDT (scheme 6b).⁵⁷

In this case precyclized precursor **51** was obtained, with 52% yield after 3 steps, by acylation reaction between **45** and compound **50**, while intramolecular DHA of compound **51** was performed with Pd(PPh₃)₄ as catalyst, KOAc as base in DMAc under diluted condition (2 mM). Both intramolecular DHA reactions was achieved with good yield (90% for compound **48** and 87% for compound **51**) working in diluted conditions and without the use of phos-

phine. An easy and efficient synthesis of precyclized intermediate is fundamental to obtain scalable monomers *via* DHA reactions. The synthetic design of monomers proposed by Luping Yu take account of this aspect, in fact the synthesis of compounds **44** (81% yield), **45**, **47** (65% yield) and **51** (58% yield) make use of simple, cheap, scalable reactions.

An easier synthetic design was proposed by T.-H. Kim *et al.*⁵⁸ in the synthetic route shown in scheme 7 for the synthesis of novel classes of acceptor monomer TPTBL **58**

Scheme 7. Synthesis of TPTBL monomer



Starting from *p*-phenylenediamine **54** with 2-bromothiophene acid chloride **46** in NMP at temperature of -5°C , bisamide **56** was obtained in 87% yield. The *N*-alkylation of bisamide **56** (70% yield) in presence of NaH and alkyl iodide in DMF, followed by ring-closing Pd(OAc)₂-catalyzed DHA reaction provide desired thiophene-phenylene-thiophene fused bislactams TPTBL **57** in good yield (69%). Bromination reaction with Br₂ leads quantitatively to the TPTBL-polymerizable monomer **58**. The author incorporate intramolecular DHA reactions in a synthetic rational design that makes use of cheap reagents, easy reactions achieved in good or high yields, and minimal number of synthetic steps.

1.5 REFERENCES

- (1). Population Reference Bureau. (<http://www.prb.org/pdf16/prb-wpds2016-web-2016.pdf>)
- (2). BP Statistical Review of World Energy June 2016.

(<https://www.bp.com/content/dam/bp/pdf/energy-economics/statistical-review-2016/bp-statistical-review-of-world-energy-2016-full-report.pdf>)
- (3). International Energy Agency, 2015 Snapshot of Global PV Markets.

(http://www.iea-pvps.org/fileadmin/dam/public/report/technical/PVPS_report_-_A_Snapshot_of_Global_PV_-_1992-2014.pdf)
- (4). The Nobel Prize in Physics 1921.

(http://www.nobelprize.org/nobel_prizes/physics/laureates/1921/)
- (5). Carlson, D., Wronski, C., *Topics in Applied Physics: Amorphous Semiconductors: Amorphous silicon solar cells*, Springer Berlin / Heidelberg 1985.
- (6). Fonte Wikipedia. (https://it.wikipedia.org/wiki/Modulo_fotovoltaico)
- (7). Tang, C. W. *Appl. Phys. Lett.* **1986**, 48, 183 – 184.
- (8). Jacoby, M. *Chemical & Engineering News*, **2016**, 96, 18, 30. Only a handful of companies are already commercializing polymeric OPVs. See www.infinitypv.com or <http://www.solarte.de>
- (9). Thompson, B. C.; Fréchet, J. M. J. *Angew. Chem. Int. Ed.* **2008**, 47, 58-77.
- (10). Brabec, C. J. *Sol. Energy Mater. Sol. Cells* **2004**, 83, 273 – 292.
- (11). Yue, D.; Khatav, P.; You, F.; Darling, S. B. *Energy Environ. Sci.* **2012**, 5, 9163 – 9172.
- (12). Lizin, S.; Van Passel, S.; De Schepper, E.; Maes, W.; Lutsen, L.; Manca, J.; Vanderzan-

de, D. *Energy Environ. Sci.* **2013**, *6*, 3136 – 3149.

(13). Krebs, F. C.; Jørgensen, M. *Sol. Energy Mater. Sol. Cells* **2013**, *119*, 73 – 76.

(14). Kirchmeyer, S.; Reuter, K. *J. Mater. Chem.* **2005**, *15*, 2077 – 2088.

(15). Gevorgyan, S. A.; Madsen, M. V.; Dam, H. F.; Jørgensen, M.; Fell, C. J.; Anderson, K. F.; Duck, B. C.; Mescheloff, A.; Katz, E. A.; Elschner, A.; Roesch, R.; Hoppe, H.; Hermenau, M.; Riede, M.; Krebs, F. C. *Sol. Energy Mater. Sol. Cells* **2013**, *116*, 187 – 196.

(16). Grossiord, N.; Kroon, J. M.; Andriessen, R.; Blom, P. W. M. *Org. Electron.* **2012**, *13*, 432 – 456.

(17). Rivaton, A.; Chambon, S.; Manceau, M.; Gardette, J. L.; Lemaître, N.; Guillerez, S. *Polym. Degrad. Stab.* **2010**, *95*, 278 – 284.

(18). Yu, G.; Gao, J.; Hummelen, J.; Wudl, F.; Heeger, A. J. *Science* **1995**, *270*, 1789 – 1791.

(19). Allemand, P. M.; Koch, A.; Wudl, F. *J. Am. Chem. Soc.* **1991**, *113*, 1050-1051.

(20). Gunes, S.; Neugebauer, H.; Sariciftci, N. S. *Chem. Rev.* **2007**, *107*, 1324-1338.

(21). Singh, T. B.; Marjanovic, N.; Matt, G. J.; Gunes, S.; Sariciftci, N. S.; Montaigne Ramil, A.; Andreev, A.; Sitter, H.; Schwodiauer, R.; Bauer, S. *Org. Electron.* **2005**, *6*, 105-110.

(22). Rispens, M. T.; Meetsma, A.; Rittberger, R.; Brabec, C. J.; Sariciftci, N. S.; Hummelen, J. C. *Chem. Commun.* **2003**, 2116-2118.

(23). The Nobel Prize in Chemistry 2000.

http://www.nobelprize.org/nobel_prizes/chemistry/laureates/2000/

(24). Jørgensen, M.; Carlé, J. E.; Søndergaard, R. R.; Lauritzen, M.; Dagnæs-Hansen, N. A.; Byskov, S. L.; Andersen, T. R.; Larsen-Olsen, T. T.; Böttiger, A. P. L.; Andreasen, B.; Fu, L.;

Zuo, L.; Liu, Y.; Bundgaard, V.; Zhan, X.; Chen, H.; Krebs, F. C. *Sol. Energy Mater. Sol. Cells* **2013**, *119*, 84-93.

(25). Longo, L.; Carbonera, C.; Pellegrino, A.; Perin, N.; Schimperia, G.; Tacca, A.; Po, R. *Sol. Energy Mater. Sol. Cells* **2012**, *97*, 139 – 149.

(26). Risko, C.; McGehee, M. D.; Bredas, J.-L. *Chem. Sci.* **2011**, *2*, 1200 – 1218.

(27). Bérubé, N.; Gosselin, V.; Gaudreau, J.; M. Côté, *J. Phys. Chem. C* **2013**, *117*, 7964 – 7972.

(28). Roncali, J. *Macromol. Rapid Commun.* **2007**, *28*, 1761 – 1775.

(29). Rehahn, M.; Schlüter, A. D.; Wegner, G.; Feast, W. J. *Polymer* **1989**, *30*, 1060 – 1062.

(30). Bao, Z. N.; Chan, W. K.; Yu, L. P. *Chem. Mater.* **1993**, *5*, 2 – 3.

(31). Mercier, L. G.; Leclerc, M. *Acc. Chem. Res.* **2013**, *46*, 1597 – 1605.

(32). Zhou, H.; Yang, L.; You, W. *Macromolecules* **2012**, *45*, 607 – 632.

(33). Bundgaard, E.; Krebs, F. C. *Sol. Energy Mater. Sol. Cells* **2007**, *91*, 954 – 985.

(34). Havinga, E. E.; ten Hoeve, W.; Wynberg, H. *Synth. Met.* **1993**, *55*, 299 – 306.

(35). Zhang, Q. T.; Tour, J. M. *J. Am. Chem. Soc.* **1998**, *120*, 5355 – 5362.

(36). Po, R.; Bianchi, G.; Carbonera, C.; Pellegrino, A. *Macromolecules* **2015**, *48*, 453 – 461.

(37). Osedach, T. P.; Andrew, T. L.; Bulovic, V. *Energy Environ. Sci.* **2013**, *6*, 711 – 718.

(38). Hou, J.; Park, M.-H.; Zhang, S.; Yao, Y.; Chen, L.-M.; Li, J.-H.; Yang, Y. *Macromolecules* **2008**, *41*, 6012 – 6018.

(39). Corey, J. Y.; Chang, L. S. *J. Organomet. Chem.* **1986**, *307*, 7.

- (40). (a) Cordovilla, C.; Bartolome, C.; Martínez-Ilarduya, J. M.; Espinet, P. *ACS Catal.* **2015**, *5*, 3040–3053; (b) Maluenda, I.; Navarro, O. *Molecules* **2015**, *20*, 7528 – 7557.
- (41). Li, C.; Bo Z.; CHAPTER 1 : New Chemistry for Organic Photovoltaic Materials, in ‘*Polymer Photovoltaics: Materials, Physics, and Device Engineering*’, 2015
- (42). Selected example of Buchwald-Hartwig cross-coupling: Zhou, Y.; Verkade, J. G. *Adv. Synth. Cat.* **2010**, *352*, 616.
- (43). Selected example of Cu-catalyzed oxidative coupling: Melkonyan, F. S.; Zhao, W.; Dress, M.; Eastham, N. D.; Leonardi, M. J.; Butler, M. R.; Chen, z.; Yu, X.; Chang, R. P. H.; Ratmer, M. A.; Facchetti, A. F.; Marks, T. J. *J. Org. Chem. Soc.* **2016**, *138*, 6944.
- (44). Selected example of Fe-catalyzed oxidative coupling: Tovar, J. D.; Rose, A.; Swager, T. M. *J Am. Chem. Soc.* **2002**, *124*, 7762 – 7769.
- (45). D., Alberico; Scot, M. E.; Lautens, M. *Chem. Rev.* **2007**, *107*, 174 – 238.
- (46). Chang, S.-W.; Waters, H.; Kettle, J.; Horie, M. *Org. Electronics* **2012**, *13*, 2967 – 2974.
- (47). Chang, S.-W.; Waters, H.; Kettle, J.; Kuo, Z-R.; Li, C.-H.; Yu, C.-Y.; Horie, M. *Macromol. Rapid Commun.* **2012**, *33*, 1927 – 1932.
- (48). Wang, M.; Ford, M.; Phan, H.; Coughlin, J.; Nguyena, T.-Q.; Bazan, G. C. : *Chem. Commun.* **2016**, *52*, 3207 – 3210.
- (49). Sharma, B.; Sarothia, Y.; Singh, R.; Kan, Z.; Keivanidis, P. E.; Jacob *Polym. Int.* **2016**; *65*, 57 – 65.
- (50). Wang, X.; Wang, K.; Wang, M. *Polym. Chem.* **2015**, *6*, 1846 – 1855.
- (51). (a) Liu, Y.; Zhao, J.; Li, Z.; Mu, C.; Ma, W.; Hu, H.; Jiang, K.; Lin, H.; Ade, H.; Yan,

H. *Nat. Commun.* **2014**, *5*, 5293. (b) pv Magazine, Raynergy Tek Sets World Record Solution Processed Single Junction OPV PCE 11.51% Using Halogen-Free Ink Formulation.

(http://www.pv-magazine.com/services/press-releases/details/beitrag/raynergy-tek-sets-world-record-solution-processed-single-junction-opv-pce-1151-using-halogen-free-ink-formulation_100025157/#axzz4PVH1n83S)

(52). (1) Hou, Q.; Xu, Y. S.; Yang, W.; Yuan, M.; Peng, J. B.; Cao, Y. *J. Mater. Chem.* **2002**, *12*, 2887 – 2892. (2) Liu, B., Najari, A.; Pan, C. Y.; Leclerc, M.; Xiao, D. Q.; Zou, Y. P. *Macromol. Rapid Commun.* **2010**, *31*, 391 – 397.

(53). Chàvez, P.; Ngov, C.; Frémont, P.; Lévêque, Leclerc, N. *J. Org. Chem.* **2014**, *79*, 10179 – 10188.

(54). Guo, Q.; Jiang, R.; Wu, D.; You, J. *Macromol. Rapid Commun.* **2016**, *37*, 794 – 798.

(55). Liégault, B.; Lee, D.; Huestis, M. P.; Stuart, D. R.; Fagnou, K. *J. Org. Chem.* **2008**, *73*, 5022 – 5028.

(56). Schneider, A. M.; Lu, L.; Manley, E. F.; Zheng, T.; Sharapov, V.; Xu, T.; Marks, T. J., Chen, L. X.; Yu, L. *Chem. Sci.* **2015**, *6*, 4860 – 4866.

(57). Jung, I. H.; Lo, W.-Y.; Jang, J.; Chen, W.; Zhao, D.; Landry, E. S.; Lu, L.; Talapin, D. V.; Yu, L. *Chem. Mater.* **2014**, *26*, 3450 – 3459.

(58). Poduval, M. K.; Burrezo, P. M.; Cadaso, J.; Navarrete, Ortiz, R. P.; Kim, T.-H. *Macromolecules* **2013**, *46*, 9220–9230.

Motivation Section

2.1 DONOR-ACCEPTOR CONJUGATED COPOLYMERS INCORPORATING TETRAFLUORO-BENZENE AS THE π - ELECTRON DEFICIENT UNIT

Conjugated polymers are used for a number of technological applications, and they are currently developed as components in organic devices for photovoltaic (OPV) applications.¹⁻⁴ As discussed in the introduction section (paragraph 1.2), the active layer of the most promising OPV devices with bulk-heterojunction architectures is composed of a conjugated polymer, acting as the "donor polymers", in combination with an "acceptor materials", more frequently, a fullerene derivative.

Two categories of conjugated homopolymers have been thoroughly studied in the very early stage of OPV research as "donor polymers": a) soluble, 2,5-dialkoxy-substituted poly(phenylenevinylene)s (PPVs), and: b) poly-3-alkylthiophenes, which were for several time the "workhorses" in photovoltaic applications.⁵⁻⁶ These conjugated homopolymers, which show PCEs of 5-6% after thorough optimization for rrP3HT and 2-3% for PPVs, have non optimal band gaps (≥ 1.9 eV), solar light absorption and morphological properties.

The most important breakthrough in the field of polymer design for bulk heterojunction cells has been the introduction of materials based on the donor-acceptor concept, affording more finely tuned and efficient conjugated donor polymer.⁷⁻⁹ Low-band-gap polymers achievable by alternating of different electron-rich moiety and an electron-deficient moiety lead to important benefit in absorption efficiency, HOMO and LUMO energy levels require to

achieve the ideal conditions, good mobility and morphological properties.

In the context of donor-acceptor conjugated polymers for bulk heterojunction applications, the introduction of fluorine atoms into the skeleton of conjugated polymers is increasingly pursued. The resulting materials have increased thermal and oxidative stability compared to their nonfluorinated counterparts, together with more optimal and decreased bandgaps. In addition to effects on the electronic energy levels, fluorine substitution has an influence on the morphology, promoting specific noncovalent interactions which can yield semicrystalline, more ordered materials, with important consequences related to their electronic performances.¹⁰⁻¹⁷

In this work, we investigate the synthesis and characterization the structures of the new polymers shown in Figure 1, in which the 2,3,5,6-tetrafluorobenzene π -electron deficient unit is combined with two types of π -electron rich units. The polymeric structures are obtained through different synthetic methodologies (Stille, Direct Arylation, and Horner–Wadsworth–Emmons polymerizations), affording direct aryl-aryl linkages between the π -electron deficient and π -electron rich units (**P3** and **P4**), or separating them through a vinylene bridge (**P1** and **P2**).

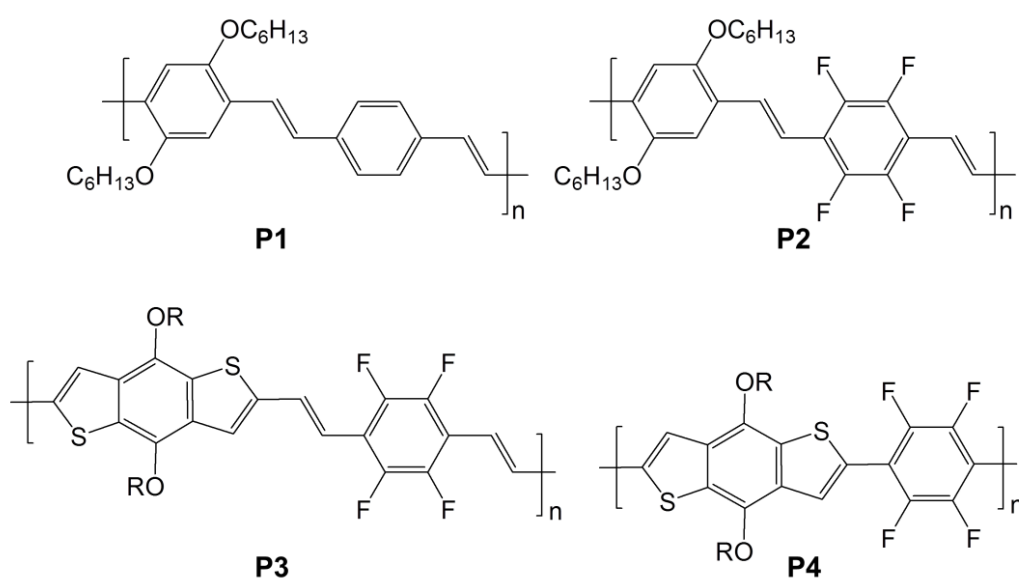


Figure 1. Structures of the polymers synthesized in this work.

2.2 CONJUGATED THIOPHENE-FUSED ISATIN DYES THROUGH INTRAMOLECULAR DIRECT ARYLATION

Organic dyes constitute a large and important class of industrial products. They are generally characterized by good optical absorption and mechanical properties, and by solution processability and stability; these properties are also desirable for solid-state applications, therefore major classes of industrial dyes and pigments (phthalocyanines, naphthalene diimides, diketopyrrolopyrroles, indigos and isoindigos, squaraines) have already found applications in the broad world of organic electronics.¹⁸ In fact, organic dyes such as diketopyrrolopyrrole or naturally-occurring isoindigo, when incorporated in a π -conjugated polymer scaffold, have yielded efficient materials to be used in the field of organic photovoltaics (OPV).¹⁹

Isatin (1*H*-indole-2,3-dione) and its derivatives are synthetically versatile natural dyes, extensively used in organic synthesis. The advances in the use of isatins for organocatalysis, as well as their biological and pharmacological properties, have been recently reviewed.²⁰ Although isatin is the synthetic precursor of isoindigo (Figure 2), its direct incorporation into functional fragments for OPV or organic electronic applications has been far from fully explored.²¹ The isatin skeleton contains formally an amide functionality, linked to the aromatic ring, combined with an electron-withdrawing C3 ketone functionality, *ortho*-linked to the aromatic ring with respect to the amide; it thus possesses a Donor-Acceptor structure giving the compound a bright red color. The C3 ketone possesses orthogonal reactivity with respect with the C2 carbonyl amide, and its derivatization occurs with relative ease.²⁰

Since low-band-gap polymers for OPV are currently engineered by alternating electron-rich and electron-deficient units in order to match and optimize solar photon harvesting,²² suitable isatin derivatives can be ideal monomers. Simple and efficient synthetic pathways, that present a more high "synthetic accessibility", are of the foremost importance in the design

of π -conjugated polymers for OPV, demanding for the removal of synthetic steps requiring stoichiometric organometallic reagents.²³

In this work, we present the design, synthesis and evaluation of a series of fully π -conjugated dyes in which a thiophene ring is fused into the isatin core. The synthesis adopts an intramolecular, direct hetero-arylation (DHA) cyclization protocol as the key step, in order to ensure potential for industrial scalability.^{22,23}

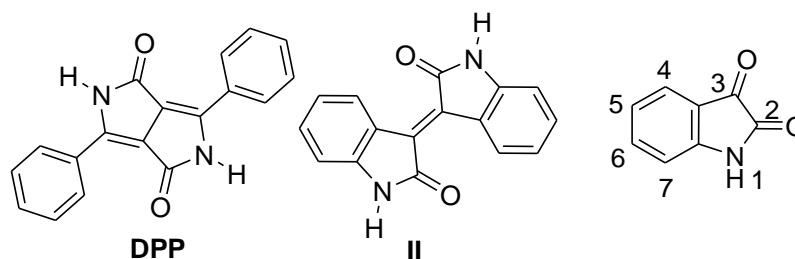


Figure 2. The most popular dyes used for OPV applications (diketopyrrolopyrrole **DPP**, right and Isoindigo **II**, center, and the isatin core structure with numbering).

2.3 ONE POT DIRECT ARYLATION AND CROSS-ALDOL CONDENSATION FOR THE RAPID CONSTRUCTION OF π -EXTENDED THIOPHENE AND FURAN-BASED SCAFFOLDS

Conjugated π -extended organic compounds based on aromatic heterocycles such as thiophene and furan are enjoying a continuously increasing popularity in the organic electronics. Their attractive properties at the molecular, supramolecular and macromolecular level have prompted their use as organic materials in organic photovoltaic cells (OPVs)¹⁻⁴. Incredible efforts have been devoted in recent years towards the development of complex molecular architectures able to afford more and more efficient and tunable monomers, often at the expense of the scalability of the synthetic sequence, as well as its industrial suitability. In fact, the combination of expensive reagents and catalysts, a high number of synthetic steps and chromato-

graphic methods of purification make the large scale synthesis of many of these materials not approachable.²⁴

The development of efficient methodologies for the rapid construction of π -extended organic compounds and polymers is therefore becoming more and more in demand in the field of material science. In this context, crossfertilization from “classical” synthetic organic fields, such as total synthesis, where domino/cascade and/or multicomponent reaction approaches, valorizing atom economy, are often used, can be a powerful strategy.²⁵ Reports about using Pd-catalyzed (Stille or Suzuki) coupling reactions, in sequence with traditional C–C or C–N bond formation methodologies, such as aldol condensation²⁶ or Michael reaction,²⁷ have already appeared in the recent literature. Stille and Suzuki reactions, however, require preactivation of the reacting monomer by the formation of organometallic and halide-substituted derivatives, with intrinsic toxicity considerations to be added, especially for the trialkyltin derivatives used in the Stille protocols.

Direct heteroarylation reactions (DHA) are becoming increasingly popular as Pd-catalyzed carbon-carbon forming methodologies in organic and macromolecular syntheses, since no such preactivation of the starting monomers with organometallic reagents is required, and they are usually regioselective and efficient.²⁸ In fact, it prompted our attention that DHAs are conducted in aprotic polar organic solvents, and need relatively weak bases to function, similarly to cross-aldol reactions, so that multicomponent domino/cascade processes lining up both methodologies could indeed be feasible.²⁹

In this work we report a regioselective and efficient one-pot cross aldol-DHA strategy for construction of fully π -conjugated compounds in which thiophene or furan rings are fused to arene or heteroarene moieties. Two alternative synthetic strategies (presented in Figure 3) have been used, differing from the relative positioning of the aldehyde and the acidic protons involved in the aldol condensation. Instead, the halide atom and the electrophilic portion the α -thiophene or furan carbon atom in the DHA are kept unchanged, as this is reported and

demonstrated to be the best combination in order to ensure high regioselectivity in related systems.³⁰ We also reported our studies regarding the synthetic approach for the synthesis of new DIPID-based monomers.

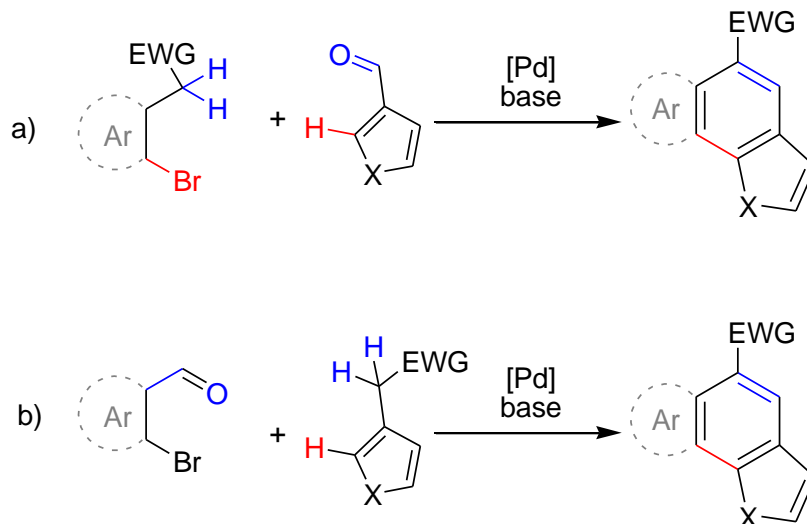


Figure 3. Strategies for cross aldol-DHA cyclization reactions. EWG = Electron-withdrawing group. X = Sulfur or Oxygen.

2.4 ANTHRADITHIOPHENE-BASED AND DIHYDROBENZODITHIOPHENE -BASED MONOMER FOR THE SYNTHESIS OF INNOVATIVE POLYMERS FOR PHOTOVOLTAIC APPLICATIONS

π -Conjugated organic compounds based on extended aromatic systems have attracted considerable attention over the past decade for their potential use as semiconductors in photovoltaic devices.¹⁻⁴ These extended π -conjugation systems feature enforced planarity and more effective π -electron delocalization, which can lead to broader light absorption and improve π - π interactions between polymer chains in thin solid films to enhance the charge carrier mobility.³¹ In addition, the HOMO energy levels of related polymers can be tuned through adjusting the fused aromatic moieties within these polycyclics. The introduction of thiophene

ring in oligoacenes framework led to important benefit such as ease of functionalization and better chemical stability compared to analogue polyacenes without thiophene rings.³²

The most simple extended thiophene-fused π -conjugated system are a benzene nucleus fused with two thiophene rings in thienophenylene framework of benzodithiophene (BDT) shown in figure 4a. The synthetic ease and large-scale production of IBDT and aBDT makes these monomers widely used for the construction of highly-performance polymers.³³

On the other end, thienoacenes (Figure 4) are promising candidates for device applications since their linearly fused benzenoid structures give rise to a substantial increase in conjugation compared to their thienophenylene analogues. NDT1 and QTN (Figure 4) are widely studied when incorporated in polymer due to our easy synthesis.³⁴ Pentacene incorporating thiophene rings into π -extended framework, known as anthradithiophenes (Figure 4), has also been explored, however, there are only a few reported cases due to synthetic difficulties.³⁵

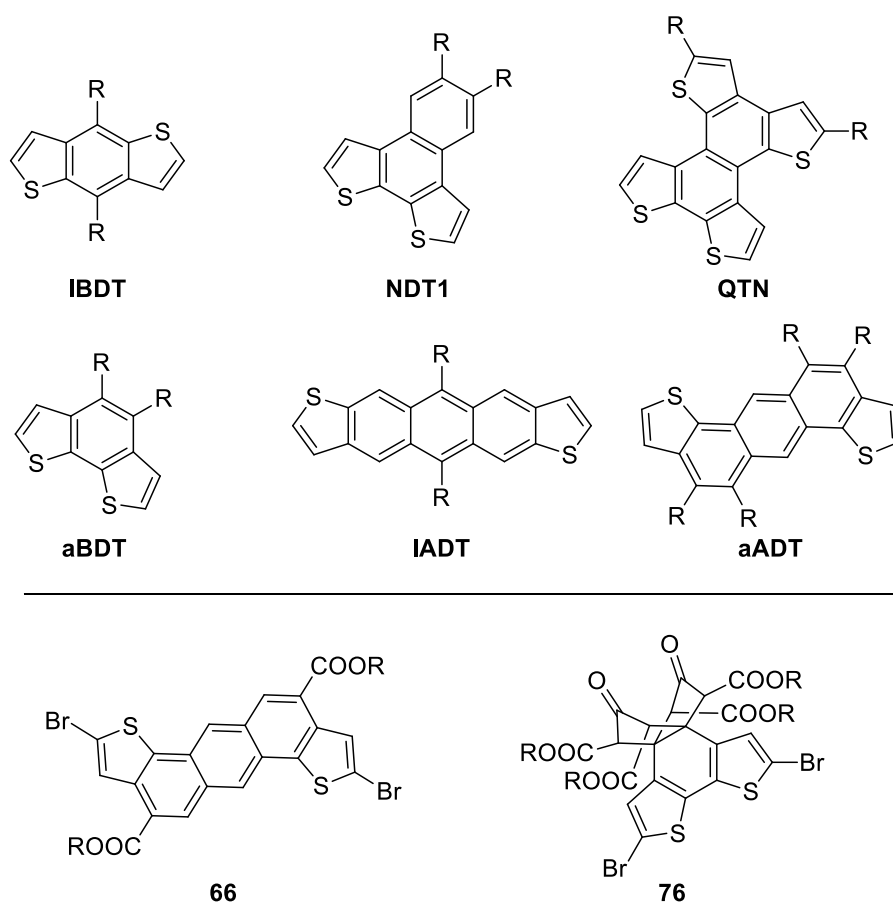


Figure 4. Chemical structure of oligophenylene and oligoacenes donor units.

In this work, we present the design, synthesis and evaluation of a series of novel anthra[1,2-*b*:5,6-*b'*]dithiophene scaffold (**66**), in which carboxylic groups are present in the 4 and 10 positions. The synthesis adopts an one-pot direct arylation and cross-aldol condensation, developed in our laboratories, as key step for construction of aADT framework. We also present our preliminary work on the synthesis of new dihydrobenzodithiophene-based monomer **76**, obtained from benzodithiophenedione through the Weiss reaction. Both these compounds shows interesting properties and could be polymerized with acceptor units already reported in literature.

2.5 REFERENCES

- (1). A. C. Grimsdale, K. L. Chan, R. E. Martin, P. G. Jokisz, A. B. Holmes, *Chem. Rev.* **2009**, *109*, 897-1091.
- (2). L. Dou, J. You, Z. Hong, Z. Xu, G. Li, R. A. Street, Y. Yang, *Adv. Mater.* **2013**, *46*, 6642–6671.
- (3). G. Li, R. Zhu, Y. Yang, *Nat. Photonics* **2012**, *6*, 153-161.
- (4). G. Marzano, C.V. Ciasca, F. Babudri, G. Bianchi, A. Pellegrino, R. Po, G.M. Farinola, *Eur. J. Org. Chem.* **2014**, *30*, 6583-6614.
- (5). B. C. Thompson, J. M. J. Fréchet, *Angew. Chem. Int. Ed.* **2008**, *47*, 58-77.
- (6). For all-polymer photovoltaic cells, see: J. Wang, Y. Yao, S. Dai, X. Zhang, W. Wang, Q. He, L. Han, Y. Lin, X. Zhan, *J. Mater. Chem. A* **2015**, *3*, 13000-13010.
- (7). H. Zhou, L. Yang, W. You, *Macromolecules* **2012**, *45*, 607-632.
- (8). K. Okamoto, J. Zhang, J. B. Housekeeper, S. R. Marder, C. K. Luscombe, *Macromolecules* **2013**, *46*, 8059–8078.
- (9). J. Chen, Y. Cao, *Acc. Chem. Res.* **2009**, *42*, 1709-1718.
- (10). F. Babudri, G. M. Farinola, F. Naso, R. Ragni, *Chem. Commun.* **2007**, *10*, 1003-1022.
- (11). J. E. Carlé, M. Helgesen, N. K. Zawacka, M. V. Madsen, E. Bundgaard, F. C. Krebs, *J. Polym. Sci., Part B: Polym. Phys.* **2014**, *52*, 893–899.
- (12). K. Reichenbacher, H. I. Suss, J. Hulliger, *Chem. Soc. Rev.* **2005**, *34*, 22-30.
- (13). T. L. Nguyen, H. Choi, S.-J. Ko, M. A. Uddin, B. Walker, S. Yum, J.-E. Jeong, M. H. Yun, T. J. Shin, S. Hwang, J. Y. Kim, H. Y. Woo, *Energy Environ. Sci.* **2014**, *7*, 3040–3051.
- (14). Y. Wang, S. R. Parkin, J. Gierschner, M. D. Watson, *Org. Lett.* **2008**, *10*, 3307-3310.
- (15). G. Li, V. Shrotriya, J. Huang, Y. Yao, T. Moriarty, K. Emery, Y. Yang, *Nat. Mater.* **2005**, *4*, 864-868.
- (16). F. Meyer, *Prog. Polym. Sci.* **2015**, *47*, 70–91.

- (17). H. Zhou, L. Yang, A. C. Stuart, S. C. Price, S. Liu, W. You, *Angew. Chem. Int. Ed.* **2011**, *50*, 2995-2998.
- (18). (a) Gsänger, M.; Bialas, D.; Huang, L.; Stolte, M.; Würthner, F. *Adv. Mater.* **2016**, *28*, 3615–3645; (b) Ghazvini Zadeh, E. H.; Tang, S.; Woodward, A. W.; Liu, T.; Bondarc, M. V.; Belfield, K. D. *J. Mater. Chem. C* **2015**, *3*, 8495–8503; (c) Robb, M. J.; Ku, S. Y.; Brunetti, F. G.; Hawker, C. J. *J. Polym. Sci. Polym. Chem. A* **2013**, *51*, 1263–1271; (d) Chevrier, M.; Kesters, J.; Blayo, C.; Richeter, S.; Van der Lee, A.; Coulembier, O.; Surin, M.; Mehdi, A.; Lazzaroni, R.; Evans, R. C.; Maes, W.; Dubois, P.; Clément, S. *Macromol. Chem. Phys.* **2016**, *217*, 445–458; (e) Beverina, L.; Salice, P. *Eur. J. Org. Chem.* **2016**, 1207–1225.
- (19). (a) Qua, S.; Tian, H. *Chem. Commun.* **2012**, *48*, 3039-3051. (b) Wang, E.; Mammo, W.; Andersson, M. R. *Adv. Mater.* **2014**, *26*, 1801–8122. (c) Deng, P.; Zhang, Q. *Polym. Chem.* **2014**, *5*, 3298–3305. (d) Ma, Z. F.; Sun, W. J.; Himmelberger, S.; Vandewal, K.; Tang, Z.; Bergqvist, J.; Salleo, A.; Andreasen, J. W.; Inganäs, O.; Andersson, M. R.; Müller, C.; Zhang, F. L.; Wang, E. *Energy Environ. Sci.* **2014**, *7*, 361–369.
- (20). (a) da Silva, J. F. M.; Garden, S. J.; Pinto, A. C. *J. Braz. Chem. Soc.* **2001**, *12*, 273-324. For selected recent examples of the use of isatin derivatives for organocatalytic reactions, see: (b) Stucchi, M.; Lesma, G.; Meneghetti, F.; Rainoldi, G.; Sacchetti, A.; Silvani, A.; *J. Org. Chem.* **2016**, *81*, 1877–1884 (c) Monari, M.; Montroni, E.; Nitti, A.; Lombardo, M.; Trombini, C.; Quintavalla, A. *Chem. Eur. J.* **2015**, *21*, 11038-11049.
- (21). (a) Wu, J.; Chen, J.; Huang, H.; Li, S.; Wu, H.; Hu, C.; Tang, J.; Zhang, Q. *Macromolecules* **2016**, *49*, 2145–2152; (b) Marchioni, F.; Yang, J.; Walker, W.; Wudl, F. *J. Phys. Chem. B* **2006**, *110*, 22202–22206; (c) Tormos, G. V.; Belmore, K. A.; Cava, M. P. *J. Am. Chem. Soc.* **1993**, *115*, 11512–11515.
- (22). (a) Zhou, H.; Yang, L.; You, W. *Macromolecules* **2012**, *45*, 607–632. (b) Okamoto, K.;

Zhang, J.; Housekeeper, J. B.; Marder, S. R.; Luscombe, C. K. *Macromolecules* **2013**, *46*, 8059–8078; (c) Bundgaard, E.; Krebs, F. C. *Solar Energy Mat. Solar Cells* **2007**, *91*, 954-985.

(23). (a) Po, R.; Bianchi, G.; Carbonera, C.; Pellegrino, A. *Macromolecules* **2015**, *48*, 453-461. (b) Po', R.; Bernardi, A.; Calabrese, A.; Carbonera, C.; Corso, G.; Pellegrino, A. *Energy Environ. Sci.* **2014**, *7*, 925-943. (c) Mercier, L. G.; Leclerc, M. *Acc. Chem. Res.* **2013**, *46*, 1597-1605.

(24) (a) Po, R.; Bianchi, G.; Carbonera, C.; Pellegrino, A.; *Macromolecules* **2015**, *48*, 453-461; (b) Po', R.; Bernardi, A.; Calabrese, A.; Carbonera, C.; Corso, G.; Pellegrino, A.; *Energy Environ. Sci.* **2014**, *7*, 925-943. (c) Boutreault, P. L. T.; Najari, A.; Leclerc, M.; *Chem. Mater.* **2011**, *23*, 456-469.

(25) (a) Nicolaou, K. C.; Edmonds, D. J.; Bulger P. G.; *Angew. Chem. Int. Ed.* **2006**, *45*, 7134–7186. For selected recent example of the use of cascade reactions, see: (b) Rene, O.; Lapointe, D.; Fagnou, K. *Org. Lett.* **2009**, *11*, 4560–4563; (c) Monari, M.; Montroni, E.; Nitti, A.; Lombardo, M.; Trombini, C.; Quintavalla, A *Chem. Eur. J.* **2015**, *21*, 11038-11049.

(26) (a) Choi, Y. L.; Yu, C. M.; Kim, B. T.; Heo, J. N.; *J. Org. Chem.* **2009**, *74*, 3948–3951; (b) Han, W.; Zhou, X.; Yang, S.; Xiang, G.; Cui, B.; Chen, Y. *J. Org. Chem.* **2015**, *80*, 11580–11587.

(27) Mousseau, J. J; Fortier, A.; Charette, A. B. *Org. Lett.* **2010**, *12*, 516–519.

(28) Alberico, D.; Scot, M. E.; Lautens, M. *Chem. Rev.* **2007**, *107*, 174–238.

(29) (a) Dhiman, S.; Pericherla, K.; Nandwana, N. K.; Kumar, D.; Kumar, A. *J. Org. Chem.* **2014**, *79*, 7399-7404. (b) Fu, M.; Lin, D.; Deng, Y.; Zhang, X. Q.; Liu, Y.; Lai, C.; Zeng, W.; *RCS Adv.* **2014**, *4*, 23595-23603. (c) Ruan, J.; Iggo, J. A.; Xiao, J.; *Org. Lett.* **2011**, *13*, 268-

271.

(30) (a) Takeda, D.; Yamashita, M.; Hirano, K.; Satoh, T.; Miura, M. *Chem. Lett.* **2011**, *40*, 1015-1017. (b) Dong, J. J.; Doucet, H.; *Eur. J. Org. Chem.* **2010**, 611–615. (c) Glover, B.; Harvey, K. A.; Liu, B.; Sharp, M. J.; Tymoschenko, M. F.; *Org. Lett.* **2003**, *5*, 301-304.

(31). Coropceanu, V.; Kwon, O.; Wex, B.; Kaafarani, B. R.; Gruhn, N. E.; Durivage, J. C.; Neckers, D. C.; Brédas, J.-L. *Chem. Eur. J.* **2006**, *12*, 2073–2080.

(32). Takimiya, K.; Shinamura, S.; Osaka, I.; Miyazaki, E. *Adv. Mater.* **2011**, *23*, 4347–4370.

(33). (a) Hou, J.; Park, M.-H.; Zhang, S.; Yao, Y.; Chen, L.-M.; Li, J.-H.; Yang, Y. *Macromolecules* **2008**, *41*, 6012 – 6018; (b) Tovar, J. D.; Rose, A.; Swager, T. M. *J. Org. Chem. Soc.* **2002**, *124*, 7762–7769.

(34). (a) Xiao, S.; Zhou, H.; You, W. *Macromolecules* **2008**, *41*, 5688–5696; (b) Xiao, S.; Stuart, A. C.; Liu, S.; Zhou, H.; You, W. *Adv. Funct. Mater.* **2010**, *20*, 635–643.

Discussion of Results

and Conclusions

3.1 DONOR-ACCEPTOR CONJUGATED COPOLYMERS INCORPORATING TETRAFLUORO-BENZENE AS THE π -ELECTRON DEFICIENT UNIT

This paragraph is based on the following publication:

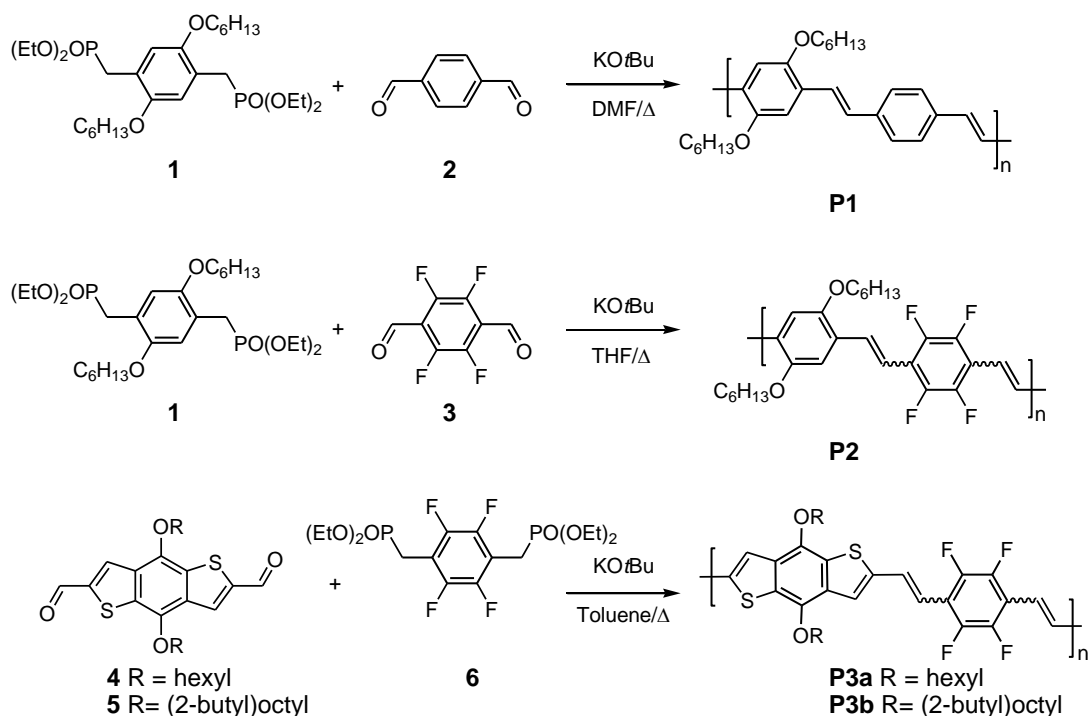
Andrea Nitti, Federico Debattista, Luigi Abbondanza, Gabriele Bianchi, Riccardo Po and Dario Pasini, accepted (*Journal of Polymer Science, Part A: Polymer Chemistry*).

3.1.1 Results and Discussion

Synthesis of modified PPVs. Several approaches for the synthesis of PPV and its processable dialkoxy derivatives have been explored to date; dehydrohalogenation routes (Gilch synthesis) or thermal elimination of sulfonium salt precursor polymers (Wessling route) are the most applied synthetic methodologies, but they suffer from undesirable side reactions which are difficult to control, affording, if carefully controlled conditions are not applied, partial gelation by cross linking or incomplete elimination.¹ A further limitation to both polymerization routes is the fact that perfectly alternating copolymers cannot be prepared. The use of an olefination-based methodology (the Horner-Wadsworth-Emmons HWE reaction) overcomes the mentioned problems, and has been applied for the synthesis of alternating PPVs.²⁻⁵

All the before mentioned polymerization protocols to obtain PPV and derivatives follow typical polycondensation kinetics, with poor control of molecular weight and polydispersities. More recently, routes utilizing the ring opening metathesis polymerization (ROMP) of cyclophanedienes as strained monomers are able to afford PPVs with controlled molecular weights;⁶⁻¹² this strategy can clearly pave the way to the production of block/alternating PPV-like *copolymers*,¹³ and it has refreshed scientific attention towards this class of conjugated polymers. Given the complex synthesis of the strained monomers,¹⁴ particularly promising alternating copolymers for functional applications can be initially scouted by uncontrolled HWE techniques, leaving the fine tuning of the most promising structures using more refined ROMP methodologies to a later stage.

Scheme 1. Synthesis of polymers P1-P3 by HWE polymerization



The monomers required for HWE condensation polymerization, namely the dialdehydes and bisphosphonates shown in Scheme 1, could be prepared by conventional organic synthesis. Benzodithiophene (BDT) derivatives **4** and **5** could be obtained in good yields by double formylation in the a position of the thiophene rings following methods reported in the litera-

ture. The chemical shift of the key aromatic protons in the b-position of the thiophene rings, are identical to those reported in the literature for a longer unbranched alkyl chain derivative (n-dodecyl substituted diformyl BDT, analogous to **4**)¹⁵ and a branched alkyl chain derivative (2-ethylhexyl substituted diformyl BDT, analogous to **5**).¹⁶ This data confirms the accessibility of the p-surfaces and the absence of self-aggregation and p-p stacking independently by the steric hindrance of the O-alkyl substituents.

HWE polymerizations were carried out by the addition of 3 equiv of KOtBu (0.1-0.3 M) as the base to rigorously stoichiometric amounts of phosphonates **1** or **6** and dialdehydes **2-5**

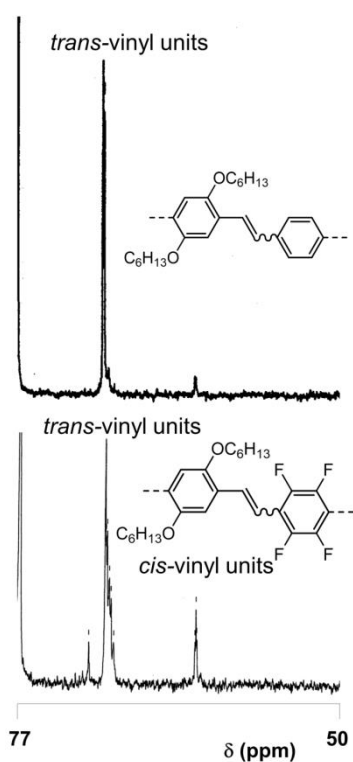


Figure 1. Partial ¹³C NMR spectra (75 MHz, CDCl₃) of polymer **P1** (top), and **P2** (bottom, related to the -OCH₂ carbon resonances of the hexyl chains.

in THF, toluene or DMF, chosen accordingly to the solubility characteristics of the monomer couples. Polymer **P1** was synthesized as a control since it has not been, to our knowledge, previously reported. All polymers were obtained in reasonable yields and as red powders, with virtually no traces of residual, unreacted monomers detectable in the ¹H NMR spectra of the crude reaction mixtures (see Appendix). The polymers were readily soluble in common organic solvents such as chloroform, toluene, THF, and chlorobenzene.

Although HWE polymerization has been reported to afford *trans*-vinylene linkages with high stereochemical control,²⁻⁵ differences in the stereoregularity achieved between polymers **P1** and **P2** were immediately detected by both ¹H and ¹³C NMR spectroscopy. Polymer **P1** could be characterized as being composed of almost exclusively *trans* vinyl units, whereas in polymer **P2** a substantial amount (ca. 30% by ¹H NMR integration of the relevant signals) of *cis* linkages were present. The characterization could take advantage of the fact that alkoxy-substituted PPVs with *cis-trans* alternat-

tion could take advantage of the fact that alkoxy-substituted PPVs with *cis-trans* alternat-

ing configuration of their vinylene linkages have been obtained and characterized by Turner et al using the ROMP synthesis.¹¹ According to their assignments, in polymer **P1**, the resonances associated to the α -CH₂ carbon atoms of the hexyl chains appear as a broad singlet centered at 4.1 ppm, whereas in **P2** a substantial peak at 3.6 ppm appears, corresponding to the α -CH₂ carbon atoms of the hexyl chains neighbouring *cis*-vinylene units. Analysis of the ¹³C NMR spectra confirmed the above stereochemical analysis, with the carbon associated to the α -CH₂ carbon atoms of the hexyl chains being a single resonance in the case of **P1**, whereas two signals are present in the case of **P2** (Figure 1).

A lack of stereochemical definition of the newly generated double bond is suggested also in the ¹H NMR spectra of **P3a**, in which two signals for the resonances associated to the α -CH₂ carbon atoms at 4.1 ppm and 3.4 ppm (see Appendix). In this case, the percentage of stereochemical confusion is higher than in **P2**, reaching ca. 50%. However, this attribution is only tentative as this polymer with *cis-trans* alternating configuration of their vinylene units has not been previously reported.

Molecular weights for these polymers were measured by GPC relative to polystyrene standards eluted by THF. Further GPC analysis were conducted in TCB at high temperatures in order to overcome aggregation phenomena. Polymers had M_n in the range of 4000, corresponding to average degrees of polymerizations of around 10, and with dispersity largely dependent from the purification procedures used for the polymers (Table 1). Very large PDIs could be detected when a nonsolvent could not be found for purification (polymer **P2**, entry 2 in Table 1), and very low when thorough fractionation/soxhlet extraction was extensively performed (entry 4 in Table 1).

The room temperature ¹H NMR spectra of polymer **P3a** and **P3b** in CHCl₃ showed a particularly broad profile indicating aggregation in these solvent at room temperature. It is likely that the higher aggregation tendency of **P3** when compared with **P1** and **P2**, is indicative of the stronger tendency of the *p*-electron deficient fluorinated moiety to stack over the *p*-rich

BDT moiety, both intramolecularly, through the steric constraint imposed by the *cis*-carbon-carbon double bond units, and intermolecularly.

Table 1. Reaction conditions, yields and molecular weight characterization of P1-P3.

Entry	Monomer	Solvent/T(°C) ^a	Yield[%] ^b	M_n	PDI	Polymer
1	1 + 2	DMF/80	40	4000 ^c	1.5 ^c	P1
2	1 + 3	THF/60	69	3200 ^c	9.2 ^c	P2
3	4 + 6	Toluene/110	77	4200 ^c	2.9 ^c	P3a
4	5 + 6	Toluene/110	59	3900 ^d	1.2 ^d	P3b

^a Dry solvents were used. ^b After purification by precipitation, liquid-liquid extraction and/or soxhlet extraction, as described in the experimental section. ^c As determined by GPC method a (THF as the mobile phase, 40°C). ^d As determined by GPC method b (trichlorobenzene as the mobile phase, 90°C).

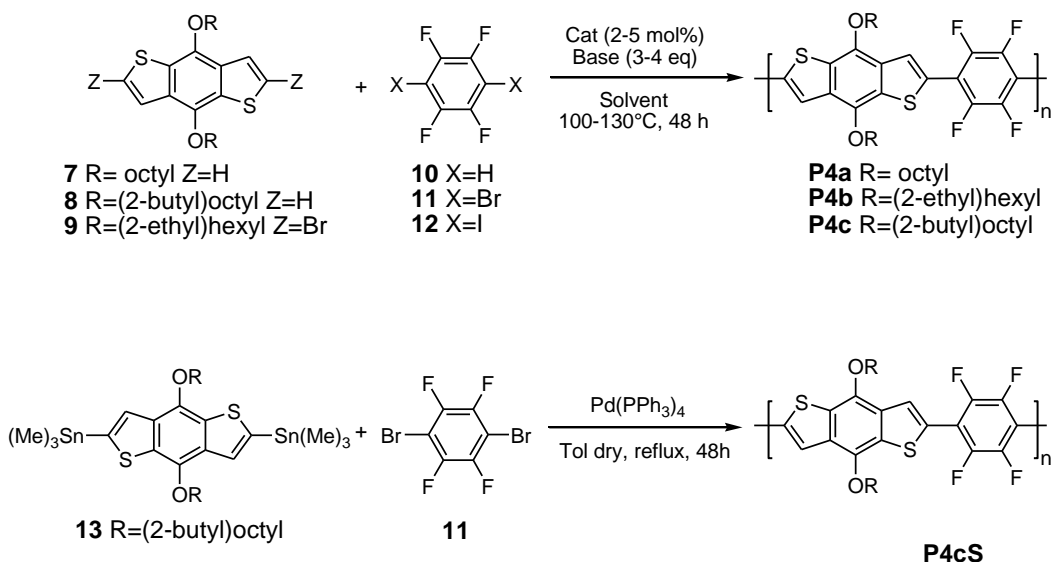
Synthesis and Polymerization of Alternating BDT-tetrafluorobenzene Polymers by Stille and DHAP. We compare the previous results obtained through HWE with analogous donor-acceptor conjugated polymeric structures obtained through Stille Polymerization (SP) and Direct Arylation Polymerization (DHAP) using suitable 1,2,4,5-tetrafluorobenzene derivatives. The latter method is particularly envisaged in the light of possible process scale-up, and of the potential toxicity of the stannane functionalized monomers and the stannane by-products obtained using the SP. A sensible reduction of synthetic steps is envisaged using DHAP *vs* SP.

Conjugated polymers containing aromatic fluorinated substrates have been synthesized via DHAP, including 1,2,4,5-tetrafluorobenzene, and 5,6-difluoro-2,1,3-benzothiadiazole.¹⁸⁻²² These examples however apply to systems where the fluorinated substrate is the only significant acidic proton. Most donor units, including BDT derivatives, possess thiophene rings, which, like fluorinated benzenes, have aromatic protons suitable for C-H activation. Thompson *et al.*¹⁷ have recently approached this problem and reported a screening of direct arylation conditions on a model small molecule system (a 2-substituted thiophene and a pentafluoro-

benzene), to develop suitable conditions for the direct arylation polymerization (DHAP) of fluorinated copolymers. Optimal functionalization for direct arylation has been found by reacting a thiophene-based halogenated donor and an unfunctionalized highly fluorinated acceptor, which is opposite of typical cross coupling reactions, where the acceptor is typically halogenated. Recently, Marzano *at al.* have reported successful DHAP reaction by activation of the C-H bond on the benzobisthiophene with halogenated benzothiadiazole and benzotriazole as acceptor unit.^{18, 19}

Our results using the substituted BDT and tetrafluorobenzene couples are illustrated in Scheme 2.

Scheme 2. Synthesis of polymers P4 by DHAP and SP



DHAPs were carried out (excluding entry 2 in Table 2 where the more active Pd₂(dba)₃ catalyst was used) using Pd(OAc)₂, acetates or carbonates as bases, to rigorously stoichiometric amounts of monomer couples in Toluene or DMF (0.1 M), chosen according to the solubility characteristics of the monomer couples. These conditions were previously reported by some of us to give excellent yields and polydispersities in the DHAPs of Donor/Acceptor monomer couples.²⁵ SP was conducted with the halogenated acceptor and tinylated BDT donor as these were the optimal reported conditions.²⁰⁻²⁴ All polymer samples were thoroughly purified by precipitation and Soxhlet cycles. *M_n* of the polymers obtained were somewhat dis-

appointing in all cases (Table 2).

Table 2. Reaction conditions and yields for DHAP and SP obtaining polymers 4

Entry	Monomer	Solvent/Base/T(°C) ^a	Yield[%] ^b	M_n^c	\bar{D}^c	Polymer
1	7 + 12	DMA/KOAc/100	81	low	1.1	P4a
2 ^d	9 + 10	Toluene/K ₂ CO ₃ /130	60	1600	1.6	P4b
3	8 + 12	Toluene/CsOAc/100	n.d.	1100	2.6	P4c
4 ^e	13 + 11	Toluene/110	42	4100	1.4	P4cS

^a Dry solvents were used. ^b After purification by precipitation, liquid-liquid extraction and/or soxhlet extraction, as described in the experimental section. ^c As determined by GPC method b (trichlorobenzene as the mobile phase, 90°C). ^d Run with Pd₂(dba)₃ instead of Pd(OAc)₂ as the catalyst. ^e Run with Pd(PPh₃)₄ as the catalyst.

NMR, Thermal and Theoretical Characterization. Even in the presence of low degree of polymerizations, ¹H NMR spectra showed broad signals (especially in the aromatic region), and the absence of any residual monomers in the purified polymer samples. Substantial differences could be found in comparing the spectra of **P4a** vs. **P4b** or **P4cS**, with the former showing a much sharper profile, and peaks which could be attributed to a BDT dimer, obtained in high yields presumably through an undesired homocoupling activated by Pd(II) through the acidic α -thiophene positions (Figure A1). This is to be attributed to a lack of selectivity in the course of the DHAP. The ¹H NMR spectrum of polymer **P4b**, instead, show a pattern much more similar to the SP product **P4cS**. The cleaner polymerization in the case of **P4b** strengthens Thompson's indication¹⁷ about the use thiophene-based donor and an unfunctionalized fluorinated acceptor for DHAPs.

The optical bandgaps (calculated on the basis of the onset of the λ_{max} of their UV/Vis spectra in CHCl₃ solutions, see Figure A2) of selected polymers were as follows: 2.3 eV for **P2**, 2.2 eV for **P4cS** and 1.9 eV for **P3b**. The thermal stability of **P4b**, obtained by DHAP, is very good and up to 350°C (Figure A3).

Given the clear indication about self-aggregation of the macromolecular structures by the GPC and NMR results, we set out to investigate this phenomena computationally. We calcu-

lated the self-interaction surface energies of the monomeric and dimeric repeating units for polymers **P1-P4**, plotted by increasing the numbers of stacked units. The energy variation is calculated as the difference between the energy in the gas phase, and energy of the units inserted into the stacked aggregate (Figures A5-A8). In order to highlight how the chemical nature of the molecule influences the supramolecular packing, the energy differences were normalized according to surfaces of the molecular structures.

Figure 2 (left) shows dimer units (of the repeating unit) of the polymer synthesized are compared with dimeric unit of rrP3HT as reference, while on the right monomeric units (repeating units) of the polymer synthesized are compared with 3-hexylthiophene (HT). In the case of monomers, results were also compared with the modelled structures of **P3H** and **P4H**, possessing the structures of **P3** and **P4** repeating units, respectively, but bearing hydrogen atoms instead of fluorine. In Figure A4, for a comparison, normalization according to surfaces of the molecular structures was not carried out.

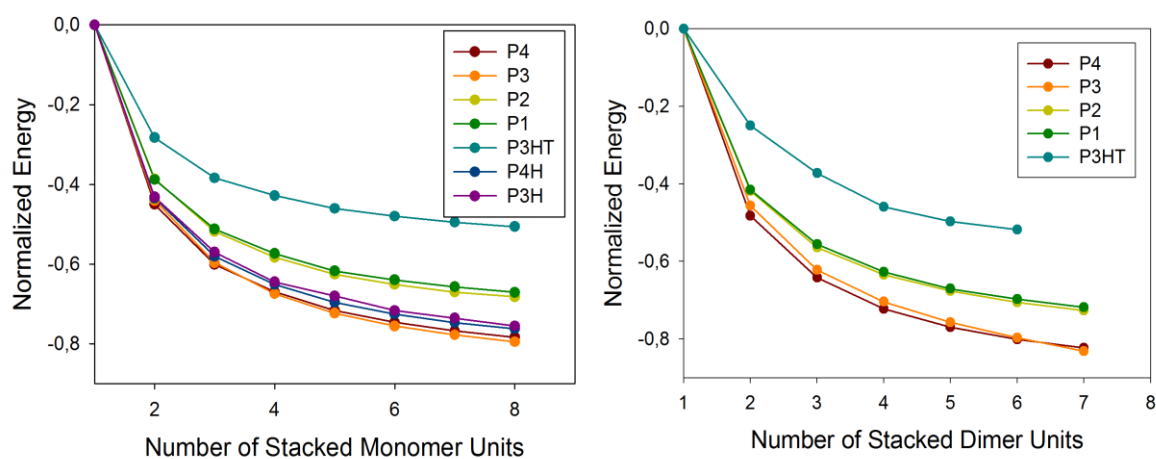


Figure 2. Self-interaction surface energies, normalized by surface unit, of the number n of units in ordered arrangement.

It is evident how all polymers synthesized in this work show stronger self-interaction energies than to the self-interaction energy of rrP3HT, to confirm aggregation interactions ob-

servables by GPC and NMR experiments. **P3** and **P4**, incorporating the BDT donor unit, are by far the most aggregating of the lot, so that BDT is much more efficient in interacting by stacking with the acceptor units. The introduction of fluorination in the monomeric unit (**P3** and **P4**) slightly increase the aggregation interactions than calculated monomeric unit with benzene portions (**P3H** and **P4H**).

The polymers **P1-4** with donor-acceptor architecture have an electronic distribution on carbon frameworks in which the HOMO orbital is placed on the electron-rich moiety of the monomeric unit, while the LUMO orbital is placed on the electron-poor moiety of the monomeric units (Figure 3). The HOMO orbitals are always localized on the electron-rich moiety 2,5-dialkoxybenzene units (polymers **P1** and **P2**) and BDT units (polymers **P3** and **P4**).

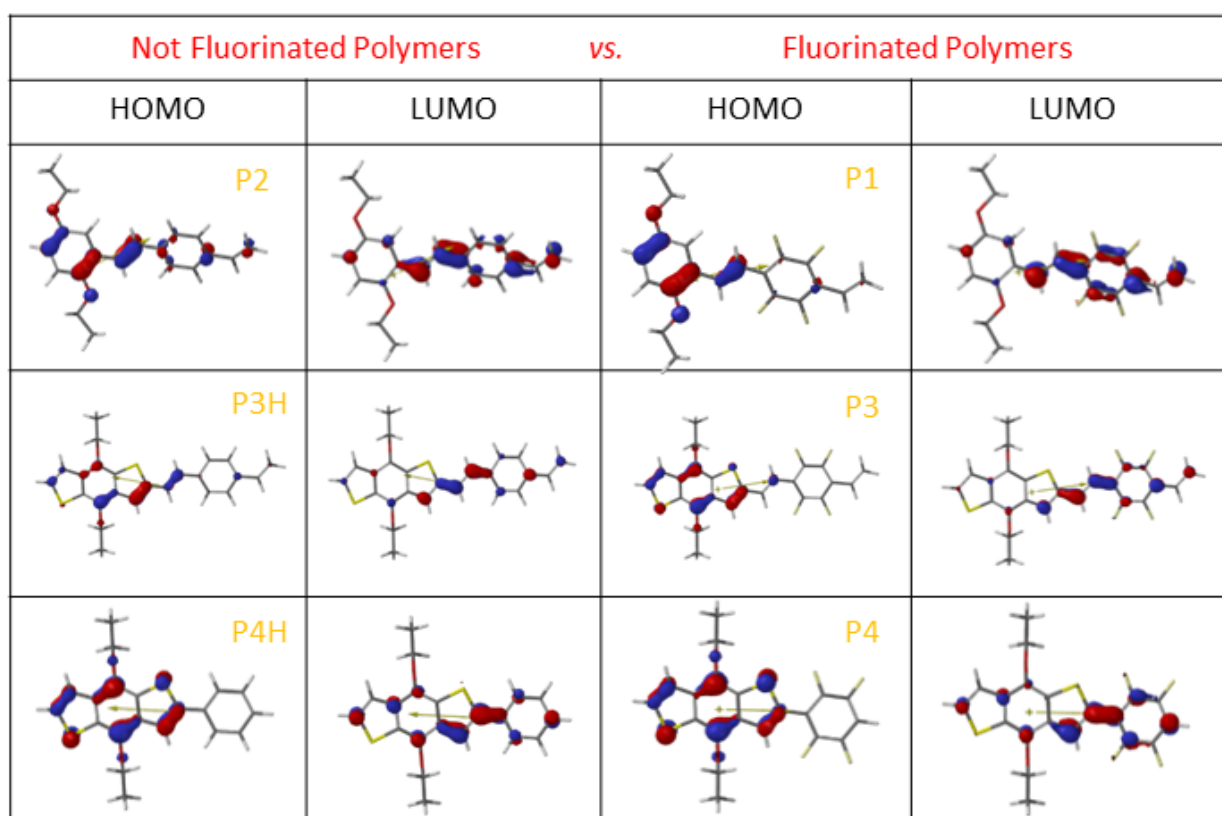


Figure 3. Calculated HOMO and LUMO levels of polymers **P1-P4**, and for analogues **P3H** and **P4H**. Structures are orderly arranged according to fluorine substitution (from left to right in the same row), and insertion of vinylene bridges (from top to bottom in the same column).

The analysis of the LUMO orbitals is more complex and requires a separate discussion for each case. In polymer **P1**, the LUMO distribution density show a low probability on the benzene moiety, which is in a quinoid form, and a high density of probability on vinylene bridge. In fluorinated polymer **P2**, the LUMO distribution shows an important density of probability on the tetrafluorobenzene moiety, which is in a quinoid form. This observation suggests an increased acceptor ability of the tetrafluorobenzene moiety of the polymer **P2** when compared to the benzene moiety of the polymer **P1**. In polymers **P3** and **P3H** the LUMO orbitals are prevalently localized on the vinylene bridge. The presence of fluorine atoms does not influence the acceptor ability of the benzene ring when it is linked with a BDT donor moiety. In polymers **P4** and **P4H**, instead, the LUMO orbitals are prevalently localized on the aryl-aryl bond linking the BDT donor unit with the benzene ring.

3.1.2 Conclusions

We have reported on the introduction of simple, symmetric and highly fluorinated aromatic moieties as electron poor components in π -conjugated polymers for BHJ using by several polymerization techniques. HWE gives stereoirregular polymers, perhaps a consequence of the high tendency of π -stacking of the fluorinated moieties over the π -rich units. Our results using DHAPs confirm the need to place the acidic CH on the fluorine units in the monomer design, substantially confirming what previously reported.¹⁷ In both cases, the tendency to aggregation, evident by NMR spectroscopy and fully substantiated by calculations, is probably detrimental for the achievement of high degrees of polymerization. The polymers have however interesting HOMO-LUMO gaps. In the light of the possibility to use oligomer molecules for photovoltaics, which overcome shortcomings of both vapor-deposited small molecules and solution processed polymers,²⁶ these structures can represent, once thorough optimization of the polymerization methodology has been successfully carried out, promising alternatives for state-of-the-art organic photovoltaics.

3.2 CONJUGATED THIOPHENE-FUSED ISATIN DYES THROUGH INTRAMOLECULAR DIRECT ARYLATION

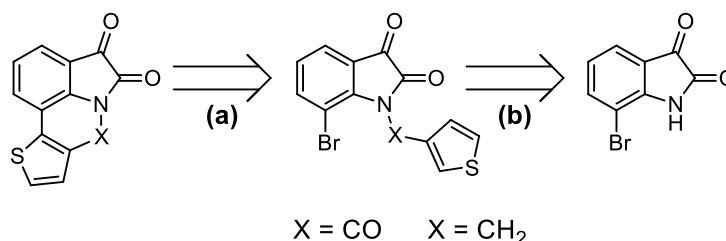
This paragraph is based on following publication:

Nitti, A.; Signorile, M.; Boiocchi, M.; Bianchi, G.; Po, R.; Pasini, D. *J. Org. Chem.* **2016**, *81*, 11035–11042.

3.2.1 Results and Discussions

Molecular Design and Synthesis. Our retrosynthetic analysis is presented in Scheme 3. It develops starting from commercially-available 7-bromoisatin, possessing a bromine atom at a suitable position for intramolecular DHA reaction, forming a stable six-membered ring system. The introduction of the thiophene moiety (step b in Scheme 3) takes advantage of the amide nitrogen at position 1, which has been reported to be acylated²⁷ or alkylated.²⁸

Scheme 3. Retrosynthetic analysis for the synthesis of target dyes

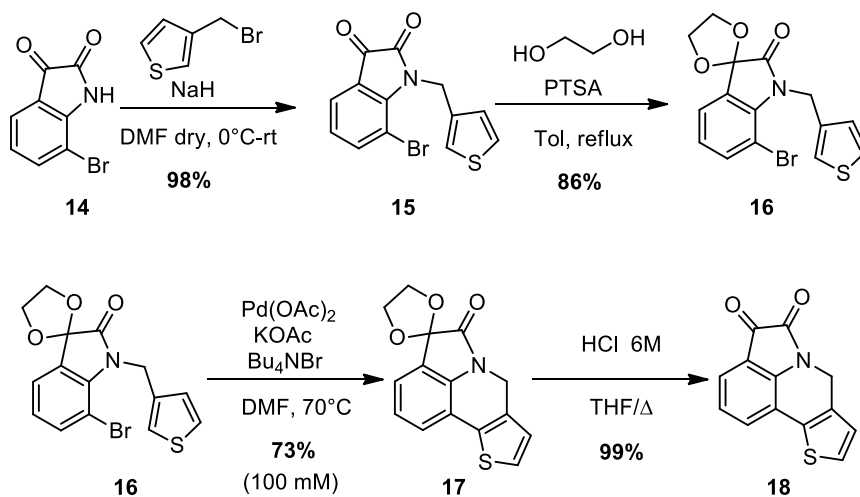


Regarding the acylation approach, the reaction between 7-bromoisatin and 3-thiophenecarbonyl chloride was explored under several conditions, by changing the nature of the reaction solvent and base and adapting protocols reported in the literature,²⁷ but in all cases the conversion of the isatin starting material was minimal (see Appendix).

We thus turned our attention to the *N*-alkylation of 7-bromoisatin **14** with 3-bromomethylthiophene (Scheme 4).²⁸ The reaction was successfully carried out in the presence of NaH in dry DMF at 0°C to give compound **15** in excellent yields (98%). *N*-alkyl isatin derivative **15** was then protected on C-3 keto-carbonyl group with ethylene glycol to give *spi*-

ro-dioxolane **16** (86% yield). The key DHA ring closing reaction was carried out in the presence of Pd(OAc)₂ as catalyst, an excess of potassium acetate as base and in moderate dilution conditions (100 mM for reagent **16** in dry DMF). The desired compound **17** was isolated after purification by flash chromatography in good yields (73%). The reaction was also carried out under substantially different dilution conditions (10 mM), but yields were essentially the same. Finally, deprotection under acidic conditions, and purification by flash chromatography afforded isatin-based dye **18** as a red solid (Scheme 4). The protection at the C3 carbonyl was adopted since similar substrates were identically protected before DHA reaction using Palladium as the catalyst.²⁹ Avoiding the protection/deprotection steps would advantageously lower the number of synthetic steps and raise the total yield of the final compound; however, the DHA ring closing protocol, successfully applied on protected compound **16**, did not work at all when attempted directly on compound **15**. Presumably, since all starting material was recovered, the oxophilicity of the Pd(II) catalyst, which can coordinate to the C2 and C3 neighboring carbonyls was detrimental in this case. We also attempted recently reported³⁰ organocatalytic DHA reaction protocols (*o*-phenantroline, *t*-BuOK), for the ring closing reaction of **15** to afford directly **18**, but in this case degradation of the isatin lactam ring could be detected.³¹

Scheme 4. Synthesis of Thiophene-Fused Isatin Dye **18**

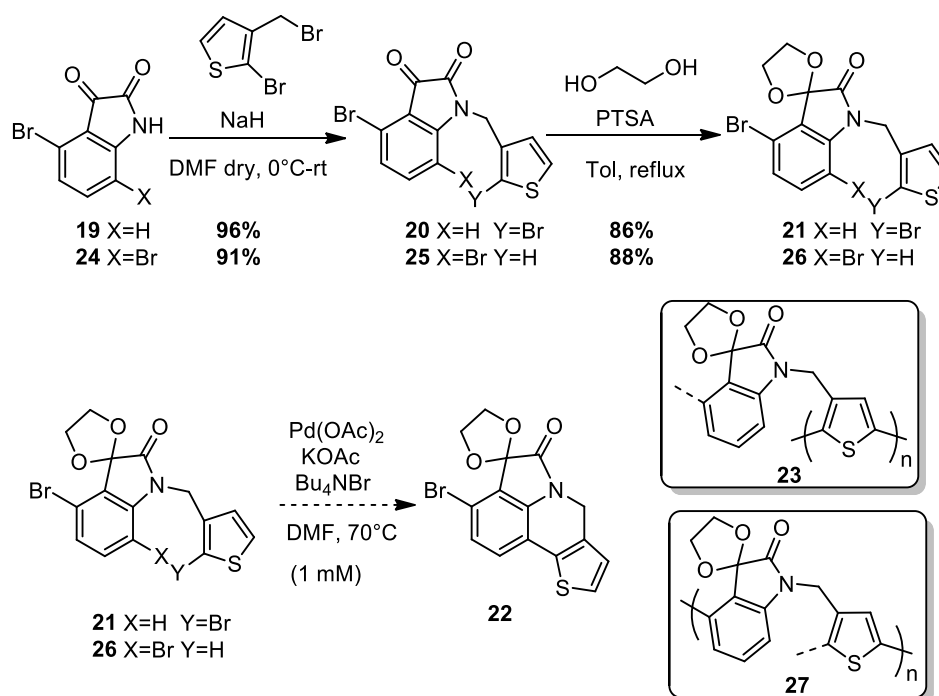


Encouraged by the successful synthetic route presented in Scheme 4, we aimed at obtain-

ing fused substrates presenting a bromine atom at position 4 of the isatin core. Compound **22** (Scheme 5), presenting a nucleophilic (the carbon linked to the bromine atom) and an electrophilic (the α -carbon on the thiophene residue) site on the same molecule, could be an interesting monomer to be polymerized or copolymerized head to tail using a DHA protocols. The *spiro*-dioxolane protecting group, with its quaternary carbon atom, could be advantageous in solubilizing the growing polymer chains, preventing π -stacking, aggregation and precipitation from the reaction mixture.³²

Our first approach to compound **22** was elaborated by implementing the use of commercially available 4-bromo-1*H*-indole-2,3-dione **19** (Scheme 5). We envisaged it could be possible, by utilizing high dilution reaction conditions, to activate a regioselective intramolecular DHA between position 7 of the isatin core and the position 2 of the thiophene ring.

Scheme 5. Attempted synthesis of DHA polymerizable monomer **22, and probable structures of the obtained polymers **23** and **27****

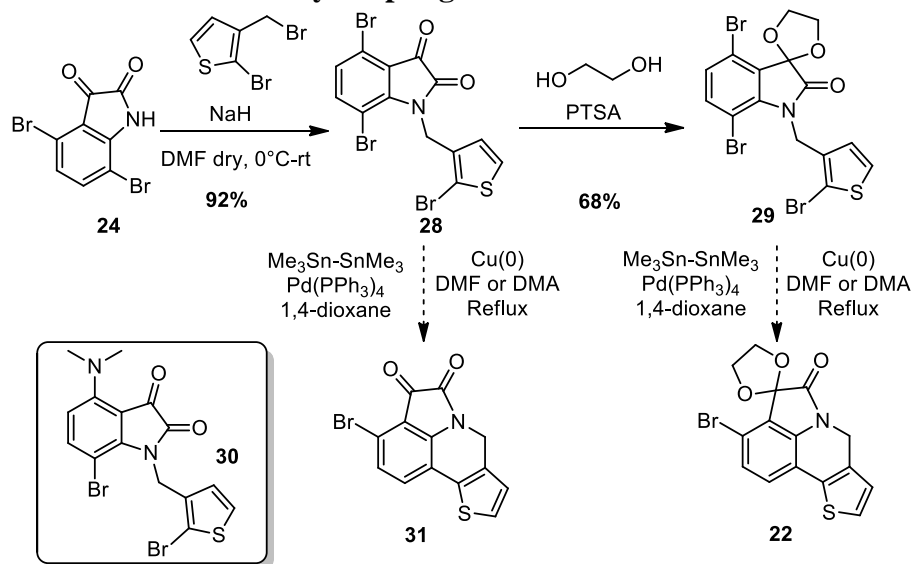


4-Bromo-1*H*-indole-2,3-dione **19** was alkylated with 2-bromo-3-bromomethylthiophene under conditions identical to those used for **15**, to give compound **20** in excellent yields (96%). Protection with ethylene glycol gave *spiro*-dioxolane **21** (86% yield), but the key in-

tramolecular DHA ring closing reaction, attempted in high dilution conditions, did not yield the desired compound **22**, but rather an insoluble oligomeric or polymeric baseline red material. Since intermediate **21** presents a thiophene ring with α positions orthogonally reactive in the DHA reaction, a plausible hypothesis provides for a polythiophene-type structure **23** (boxed in Scheme 5) of the polymer formed. The negligible but probably not suppressed reactivity of the isatin carbon atom in position 4, linked to the bromine, in the carbon-carbon bond formation with DHA, result in the crosslinking of the structure, and in the resulting insolubility properties.

We pursued a further possibility to obtain **22**, in which both bromine atoms (the one needed for the intramolecular DHA ring closing step, and the one to be remaining in the final product for subsequent polymerization), are placed on the isatin core. Derivative **24** is not commercial available and was synthesized starting from 2,5-dibromoaniline following a general reported procedure for isatins.³³

Scheme 6. Attempted synthesis of DHA Polymerizable monomer 22 and 31 through Ullmann or Stille/Kelly coupling

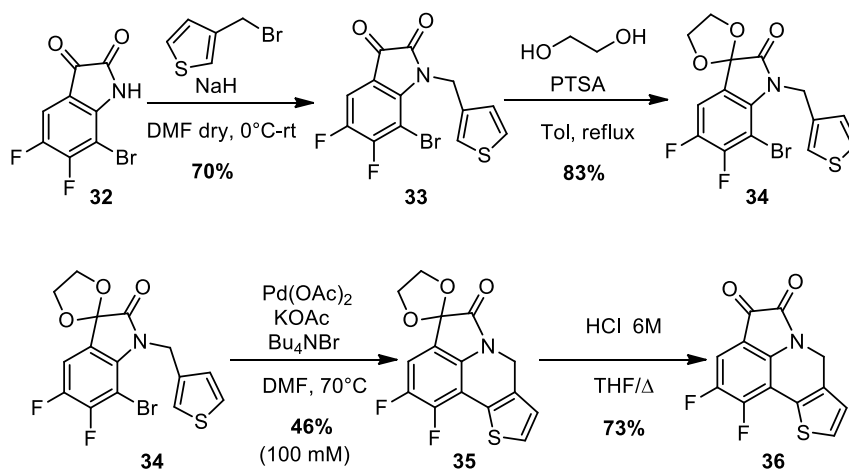


Alkylation with 3-bromomethylthiophene, to afford compound **25** (91% yield), and protection, for compound **26** (88% yield), went smoothly as before, but again the key intramolecular DHA ring closing reaction, attempted in high dilution conditions, did not yield even trace

amounts of the desired compound **22** (Scheme 5). Also in this case an insoluble oligomeric or polymeric baseline red material was formed; it is likely in this case that the nucleophilic character of the bromine in position 4 is much higher than of the one in position 7 of the isatin core, so that intermolecular DHA reaction, on either of the α -carbons of the appended thiophene residue is competitive with the intramolecular DHA ring closing, thus affording cross-linking and intractability of the resulting material.

An indirect proof of the higher reactivity as a nucleophile in metal-catalyzed cross-coupling reactions of the carbon atom at the 4-position with respect to the 7-position is reinforced by the results illustrated in Scheme 6, where further attempts were made by synthesizing derivatives with three bromine atoms, in order to develop Ulmann³⁴ or Stille-Kelly³⁵ ring closing strategies. However, when attempted on compounds **28** or **29**, both methodologies failed to give the desired, cyclized dyes **22** or **31**. Interestingly, when the Ulmann protocol was adopted on compound **28** in the presence of solvents such as DMF or DMA, derivative **30**, in which a dimethylamino group has *regioselectively* substituted the bromine atom in position 4, was obtained in high yields. Both compounds **28** and **30** have been characterized by X-ray crystallography, and their crystal data, plots showing thermal ellipsoids and crystallographic details are reported in the Appendix.

Scheme 7. Completion of the synthesis of thiophene-fused isatin-based dye **36**



Held by the success of the DHA route presented in Scheme 7, we set out to demonstrate

its feasibility with other isatin derivatives. In particular, we considered isatin **32**, bearing two fluorinated atoms on the aromatic ring, for two reasons: a) the availability of the precursor 2-bromo-3,4-difluoroaniline for its synthesis³³; b) the fact that the aromatic ring has only one aromatic hydrogen, possibly allowing a selective late stage further introduction of a bromine atom through electrophilic aromatic substitution once dye **36** has been synthesized (Scheme 7). Indeed, alkylation, protection, intramolecular DHA and deprotection occurred smoothly, to generate dye **36**, although in sensibly reduced yields when compared to **18**. Attempts to use Pd(0) sources, namely by employing Pd₂(dba)₃, resulted in negligible yields of the desired compound, probably because of the increased steric hindrance around the Pd catalytic center.

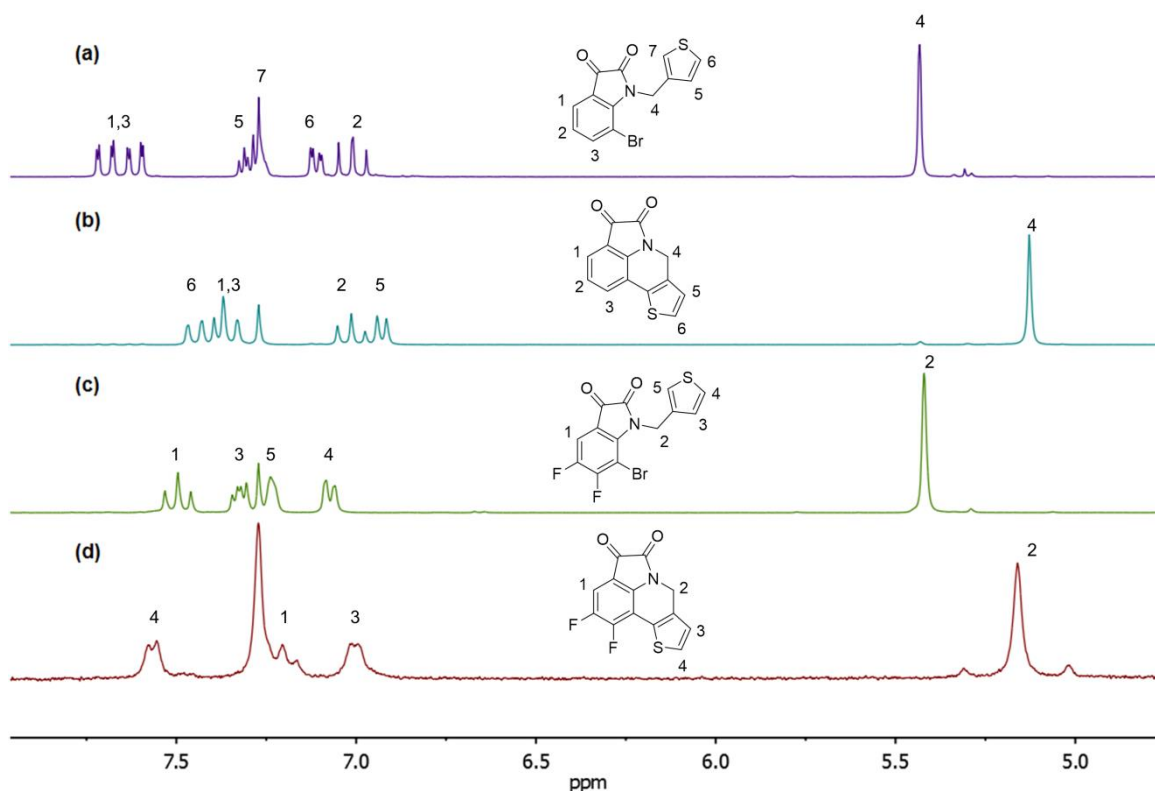


Figure 4. Stacked ¹H-NMR spectra (200 MHz, CDCl₃) of compounds: (a) **15**, (b) **18**, (c) **33** and (d) **36**.

NMR, UV/Vis and Cyclic Voltammetry. Characterization by ¹H NMR spectroscopy was able to substantiate the interaction between the thiophene and isatin moieties, placed in direct conjugation. We report in Figure 4 a comparison between the ¹H NMR spectra of com-

pounds **15** and **18** on one side, and **33** and **36** on the other. In both cases, peaks related to the isatin core in **15** and **33** above 7.5 ppm, markedly shift to higher fields in **18** and **36**, probably also as a consequence of the loss of the bromine atom as a substituent on the aromatic ring. Peaks of the thiophene moieties (labelled 5 and 6 for compounds **15** and **18**, 3 and 4 for compounds **33** and **36**) shift in opposite directions upon ring closure. A large shift upon cyclization is also detected for the benzylic CH₂ proton resonances (labelled 4 for compounds **15** and **18**, 3 and 2 for compounds **33** and **36**) demonstrating an effective charge transfer and cross-talking between the moieties within the fully π -conjugated molecular structure.

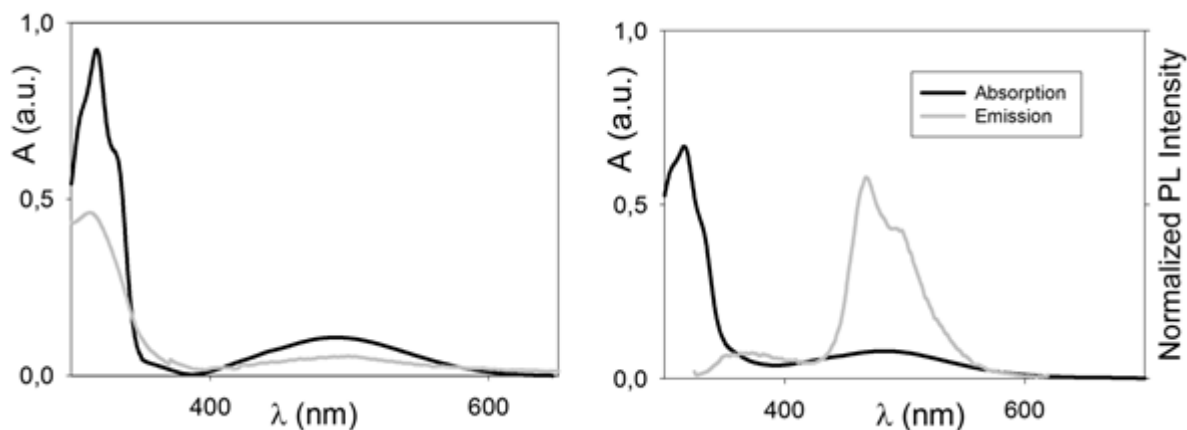


Figure 5. Left: UV/Vis spectra 10^{-4} M in CHCl_3 of compounds **18** (black line) and **36** (grey line). Right: absorption and emission spectra ($\lambda_{\text{ex}} = 318$ nm) of compound **18** ($5 \cdot 10^{-5}$ M in MeCN).

Such cross talking is also evidenced by the UV/Vis spectra of compounds **18** and **36** (Figure 3, left). Whereas the λ_{max} is centered around 320 nm ($\epsilon = 4000\text{-}9000 \text{ M}^{-1}\text{cm}^{-1}$ in CHCl_3), a weaker intramolecular charge transfer band centered around 490 nm is detected in both compounds ($\epsilon = 600\text{-}1000 \text{ M}^{-1}\text{cm}^{-1}$ in CHCl_3). The latter band showed solvent dependence in the case of compound **18** (the maximum shifting from 490 nm in CHCl_3 to 478 nm in toluene, see Figure A9). Compound **18** demonstrated to be weakly emissive (Figure 2, right) when excited at 318 nm, and nonemissive when excited on the charge-transfer band at 480 nm.

Data for the HOMO-LUMO gaps of the final compounds **18** and **36**, could be determined both by optical and electrochemical methods, and they are compared with isoindigo (**II**) and diketopyrrolopyrrole (DPP), for which literature data are available (Table 3). The effect of the introduction of the fluorine substituents is to lower both HOMO and LUMO levels, thus maintaining the band gap at 2.1 eV. For both compounds **18** and **36**, the reduction peak is reversible, whereas it is not reversible in the oxidation mode, indicating that the compound does not polymerize electrochemically, even by lowering the scan rate from 200 mV/s to 20 mV/s. A slight shift of the cathode potential is observed upon successive reduction cycles.

Table 3. Experimental values for semiconducting properties of the new dyes synthesized, and comparison with literature values of relevant compounds

Compound	HOMO-LUMO gap (eV) CV	HOMO-LUMO gap (eV) opti-cal	HOMO (eV)	LUMO (eV)
DPP ^a	2.1	2.1	-5.4	-3.3
II ^b	2.8	2.5	-5.9	-3.1
18 ^c	2.1 ^d	2.1	-5.6	-3.5
36 ^c	2.1 ^d	2.1	-5.8	-3.7

^a Data taken from ref. 36. ^b Data taken from ref. 37. UV/Vis and CV spectra are shown in Figures A9 and A10, respectively. ^d HOMO-LUMO values obtained by the analysis of the first cycle.

X-ray crystal structure of 18. The dye **18** originates in the solid state two polymorphs: the **18_1** crystal, triclinic, and the **18_2** crystal, monoclinic. In both crystals the asymmetric units contain two very similar but crystallographically-independent molecules of **18**; all of them are essentially planar. Plots showing thermal ellipsoids are drawn in Figure A11, and relevant bond distances in each independent molecule **18** are reported in Table A3.

The bond distances for the thiophene moiety change slightly but significantly upon fusion with the isatin core with respect to those observed in the isolated system. In all molecular structures **18**, the *sp*² thiophene carbon atoms directly connected to the isatin groups originate thiophene C-C and C-S bonds significantly longer (by 0.02-0.05 Å) than the symmetrically

placed C-C and C-S bonds, linked with CH groups. All bonds are significantly different than those in isolated thiophene.³⁸ A transfer of electron density towards the C-C bonds connecting the thiophene rings and the isatin aromatic groups is also evident by their shortening (1.451 for **18_1** and 1.457 Å for **18_2**) with respect to a $C_{sp^2}-C_{Ar}$ single bond (1.470 Å) observed in related structures.³⁸

In the solid state the two polymorphs of compound **18** differ in the dihedral angle between the two independent molecules forming the crystal: in **18_1**, the dihedral angle between the two independent polycyclic compounds is 21°, whereas in **18_2** the dihedral angle is 89°. In the **18_1** crystal, the two independent molecules originate two face-to-face π -stacked molecular rows extending along the direction of the *a* crystallographic axis. Each row is made by centrosymmetrically related molecules, as shown in Figure 6.

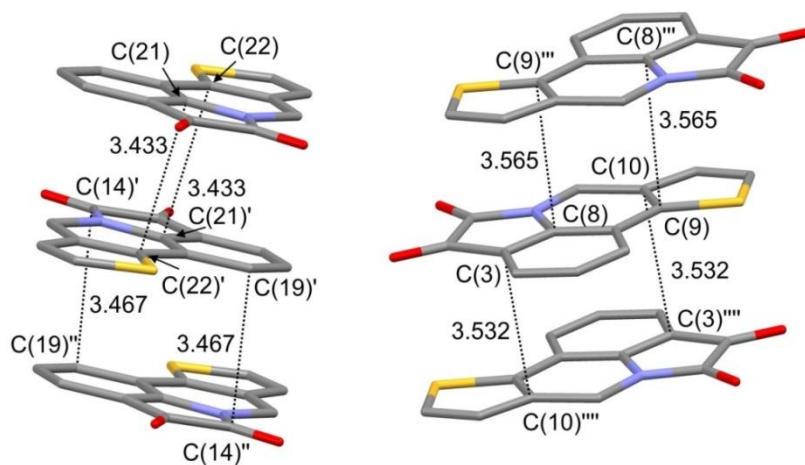


Figure 6. A simplified sketch of the molecular rows made by face-to-face π -stacked molecules in the **18_1** crystal. The shortest intermolecular contacts are drawn with dashed lines (values are in Å). H-atoms are omitted for clarity.

The stacked molecules are placed on overlying planes having interplanar distances in the range 3.41-3.56 Å. Molecular rows are kept together by weak non-conventional C-H \cdots O interactions involving the CH group of the thiophene unit linked to the Sulphur atom (H-donor)

and one Oxygen atom of isatin (H-acceptor) of adjacent molecules of **18**. Features of these interactions are shown in Figure A12.

In the **18_2** crystal, the two independent molecules of the polycyclic compound originate two molecular rows already characterized by face-to-face π -stacking interactions: the stacked molecules are placed on overlying planes having interplanar distances of 3.31 and 3.32 Å. However, the stacked units along the two independent molecular rows are the pentagonal rings of the polycyclic compound **18**, i.e. the thiophene group and the pyrrole subunit of the isatin group. In particular, as shown in Figure 7, each molecule has the pyrrole subunit placed above the thiophene group of a symmetrically equivalent molecule placed in the underlying plane, whereas it has the thiophene group placed below the pyrrole subunit of a symmetrically equivalent molecule placed in the overlying plane.

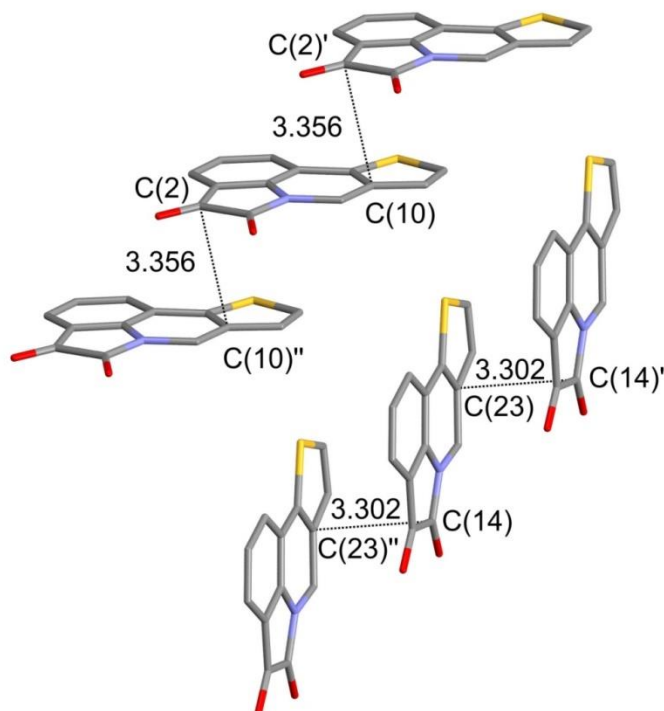


Figure 7. A simplified sketch of the molecular rows made by face-to-face π -stacked molecules in the **18_2** crystal. H-Atoms were omitted for clarity.

The molecular offset promotes the formation of zigzag like molecular rows extending along the direction of the *a* crystallographic axis. The molecular rows are interconnected by

weak non-conventional C-H...O interactions having as H-acceptor species the O atoms of isatin groups and as H-donor groups three different groups: the CH group of thiophene rings bonded to the Sulphur atom; one CH group of the phenyl ring of the isatin moiety; the CH group of the C_{sp3} atom of the fused rings. Features of these interactions are shown in Figure A13.

3.2.2 Conclusions

We have successfully synthesized fully conjugated molecular hybrids, in which the core of the naturally-occurring dye isatin has been fused with a thiophene residue. We have demonstrated that the synthesis is feasible using the mild and scalable conditions associated with the DHA reaction, used as the key intramolecular ring closing step. The DHA reaction has however to be performed with the correct set up in terms of nucleophilic and electrophilic atom, that is the halogen atom on the isatin residue, and hydrogen atoms on both the α -positions of the thiophene residue, to avoid intermolecular propagation and crosslinking which cannot be suppressed using high dilution reaction conditions. We have also demonstrated that the synthetic protocol is adaptable to other substituents, namely fluorine atoms, on the aromatic isatin residue. The synthetic flexibility has afforded tunable energy levels of the final dyes, with the fluorinated compound **36** having identical bandgap with respect to **18**, but lower HOMO and LUMO levels. We are currently engaged in tuning reaction protocols for late stage dibromination of both **18** and **36**, to afford isatin-based conjugated monomers capable of polymerization for organic photovoltaic applications.

3.3 ONE POT DIRECT ARYLATION AND CROSS-ALDOL CONDENSATION FOR THE RAPID CONSTRUCTION OF π -EXTENDED THIOPHENE AND FURAN-BASED SCAFFOLDS

This paragraph is partially based on the following publication:

Nitti, A.; Bianchi, G.; Po, R.; Pasini, D. "One Pot Direct Arylation and Cross-Aldol Condensation for the Rapid Construction of π -Extended Thiophene and Furan-based Scaffolds", to be submitted

3.3.1 Results and discussions

We have initially investigated the synthesis of new conjugated donor-acceptor monomers **44** in which two thiophene rings are fused with dihydro-pyrroloindoleone (DIPID) nucleus. DIPID is known to be a acceptor unit of polymers with good efficiencies. The fusion of the DIPID with two thiophene rings would lead to a monomer with new electronic properties compared to the DIPID-based monomer reported in the literature. The retrosynthetic analysis for the synthesis of the hypothesized monomer is shown in Figure 8. The crucial steps in the synthesis of **44** are: a) bromination reaction of DIPID, and b) a double cascade cyclization reaction between dibrominated DIPID **41** and 3-formylthiophene **43**, both not reported in literature.

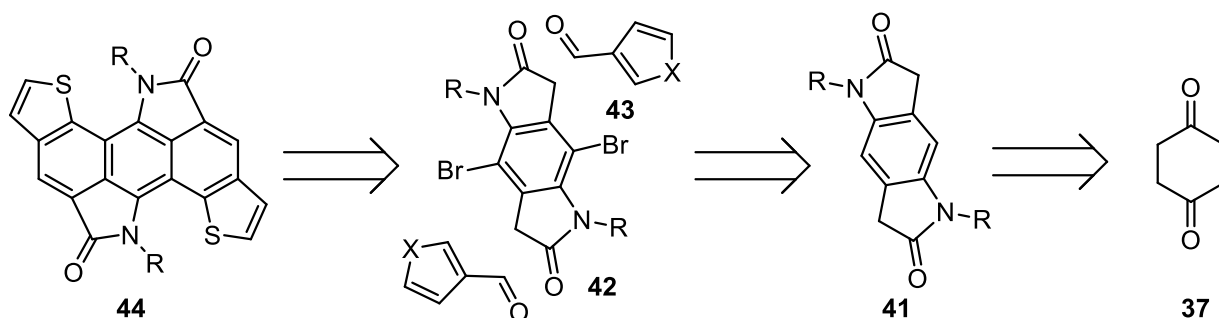
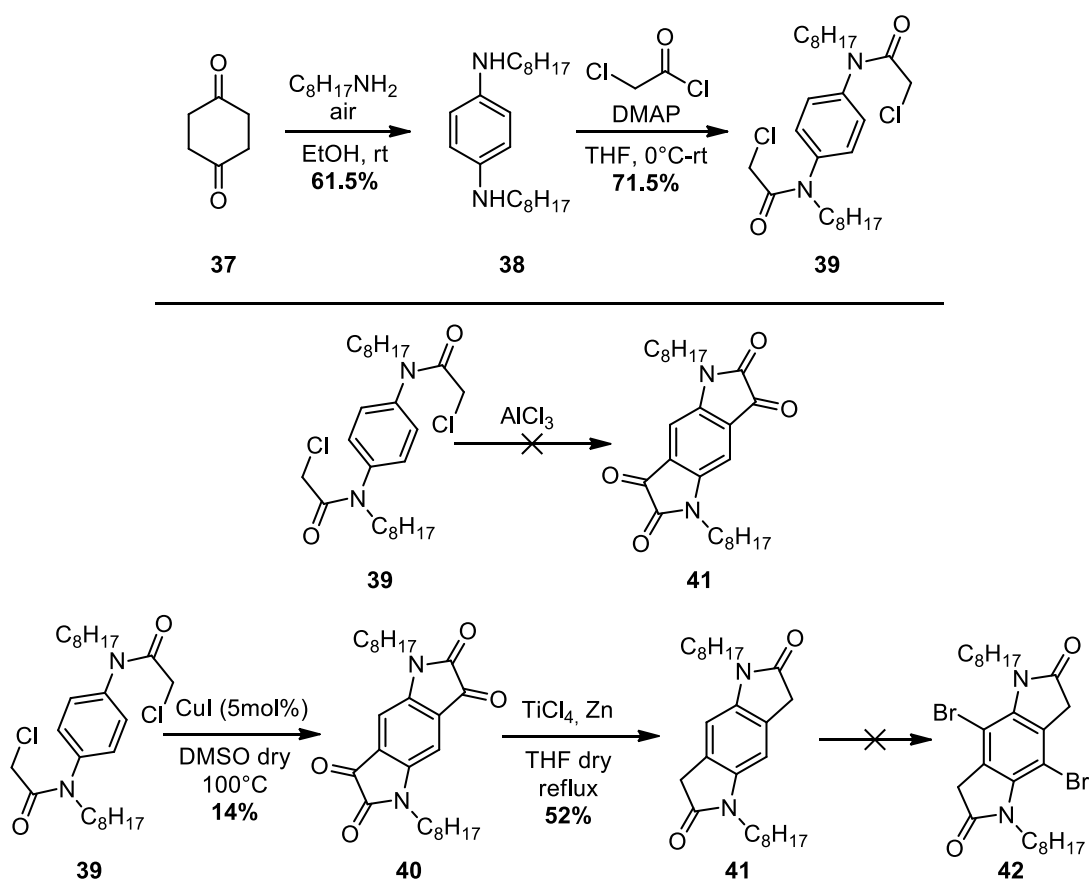


Figure 8. Retrosynthetic analysis of target monomer **44**.

The synthesis of DIPID following literature procedures (Figure 8), has not led to the de-

sired product. Several experiments for the synthesis of DIPID have been conducted to bypass the non-reproducibility of the final step consisting in a Friedel-Crafts cyclization AlCl_3 -catalyzed (see Appendix). The successful way (Scheme 13) develops a Cu-catalyzed cyclization followed by reduction of the carbonyl moiety with TiCl_4 and Zn. The bromination reaction of DIPID **41** did not lead to the expected product **42**; for this reason the synthesis of the monomer **44** was abandoned.

Scheme 8. Synthesis of DIPID unit through oxidative cyclization Cu-catalyzed



Simultaneously to the synthesis of DIPID, stimulated by the work of Heo *et al.*,³⁹ we set out to investigate the reaction of *N*-methyl-4-bromooxindole **45a** (derived from alkylated isatin by reduction at its C3 carbonyl) and 3-formylthiophene **43a**, to form **46a** (Scheme 8).

Using $\text{Pd}(\text{OAc})_2$ as the catalyst, KOAc and dry DMF at 150°C in moderate dilution conditions (50 mM), we were pleased to isolate the desired compound **46a** after purification by flash column chromatography, albeit in relatively low yield (Table 4, entry 1).

pendently from the CH⁻ containing acceptor substrate (thiophene or furan) used in the DHA reaction, seems to indicate that cross aldol occurs faster, forming the new carbon-carbon double bond probably in both *E* (useful for subsequent ring closure) and *Z* stereochemical configurations. The reactions were also characterized by a substantial amount of baseline material, given probably by oligomeric species formed by intermolecular DHA when the stereochemistry is not correctly set up for the ring closure. The crosstalking between the fused thiophene (*vs* fused furan) and oxindole fragments of **46a** *vs.* **46b** vary substantially, as testified by their ¹H NMR spectra (see figure A15, Appendix). Further characterization by UV/Vis and emission spectroscopies confirmed the “push-pull” nature of the new molecular structures **46a** and **46c** (Figure A17).

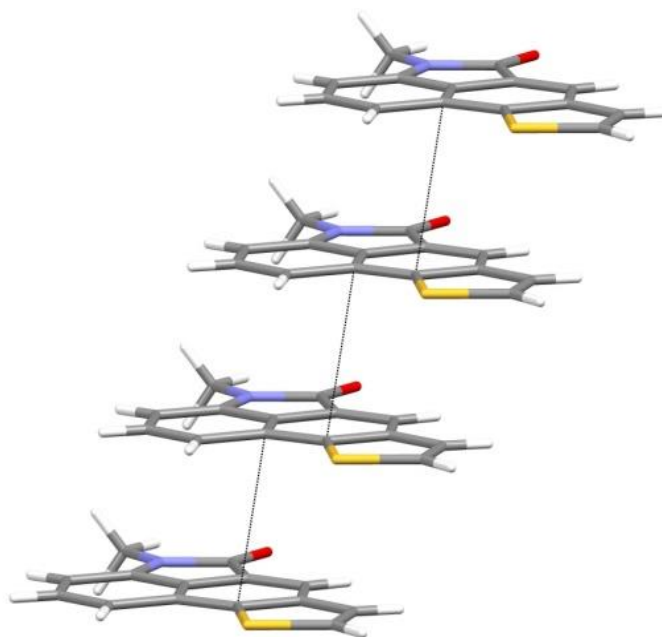


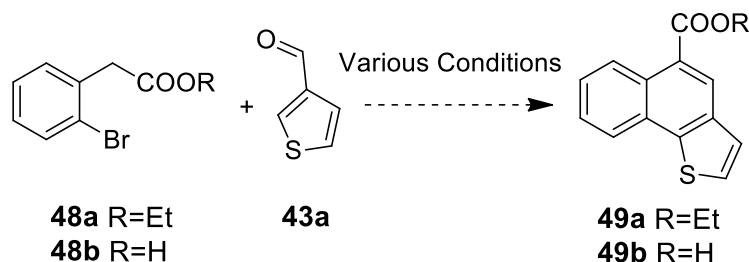
Figure 9. Structure of compound **46a** in the crystal.

The structure of compound **46a** was confirmed by X-ray crystallography (Figure 9). The polycyclic molecules are essentially flat, and lie on overlying layers having interplanar distance of 3.51 Å. Face-to-face π - π stacking interactions occur between the aromatic rings of adjacent molecules, which remain parallel to each other in terms of orientation of their molecular dipoles.

To demonstrate the effective potential of our cross aldol-DHA strategy, we evaluated the use of simpler, commercially available reagents. The reaction of ethyl 2-bromophenylacetate **48a** or the corresponding acid **48b** and 3-formylthiophene **43a** (Scheme 10), however, when screened under a variety of conditions, did not afford the desired product **49**; essentially, only baseline material could be detected (see Table A5).

Both electronic and steric effects are likely to be responsible for the different outcomes in the synthesis of **46** and **49**, involving the same aldehyde **43a**; as for the former, ester (in **46**) and amide (in **49**) moieties have differing electron-withdrawing abilities, and may tune the nucleophilic nature of the CH₂ groups in the cross aldol reaction; as for the latter, a high stereoselectivity in the newly formed double bond of the aldol adduct towards the *E*-configuration would inevitably preclude cyclization in the subsequent DHA.

Scheme 10. Attempted synthesis of compound 49

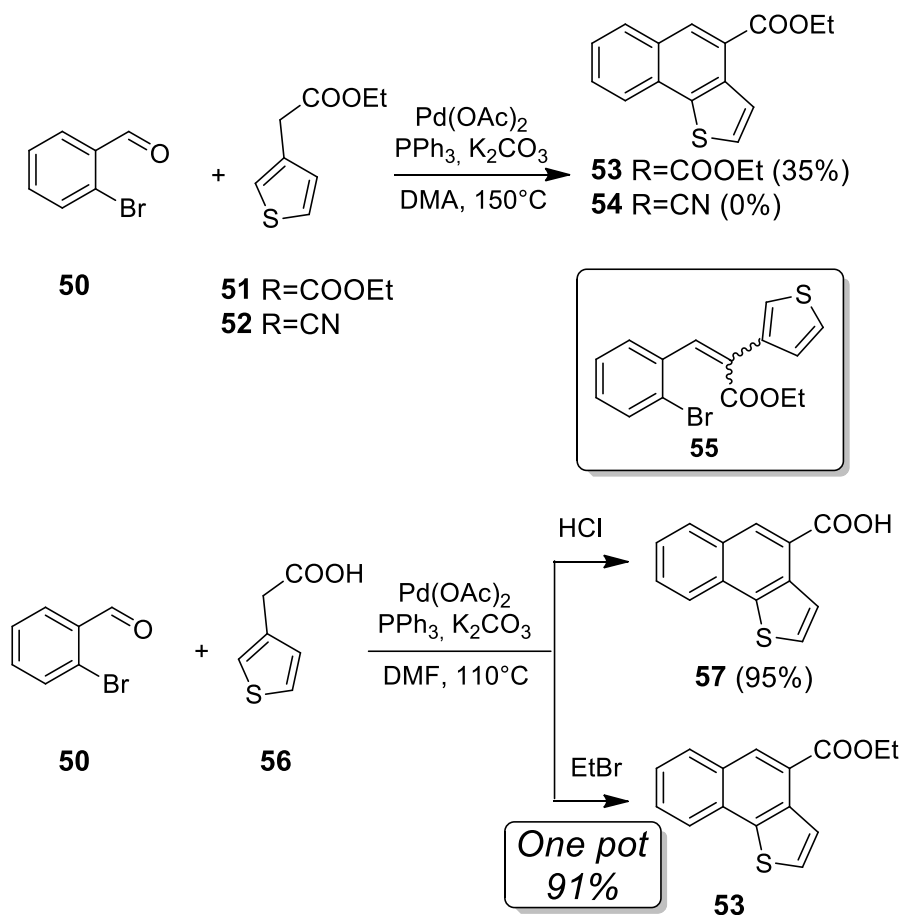


By reversing the position of nucleophilic and electrophilic moieties of the cross-aldol reaction (such as in pathway *b*) in Figure 3, paragraph 2.3) 2-bromobenzaldehyde and ethyl 3-thiopheneacetate gave, in the presence of Pd(OAc)₂, PPh₃, K₂CO₃ in dry DMAc at temperature of 150°C compound **53** (Scheme 11) in 35% yield after extensive optimization (Table A6).

In analogy to **46a**, GC-MS experiments on the crude reaction evidenced the presence, in variable ratios, of byproduct **55**, in which aldol condensation had occurred without subsequent DHA occurring (presumably the compound with the uncorrected stereochemistry at the carbon-carbon double bond). Furthermore, in the case of cyano substituted substrate **52**, none of the correct product could be isolated. Gratifyingly, however, the commercially-available 3-

thiopheneacetic acid, in place of the corresponding ethyl ester, gave after acidification and simple filtration compound **57** in almost quantitative yield. The reaction could be carried forward one pot by the addition of ethyl bromide at room temperature, giving π -extended compound **53** in 91% and purification by column chromatography.

Scheme 11. Highly efficient construction of Naphthothiophene-fused compounds

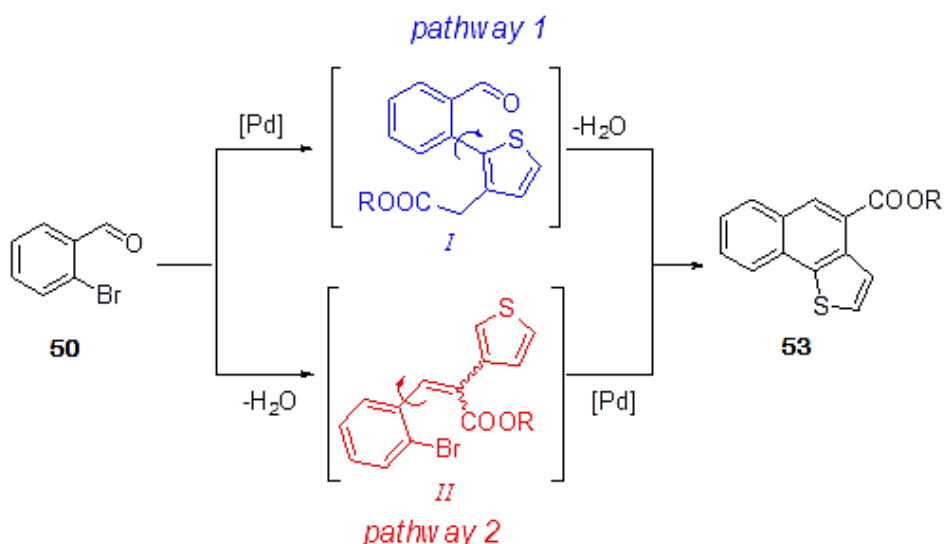


In case of substrate **56**, the cross-aldol intermediate byproduct was not observed in the crude reaction mixture. Control experiments in the absence of the Pd(II) catalyst and the phosphine, other conditions equal, were revealing: in the case of reactants **50** and **51**, product **55** was formed in good yield, as a mixture of stereoisomers, of which the major one could be separated by flash chromatography and isolated in 43% yield. In the case of reactants **50** and **56**, after esterification with ethyl bromide, the reaction mixture showed no cross-aldol product, with **50** left unreacted and esterification of the other starting material **56** proceeding to afford compound **51**.

The different electron-withdrawing abilities of cyano, ester and carboxylate groups (Hammett's $\sigma_p = 0.66, 0.45$ and 0.00 , respectively)⁴¹ influence the acidity of the neighboring α -hydrogens, presumably lowering the rate of the aldol condensation with respect to the DHA, and promoting the synthetic pathway 1 instead of 2 (Scheme 12).

An alternative explanation could be the activation of the DHA pathway by the carboxylate functionality, possibly able to coordinate intramolecularly the Pd(II) catalyst during the oxidative addition step, and thus also promoting the synthetic pathway 1. However, when control experiments with **50** and **56**, other conditions equal, were conducted in the presence of increasing amounts of pivalic acid (up to 100% mol with respect to the starting materials), no dramatic suppression of the yield of compound **53** was obtained (yields dropped from 91% to 80%). Pivalic acid is known to coordinate preferentially with respect to other aliphatic carboxylic acids to Pd(II) in such reaction solvents, thus should dramatically compete with the carboxylic acid functionality of **56**, in the case such functionality would have a key kinetic role.

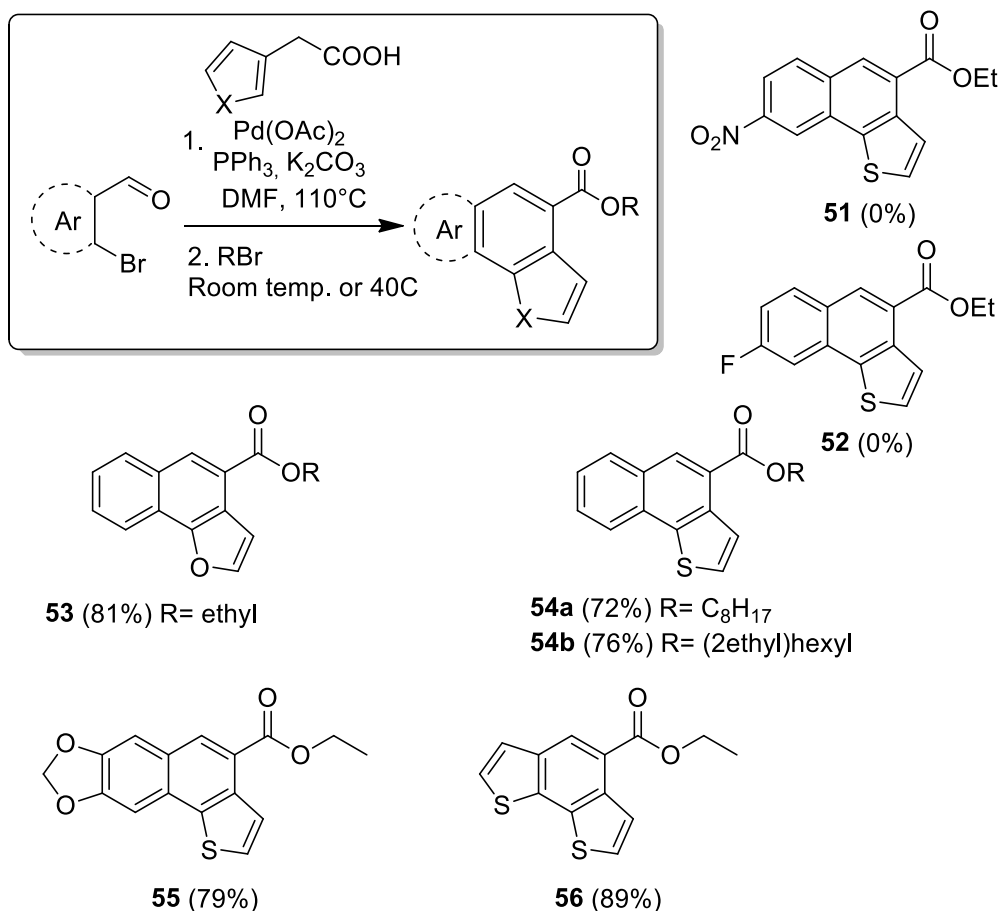
Scheme 12. Competing cross-aldol and DHA pathways



We therefore set out to investigate the generality of this approach. The optimal reaction conditions were used for the synthesis of compounds **60-63** (Scheme 13). The introduction of electro-withdrawing substituents in the *para* position with respect to the aldehyde did not af-

ford the expected product, presumably because pathway 1 is favored by the more reactive aldehyde, with additional consequences of the stereochemical outcome of the aldol addition favoring the incorrect stereoisomer for ring closure. However, the introduction of long side chains is equally efficient as in **60**, affording compounds **61** in good yields. The introduction of a furan ring instead of thiophene occurred smoothly (compound **60**). Above all, the introduction of electron rich functionalities on the aldehydes, as expected, worked equally well (compounds **62** and **63**).

Scheme 13. Synthesis of compounds 51-56 with optimized DHA-aldol cascade protocol



It is certainly worthwhile noting that compound **53** was previously reported in literature as byproduct of the catalytic cyclization *via* ruthenium-carbene/oxidation, following a complex procedure.⁴² Ethyl benzo[1,2-b:6,5-b']dithiophene-4-carboxylate **63**, an interesting and promising compound incorporated in successful polymer for Bulk-Heterojunction OPV de-

vices firstly described by Kirner *et al.*⁴³, was obtained after a synthetic sequence of 7 steps (*vs.* 1 in our sequence from commercially available materials).

3.3.2 Conclusions

We have developed an efficient methodology for the selective C–H activation followed by intramolecular cross-aldol reaction for the construction of conjugated thiophene-based and furan-based compounds using cheap commercial starting materials or easily achievable starting materials. We have applied this strategy to the synthesis of a series of D–A benzindol-5-ones fused with electron–rich thiophene or furan rings, and to a series of naphthothiophenes and naphthofurans. Using commercial 2-bromo-3-formylthiophene and 3-thiopheneacetic acid we have synthesized compound **63** in only one step, dramatically simplifying its synthesis. Our strategy paves the way for its full exploitation for the synthesis of other, more complex, difunctional monomers through easily scalable procedures.

3.4 ANTHRADITHIOPHENE-BASED AND DIHYDROBENZODITHIOPHENE-BASED MONOMER FOR THE SYNTHESIS OF INNOVATIVE POLYMERS FOR PHOTOVOLTAIC APPLICATIONS

This paragraph is based on work carried out during my second and third year at University of Pavia and during my external stay at the Department of Chemistry of the Massachusetts Institute of Technology (USA), in the group of Prof. Timothy M. Swager.

3.4.1 Synthesis of Anthradithiophene-Based Monomer

Anthradithiophene compounds (ADT), shown in Figure 10, have attracted considerable attention due to their high charge carrier mobility,⁴⁴ photoconductivity,⁴⁵ and luminescence.⁴⁶

In particular, charge carrier (hole) mobilities of over 1.2 cm²/V·s have been observed in

solution-deposited films.⁴⁷ Despite its interesting properties, few reports on photovoltaic applications were published in literature due to the difficulties in their synthesis. The main way to construct the ADT scaffold is an intermolecular or intramolecular cyclization on pre-formed precursors (Scheme 1).

The intramolecular cyclization methodologies illustrated in Figure 10a for the synthesis of aADT, make use of pre-cyclized precursor ease to obtain. However these methodologies were used for the synthesis of aADT with side chains in α position of thiophene ring wide for OFET applications.⁴⁸⁻⁴⁹ The one-pot two component reaction shown in Figure 10b is an interesting approach to the synthesis of aADT scaffolds for photovoltaic applications. In this case, however, several and tedious steps were required for the synthesis of precursors.⁵⁰

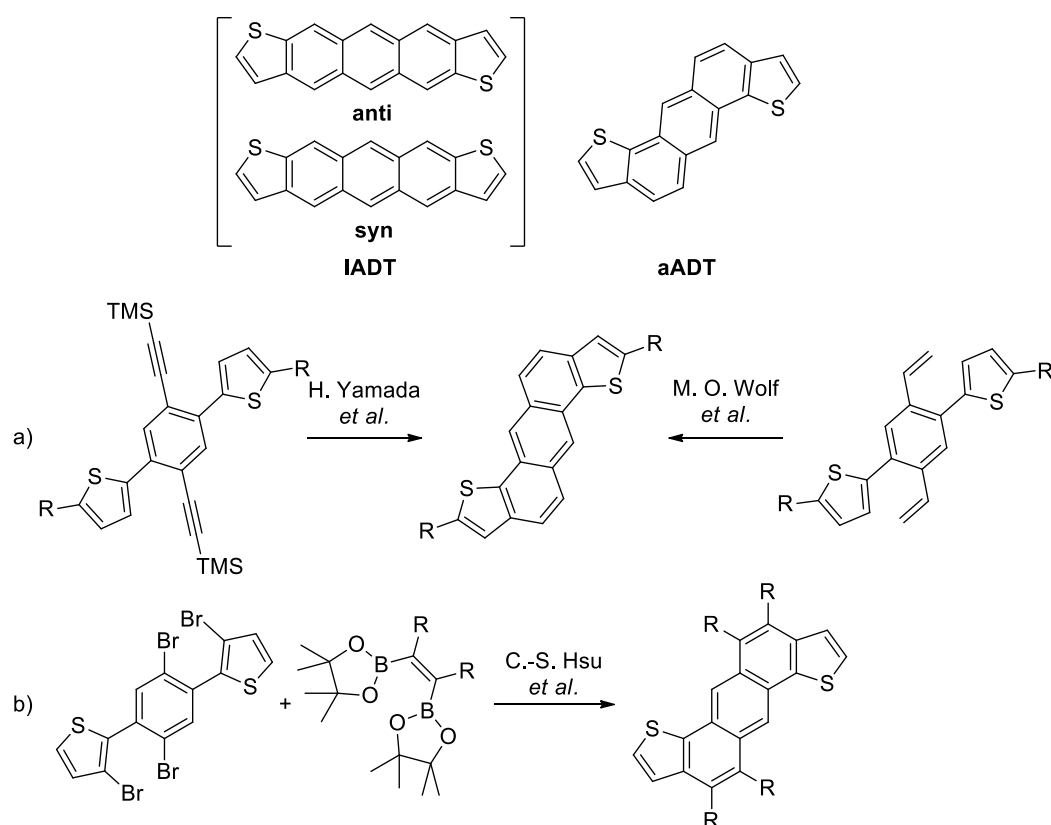


Figure 10. Structure of ADT scaffold and synthetic methodologies for the synthesis of aADT.

Our proposed synthesis of anthradithiophene scaffold make use of the one-pot protocol of DHA and cross-aldol condensation to construct a series of naphthothiophene compounds (see

paragraph 3.3). Our retrosynthetic analysis is presented in Figure 11.

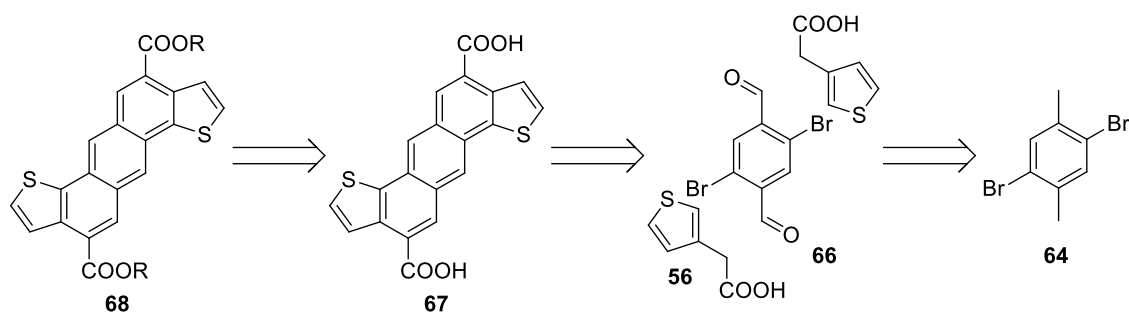
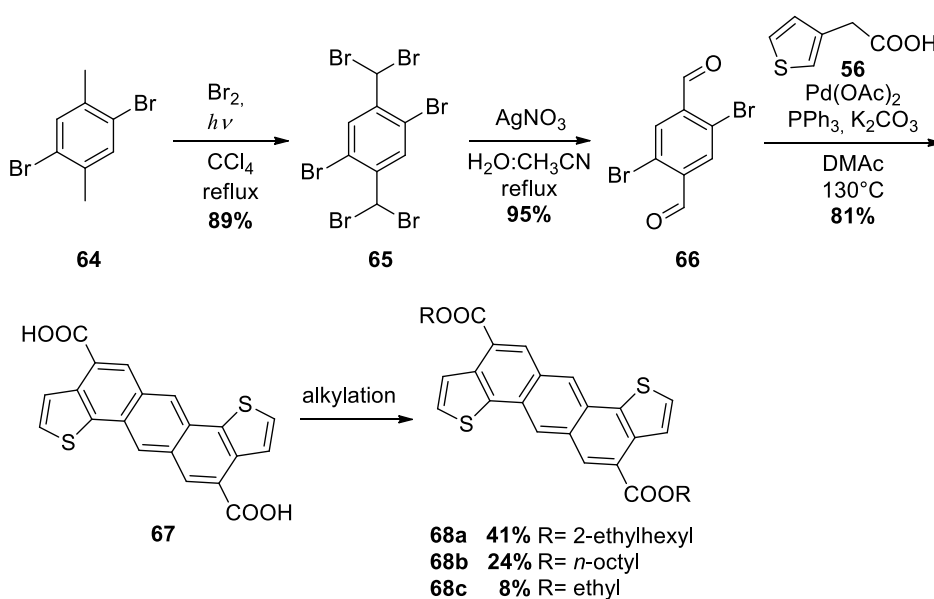


Figure 11. Retrosynthetic analysis for the synthesis of aADT **66**.

The key step of developed synthesis is an one-pot two component DHA Pd-catalyzed and cross-aldol condensation between commercially available 3-thiopheneacetic acid **56** and 2,5-dibromoterephthalaldehyde **66** performing in two steps starting 2,5-dibromo-*p*-xylene **64**.

The synthesis of ADT-based monomer, can be scaled because no expensive reagent, mild reaction condition and no exotic reactions were used, and all reactions were conducted in air atmosphere. The synthesis of pre-cyclized precursor **66** was achieved after two steps with a total yield of 85%, using as purification technique only crystallization and obtaining pure compound in scale of 30 g.⁵¹

Scheme 14. Synthesis of aADT monomer **68**



Starting from 2,5-dibromo-*p*-xylene **64** radical bromination was successfully carried out

in the presence of Br₂ in dry CCl₄ at reflux under irradiation with 500 W incandescent lamp to give compound **65** in high yields (89%). Brominated derivative **65** was then oxidized on the dibromomethyl groups with AgNO₃ in H₂O:acetonitrile to give pre-cyclized precursor **66** (95% yield). The key step of the one-pot two component DHA and cross-aldol condensation cyclization was carried out in the presence of 3-thiopheneacetic acid **56** as co-reagent, Pd(OAc)₂ and PPh₃ as catalytic system, an excess of potassium carbonate as base and in moderate dilution conditions (100 mM for reagent **66** in DMAc). Desired compound **67** was isolated in good yields (81%) as dark green powder after precipitation in 3M HCl (aq) and washings with methanol. Closing the synthesis, the ADT dicarboxylic acid **67** was alkylated to obtain the desired products **68a–c** in low or moderate yield.

A previous experiment of one-pot cyclization was conducted using pre-cyclized precursor with octyl 3-thiopheneacetate. The desired product was isolated in very low yield (2%) after flash-chromatography, demonstrating that the use of acid substrate **56** to achieve the formation of aADT framework with this methodology (see paragraph 3.3).

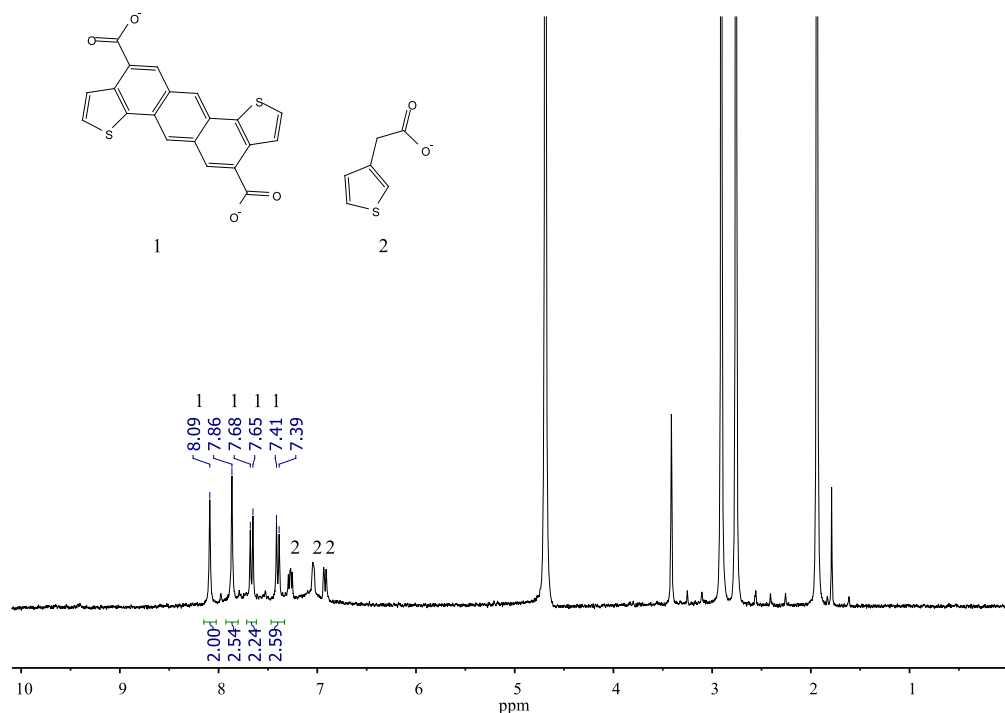
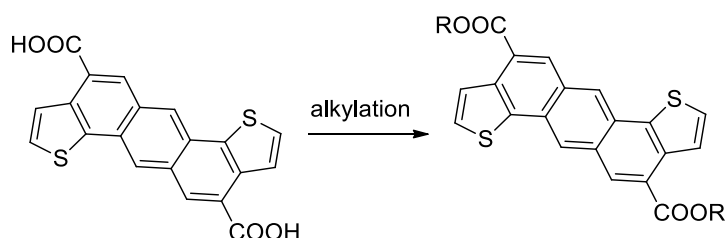


Figure 12. ¹H NMR spectra recorded in D₂O of reaction crude of double cyclization using 3-thiopheneacetic acid **56** as substrate.

^1H NMR of crude of reaction when substrate **66** was reacted with acid **56**, recorded in D_2O (Figure 12), show as the double cyclization reaction do not result in byproducts.

Alkylation reaction of **67** was conducted in several reaction conditions summarized in Table 5. Alkylation with ethyl iodide (entry 1–3) led to the desired product **68c** in low yield (8%). The inability to increase the temperature, due to the low b.p. of the ethyl iodide, did probably have an important impact on the yield of reaction. Several alkylation experiments were conducted with 1-octylbromide (entry 4–10), leading to maximum yield of 24% for **68b** (entry 10).

Table 5. Alkylation reaction of 67



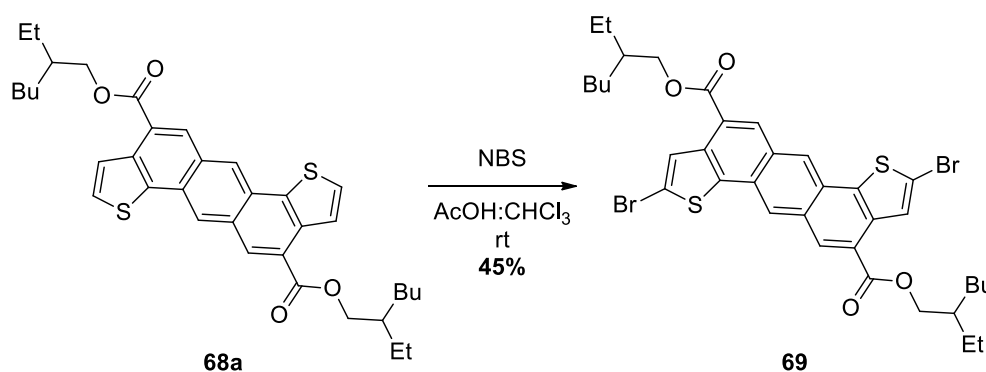
Entry	Compound	Method	Yield [%]
1	68c	EtI (2 eq), K_2CO_3 , DMAc, rt	2
2	68c	EtI (20eq), K_2CO_3 , DMAc, rt	8
3	68c	EtI (2 eq), KOH, $\text{H}_2\text{O}:\text{DCM}$, rt	0
4	68b	$\text{C}_8\text{H}_{17}\text{Br}$, K_2CO_3 , DMAc, 70°C	8
5	68b	$\text{C}_8\text{H}_{17}\text{Br}$, K_2CO_3 , Bu_4NBr , DMAc, 100°C	10
6	68b	$\text{C}_8\text{H}_{17}\text{Br}$, KOH, H_2O , 100°C	0
7	68b	a) oxalyl chloride, toluene, 100°C b) $\text{C}_8\text{H}_{17}\text{OH}$, Et_3N , CHCl_3 , 40°C	0
8	68b	a) SOCl_2 , 100°C b) $\text{C}_8\text{H}_{17}\text{OH}$, Et_3N , CHCl_3 , 40°C	14
9	68b	a) SOCl_2 , 100°C b) $\text{C}_8\text{H}_{17}\text{OH}$, Et_3N , THF, 60°C	16
10	68b	a) SOCl_2 , 100°C b) $\text{C}_8\text{H}_{17}\text{OH}$, Et_3N , THF, 60°C	24
11	66a	1-bromo-2-ethylhexane, K_2CO_3 , DMAc, 130°C	41

Surprisingly, the alkylation of **67** with 1-bromo-2-ethylhexane in presence of K_2CO_3 as base in DMAc at temperature of 130°C provides **68a** in 41% yield after crystallization with

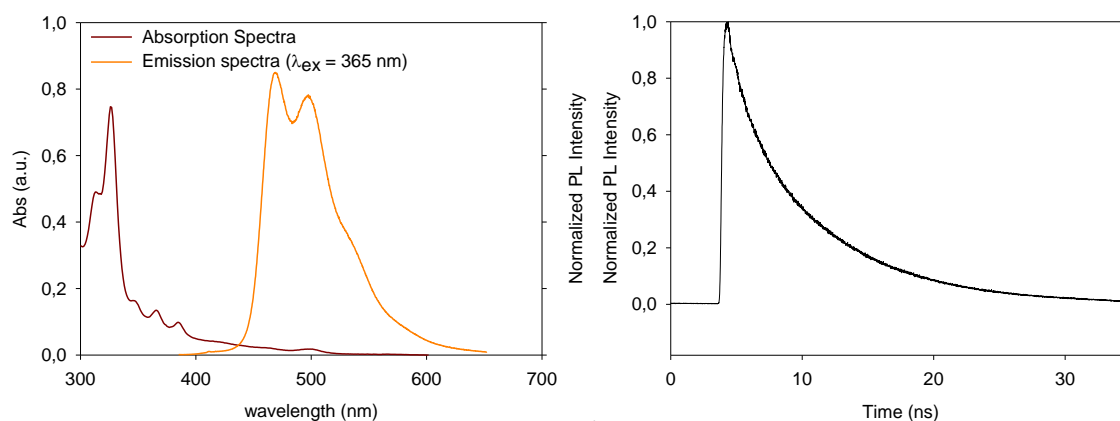
ethanol (entry 11). The increase of yield recorded using branched chains could be due to an increment of the solubility of the monomer.

To obtain a polymerizable aADT monomer, a final step of bromination is required. In Scheme 15 is reported the experiment of bromination conducted on substrate **68a**.

Scheme 15. Bromination reaction of **68a**



The experiment conducted shown as a selective bromination of α position of thiophene rings was obtained using NBS as the brominating agent and a mixture of AcOH and CHCl_3 as the solvent system at room temperature. Compound **69** was isolated after crystallization from ethanol. Other bromination protocols were tested (NBS in CHCl_3 at room temperature and NBS in DMF at 100°C), but the correct compound was not isolated.



Compound	λ_{abs} (nm)	λ_{em} (nm)	Φ_{F}	τ (ns)	ϵ ($\text{L}\cdot\text{mol}^{-1}\cdot\text{cm}^{-1}$)
68b^a	356	495	0,15	14.2	$9,9\cdot 10^3$

Figure 13. Optical properties of compound **68a** (solution 10^{-5} M in CH_2Cl_2).

Preliminary spectroscopical and photophysical studies in solution were conducted on compound **68b** and results are reported in Figure 13.

3.4.2 Synthesis of Dihydrobenzodithiophene-Based Monomer

Buckminsterfullerene (C_{60}) and its derivatives possess an number of interesting and useful magnetic,⁵² electronic⁵³ and chemical properties.⁵⁴ To utilize these properties more efficiently, the solubility of fullerenes in organic solvents must be improved so that it can be more processable for technological applications.

For organic photovoltaic applications fullerenes derivatives functionalized with solubilizing long chains, such as $PC_{61}BM$ and $PC_{71}BM$, are widely used as standard acceptor compounds for the construction of devices with Bulk-Heterojunction architecture.⁵⁵ Much efforts have been devoted to the synthesis of new electron acceptors and, despite some interesting results leading to a better understanding of the active layer,⁵⁶ the performances are still much lower when compared with fullerene derivatives. However, the high cost of $PC_{61}BM$ and $PC_{71}BM$ (0.1 g – 264 €)⁵⁷ affects considerably the total cost of the devices.

The functionalization of fullerenes with polymers would potentially endow the polymer of most of the fullerene properties. On the other hand, fullerenes embedded in polymers become more easily processable. The resulting materials can be used for surface coating, photoconducting devices, and also to create new molecular networks.⁵⁸ For photovoltaic applications, a reversible bond between the fullerene and the donor polymer is necessary to restore the fullerene/donor polymer separated couple for the correct working of the active layer in solar cell devices.

The Diels–Alder (DA) reaction is one of the most common reactions used in organic chemistry, included in the category of “click reactions” for its unique characteristic of operation simplicity, efficiency, versatility, selectivity and easy access to precursors.⁵⁹ DA reaction are also widely used as methodologies for the functionalization of polymers.⁶⁰ Involving a

straightforward [4 + 2] cycloaddition reaction between an electron-rich diene (furan and derivatives, cyclopentadiene and derivatives, indene and derivatives, etc.) and an electron-poor dienophile, it is particularly indicated for the functionalization of fullerenes. Cyclopentadienes,⁶¹ indenenes,⁶² anthracenes⁶³ and furan⁶⁴ derivatives are reported as dienes able to react with fullerene in reversible Diels-Alder reactions. The reversible properties is most important for a functionalization able to restore the fullerene/donor polymer couple into the active layer of solar cells.

During my external stay at MIT, the aim of the project was the synthesis of indene-based monomers able to promote reversible Diels-Alder reactions with C₆₀ (Step A in figure 14). This new monomer, when incorporated in π -conjugated polymers, could be able to functionalize fullerene increasing its solubility.

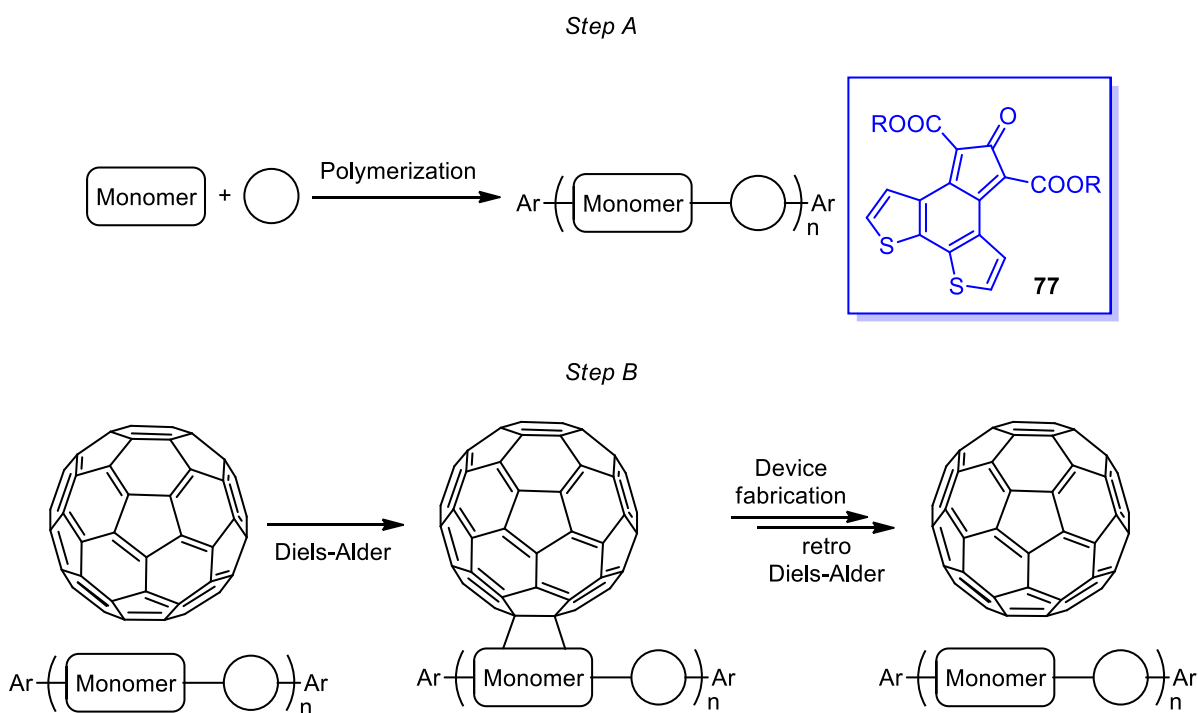


Figure 14. Aim of the project at MIT. Target molecule is illustrated in blue box.

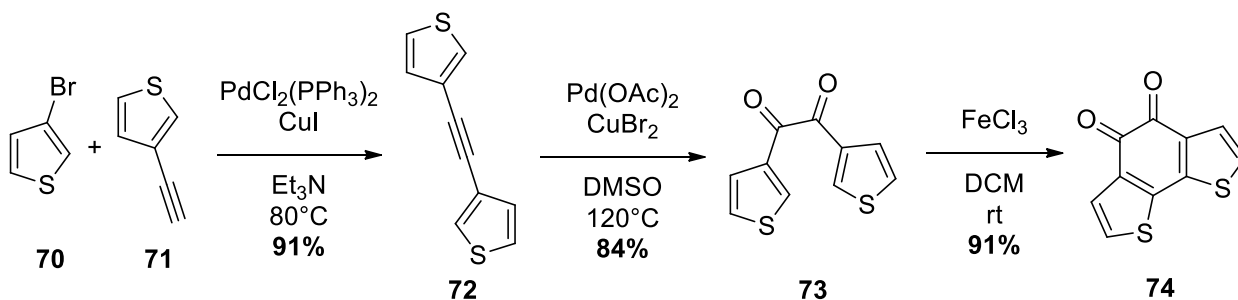
At this point, the fullerene functionalized with the donor polymer could be deposited to form a layer of material as an inactive BHJ device. The activation of device occurs after of a post-heating treatment that promotes a retro Diels-Alder with consequent generation of the ac-

tive layer composed of fullerene and donor polymer (Step B in figure 14). In detail, I dealt with the synthesis of molecule **77** in blue box of figure 14. This compound presents two thiophene rings, able to be polymerized with other monomers after preactivation of α position, fused with an indene-5-one framework able to react in reversible Diels-Alder reactions with fullerene.

The key step of the synthesis consists in a cross-aldol reaction between a benzo[1,2-*b*:6,5-*b'*]dithiophene-4,5-dione **74** and 1,3-dicarboxylate acetone **75a**, previously reported for the synthesis of analogous compounds.⁶⁵

Starting from 3-bromothiophene **70** and 3-alkynylthiophene **71**, a Sonogashira protocol was successfully carried out using $\text{PdCl}_2(\text{PPh}_3)_2$ as catalyst, CuI as typical copper salt additive for this coupling and triethylamine as base and solvent of reaction at a temperature of 80°C , to give compound **72** in high yields (91%) after purification with flash chromatography (Scheme 16).

Scheme 16. Synthesis of precursor **74**

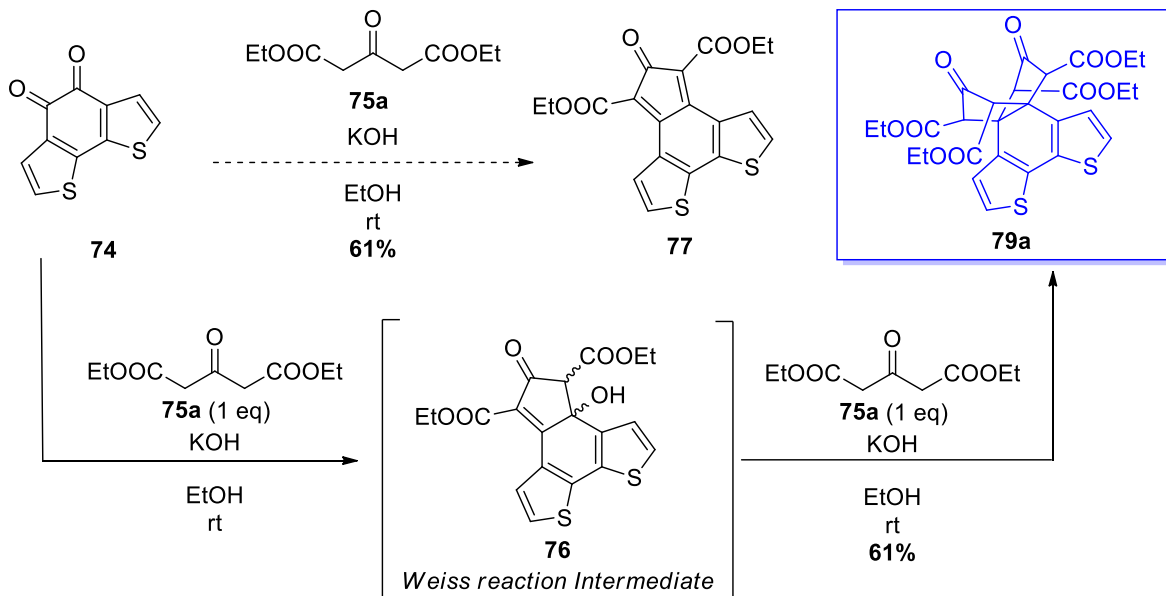


The alkynyl moiety of compound **72** was oxidized in presence of $\text{Pd}(\text{OAc})_2$ as the catalyst and CuBr_2 as the co-catalyst in DMSO at a temperature of 120°C affording compound **73** in high yield (84%) after flash-chromatography. The ring closing of compound **73** was carried out with oxidative FeCl_3 -catalyzed cyclization in DCM at room temperature, leading to the desired benzo[1,2-*b*:6,5-*b'*]dithiophene-4,5-dione **74** in 91% yield after a simple percolation.

The final step of the cross-aldol reaction on precursor **74** using 2 equivalents of diethylcarboxylate-1,3-acetone **75a** and 3 equivalents of KOH as base in ethanol after 6 h did not

lead to the desired cross-aldol product **77** but to a compound with the structure **79a**, coming from the Weiss reaction (scheme 17).⁶⁶

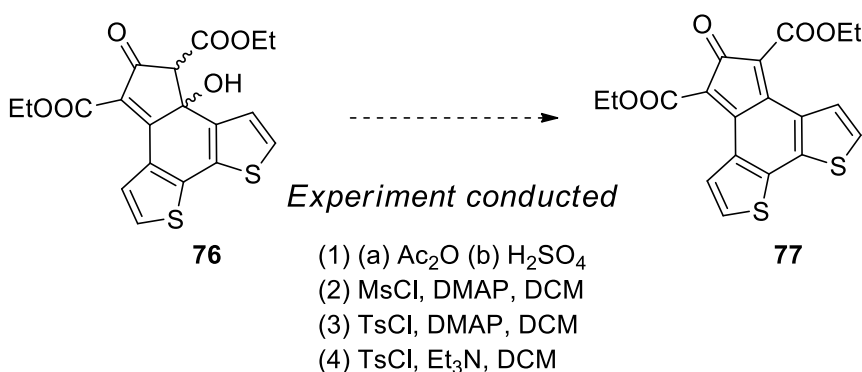
Scheme 17. Weiss reaction for the synthesis of 78a



The use of 2 equivalents of **75a** leads to the formation of aldol intermediate **76**, which reacting with a second equivalent of **75a** promote the formation of compound **79a** in 61% yield (scheme 17).⁶⁷

Using only one equivalent of **75a**, compound **76** was isolated after 1h of reaction in 52% yield. Compound **76** could be used for the synthesis of **77** through a formal dehydration reaction. Several condition were tested, however in all cases compound **77** was not isolated (scheme 18).

Scheme 18. Dehydration protocol tested for the synthesis of 77

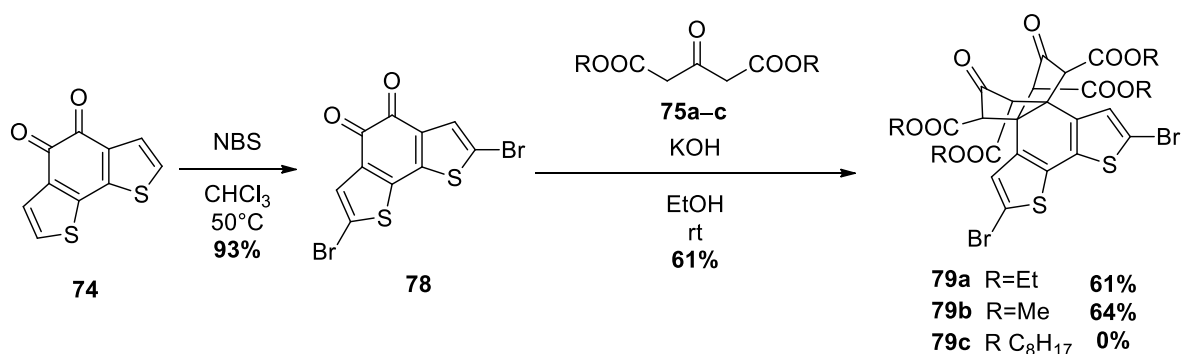


Compound **79a** cannot be used for the synthesis of donor polymer able to react in re-

versible Diels-Alder reactions with fullerene, but it is an interesting monomer to be polymerized with other monomers previous bromination of the α positions of the thiophene rings. The synthesis of polymerizable monomers is reported in scheme 19.

Compound **74** was brominated on α position obtaining compound **78** in high yields (93%) using NBS in CHCl_3 at 50°C . The Weiss reaction protocol on compound **78** was applied to the synthesis of a series of dihydrobenzodithiophene-based monomers **79a-c**. The use of two equivalents of **75a** and **75b** led to the synthesis of expected monomers **79a** and **79b**. The use of **75c**, with the *n*-octyl chains, did not lead to **79c** presumably because of the steric hindrance of the side chains.

Scheme 19. Synthesis of polymerizable monomer 79a and 79b



3.4.3 Conclusions

We have synthesized two new polymerizable monomers that require conclusive experiments to define their optical and electrochemical properties. Other experiments will be conducted on **68** to clarify some aspects regarding both the formation of byproducts in the double cyclization via DHA/cross-aldol condensation, both the influence of branched and linear side chains on the yield of alkylation reactions. Optical and electrochemical experiments will be conducted to understand the electronic properties for optoelectronic applications. Finally, monomer **68** and analogues, and monomers **79**, will be polymerized with other donor or acceptor compounds to synthesize new polymers with donor-acceptor architectures for BHJ applications.

3.5 REFERENCES

- (1). (a) Gsänger, M.; Bialas, D.; Huang, L.; Stolte, M.; Würthner, F. *Adv. Mater.* **2016**, *28*, 3615–3645; (b) Ghazvini Zadeh, E. H.; Tang, S.; Woodward, A. W.; Liu, T.; Bondarc, M. V.; Belfield, K. D. *J. Mater. Chem. C* **2015**, *3*, 8495–8503; (c) Robb, M. J.; Ku, S. Y.; Brunetti, F. G.; Hawker, C. J. *J. Polym. Sci. Polym. Chem. A* **2013**, *51*, 1263–1271; (d) Chevrier, M.; Kesters, J.; Blayo, C.; Richeter, S.; Van der Lee, A.; Coulembier, O.; Surin, M.; Mehdi, A.; Lazaroni, R.; Evans, R. C.; Maes, W.; Dubois, P.; Clément, S. *Macromol. Chem. Phys.* **2016**, *217*, 445–458; (e) Beverina, L.; Salice, P. *Eur. J. Org. Chem.* **2016**, 1207–1225.
- (2) T.-L. Choi, K.-M. Han, J.-I. Park, D. H. Kim, J.-M. Park, S. Lee, *Macromolecules* **2010**, *43*, 6045-6049.
- (3) L. Liao, Y. Pang, L. Ding, F. E. Karasz, *Macromolecules* **2002**, *35*, 6055-6059.
- (4) L. Liao, Y. Pang, L. Ding, F. E. Karasz, *Macromolecules* **2001**, *34*, 6756-6760.
- (5) G. Bounos, S. Ghosh, A. K. Lee, K. N. Plunkett, K. H. DuBay, J. C. Bolinger, R. Zhang, R. A. Friesner, C. Nuckolls, D. R. Reichman, P. F. Barbara, *J. Am. Chem. Soc.* **2011**, *133*, 10155–10160.
- (6) C. Y. Yu, M. Horie, A. M. Spring, K. Tremel, M. L. Turner, *Macromolecules* **2010**, *43*, 222–232.
- (7) C. Y. Yu, J. W. Kingsley, D. G. Lidzey, M. L. Turner, *Macromol. Rapid Commun.* **2009**, *30*, 1889–1892.
- (8) A. M. Spring, C. Y. Yu, M. Horie, M. L. Turner, *Chem. Commun.* **2009**, 2676-2678.
- (9) C. Y. Yu, M. L. Turner, *Angew. Chem. Int. Ed.* **2006**, *45*, 7797-7800.
- (10) B J. Lidster , J. M. Behrendt, M. L. Turner, *Chem. Commun.* **2014**, *50*, 11867-11870.
- (11) C.-Y. Yu, M. Helliwell, J. Raftery, M. L. Turner, *Chem. Eur. J.* **2011**, *17*, 6991-6997.
- (12) F. Menk, M. Mondeshki, D. Dudenko, S. Shin, D. Schollmeyer, O. Ceyhun, T.-L. Choi, R. Zentel, *Macromolecules* **2015**, *48*, 7435-7445.
- (13) S.-W. Chang, M. Horie, *Chem. Commun.* **2015**, *51*, 9113-9116.

- (14) M. Montanari, A. Bugana, A. K. Sharma, D. Pasini, *Org. Biomol. Chem.* **2011**, *9*, 5018-5020.
- (15) P. Si, J. Liu, Z. Zhen, X. Liu, G. Lakshminarayana, I. V. Kityk, *Tetrahedron Lett.* **2012**, *53*, 3393.
- (16) P. Si, J. Liu, G. Deng, H. Huang, H. Xu, S. Bo, L. Qiu, Z. Zhen, X. Liu, *RSC Adv.* **2014**, *4*, 25532-25539.
- (17) F. Livi, N. S. Gobalasingham, E. Bundgaard, B. C. Thompson, *J. Polym. Sci. A: Polym. Chem. J. Polym. Sci. A Polym. Chem.* **2016**, *54*, 2907-2918.
- (18) G. Marzano, D. Kotowski, F. Babudri, R. Musio, A. Pellegrino, S. Luzzati, R. Po, G. Farinola, *Macromolecules* **2015**, *48*, 7039-7048.
- (19) G. Marzano, F. Carulli, F. Babudri, A. Pellegrino, R. Po, S. Luzzati, G.M. Farinola, *J. Mater. Chem. A* **2016**, *4*, 17163-17170.
- (20) M. Wakioka, Y. Kitano, F. Ozawa, *Macromolecules* **2013**, *46*, 370-374.
- (21) D.-P. Liu, Q. Chen, Y.-C. Zhao, L.-M. Zhang, A.-D. Qi, B.-H. Han, *ACS Macro Lett.* **2013**, *2*, 522-526.
- (22) W. Lu, J. Kuwabara, T. Iijima, H. Higashimura, H. Hayashi, T. Kanbara, *Macromolecules* **2012**, *45*, 4128-4133.
- (23) H.-H. Zhang, J. Dong, Q.-S. Hu, *Eur. J. Org. Chem.* **2014**, 1327-1332.
- (24) X. Zhang, Y. Gao, S. Li, X. Shi, Y. Geng, F. Wang, *J. Polym. Sci. A Polym. Chem.* **2014**, *52*, 2367-2374.
- (25) D. Kotowski, S. Luzzati, G. Bianchi, A. Calabrese, A. Pellegrino, R. Po, G. Schimperna A. Tacca, *J. Mater. Chem. A* **2013**, *1*, 10736-10744.
- (26) Y. Lin, X. Zhan, *Acc. Chem. Res.* **2016**, *49*, 175-183.
- (27). (a) Nizalapur, S.; Ho, K. K. K.; Kimyon, O.; Yee, E.; Berry, T.; Manefield, M.; Cranfield, C. G.; Willcox, M.; Black, D. St. C.; Kumar, N.; *Org. Biomol. Chem.* **2016** *14*, 3623-3637; (b) Le, T.; Cheah, W. C.; Wood, K.; Black, D. St. C.; Willcox, M. D.; Kumar, N.; *Tet-*

- rahedron Lett.* **2011**, *52*, 3645-3647. (c) Lal, H.; Aggarwal, T. P.; Singh, V. P.; Kumar, A. *Orient. J. Chem.* **2010**, *26*, 581-588.
- (28). (a) Kamal, A.; Mahesh, R.; Nayak, V. L.; Babu, K. S.; Kumar, G. B.; Shaik, A. B.; Kapure, J. S.; Alarifi, A.; *Eur. J. Med. Chem.* **2016**, *108*, 476-485. (b) Lazreg, F.; Lesieur, M.; Samson, A. J.; Cazin, C. S. J.; *ChemCatChem* **2016**, *8*, 209-213 (c) Garden, S. J.; Torres, J. C.; Pinto, A. C. *J. Braz. Chem. Soc.* **2000**, *11*, 441-446.
- (29). Torres, J. C.; Pinto, A. C.; Garden, S. J. *Tetrahedron* **2004**, *60*, 9889-9900.
- (30). De, S.; Mishra, S.; Kakde, B. N.; Dey, D.; Bisai A. *J. Org. Chem.* **2013**, *78*, 7823-7844.
- (31). We observed *N*-(3methylthiophene)-2-bromoaniline as the major decomposition product.
- (32). Deprotection of C3 carbonyls by postmodification of the resulting polymer structures should be possible under high vacuum, continuously removing the ethylene glycol formed during the reaction.
- (33). Park, K. Y.; Kim, B. T.; Heo, J. N. *Eur. J. Org. Chem.* **2014**, 164-170.
- (34). (a) Sambigioglio, C.; Marsden, S. P.; Blackera, A. J.; McGowan, P. C. *Chem. Soc. Rev.* **2014**, *43*, 3525-3550. (b) Finet, J. P.; Fedorov, A.; Combes, S.; Boyer, G. *Curr. Org. Chem.* **2002**, *6*, 597-626.
- (35). (a) Zhang, Y.; Hubbard, J. W.; Akhmedov, N. G.; Petersen, J. L.; Söderberg, Björn C. *G. J. Org. Chem.* **2015**, *80*, 4783-4790. (b) Zhang, N.; Thomas, L.; Wu, B. *J. Org. Chem.* **2001**, *66*, 1500-1502. (c) Yue, W. S.; Li, J. *J. Org. Lett.* **2002**, *4*, 2201-2203.
- (36). Głowacki, E. D.; Coskun, H.; Blood-Forsythe, M. A.; Monkowius, U.; Leonat, L.; Grzybowski, M.; Gryko, D.; White, M. S.; Aspuru-Guzik, A.; Sariciftci, N. S. *Org. Elect.* **2014**, *15*, 3521-3528.
- (37). Estrada, L. A.; Stalder, R.; Abboud, K. A.; Risko, C.; Brédas, J. L.; Reynolds, J. R. *Macromolecules* **2013**, *46*, 8832-8844.
- (38). Allen, F. H.; Kennard, O.; Watson, D. G.; Brammer, L.; Orpen, A. G.; Taylor, R. *J.*

Chem. Soc. Perkin Trans. II **1987**, 2, S1-S19.

(39) Park, K. Y.; Kim, B. T.; Heo, J. N.; *Eur. J. Org. Chem.* **2014**, 164–170.

(41) C. Hansch, A. Leo and R. W. Taft, *Chem. Rev.* **1991**, 91, 165–195.

(42) Tsai, F. Y.; Lo, J. X.; Hsu, H. T.; Lin, Y. C.; Huang, S. L.; Wang, J. C.; Liu, Y. H.; *Chem. Asian J.* **2013**, 8, 2833-2842.

(43) Welker, M.; Turbiez, M. G. R.; Chebotareva, N.; Kirner, H. J.; Functionalized benzodithiophene polymers for electronic application, WO 2014086722.

(44). Coropceanu, V.; Kwon, O.; Wex, B.; Kaafarani, B. R.; Gruhn, N. E.; Durivage, J. C.; Neckers, D. C.; Brédas, J.-L. *Chem. Eur. J.* **2006**, 12, 2073–2080.

(45). Murphy, A. R.; Frechet, J. M. J. *Chem. Rev.* **2007**, 107, 1066–1096.

(46). Geffroy, B.; le Roy, P.; Prat, C. *Poly. Int.* **2006**, 55, 572–582.

(47). Park, S. K., Mourey, D. A., Subramanian, S., Anthony, J. E., and Jackson, T. N. *Appl. Phys. Lett.* **2008**, 93, 043301.

(48). (a) Pietrangelo, A.; Patrick, B. O.; MacLachlan, M. J.; Wolf, M. O. *J. Org. Chem.* **2009**, 74, 4918–4926.

(49). Quinton, C.; Suzuki, M.; Kaneshige, Y.; Tatenaka, Y.; Katagiri, C.; Yamaguchi, Y.; Kuzuhara, D.; Aratani, N.; Nakayama, K.; Yamada, H. *J. Mater. Chem. C* **2015**, 3, 5995—6005.

(50). Wu, J.-S.; Lin, C.-T.; Wang, C.-L.; Cheng, Y.-J.; Hsu, C.-S. *Chem. Mater.* **2012**, 24, 2391–2399.

(51). Yang, X.; Liu, D.; Miao, Q. *Angew. Chem. Int. Ed.* **2014**, 53, 6786–6790.

(52). Allemand, P.-M.; Khemani, K.C.; Koch, A.; Wudl, F.; Holkzer, K.; Donovan, S.; Gruner, G.; Thompson, J. D. *Science* **1991**, 253, 301.

(53). (a) Jehoulet, C.; Oben, Y. S.; Kim, Y.-T.; Zhou, F.; Bard, A. J. *J. Am. Chem. Soc.* **1992**, 114, 4237; (b) Xie, Q.; Perez-Cordero, E.; Echegoyen, L. *J. Am. Chem. Soc.* **1992**, 114, 3978.

(c) Wang, Y.; West, R.; Yuan, C.-H. *J. Am. Chem. Soc.* **1993**, 115, 3844.

- (54). Wudl, F.; Hirsch, A.; Khemani, K. C.; Suzuki, T.; Allemand, P. M.; Koch, A.; Eckert, H.; Srdanov, G.; Webb, H. M. *ACS Symp. Ser.*, **1992**, *481* (Fullerenes), 161-75.
- (55). Thompson, B. C.; Fréchet, J. M. J. *Angew. Chem. Int. Ed.* **2008**, *47*, 58–77.
- (56). Yan, Y.; Chenjun, S.; Gang, L.; Vishal, S.; Qibing, P.; Yang, Y. *Appl. Phys. Lett.* **2006**, *89*, 153507.
- (57). Data obtained from Sigma Aldrich web site in October 2016 (<http://www.sigmaaldrich.com/catalog/product/aldrich/684449?lang=it®ion=IT>)
- (58). Prato, M. *J. Mater. Chem.* **1997**, *7*, 1097–1109.
- (59) Nicolaou, K. C.; Snyder, S. A.; Montagnon, T.; Vassilikogiannakis, G. *Angew. Chem. Int. Ed.* **2002**, *41*, 1668–1698.
- (60). Tasdelen, M. A. *Polym. Chem.* **2011**, *2*, 2133–2145.
- (61). (a) Osuna, S.; Morera, J.; Cases, M.; Morokuma, K.; Sola, M. *J. Phys. Chem. A* **2009**, *113*, 9721–9726; (b) Nie, B.; Rotello, V. M. *J. Phys. Chem. Solids* **1997**, *58*, 1897–1899.
- (62). Sieval, A. B.; Treat, N. D.; Jan, D. R.; Hummelenac, C.; Stingelin, N. *Chem. Commun.* **2015**, *51*, 8126–8129.
- (63). Wang, G.-W.; Chen, Z.-X.; Murata, Y.; Komatsu, K. *Tetrahedron* **2005**, *61*, 4851–4856.
- (64). Nie, B.; Hasan, K.; Greaves, M. D.; Rotello, V. M. *Tetrahedron Letters* **1995**, *36*, 3617-3618.
- (65). Li, P.; Parker, T. M.; Hwang, J.; Deng, F.; Smith, M. D.; Pellechia, P. J.; Sherrill, C. D.; Shimizu, K. D. *Org. Lett.* **2014**, *16*, 5064–5067.
- (66). Bertz, S. H. *J. Am. Chem. Soc.* **1981**, *103*, 3599.
- (67). Van Ornum, S. G. ; Li, J.; Kubiak, G. G.; Cook, J. M. *J. Chem. Soc., Perkin Trans.* **1997**, *1*, 3471-3478.

Experimental Section

4.1 GENERAL EXPERIMENTAL

All commercially available reagents and solvents were used as received. THF (Na, benzophenone), CH₂Cl₂ (CaH₂) and toluene (Molecular Sieves) were dried and distilled before use. All commercially available starting materials and reagents were purchased from Aldrich, Alfa Aesar, TCI or Fluorochem and used as received. Compounds 4,8-bis(hexyloxy)-Benzo[1,2-b:4,5-b']dithiophene,¹ **1**,² **3**,³ **6**,³ **7**,⁴ **13**⁵ and **64**⁶ were prepared following previously published procedures. Analytical thin layer chromatography was performed on chromophore loaded, commercially available silica gel plates. Flash chromatography was carried out using silica gel (pore size 60 Å, 230-400 Mesh). ¹H and ¹³C NMR spectra were recorded from solutions in CDCl₃ on 200 and 300 MHz spectrometer using the solvent residual proton signal or tetramethylsilane as the internal standard.

The UV/Vis and emission spectroscopic studies were recorded using conventional spectrophotometers, with a scanning speed of 50 nm/min at 20 °C. Photoluminescence studies were conducted using an excitation slit of 2.0 nm, and emission slit of 3.0 nm with a scanning speed of 50 nm/min at 20 °C.

Diffraction data for **18_1**, **18_2** and **46a** were collected by means of a conventional diffractometer, working at ambient temperature with graphite-monochromatized Mo-K α X-radiation ($\lambda = 0.71073$ Å). Data reductions were performed with the WinGX package;⁷ absorption effects evaluated with the ψ -scan method⁸ were negligible and absorption correction was not applied to the data. All crystal structures were solved by direct methods (SIR 97)⁹ and refined

by full-matrix least-square procedures on F2 using all reflections (SHELXL 2014).¹⁰ Anisotropic displacement parameters were refined for all non-hydrogen atoms; hydrogens were placed at calculated positions with the appropriate AFIX instructions and refined using a riding model.

Melting points were measured on commercially-available instrumentation and are uncorrected.

Cyclic Voltammetry was performed with the sample at a concentration of 10^{-3} M (in the case of **18**, and **39a**) or $0,6 \cdot 10^{-3}$ M (in the case of **25**) in *o*-DCB/MeCN (1:10 by volume) solution in the presence of Bu_4NBF_4 0.1 M as the supporting electrolyte. A stationary glassy carbon (GC) disk electrode was used as the working electrode. Silver electrode Ag/AgNO_3 served as the reference electrode and the potential sweep rate was 200 mV s^{-1} . Measurements were carried out under thermostatic conditions ($20 \text{ }^\circ\text{C}$) in a nitrogen atmosphere.

Samples for the mass spectrometry were analysed with GC-MS and ESI-MS conventional instrumentation. Gel permeation chromatography (GPC) analyses were performed with two different systems: a) a Waters system equipped with a series of two universal columns (Styragel HR4A and HR5A), a refractive index detector with Tetrahydrofuran (THF) as the eluent at 40°C ; b) a Agilent 220 chromatograph equipped with a refractive index detector on 1,2,4-trichlorobenzene (TCB) as the eluent at 90°C to overcome aggregation phenomena. Molecular weight calibration was carried out in both cases using polystyrene standards.

The modeling (calculation of conformations and intermolecular interactions) and the determination of the electronic properties of the polymers **P1-4** by DFT were carried out using the Spartan'14 program suites, using B3LYP functional and 6-31G* as basic set.¹¹ The optimal geometries were obtained from DFT calculations on structures previously obtained with Force Field method, in order to cancel electrical forces on atomic nuclei and the electron density distributions (see Appendix, figure A3–5). The optimized geometries of the monomeric and dimeric clusters were obtained with the empirical method that makes use of MMFF94 param-

eterization.¹² With this method several geometries of the clusters can be obtained, thus to evaluate the intrinsic properties of the aggregates the assembly of molecules that have the lowest energy is chosen. The property that was evaluated is the energy spread between the energy of the single molecules in the gas phase and the energy of the cluster in which the same molecules are more adherent possible (see Appendix, figure A6). To better establish the relationship between molecular structure of monomeric unit and ease of aggregation, we also evaluate the microscopic tension surface in which energy spread is related to the complete surface of the cluster (see chapter 3, figure 4). Molecular surfaces were obtained by QSAR method.

4.2 SYNTHESIS OF NEW COMPOUNDS

Monomer 4. A solution of 4,8-bis(hexyloxy)-benzo[1,2-b:4,5-b']dithiophene (0.52 g, 1.32 mmol) in dry THF (20 mL) was cooled to -78°C; a solution of *n*-BuLi in hexanes (2 mL, 5.28 mmol) was added dropwise, and the solution stirred for 30 min at -78°C and a further 30 min at -10 °C. After cooling at -78°C an excess of dry DMF (2 mL) was added, the solution was stirred for 30 min and then the temperature was allowed to rise to 25°C. The reaction mixture was quenched with dropwise addition of H₂O (20 mL), then extracted with ethyl acetate (3 x 15 mL), and the organic layer dried with Na₂SO₄. The orange residue was purified by column chromatography (SiO₂; hexanes/dichloromethane 9:1 to 1:1), to yield the title compound as an orange solid (0.48 g, 81%). ¹H-NMR (200 MHz, CDCl₃, δ): 10.13 (s, 2H), 8.18 (s, 2H), 4.35 (t, 4H), 1.91 (m, 4H), 1.57-1.26 (m, 12H), 0.94 (t, 6H).

Monomer 5. A solution of commercially available 4,8-bis[(2-butyloctyl)oxy]-Benzo[1,2-b:4,5-b']dithiophene **8** (0.59 g, 1 mmol) in dry THF (10 mL) was cooled to -78°C, and a solution of *n*-BuLi in hexanes (2.5 mL, 4 mmol, 4 eq) was added dropwise, and the solution stirred for 30 min at -78°C and a further 30 min at -10 °C. After cooling at -78°C an excess of dry DMF (2 mL) was added, the solution was stirred for 30 min and the temperature was al-

lowed to rise to 25°C. The reaction mixture is quenched with addition of H₂O dropwise (20 mL), then extracted with ethyl acetate (3x15 mL), and the organic layer dried with Na₂SO₄. The orange residue was purified by column chromatography (SiO₂; hexanes:dichloromethane 9:1), to yield the title compound as an orange solid (0.60 g, 93%). ¹H-NMR (300 MHz, CDCl₃, δ): 10.15 (s, 2H), 8.19 (s, 2H), 4.29 (d, 4H), 1.92 (m, 2H), 1.6-1.2 (m, 36H), 0.94 (t, 6H).

Polymer P1 (entry 1 in Table 1). A solution of 1,4-dibenzaldehyde (0.069 g, 0.52 mmol) and compound **1** (0.30 g, 0.52 mmol) in dry DMF (10 mL) was warmed under stirring and nitrogen atmosphere to 80°C, then KO^tBu (0.18 g, 1.55 mmol) was added and heating was continued with stirring at 80°C for a further 4 h. The reaction mixture was quenched with H₂O, and the aqueous layer extracted with Toluene (3x10 mL). The organic phase was dried with Na₂SO₄, filtered and the solvent removed *in vacuo*. The residue was dissolved in a minimum amount of CH₂Cl₂ and precipitated in MeOH as the nonsolvent. The red solid was filtered and dried (0.164 g, 40%). ¹H-NMR (300 MHz, CDCl₃, δ): 8-7 (bm, 10H), 4.1 (bm, 4H), 2-0.8 (bm, 22H). ¹³C-NMR (75 MHz, CDCl₃, δ): 151.0 (bm), 144.0, 137.1, 135.0, 130.1, 128.9-125.8, 123.1, 110.5, 69.4, 31.5, 29.3, 25.7, 22.56, 13.9. GPC (THF): *M*_n = 4000, PDI = 1.5

Polymer P2. (entry 2 in Table 1). A solution of compound **3** (0.14 g, 0.69 mmol) and compound **1** (0.40 g, 0.69 mmol) in dry THF (10 mL) was warmed under stirring and nitrogen atmosphere to 45°C, then KO^tBu (0.23 g, 2.07 mmol) was added and heating was continued with stirring at 60°C for a further 24 h. The reaction mixture was quenched with H₂O, and the aqueous layer extracted with dichloromethane (3x10 mL). The organic phase was dried with Na₂SO₄, filtered and the solvent removed *in vacuo*, to yield a red solid which could not be precipitated in a nonsolvent (0.24 g, 69%). ¹H-NMR (300 MHz, CDCl₃, δ): 7.6-6.5 (bm, 6H), 4.5-3.5 (bm, 4H), 2-0.8 (bm, 22H). ¹³C-NMR (75 MHz, CDCl₃, δ): 151.0, 125.8, 123.1, 110.4, 68.9, 31.4, 29.2, 25.8, 22.6, 13.9. Major isomer only. Aromatic fluorinated carbon signals are broad and not visible. GPC (THF): *M*_n = 3200, PDI = 9.2. UV (CHCl₃) λ_{max} = 462 nm

($\epsilon = 14.000$).

Polymer P3a. (entry 3 in Table 1). A solution of compound **4** (0.106 g, 0.241 mmol) and compound **6** (0.108 g, 0.241 mmol) in dry toluene (5 mL) was warmed under stirring and nitrogen atmosphere to reflux, then KO t Bu (0.081 g, 0.723 mmol) was added and heating was continued with stirring for a further 5 h. The reaction mixture was quenched with H₂O, and the aqueous layer extracted with toluene (1x10 mL) and CH₂Cl₂ (2x10 mL). The organic phase was dried with Na₂SO₄, filtered and the solvent removed *in vacuo*, to yield a red solid which could not be precipitated in a nonsolvent (0.11 g, 77%). ¹H-NMR (200 MHz, CDCl₃, δ): 7.6-7.1 (bm, 6H), 4.2-3.5 (bm, 4H), 2.5-0.5 (bm, 22H). ¹³C-NMR (75 MHz, CDCl₃, δ): major isomer only 143.0, 135.6, 128.1, 125.4, 109.4, 59.4, 31.4, 29.3, 25.8, 22.6, 14.0. Aromatic fluorinated carbon signals are broad and not visible. GPC (THF): M_n = 4200, PDI = 2.9.

Polymer P3b (entry 4 in Table 1). A solution of compound **5** (0.240 g, 0.39 mmol) and compound **6** (0.178 g, 0.39 mmol) in dry Toluene (4 mL) was warmed under stirring and nitrogen atmosphere to reflux, then KO t Bu (0.131 g, 1.17 mmol) was added and heating was continued with stirring for a further 48 h. The reaction mixture was quenched with drops of H₂O, and the solvents removed *in vacuo*, to yield a red solid which was dissolved in a minimum amount of CHCl₃ and precipitated in MeOH as the nonsolvent, and further purified by Soxhlet extraction with acetone and hexanes. The final product was recovered via Soxhlet refluxing with CHCl₃, in which it is soluble (0.154 g, 54%). ¹H-NMR (200 MHz, CDCl₃, δ): 8-7 (very broad signals, aromatic and vinyl), 4.2-3.5 (very broad signal, -OCH₂CH₂), 2.5-0.5 (bm, 22H). GPC (TCB): M_n = 3900, PDI = 1.2. UV (CHCl₃) λ_{\max} = 553 nm ($\epsilon = 29.700$).

Polymer P4a. A solution of compound **7** (0.100 g, 0.24 mmol), compound **12** (0.090 g, 0.24 mmol), Pd(OAc)₂ (1 mg, 0.0045 mmol, 0.02 eq) and KOAc (0.046 g, 0.47 mmol, 2 eq) in dry dimethylacetamide (3 mL) was warmed under stirring and nitrogen atmosphere to 100°C for 48 h. The reaction mixture was cooled to room temperature, and the solvent removed *in vacuo*, to yield a red solid which was dissolved in a minimum amount of CH₂Cl₂ and precipitated

in MeOH as the nonsolvent, and further purified by Soxhlet extraction with MeOH, acetone and hexanes. The final product was recovered via Soxhlet refluxing with CHCl₃, in which it is soluble (0.107 g, 81%). ¹H-NMR (200 MHz, CDCl₃, δ): 7.6-6.8 (very broad signals; aromatic), 4.4-3.5 (very broad signal, -OCH₂CH₂), 2.0-0.7 (bm, 22H). ¹³C-NMR (75 MHz, CDCl₃, δ): 143.0, 129.2, 123.3, 109.4, 73.3, 31.8, 30.4, 29.3, 27.4, 22.7, 14.0. Aromatic fluorinated carbon signals are broad and not visible. GPC (TCB): $M_n = 2700$, PDI = 1.1

Polymer P4b. A solution of compound **9** (0.302 g, 0.5 mmol), compound **10** (0.075 g, 0.5 mmol), Pd₂(dba)₃ (23 mg, 0.025 mmol) and K₂CO₃ (0.207 g, 1.5 mmol) in dry toluene (5 mL) was degassed for 5 min, warmed under stirring and nitrogen atmosphere to 130°C for 48 h. The reaction mixture was cooled to room temperature, and the solvent removed *in vacuo*, to yield a red solid which was dissolved in a minimum amount of CH₂Cl₂ and precipitated in MeOH as the nonsolvent, and further purified by Soxhlet extraction with acetone and hexanes. The final product was recovered via Soxhlet refluxing with CHCl₃ (0.178 g, 60%). ¹H-NMR (300 MHz, CDCl₃, δ): 7.8-6.2 (very broad signals; aromatic), 4.0-3.5 (very broad signal, -OCH₂CH₂), 2.0-0.5 (bm, 22H). GPC (TCB): $M_n = 1600$, PDI = 1.6

Polymer P4c. A solution of compound **8** (0.100 g, 0.17 mmol), compound **12** (0.069 g, 0.17 mmol), Pd(OAc)₂ (1 mg, 0.0034 mmol) and CsOAc (0.130 g, 0.68 mmol) in dry Toluene (2 mL) was degassed for 5 min, warmed under stirring and nitrogen atmosphere to 100°C for 48 h. The reaction mixture was cooled to room temperature, and the solvent removed *in vacuo*, to yield a red solid. GPC (THF): $M_n = 1100$, PDI = 2.6

Polymer P4cS. A solution of compound **13** (0.028 g, 0.03 mmol), compound **11** (0.009 g, 0.03 mmol) and Pd(PPh₃)₄ (0.35 mg, 0.0003 mmol) in dry toluene (1 mL) was degassed for 5 min, warmed under stirring and nitrogen atmosphere to 110°C for 48 h. The reaction mixture was cooled to room temperature, and the solvent removed *in vacuo*, to yield a red solid which was dissolved in a minimum amount of CH₂Cl₂ and precipitated in MeOH as the nonsolvent (9 mg, 42%). GPC (TCB): $M_n = 4100$, PDI = 1.4.

3-Bromomethylthiophene. 3-bromomethylthiophene was synthesized by modifying of the protocol reported in literature.¹³ A suspension of NBS (1.78 g, 10 mmol) and benzoyl peroxide (3 mg, 0.001 mmol) in CCl₄ (10 mL) was heated at 40 °C for 30 min, then 3-methylthiophene (10 mmol) was added dropwise. The mixture was refluxed for 2h. The precipitate was filtered and washed with hexanes. The organic solvent was removed and the crude reaction was distilled *in vacuo* to yield the desired product (1.54 g, 87%); ¹H NMR (200 MHz, CDCl₃) δ 7.33-7.31 (m, 2H), 7.14 (d, *J* = 5.0 Hz, 1H), 4.54 (s, 2H).

2-Bromo-3-methylthiophene. 2-bromo-3-methylthiophene was synthesized by modifying of the protocol reported in literature.¹⁴ NBS (1.74 g, 9.8 mmol) was added slowly to solution of 3-methylthiophene (10 mmol) in glacial AcOH (7 mL) at 0 °C. The mixture was maintained at room temperature for 1 h. The reaction mixture was then quenched with water and extracted with ether. The organic solvent was removed and the crude material was purified by flash column chromatography using hexanes as eluent. 2-Bromo-3-methylthiophene was obtained as a pale yellow oil (1.47 g, 83%); ¹H NMR (200 MHz, CDCl₃) δ 7.18 (d, *J* = 5.6 Hz, 1H), 6.79 (d, *J* = 5.5 Hz, 1H), 2.21 (s, 3H).

2-Bromo-3-Bromomethylthiophene. 2-bromo-3-bromomethylthiophene was synthesized by modifying of the protocol reported in literature.¹³ A suspension of 2-bromo-3-methylthiophene (1.77 g, 10 mmol), NBS (1.78 g, 10 mmol) and benzoyl peroxide (3 mg, 0.001 mmol) in CCl₄ (10 mL) was heated to reflux for 8h. The mixture of reaction was filtered and precipitate washed with hexanes. The organic solvent was removed and organic crude was distilled *in vacuo* to yield the desired product as a pale colorless oil (2.93 g, 87%); ¹H NMR (200 MHz, CDCl₃) δ 7.27 (d, *J* = 5.6 Hz, 1H), 7.01 (d, *J* = 5.7 Hz, 1H), 4.47 (s, 1H).

General Procedure for the Synthesis of *N*-benzylisatins. *Example for the synthesis of 15.* 7-Bromoisatin (226 mg, 1 mmol) and dry DMF (5 mL) were introduced at 0 °C, under nitrogen, in a flame-dried Schlenk flask. NaH (60 mg, 1.5 mmol) was added slowly and the reaction mixture was stirred at 0 °C for 30 min. 3-Bromomethylthiophene (194 mg, 1.1 mmol) was

then added *via* syringe and the reaction mixture was stirred at room temperature. After full conversion of the starting material (5h, TLC monitoring), the reaction mixture was quenched with water. The aqueous phase was extracted with ethyl acetate, the combined organic extracts were removed of the solvent *in vacuo* and the crude material was purified by flash chromatography (SiO₂; *n*-hexanes:ethyl acetate 8:2) to afford pure *N*-benzylisatins **15** as red solid (315 mg, 98%).

7-bromo-1-(thiophen-3-ylmethyl)indoline-2,3-dione (15). Obtained as a red solid (315 mg, 98%); ¹H NMR (200 MHz, CDCl₃): δ 7.69 (dd, *J* = 8.1 and 1.3 Hz, 1H), 7.61 (dd, *J* = 7.3 and 1.3 Hz, 1H), 7.35 – 7.21 (m, 2H), 7.11 (dd, *J* = 4.8 and 1.5 Hz, 1H), 7.06–6.94 (m, 1H), 5.43 (s, 2H); ¹³C NMR (75 MHz, CDCl₃): δ 182.2, 158.7, 147.4, 144.0, 136.5, 126.8, 126.4, 125.1, 124.7, 122.8, 120.8, 104.3, 40.3; MS-ESI: *m/z* 322 [*M* + H]⁺, 345 [*M* + Na]⁺, 644 [2*M*]⁺; GC-MS (EI) rt: 16.94 min, *m/z* 323 [*M*]⁺; anal. calcd. for C₁₃H₈BrNO₂S: C 48.5; H 2.5; found: C 48.2; H 2.2. M.p. > 300°C (dec.).

4-bromo-1-((2-bromothiophen-3-yl)methyl)indoline-2,3-dione (20). Obtained as an orange solid (385 mg, 96%); ¹H NMR (200 MHz, CDCl₃): δ 7.45–7.20 (m, 3H), 6.92–6.81 (m, 2H), 4.88 (s, 2H); ¹³C NMR (75 MHz, CDCl₃): δ 180.3, 157.1, 151.6, 138.4, 133.8, 128.8, 127.3, 127.3, 121.7, 111.5, 109.5, 109.3, 38.6; MS-ESI: *m/z* 400 [*M* + H]⁺, 422 [*M* + Na]⁺, 798 [2*M*]⁺; anal. calcd. for C₁₃H₇Br₂NO₂S: C 38.9; H 1.8; found: C 38.6; H 1.9. M.p. > 300°C (dec.).

4,7-dibromo-1-(thiophen-3-ylmethyl)indoline-2,3-dione (25). Obtained as an orange solid (365 mg, 91%); ¹H NMR (200 MHz, CDCl₃): δ 7.50 (d, *J* = 8.7 Hz, 1H), 7.30 (dt, *J* = 5.5 and 2.7 Hz, 1H), 7.24 (s, 1H), 7.14 (d, *J* = 8.7 Hz, 1H), 7.11 – 7.04 (m, 1H), 5.45 (s, 2H); ¹³C NMR (75 MHz, CDCl₃): δ 179.6, 157.8, 149.0, 143.7, 136.1, 129.9, 126.7, 126.5, 122.8, 121.4, 118.9, 102.9, 40.4; MS-ESI: *m/z* 400 [*M* + H]⁺, 422 [*M* + Na]⁺, 798 [2*M*]⁺; anal. calcd. for C₁₃H₇Br₂NO₂S: C 38.9; H 1.8; found: C 38.7; H 2.0. M.p. > 250°C (dec.).

4,7-dibromo-1-((2-bromothiophen-3-yl)methyl)indoline-2,3-dione (28). Obtained as an orange

solid (442 mg, 92%); ^1H NMR (200 MHz, CDCl_3): δ 7.49 (d, $J = 8.7$ Hz, 1H), 7.24 (d, $J = 5.7$ Hz, 1H), 7.17 (d, $J = 8.7$ Hz, 1H), 6.66 (d, $J = 5.7$ Hz, 1H), 5.32 (s, 9H); ^{13}C NMR (75 MHz, CDCl_3): δ 179.6, 157.8, 149.0, 143.7, 136.1, 129.9, 126.7, 126.5, 122.8, 121.4, 118.9, 102.9, 40.4; MS-ESI: m/z 400 $[M + \text{H}]^+$, 422 $[M + \text{Na}]^+$, 798 $[2M]^+$; single crystals suitable for X-Ray crystallography were obtained by slow evaporation of a solution of compound in CH_2Cl_2 . M.p. $> 250^\circ\text{C}$ (dec.).

7-bromo-5,6-difluoro-1-(thiophen-3-ylmethyl)indoline-2,3-dione (33). Obtained as a pale orange solid, (251 mg, 70%); ^1H NMR (200 MHz, CDCl_3): δ 7.50 (t, $J = 7.2$ Hz, 1H), 7.32 (dd, $J = 4.9$ and 3.0 Hz, 1H), 7.24 (s, 1H), 7.07 (d, $J = 4.9$ Hz, 1H), 5.42 (s, 2H); ^{13}C NMR (75 MHz, CDCl_3): δ 180.3, 158.5, 156.1, 152.7, 149.1, 145.8, 136.0, 126.8, 126.5, 122.8, 113.8, 95.9, 40.5, 29.6; anal. calcd. for $\text{C}_{13}\text{H}_6\text{BrF}_2\text{NO}_2\text{S}$: C 43.6; H 1.7; found: C 43.4; H 1.6. M.p. $> 250^\circ\text{C}$ (dec.).

General Procedure for the Synthesis of *N*-benzylisatin ethylenedioxy ketals. *Example for the synthesis of 16.* A solution of compound **15** (322 mg, 1 mmol), ethylene glycol (1 mL, 18 mmol), *p*-toluenesulfonic acid (few crystals) in toluene (5 mL) was heated at reflux for 6h with a Dean-Stark equipment. The solvent was then removed and the solid was treated with a sat. NaHCO_3 aqueous solution, and the aqueous phase was extracted with CH_2Cl_2 . The organic extracts were concentrated *in vacuo* and the solid purified by flash chromatography (SiO_2 ; CH_2Cl_2) to afford pure product **16** as a white solid (315 mg, 86%).

7'-bromo-1'-(thiophen-3-ylmethyl)spiro[[1,3]dioxolane-2,3'-indolin]-2'-one (16). Obtained as a white solid, (315 mg, 86%); ^1H NMR (200 MHz, CDCl_3): δ 7.45 (dd, $J = 8.1$ and 1.3 Hz, 1H), 7.34 (dd, $J = 7.3$ and 1.3 Hz, 1H), 7.27 (dd, $J = 4.9$ and 3.1 Hz, 1H), 7.15 (dd, $J = 2.9$ and 1.3 Hz, 1H), 7.06 (dd, $J = 5.0$, 1.3 Hz, 1H), 6.95 (dd, $J = 8.2$, 7.3 Hz, 1H), 5.31 (s, 2H), 4.72–4.25 (m, 4H); ^{13}C NMR (75 MHz, CDCl_3): δ 173.9, 141.1, 137.3, 127.4, 126.5, 126.0, 124.5, 124.1, 121.8, 102.9, 100.9, 65.9, 40.1; GC-MS (EI) rt: 17.94 min, m/z 268 $[M]^+$; anal. calcd. for $\text{C}_{15}\text{H}_{12}\text{BrNO}_3\text{S}$: C 49.2; H 3.3; found: C 49.0; H 3.5.

4'-bromo-1'-((2-bromothiophen-3-yl)methyl)spiro[[1,3]dioxolane-2,3'-indolin]-2'-one (**21**).

Obtained as a white solid (383 mg, 86%); ^1H NMR (200 MHz, CDCl_3): δ 7.19 (td, $J = 6.7$, 6.2, 4.0 Hz, 3H), 6.81 (d, $J = 5.7$ Hz, 1H), 6.72 (dd, $J = 6.5$ and 2.2 Hz, 1H), 4.75 (s, 2H), 4.72–4.37 (m, 4H); ^{13}C NMR (75 MHz, CDCl_3): δ 180.3, 157.1, 151.6, 138.4, 133.8, 128.8, 128.6, 121.6, 116.4, 111.5, 109.6, 66.7 38.6; MS-ESI: m/z 444 $[M + \text{H}]^+$, 466 $[M + \text{Na}]^+$, 886 $[2M]^+$; anal. calcd. for $\text{C}_{15}\text{H}_{11}\text{Br}_2\text{NO}_3\text{S}$: C 40.5; H 2.5; found: C 40.9; H 2.2. M.p. > 200°C (dec.).

4',7'-dibromo-1'-(thiophen-3-ylmethyl)spiro[[1,3]dioxolane-2,3'-indolin]-2'-one (**26**). Obtained as a white solid, (392 mg, 88%); ^1H NMR (200 MHz, CDCl_3): δ 7.35–7.23 (m, 2H), 7.18–6.97 (m, 3H), 5.31 (s, 2H), 4.74–4.36 (m, 4H); ^{13}C NMR (75 MHz, CDCl_3): δ 173.6, 142.9, 138.2, 137.0, 128.7, 126.4, 126.2, 125.4, 121.8, 119.2, 102.0, 101.6, 66.7, 40.2; MS-ESI: m/z 444 $[M + \text{H}]^+$, 466 $[M + \text{Na}]^+$, 886 $[2M]^+$; $^+$; anal. calcd. for $\text{C}_{15}\text{H}_{11}\text{Br}_2\text{NO}_3\text{S}$: C 40.5; H 2.5; found: C 40.1; H 2.8.

4',7'-dibromo-1'-((2-bromothiophen-3-yl)methyl)spiro[[1,3]dioxolane-2,3'-indolin]-2'-one (**29**). Obtained as a white solid (356 mg, 68%); ^1H NMR (200 MHz, CDCl_3): δ 7.29 (d, $J = 8.1$ Hz, 1H), 7.18 (d, $J = 5.7$ Hz, 1H), 7.07 (d, $J = 8.1$ Hz, 1H), 6.60 (d, $J = 5.7$ Hz, 1H), 5.18 (s, 2H), 4.62–4.46 (m, 4H); ^{13}C NMR (75 MHz, CDCl_3): δ 173.6, 142.9, 138.2, 137.0, 128.7, 126.4, 126.2, 125.4, 121.8, 119.2, 102.0, 101.6, 66.7, 40.2; MS-ESI: m/z 444 $[M + \text{H}]^+$, 466 $[M + \text{Na}]^+$, 886 $[2M]^+$; anal. calcd. for $\text{C}_{15}\text{H}_{10}\text{Br}_3\text{NO}_3\text{S}$: C 34.4; H 1.9; found: C 34.8; H 2.1.

7'-bromo-5',6'-difluoro-1'-(thiophen-3-ylmethyl)spiro[[1,3]dioxolane-2,3'-indolin]-2'-one (**34**). Obtained as a white solid (334 mg, 83%); ^1H NMR (200 MHz, CDCl_3): δ 7.29 (dd, $J = 4.9$ and 2.9 Hz, 1H), 7.21 (t, $J = 7.6$ Hz, 1H), 7.11 (s, 1H), 7.01 (d, $J = 6.0$ Hz, 1H), 5.28 (s, 2H), 4.68–4.25 (m, 4H); ^{13}C NMR (75 MHz, CDCl_3): δ 172.6, 149.4, 148.5, 146.1, 145.1, 130.6, 128.4, 116.6, 116.5, 111.7, 103.0, 65.9, 41.7; MS-ESI: m/z 402 $[M + \text{H}]^+$, 425 $[M + \text{Na}]^+$, 804 $[2M]^+$; anal. calcd. for $\text{C}_{15}\text{H}_{10}\text{BrF}_2\text{NO}_3\text{S}$: C 44.8; H 2.5; found: C 44.7; H 2.9.

General Procedure for the intramolecular DHA reaction. Example for the synthesis of **17**.

A suspension of *N*-benzylisatin ketal **16** (366mg, 1 mmol), Pd(OAc)₂ (5 mg, 0.02 mmol), KOAc (294 mg, 3 mmol), Bu₄NBr (322 mg, 1 mmol) in dry DMF (5 mL) was stirred and heated to reflux. After full conversion of the starting material (8 h, TLC monitoring), the reaction mixture was quenched with water, and the aqueous phase was extracted with ethyl acetate. The organic extracts were concentrated *in vacuo* and the solid purified by flash chromatography (SiO₂; *n*-hexanes:ethyl acetate 8:2) to afford the pure product **17** as a white solid (208 mg, 73%).

Spiro[[1,3]dioxolane-2,4'-pyrrolo[3,2,1-ij]thieno[3,2-c]quinolin]-5'(7'H)-one (**17**). Obtained as a white solid (208 mg, 73%); ¹H NMR (200 MHz, CDCl₃): δ 7.31–7.20 (m, 2H), 7.15 (dd, *J* = 7.5 and 1.0 Hz, 1H), 6.97 (t, *J* = 7.6 Hz, 1H), 6.86 (d, *J* = 5.1 Hz, 1H), 4.99 (s, 2H), 4.67–4.23 (m, 4H); ¹³C NMR (75 MHz, CDCl₃): δ 172.9, 138.6, 130.4, 129.5, 126.2, 125.3, 123.4, 123.3, 121.9, 115.4, 103.5, 65.7, 41.5; GC-MS (EI) rt: 18.37 min, *m/z* 285 [*M*]⁺; anal. calcd. for C₁₅H₁₁NO₃S: C 63.1; H 3.9; found: C 63.4; H 3.9.

1',2'-difluorospiro[[1,3]dioxolane-2,4'-pyrrolo[3,2,1-ij]thieno[3,2-c]quinolin]-5'(7'H)-one (**35**). Obtained as a white solid (148 mg, 46%); ¹H NMR (200 MHz, CDCl₃): δ 7.47 (d, *J* = 5.2 Hz, 1H), 7.09–6.88 (m, 2H), 5.02 (s, 2H), 4.67–4.22 (m, 4H); ¹³C NMR (75 MHz, CDCl₃): δ 172.6, 149.3, 148.5, 146.1, 145.1, 130.6, 128.4, 125.4, 116.5, 111.8, 106.4, 102.9, 65.9, 41.7; MS-ESI: *m/z* 322 [*M* + H]⁺, 344 [*M* + Na]⁺, 642 [2*M*]⁺; anal. calcd. for C₁₅H₉F₂NO₃S: C 56.1; H 2.8; found: C 56.4; H 2.9.

General Procedure for the deprotection. *Example for the synthesis of 18.* A solution of compound **17** (285 mg, 1 mmol) in THF (2.5 mL) and aqueous HCl 6M (2.5 mL) was stirred and heated to reflux for 6h. THF was removed *in vacuo* and the resulting aqueous phase was extracted with ethyl acetate. The combined organic extracts were concentrated *in vacuo* and resulting crude material was purified by chromatography (SiO₂; *n*-hexanes :ethyl acetate 9:1) to afford pure product **18** in quantitative yield.

4H-pyrrolo[3,2,1-ij]thieno[3,2-c]quinoline-4,5(7H)-dione (**18**). Obtained as a red solid (241

mg, 99%); ^1H NMR (200 MHz, CDCl_3): δ 7.53–7.29 (m, 3H), 7.01 (t, $J = 7.7$ Hz, 1H), 6.93 (d, $J = 5.2$ Hz, 1H), 5.13 (s, 2H); ^{13}C NMR (75 MHz, CDCl_3): δ 180.6, 167.4, 155.6, 143.6, 127.5, 126.8, 124.3, 124.2, 121.8, 121.1, 114.6, 113.4; 40.0; MS-ESI: m/z 242 [$M + \text{H}$] $^+$, 264 [$M + \text{Na}$] $^+$; single crystals suitable for X-Ray crystallography were obtained by slow evaporation of a solution of compound in CH_2Cl_2 . M.p. > 300°C (dec.).

*1,2-difluoro-4H-pyrrolo[3,2-*l*-ij]thieno[3,2-*c*]quinoline-4,5(7H)-dione (36)*. Obtained as a red solid (202 mg, 73%); ^1H NMR (200 MHz, CDCl_3): δ 7.56 (d, $J = 4.0$ Hz, 1H), 7.19 (t, $J = 7.9$ Hz, 1H), 7.01 (d, $J = 4.5$ Hz, 1H), 5.16 (s, 2H); ^{13}C NMR (75 MHz, CDCl_3): δ 186.6, 171.4, 157.2, 152.1, 130.9, 129.6, 125.5, 122.6, 117.6, 111.2, 110.9, 110.2, 42.0; MS-ESI: m/z 278 [$M + \text{H}$] $^+$; anal. calcd. for $\text{C}_{13}\text{H}_5\text{F}_2\text{NO}_2\text{S}$: C 56.3; H 1.8; found: C 56.6; H 2.0. M.p. > 300°C (dec.).

4,7-dibromoindoline-2,3-dione 24.¹⁵ Chloral hydrate (14.7 g, 88.8 mmol) was added to a suspension of hydroxylamine hydrochloride (18.5 g, 0.266 mol), sodium sulfate (84 g, 0.59 mol), and 2,5-dibromoaniline (74.0 mmol) in water (500 mL) and 2 M HCl (25 mL). The mixture was then heated at 55 °C overnight with stirring. After cooling to room temperature, the hydroxyiminoacetanilide intermediate was collected by filtration, washed with water and dried under vacuum. The intermediate was added in small portions, with stirring, to concentrated H_2SO_4 (45 mL), which had been heated to 55 °C. The temperature of the reaction mixture was maintained below 70 °C during the addition. The dark-colored solution was heated at 80 °C for an additional 10 min and then cooled to room temperature, poured onto crushed ice, and allowed to stand for 30 min. The precipitate was collected by filtration, washed three times with water, and dried under vacuum to yield isatin **24** to be used directly in the next step without further purification. ^1H NMR (200 MHz, $\text{DMSO-}d_6$) δ 7.54 (d, $J = 8.6$ Hz, 1H), 7.12 (d, $J = 8.6$ Hz, 1H).

7-bromo-1-((2-bromothiophen-3-yl)methyl)-4-(dimethylamino)indoline-2,3-dione (30). Cu powder (0.10 g, 1.67 mmol) was added to a solution of compound **28** (0.10 g, 0.21 mmol) in

dry DMF (10 mL) under nitrogen. The reaction mixture was heated under stirring at 130 °C for 3 days. The reaction mixture was quenched with water and the resulting aqueous phase was extracted with ethyl acetate. The combined organic extracts were removed of the solvent *in vacuo* and the crude material was purified by flash chromatography (SiO₂; *n*-hexanes:ethyl acetate 8:2) to afford pure compound **30** as a red solid (43 mg, 73%). ¹H NMR (200 MHz, CDCl₃): δ 7.29 (d, *J* = 9.2 Hz, 1H), 7.19 (d, *J* = 5.7 Hz, 1H), 6.68 (d, *J* = 5.7 Hz, 1H), 6.47 (d, *J* = 9.4 Hz, 1H), 5.28 (s, 2H), 3.16 (s, 6H). ¹³C NMR (75 MHz, CDCl₃): δ 176.4, 160.7, 151.2, 146.7, 143.1, 136.4, 129.5, 126.4, 124.0, 114.1, 108.6, 90.3, 43.3, 41.0; MS-ESI: *m/z* 284 [*M* + H]⁺; single crystals suitable for X-Ray crystallography were obtained by slow evaporation of a solution of compound in CH₂Cl₂. M.p. > 300°C (dec.).

General Procedure for the Stille-Kelly reaction for the attempted synthesis of compounds 22 and 31. *Example for the synthesis of 31.* Pd(PPh₃)₄ (0.013 g, 10% mol) was added to a solution of compound **29** (0.061 g, 0.12 mmol) in dry 1,4-dioxane (3 mL). The reaction mixture was purged with nitrogen for 5 min, then hexamethylditin (0.076 g, 0.24 mmol), was added under nitrogen. The reaction mixture was quenched with water after 1d (TLC monitoring) and solvents were removed *in vacuo*. The resulting crude solid was extracted with ethyl acetate and the organic extracts were concentrated *in vacuo*. ¹H NMR spectrum on crude of reaction did not show the expected signals of compound **22**.

7-bromo-5,6-difluoroindoline-2,3-dione (32). Chloral hydrate (477 mg, 5.8 mmol) was added to a suspension of hydroxylamine hydrochloride (584 mg, 16.8 mmol), sodium sulfate (2.05 g, 28.8 mmol), and 2-bromo-3,4-difluoroaniline (500 mg, 2.4 mmol) in 2M aqueous HCl (5 mL). The mixture was refluxed overnight with vigorous stirring. After cooling to room temperature, the hydroxyiminoacetanilide intermediate was collected by filtration as a yellow solid, which was washed with water and dried under vacuum. The intermediate was added in small portions, with stirring, to concentrated H₂SO₄. The temperature of the reaction mixture was maintained below 70 °C during the addition. The dark-colored solution was heated at 80

°C for 3 h and then cooled to room temperature, poured onto crushed ice, and allowed to stand for 30 min. The precipitate was collected by filtration, washed with water and toluene, and purified by flash chromatography (SiO₂; *n*-hexanes:ethyl acetate 8:2) to give the analytically pure product as a pale orange solid (290 mg, 46%); ¹H NMR (200 MHz, DMSO-*d*₆): δ 11.41 (s, 1H), 7.66 (d, *J* = 8.6 Hz, 1H), 7.17 (d, *J* = 8.6 Hz, 1H); ¹³C NMR (75 MHz, DMSO-*d*₆): δ 181.8, 159.8, 154.3, 150.9, 144.4, 114.5, 113.2, 94.3. GC-MS (EI) rt: 9.94 min, *m/z* 261 [*M*]⁺; anal. calcd. for C₈H₂BrF₂NO₂: C 36.8; H 0.8; found: C 36.6; H 0.9.

General Procedure for the Synthesis of 39a–c. *Example for the synthesis of 39a.* A solution of 4-bromo-1-methylindolin-2-one **37a** (226 mg, 1 mmol), Pd(OAc)₂ (11 mg, 0.05 mmol), PPh₃ (26 mg, 0.1 mmol), KOAc (294 mg, 3 mmol) in DMF dry (5 mL) was added at rt 3-formylthiophene **38a** (0.131 mL, 1.5 mmol) and then stirred to 150°C. After full conversion of the starting material (12 h, TLC monitoring), the reaction mixture was quenched with a solution of ammonium chloride 1M, and the aqueous phase was extracted with ethyl acetate. The organic extracts was dried with sodium sulfate, filtrated and concentrated *in vacuo*. Crude of reaction was purified by flash chromatography (SiO₂; *n*-hexanes:ethyl acetate 9:1) to afford the pure product **39a** as a white cream solid (110 mg, 46%).

4-methylthieno[2',3':4,5]benzo[1,2,3-cd]indol-5(4H)-one (39a): Obtained as a white cream solid (110 mg, 46%); ¹H NMR (200 MHz, CDCl₃): δ 8.41 (s, 1H), 7.73 (d, *J* = 8.4 Hz, 1H), 7.64 (s, 2H), 7.55 (t, *J* = 8.4, 7.1 Hz, 1H), 6.93 (d, *J* = 7.1 Hz, 1H), 3.47 (s, 3H); ¹³C NMR (75 MHz, CDCl₃): δ 168.0, 140.5, 140.3, 139.6, 128.7, 126.2, 126.0, 124.7, 124.0, 121.7, 121.0, 116.2, 104.2, 26.3; GC-MS (EI) rt: 17.35 min, *m/z* 239 [*M*]⁺.

4-octylthieno[2',3':4,5]benzo[1,2,3-cd]indol-5(4H)-one (39b): Obtained as a white cream solid (134 mg, 40%); ¹H NMR (200 MHz, CDCl₃): δ 8.44 (s, 1H), 7.75 (d, *J* = 8.4 Hz, 1H), 7.66 (s, 2H), 7.55 (t, *J* = 8.4, 7.1 Hz, 1H), 6.96 (d, *J* = 7.1 Hz, 1H) 3.94 (t, *J* = 7.2 Hz, 2H), 1.73 – 1.30 (m, 2H), 1.29 – 1.23 (m, 10H), 0.91 – 0.85 (m, 3H); ¹³C NMR (75 MHz, CDCl₃): δ 168.3, 141.1, 140.6, 129.7, 128.4, 126.9, 126.7, 125.6, 125.2, 121.8, 121.4, 116.6, 105.4, 41.0,

32.5, 30.8, 29.9, 29.3, 27.7, 23.3, 14.5; GC-MS (EI) rt: 42.44 min, m/z 337 $[M]^+$.

4-methylbenzofuro[5,6,7-cd]indol-5(4H)-one (3c): Obtained as a white cream solid (102 mg, 46%); ^1H NMR (200 MHz, CDCl_3): δ 8.29 (s, 1H), 7.90 – 7.80 (m, 2H), 7.58 (t, $J = 7.2$ Hz, 1H), 7.08 (d, $J = 2.2$ Hz, 1H), 6.95 (d, $J = 7.2$ Hz, 1H), 3.48 (s, 3H); ^{13}C NMR (75 MHz, CDCl_3): δ 169.5, 141.5, 141.1, 140.6, 129.7, 126.9, 126.4, 125.7, 124.7, 122.3, 121.0, 116.6, 104.1, 26.2; GC-MS (EI) rt: 14.85 min, m/z 223 $[M]^+$.

General Procedure for the Synthesis of thiophene- and furan-based compounds. *Example for the synthesis of 46.* A solution of 3-thiopheneacetic acid **44** (146 mg, 1 mmol), $\text{Pd}(\text{OAc})_2$ (5 mg, 0.02 mmol), PPh_3 (11 mg, 0.04 mmol), K_2CO_3 (276 mg, 2 mmol) in DMF dry (5 mL) was added at rt 2-bromobenzaldehyde **43** (0.115 mL, 1 mmol) and then stirred to 110°C . After 12h, reaction suspension was warmed to rt and then ethyl iodine (0.160 mL, 2 mmol) was added in one portion. Reaction suspension was conducted to rt until completion (4 h, TLC monitoring), then was quenched with a solution of ammonium chloride 1M and the aqueous phase was extracted with ethyl acetate. The organic extracts was dried with sodium sulfate, filtrated and concentrated *in vacuo*. Crude of reaction was purified by flash chromatography (SiO_2 ; *n*-hexanes:ethyl acetate 9:1) to afford the pure product **46** as a white cream solid (233 mg, 91%).

Ethyl naphtho[1,2-b]thiophene-4-carboxylate (46): Obtained as a white cream solid (233 mg, 91%); ^1H NMR (200 MHz, CDCl_3): δ 8.59 (s, 1H), 8.35 (d, $J = 5.5$ Hz, 1H), 8.18 (d, $J = 8.1$ Hz, 1H), 8.04 (d, $J = 8.1$ Hz, 1H), 7.68 (t, $J = 7.6$ Hz, 1H), 7.62 (d, $J = 5.5$ Hz, 1H), 7.57 (t, $J = 7.6$ Hz, 1H), 4.53 (q, $J = 7.1$ Hz, 2H), 1.52 (t, $J = 7.1$ Hz, 3H); ^{13}C NMR (75 MHz, CDCl_3): δ 166.7, 139.0, 135.0, 130.8, 130.3, 130.1, 129.4, 128.9, 126.1, 125.8, 125.7, 123.6, 123.5, 61.1, 14.3; GC-MS (EI) rt: 16.77 min, m/z 256 $[M]^+$.

Naphtho[1,2-b]thiophene-4-carboxylic acid (50): Obtained as a green solid (217 mg, 95%); ^1H NMR (200 MHz, CDCl_3): δ 13.11 (s, 1H), 8.61 (s, 1H), 8.30 – 8.18 (m, 3H), 7.96 (d, $J = 5.5$ Hz, 1H), 7.80 – 7.68 (m, 2H); ^{13}C NMR (75 MHz, CDCl_3): δ 167.5, 138.2, 135.0, 131.5,

130.3, 130.0, 129.8, 129.5, 127.2, 126.6, 125.6, 124.0, 123.2; ESI-MS: m/z 227 $[M]^-$; anal. calcd. for $C_{13}H_8O_2S$: C 68.40; H 3.53; found: C 68.39; H 3.58.

Ethyl naphtho[1,2-b]furan-4-carboxylate (53): Obtained as a white cream solid (233 mg, 81%); 1H NMR (200 MHz, $CDCl_3$): δ 8.42 (s, 1H), 8.21 (d, $J = 5.5$ Hz, 1H), 7.81 (t, $J = 5.2$ Hz, 1H), 7.72 – 7.42 (m, 3H), 6.97 (d, $J = 7.5$ Hz, 1H), 4.29 (q, $J = 5.9$ Hz, 2H), 1.30 (t, $J = 5.9$ Hz, 3H); ^{13}C NMR (75 MHz, $CDCl_3$): δ 168.4, 148.3, 144.4, 133.3, 130.0, 127.5, 127.3, 126.4, 125.7, 124.2, 121.9, 121.1, 103.3, 61.2, 14.7; ESI-MS m/z 241 $[M]^+$; anal. calcd. for $C_{15}H_{12}O_3$: C 74.99; H 5.03; found: C 75.01; H 5.10.

Octyl naphtho[1,2-b]thiophene-4-carboxylate (54a): Obtained as a white cream solid (245 mg, 72%); 1H NMR (200 MHz, $CDCl_3$): δ 8.58 (s, 1H), 8.35 (d, $J = 5.5$ Hz, 1H), 8.18 (d, $J = 8.1$ Hz, 1H), 8.04 (d, $J = 7.7$ Hz, 1H), 7.74 – 7.50 (m, 3H), 4.46 (t, $J = 6.7$ Hz, 2H), 1.87 (q, $J = 7.0$ Hz, 2H), 1.57 – 1.22 (m, 10H), 0.93 – 0.87 (m, 3H); ^{13}C NMR (75 MHz, $CDCl_3$): δ 167.6, 139.8, 135.9, 131.6, 131.1, 130.9, 130.2, 129.7, 129.0, 126.9, 126.8, 126.5, 124.3, 66.1, 32.5, 29.9, 29.7, 29.5, 26.8, 23.3, 14.8; GC-MS (EI) rt: 22.39 min, m/z 340 $[M]^+$.

2-ethylhexyl naphtho[1,2-b]thiophene-4-carboxylate (54b): Obtained as a white cream solid (258 mg, 76%); 1H NMR (200 MHz, $CDCl_3$): δ 8.58 (s, 1H), 8.35 (d, $J = 5.5$ Hz, 1H), 8.18 (d, $J = 8.1$ Hz, 1H), 8.07 (d, $J = 7.8$ Hz, 1H), 7.76 – 7.48 (m, 3H), 4.10 (d, $J = 7.4$, 1.2 Hz, 2H), 1.80 (q, $J = 12.7$, 6.8 Hz, 1H), 1.74 – 1.09 (m, 8H), 0.92 (q, $J = 6.8$ Hz, 6H); ^{13}C NMR (75 MHz, $CDCl_3$): δ 166.7, 139.0, 135.0, 130.8, 130.3, 130.1, 129.4, 128.9, 126.1, 125.8, 125.7, 123.6, 123.5, 44.3, 37.2, 30.4, 28.5, 23.8, 22.9, 13.9, 10.4; ESI-MS: m/z 341 $[M]^+$; anal. calcd. for $C_{21}H_{24}O_2S$: C 74.08; H 7.10; found: C 74.05; H 7.14.

Ethyl thieno[2',3':5,6]naphtho[2,3-d][1,3]dioxole-4-carboxylate (55): Obtained as a white cream solid (237 mg, 79%); 1H NMR (200 MHz, $CDCl_3$): δ 8.52 (d, $J = 1.5$ Hz, 1H), 7.72 (s, 1H), 7.57 (d, $J = 7.5$ Hz, 1H), 7.42 (d, $J = 7.4$ Hz, 1H), 7.30 (d, $J = 1.5$ Hz, 1H), 4.29 (q, $J = 5.9$ Hz, 2H), 3.92 (s, 2H), 1.30 (t, $J = 5.9$ Hz, 3H); ^{13}C NMR (75 MHz, $CDCl_3$): δ ; ESI-MS:

m/z 301[M]⁺.

Ethyl benzo[1,2-b:6,5-b']dithiophene-4-carboxylate (**56**): ¹H NMR (400. MHz, CDCl₃): δ 8.57 (1H, s), 8.32 (d, *J* = 5.5 Hz, 1H), 7.53 (d, *J* = 5.5 Hz, 1H), 7.49 (d, *J* = 5.5 Hz, 1H), 7.45 (d, *J* = 5.5 Hz, 1H), 4.02 (q, *J* = 7.1 Hz, 2H), 1.52 (t, *J* = 7.1 Hz, 3H); ¹³C NMR (100.1 MHz, CDCl₃): δ 167.3, 138.0, 136.1, 135.5, 134.8, 125.7, 125.6, 125.2, 125.1, 124.3, 121.9, 52.0, 14.3; GC-MS (EI): rt 21.29, 262 [M]⁺.

anthra[1,2-b:5,6-b']dithiophene-4,10-dicarboxylic acid (**65**). 2,5-Dibromobenzene-1,4-dicarbaldehyde (1 mmol, 291 mg) and K₂CO₃ (4 mmol, 552 mg) was added to a stirred mixture of 3-thiopheneacetic acid (2 mmol, 284 mg), triphenylphosphine (0,04 mmol, 10.5 mg) and Pd(OAc)₂ (0,02 mmol, 4,5 mg) in dry DMAc (5 mL). The resulting mixture was stirred at 130°C for 48h. The mixture was cooled to room temperature and quenched with water, the solvent was removed *in vacuo*. The crude of the reaction was treated with HCl 1M and filtered under vacuum. The green solid obtained was washed several times with methanol to afford pure compound **5** as a dark powder (275 mg, 73%). ¹H NMR (200 MHz, DMSO-*d*₆): δ 13.28 (bs, 2H), 9.16 (s, 2H), 8.88 (s, 2H) 8.30 (d, *J* = 5.4 Hz, 2H), 8.50 (d, *J* = 5.4 Hz, 2H).

General procedure for the synthesis of 66a–c. *Example for the synthesis of 66a.* 1-Bromo-2-ethylhexane (3 mmol, 0.53 mL) was added to a stirred mixture of anthra[1,2-b:5,6-b']dithiophene-4,10-dicarboxylic acid **65** (1 mmol, 378 mg) and K₂CO₃ (4 mmol, 552 mg) in DMAc dry (5 mL). The resulting mixture was stirred at 130°C for 48h. The reaction mixture was quenched with water and solvent was removed *in vacuo*. A solution of ammonium chloride was added and the aqueous phase was extracted with diethyl ether. The combined organic extracts were washed with brine and the solvent was removed *in vacuo*. The crude material was purified by crystallization with methanol to give pure compound **66a** as yellow solid (295 mg, 49%).

bis(2-ethylhexyl) anthra[1,2-b:5,6-b']dithiophene-4,10-dicarboxylate (**66a**). Obtained as yellow solid (295 mg, 49%). ¹H NMR (200 MHz, CDCl₃): δ 8.89 (s, 2H), 8.79 (s, 2H), 8.40 (d, *J*

= 5.4 Hz, 2H), 7.67 (d, $J = 5.4$ Hz, 2H), 4.47 (t, $J = 6.7$ Hz, 4H), 1.91 (m, 4H), 1.43 (m, 20H), 0.91 (m, 6H).

*diocetyl anthra[1,2-*b*:5,6-*b'*]dithiophene-4,10-dicarboxylate (66b)*. Obtained as yellow solid (144 mg, 24%). ^1H NMR (200 MHz, CDCl_3): δ 8.89 (s, 2H), 8.79 (s, 2H), 8.40 (d, $J = 5.4$ Hz, 2H), 7.67 (d, $J = 5.4$ Hz, 2H), 4.47 (t, $J = 6.7$ Hz, 4H), 1.91 (m, 4H), 1.43 (m, 20H), 0.91 (m, 6H); ^{13}C NMR (75 MHz, CDCl_3): δ 166.4, 138.9, 134.4, 130.7, 129.9, 128.5, 126.4, 125.5, 125.1, 124.5, 65.5, 31.7, 29.2, 29.1, 28.7, 26.1, 22.6, 14.0.

*diethyl anthra[1,2-*b*:5,6-*b'*]dithiophene-4,10-dicarboxylate (66c)*. Obtained as yellow solid (34.6 mg, 8%). ^1H NMR (200 MHz, CDCl_3): δ 8.87 (s, 2H), 8.78 (s, 2H), 8.39 (d, $J = 5.4$ Hz, 2H), 7.66 (d, $J = 5.4$ Hz, 2H), 4.53 (q, $J = 7.1$ Hz, 4H), 5.43 (t, $J = 5.1$ Hz, 6H); ^{13}C NMR (75 MHz, CDCl_3): δ 182.2, 158.7, 147.4, 144.0, 136.5, 126.8, 126.4, 125.1, 124.7, 122.8, 120.8, 104.3, 40.3; MS-ESI: m/z 322 [$M + \text{H}$] $^+$

Bis(2-ethylhexyl) 2,8-dibromoanthra[1,2-*b*:5,6-*b'*]dithiophene-4,10-dicarboxylate (67). NBS (3 mmol, 0.53 mL) was added portionwise over 15 min to a stirred solution of bis(2-ethylhexyl) anthra[1,2-*b*:5,6-*b'*]dithiophene-4,10-dicarboxylate **66a** (1 mmol, 761 mg) in CHCl_3 :AcOH (8 mL:0.8 mL). The resulting mixture was stirred overnight at room temperature, then quenched with water, extracted with chloroform and washed with brine. The collected organic layer was dried over Na_2SO_4 . After removal of the solvent under reduced pressure, the residue was crystallized in a mixture of dichloromethane and ethanol to give **67** as yellow solid (556 mg, 73%). ^1H NMR (400 MHz, CDCl_3): δ 8.62 (s, 2H), 8.55 (s, 2H), 8.37 (s, 2H), 4.42 (m, 4H), 1.87 (m, 2H); 1.58 (m, 18H), 1.47 (m, 6H).

3-[2-(thiophen-3-yl)ethynyl]thiophene (70). Tryethylamine (30 mL) and 3-ethynylthiophene (2.163 g, 20 mmol) were introduced at room temperature, under nitrogen, in a flame-dried Schlenk flask. 3-bromothiophene (3.912 g, 24 mmol), copper(I)iodide (0.076 g, 0.4 mmol) and $\text{PdCl}_2(\text{PPh})_3$ (0.140 g, 0.2 mmol) were added sequentially. The resulting mixture was stirred for 3h at 80°C. The mixture was cooled to room temperature and quenched with a so-

lution of HCl 1M, extracted with ethyl acetate and washed with brine. The collected organic layer was dried over Na₂SO₄. After removal of the solvent under reduced pressure, the residue was purified by flash-chromatography (SiO₂; *n*-hexanes:ethyl acetate 9:1) to afford pure **70** as white solid (3.45 g, 91%). ¹H NMR (400 MHz, CDCl₃): δ 7.51 (dd, *J* = 3.0, 1.0 Hz, 1H), 7.31 (dd, *J* = 5.0, 3.0 Hz, 1H), 7.19 (dd, *J* = 3.0, 1.0 Hz, 1H).

bis(thiophen-3-yl)ethane-1,2-dione (71). A flame-dried Schlenk flask was charged with 3-[2-(thiophen-3-yl)ethynyl]thiophene **70** (3.043 g, 16 mmol), DMSO (70 mL), Pd(OAc)₂ (0.359 g, 1.6 mmol) and CuBr₂ (0.358 g, 1.6 mmol). The resulting mixture was stirred for 4h at 120°C. The mixture was cooled to room temperature and quenched with brine, extracted with diethyl ether and washed with brine. The collected organic layer was dried over Na₂SO₄. After removal of the solvent under reduced pressure, the residue was purified by flash-chromatography (SiO₂; *n*-hexanes:ethyl acetate 9:1) to afford pure **71** as white solid (2.96 g, 84%). ¹H NMR (400 MHz, CDCl₃): δ 8.26 (dd, *J* = 3.0, 1.0 Hz, 1H), 7.59 (dd, *J* = 5.0, 3.0 Hz, 1H), 7.24 (dd, *J* = 3.0, 1.0 Hz, 1H).

benzo[1,2-b:6,5-b']dithiophene-4,5-dione (72). A flame-dried Schlenk flask was charged with bis(thiophen-3-yl)ethane-1,2-dione **71** (2.89 g, 13 mmol), dichloromethane (80 mL) and FeCl₃ dry (4.92 g, 39 mmol). The resulting mixture was stirred for 2 h at room temperature. The mixture was quenched with water and the solvent was removed under reduced pressure. The dark solid was collected by filtration under *vacuum* and the solid residue was purified by crystallization with acetonitrile to give **72** as dark crystalline solid (2.61 g, 95%). ¹H NMR (400 MHz, CDCl₃): δ 7.52 (dd, *J* = 5.2 Hz, 2H), 7.23 (dd, *J* = 5.2 Hz, 2H).

2,7-dibromobenzo[1,2-b:6,5-b']dithiophene-4,5-dione (73). NBS (20 mmol, 3.56 g) was added portionwise over 15 min to a stirred solution of benzo[1,2-b:6,5-b']dithiophene-4,5-dione **72** (10 mmol, 2.20 g) in CHCl₃ (80 mL). The resulting mixture was stirred for 6h at room temperature. The mixture was quenched with water and the solvent was removed under reduced pressure. The dark solid was collected by filtration under *vacuum* and the solid resi-

due was purified by crystallization with acetonitrile to give **73** as violet-dark crystalline solid (3.51 g, 93%). ¹H NMR (400 MHz, CDCl₃): δ 7.47 (s, 2H).

General procedure for the synthesis of 76a–b. *Example for the synthesis of 76a.* To a stirred mixture of benzo[1,2-b:6,5-b']dithiophene-4,5-dione **72** (1 mmol, 378 mg) and K₂CO₃ (4 mmol, 552 mg) in ethanol (5 mL) was added diethylcarboxylic-1,3-acetone (2 mmol, 0.53 mL). The resulting mixture was stirred at room temperature for 6h. Reaction mixture was quenched with water and the white solid was filtrated under *vacuum* and washed with ethanol. The white solid was dried under vacuum to give 16a (0.359 g, 61%).

(4R,6S,10S,12R)-tetraethyl 5,11-dioxo-5,6-dihydro-4H-3b,6a-propanoindeno[5,4-b:6,7-b'] dithiophene-4,6,10,12-tetracarboxylate (76a). Obtained as a white solid (358 mg, 61%). ¹H NMR (200 MHz, DMSO-*d*₆): δ 8.87– 7.28 (m, 4H), 5.16 – 3.89 (m, 12H), 1.27 – 0.99 (m, 12H).

(4R,6S,10S,12R)-tetramethyl 5,11-dioxo-5,6-dihydro-4H-3b,6a-propanoindeno[5,4-b:6,7-b'] dithiophene-4,6,10,12-tetracarboxylate (76b). Obtained as a white solid (358 mg, 61%). ¹H NMR (200 MHz, DMSO-*d*₆): δ 7.97– 7.02 (m, 4H), 5.56 – 4.24 (m, 4H), 3.64 – 3.31 (m, 9H).

4.3 REFERENCES

- (1). C. Kanimozhi, P. Balraju, G. D. Sharma, S. Patil, *J. Phys. Chem. B* **2010**, *114*, 3095-3103.
- (2). M.-J. Baek, G. Fei, S.-H. Lee, K. Zong, Y.-S. Lee, *Synth. Met.* **2009**, *159*, 1261-1266.
- (3). A. K. Sharma, D. Pasini, *J. Fluorine Chem.* **2011**, *132*, 956-960.
- (4). Y. Liang, Y. Wu, D. Feng, S.T. Tsai, H.J. Son, G. Li, *J. Am. Chem. Soc.* **2009**, *131*, 56-57.
- (5). C.-Y. Mei, L. Liang, F.-G. Zhao, J.-T. Wang, L.-F. Yu, Y.-X. Li, W.-S. Li, *Macromolecules* **2013**, *46*, 7920-7931.
- (6). Yang, X.; Liu, D.; Miao, Q. *Angew. Chem. Int. Ed.* **2014**, *53*, 6786–6790.
- (7). Farrugia, L.J. *J. Appl. Crystallogr.* **2012**, *45*, 849-854.
- (8). North, A.C.T.; Phillips, D.C.; Mathews, F.S. *Acta. Crystallogr.* **1968**, *A24*, 351-359.
- (9). Altomare, A.; Burla, M. C.; Camalli, M.; Cascarano, G. L.; Giacovazzo, C.; Guagliardi, A.; Moliterni, A. G. G.; Polidori, G.; Spagna, R. *J. Appl. Crystallogr.* **1999**, *32*, 115-119.
- (10). Sheldrick, G. M. *Acta Crystallogr.* **2008**, *A64*, 112-122.
- (11). (a) Becke, A. D. *J. Chem. Phys.* **1993**, *98*, 1372-1377; (b) Becke, A. D. *J. Chem. Phys.* **1993**, *98*, 5648-5652; (c) Becke, A. D. *J. Chem. Phys.* **1996**, *104*, 1040-1046.
- (12). Halgren, T. A. *J. Comput. Chem.* **1996**, *17*, 490-519.
- (13). Ngwendson, J. N.; Atemnkeng, W. N.; Schultze, C. M.; Banerjee, A.; *Org. Lett.* **2006**, *8*, 4085-4088.
- (14). Zhuang, W; Bolognesi, M.; Seri, M.; Henriksson, P.; Gedefaw, D.; Kroon, R.; Jarvid, M.; Lundin, A.; Wang, E.; Muccini, M.; Andersson, M. R.; *Macromolecules* **2013**, *46*, 8488-8499.
- (15). Miljanic, O. S.; Vollhardt, K. P. C.; Whitener, G. D.; *Synlett* **2003**, 29-34.

Appendix

DONOR-ACCEPTOR CONJUGATED COPOLYMERS INCORPORATING TETRAFLUORO-BENZENE AS THE π -ELECTRON DEFICIENT UNIT

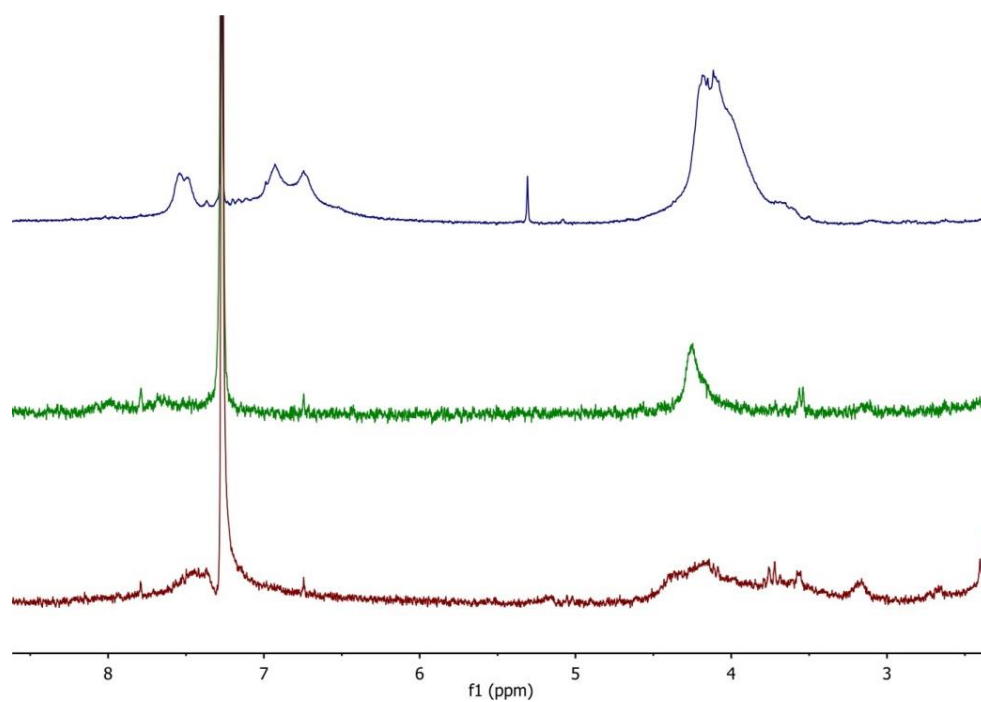


Figure A1. Partial ¹H NMR spectra (200 MHz, CDCl₃, 25°C) of polymer **P4a** (blue, top), **P4cS** (green, middle) and **P4b** (red, bottom)

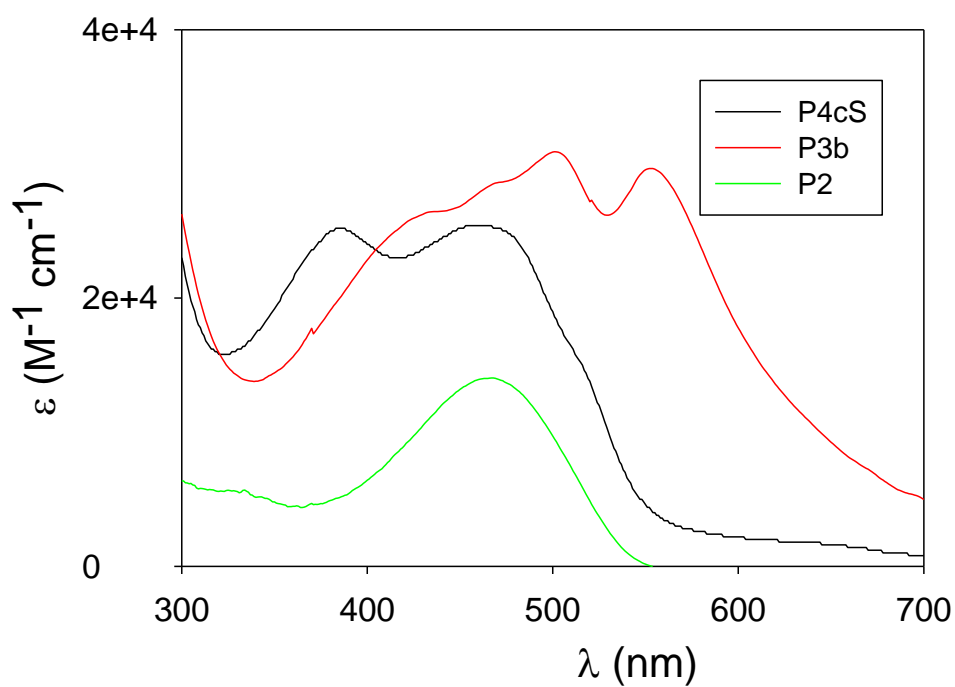


Figure A2. UV/Vis spectra of polymers **P2**, **P4cS** and **P3b** (CHCl_3 , 10^{-4} - 10^{-5} M)

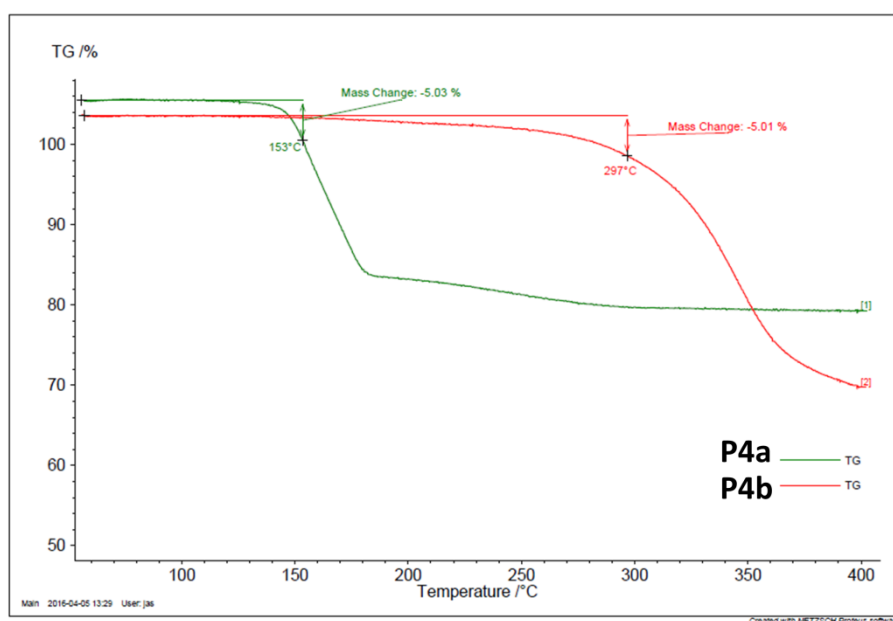


Figure A3. TG analysis of **P4a** and **P4b**

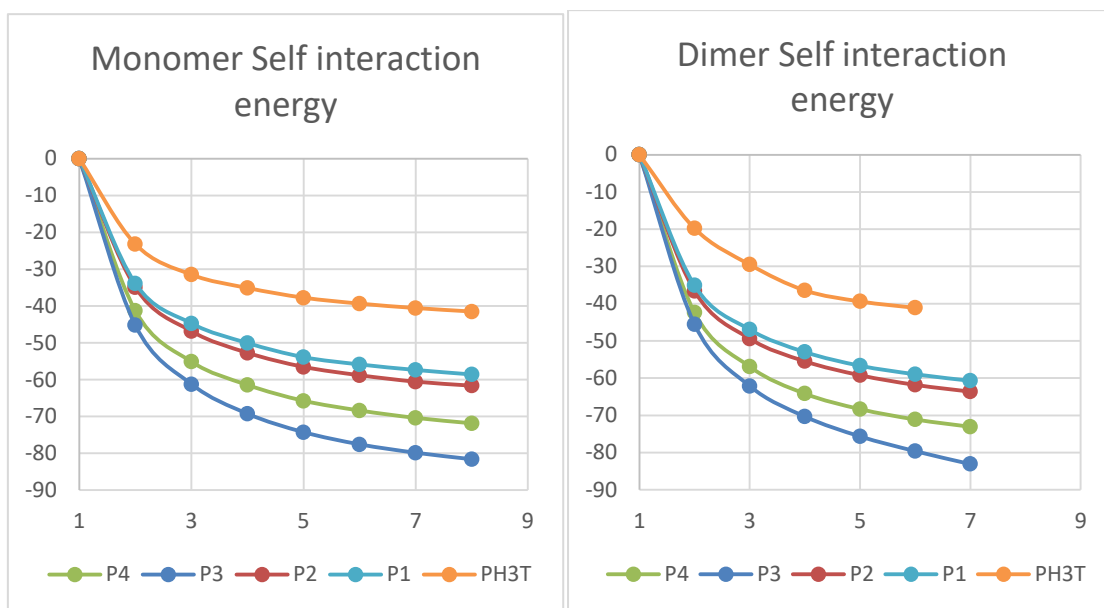
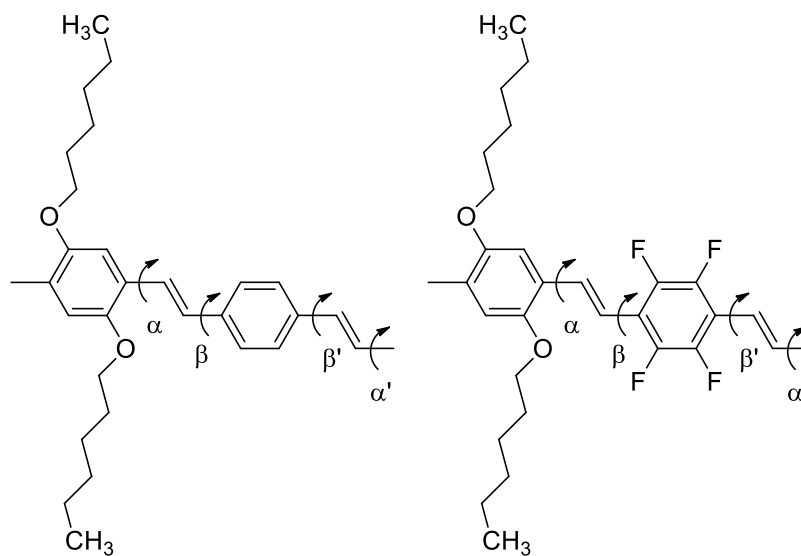


Figure A4. Absolute self interaction energy per monomer (left) or dimer (right) are plotted in kJ/mol unit versus number of stacked units

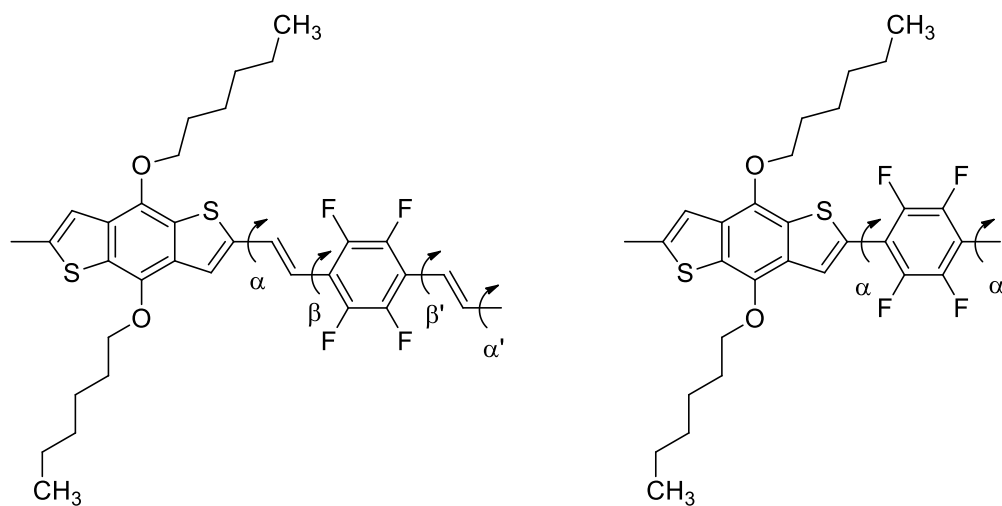
Table A1. Torsion angles in polymers P1, P2, P3, P4, P3H and P4H (in degrees)

Polymer	α	β	$\beta\delta$	$\alpha\epsilon$
P1	45.0	39.0	-44.0	-43.0
P2	45.5	38.4	-44.8	-39.9
P3	7.83	37.0	-10	-36.9
P4	-50.1	-	-	50.1
P3H	-18.0	24.7	-25.0	17.0
P4H	-51.0	-	-	51.0



P1

P2



P3

P4

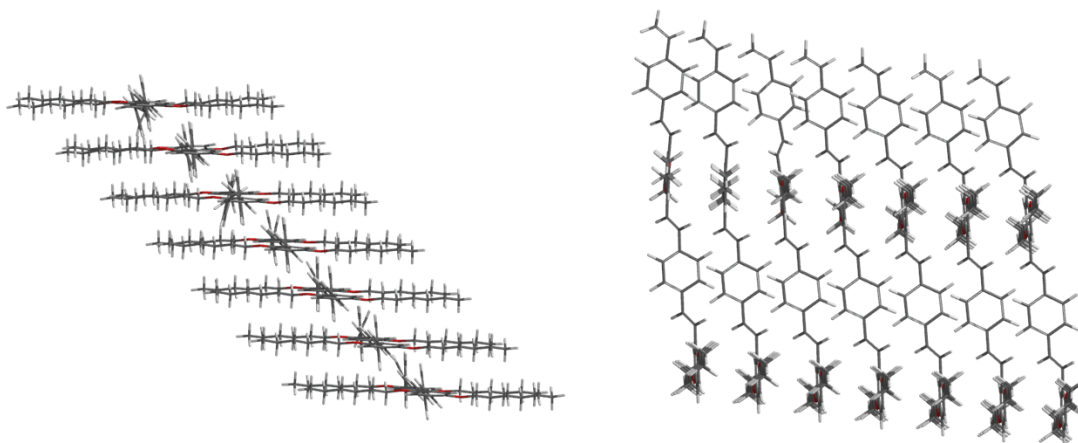


Figure A5. Optimized stacked dimeric units of polymer **P1**. Left: view interaction of side chains in a plane orthogonal to the plane of backbone. Right: view interaction of conjugated backbone.

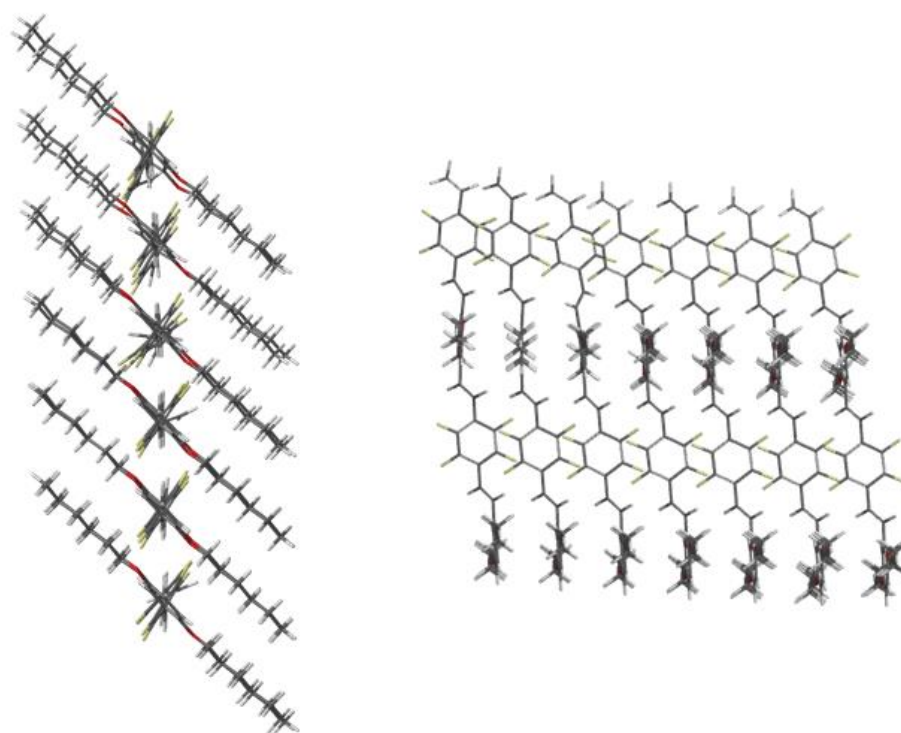


Figure A6. Optimized stacked dimeric unit of polymer **P2**. Left: view interaction of side chains in a plane orthogonal to the plane of backbone. Right: view interaction of conjugated backbone.

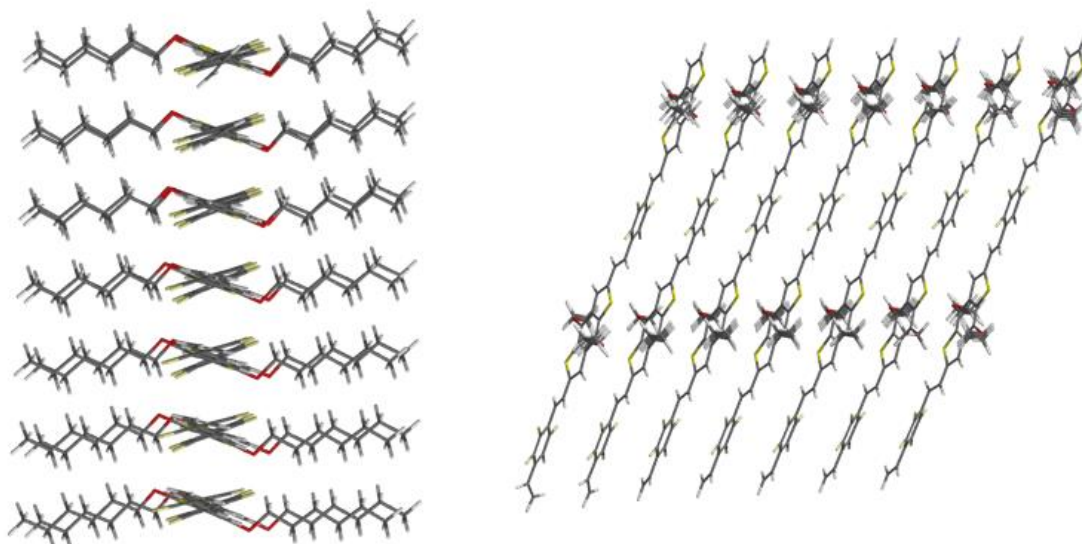


Figure A7. Optimized stacked dimeric unit of polymer **P3**. Left: view interaction of side chains in a plane orthogonal to the plane of backbone. Right: view interaction of conjugated backbone.

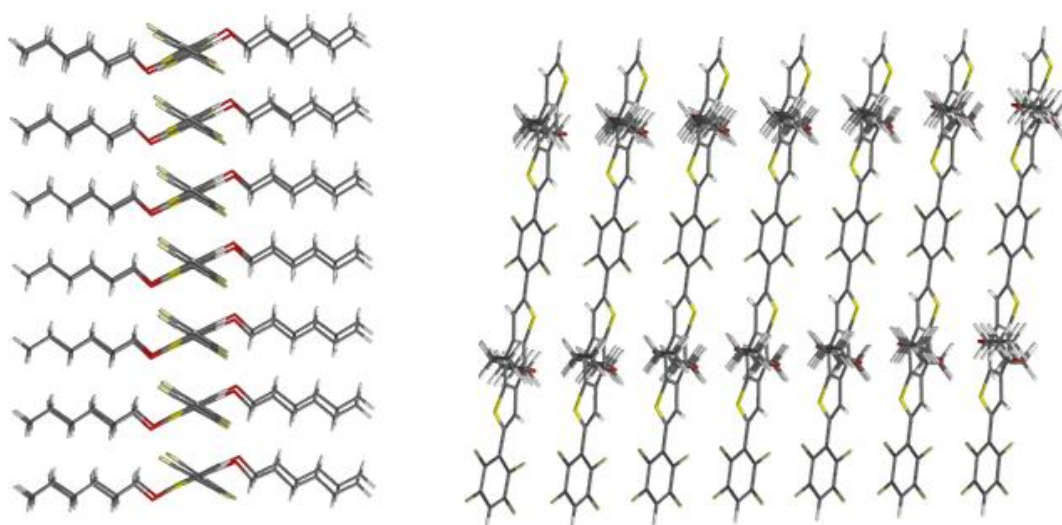
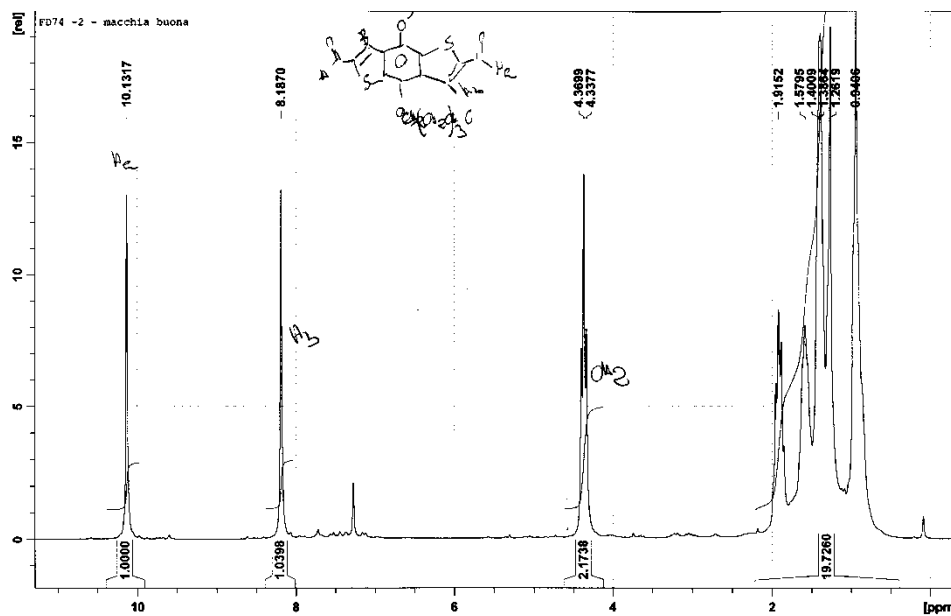


Figure A8. Optimized stacked dimeric unit of polymer **P4**. Left: view interaction of side chains in a plane orthogonal to the plane of backbone. Right: view interaction of conjugated backbone.

Copies of NMR of Newly Synthesized Compounds and Polymers

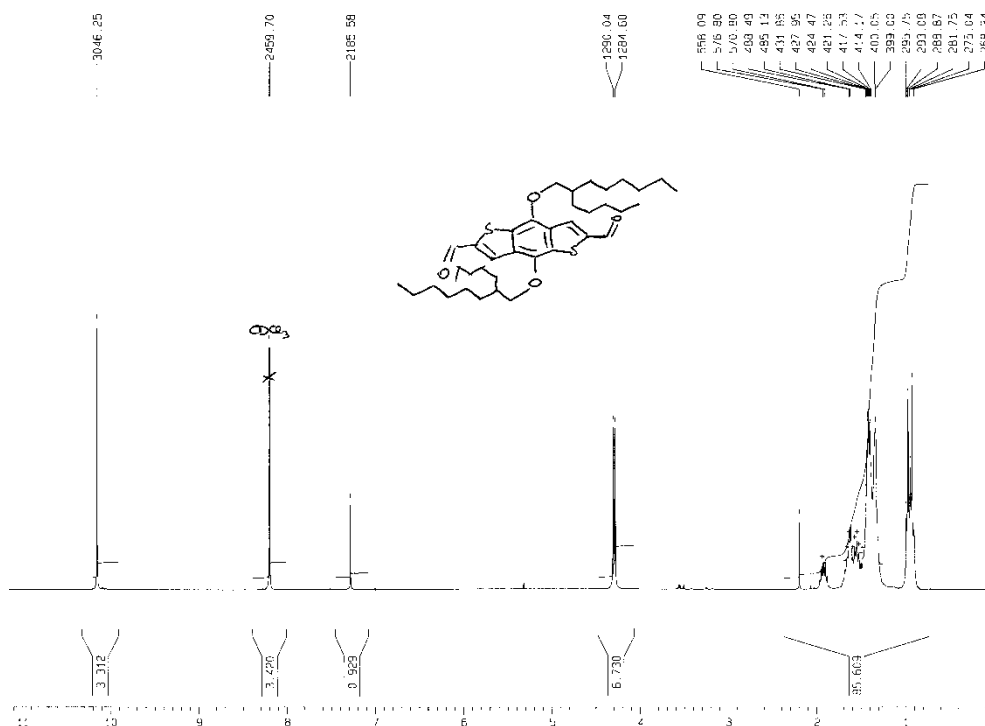
Monomer 4.

^1H NMR (CDCl_3 , 200 MHz)



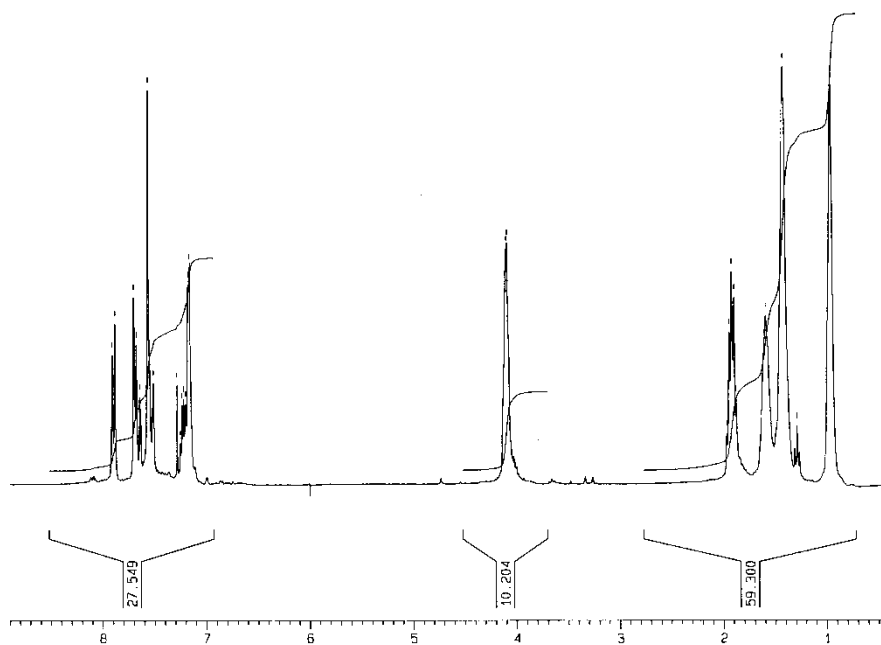
Monomer 5

^1H NMR (CDCl_3 , 200 MHz)

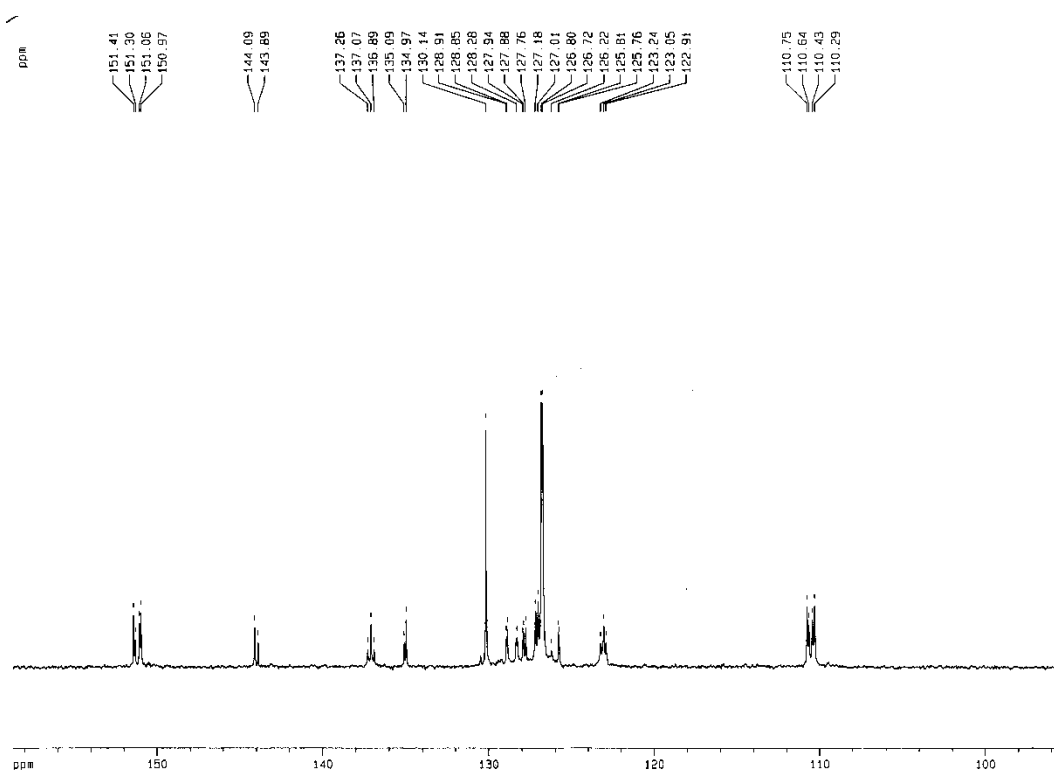


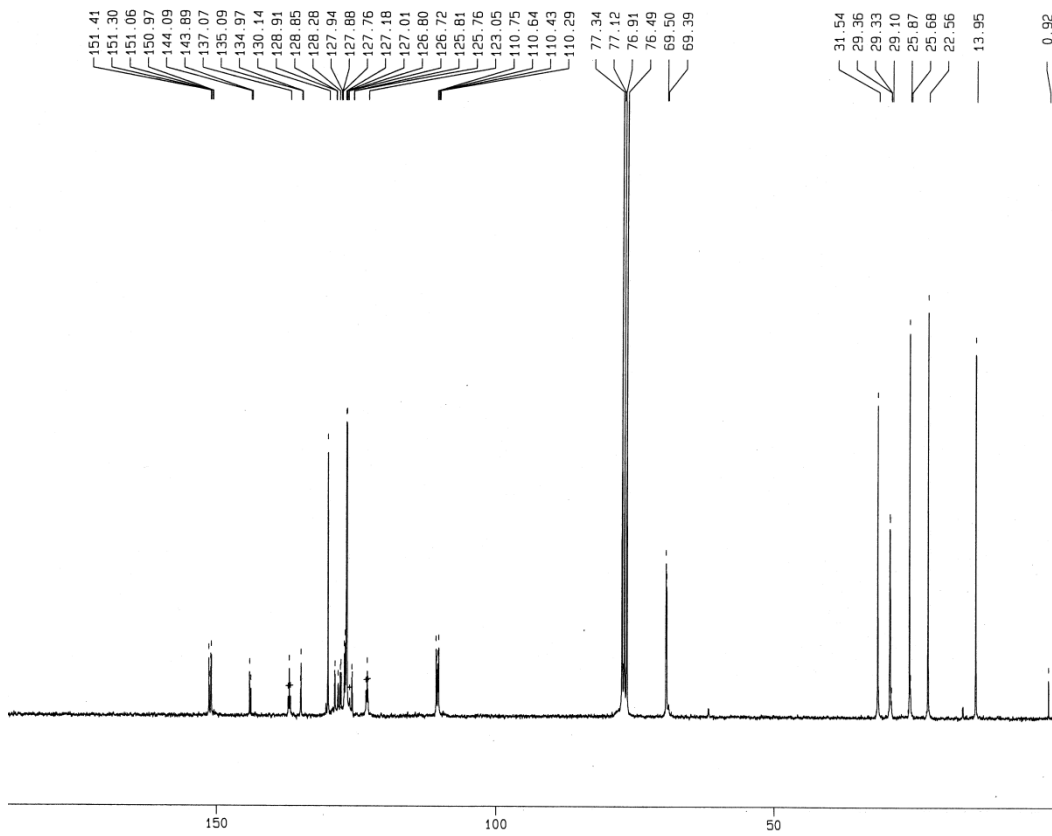
Polymer **P1**.

^1H NMR (CDCl_3 , 300 MHz)



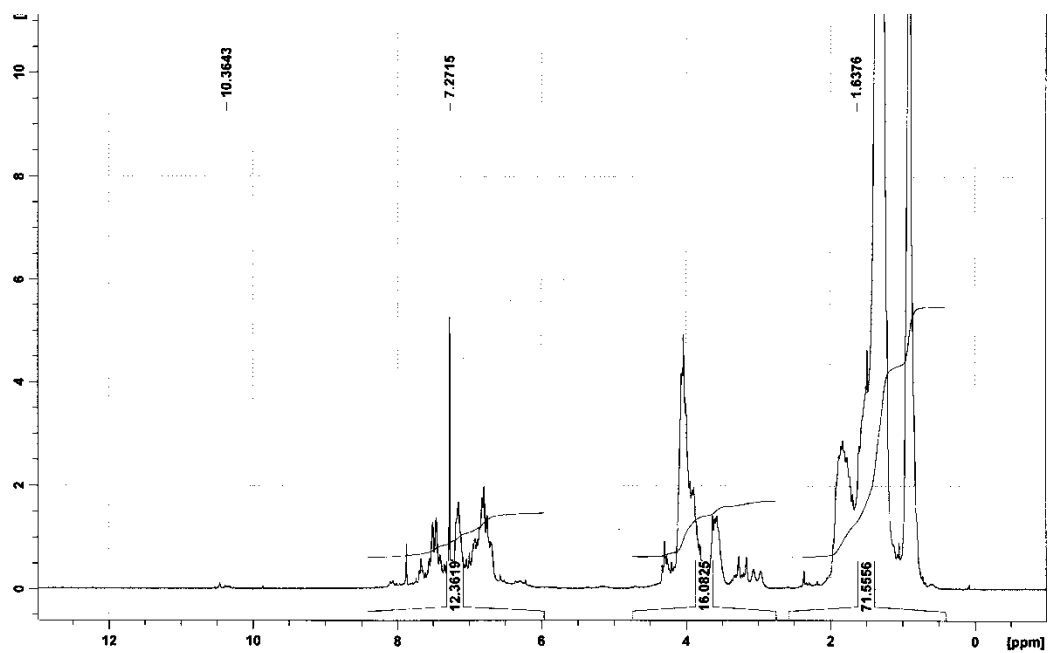
^{13}C NMR (CDCl_3 , 75 MHz)



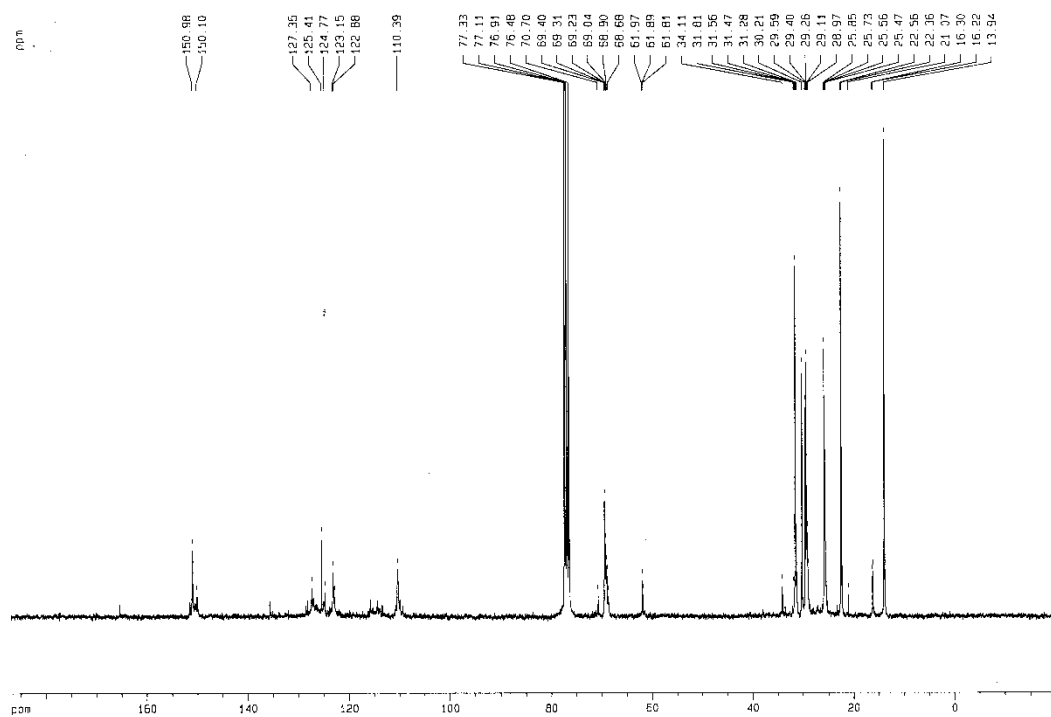


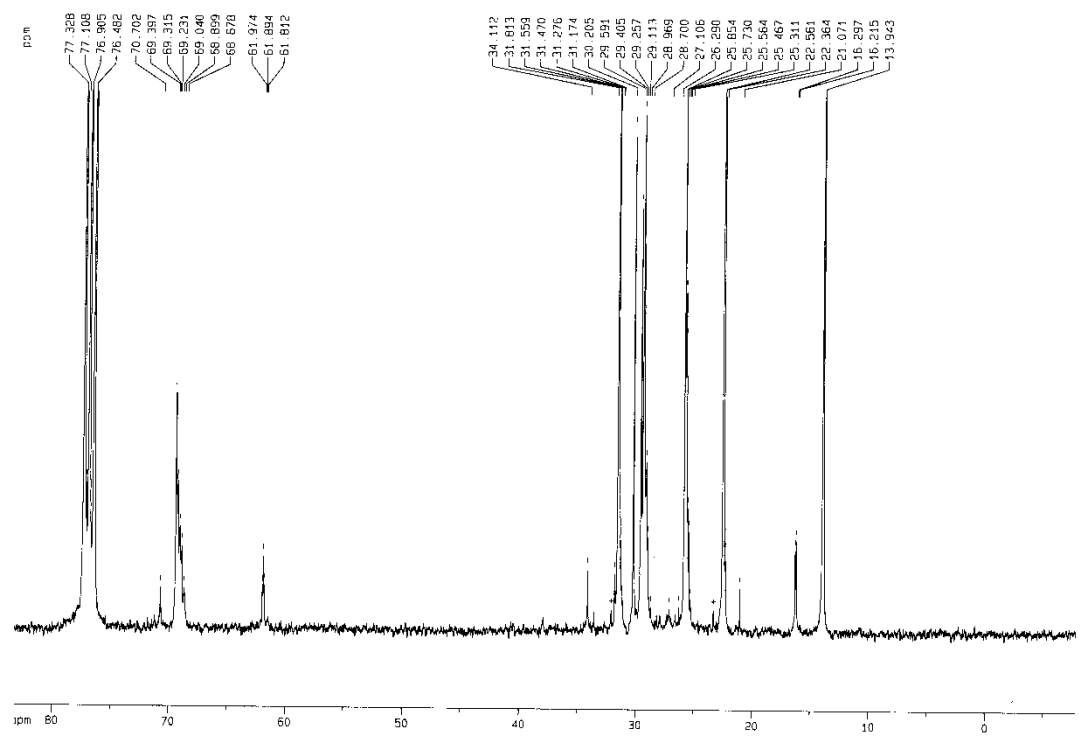
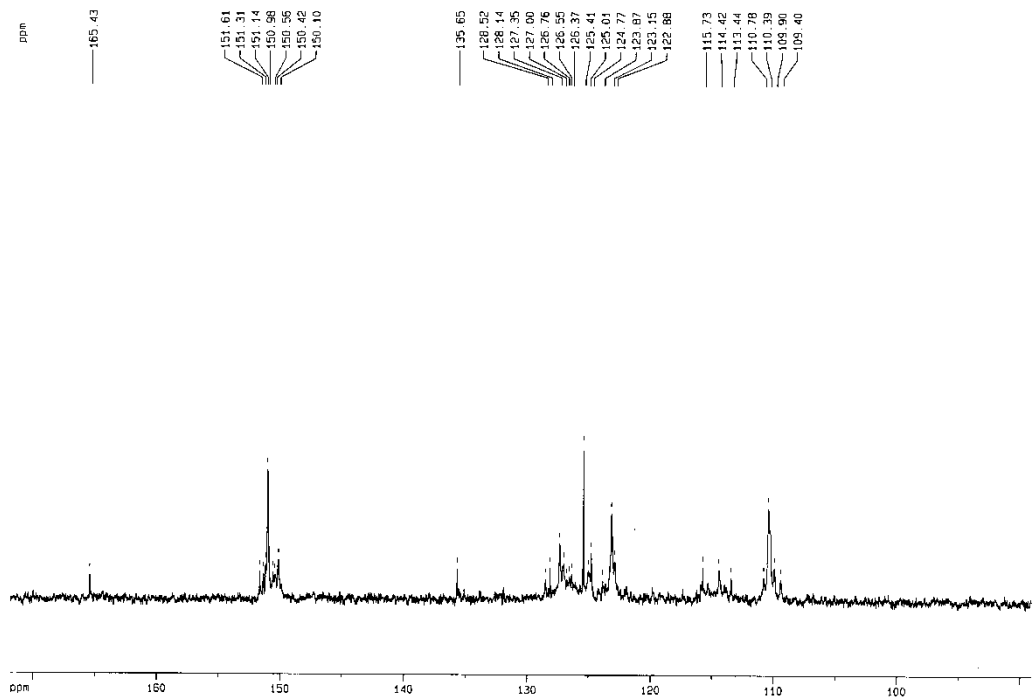
Polymer **P2**.

^1H NMR (CDCl_3 , 200 MHz)

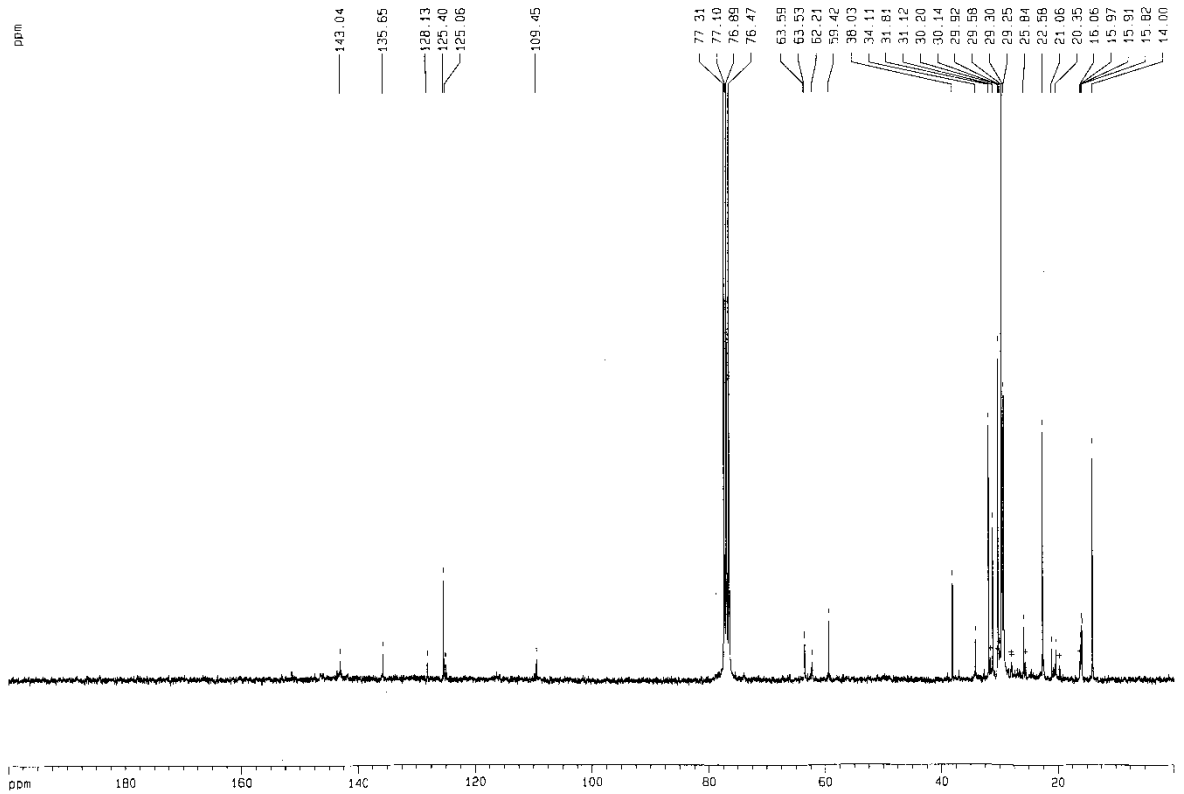
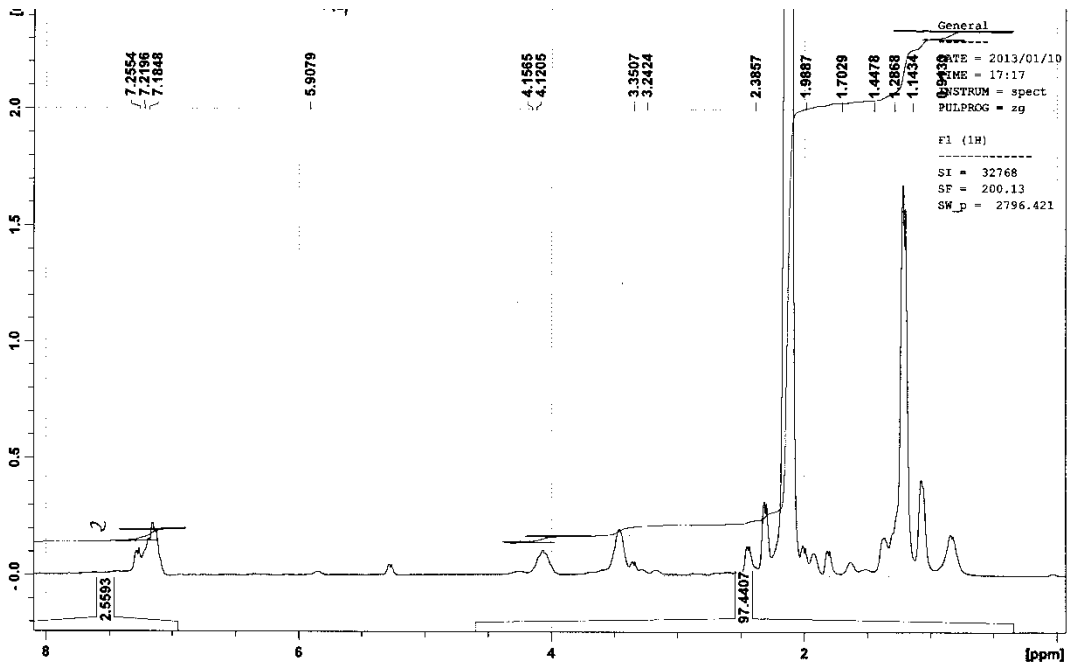


^{13}C NMR (CDCl_3 , 75 MHz)

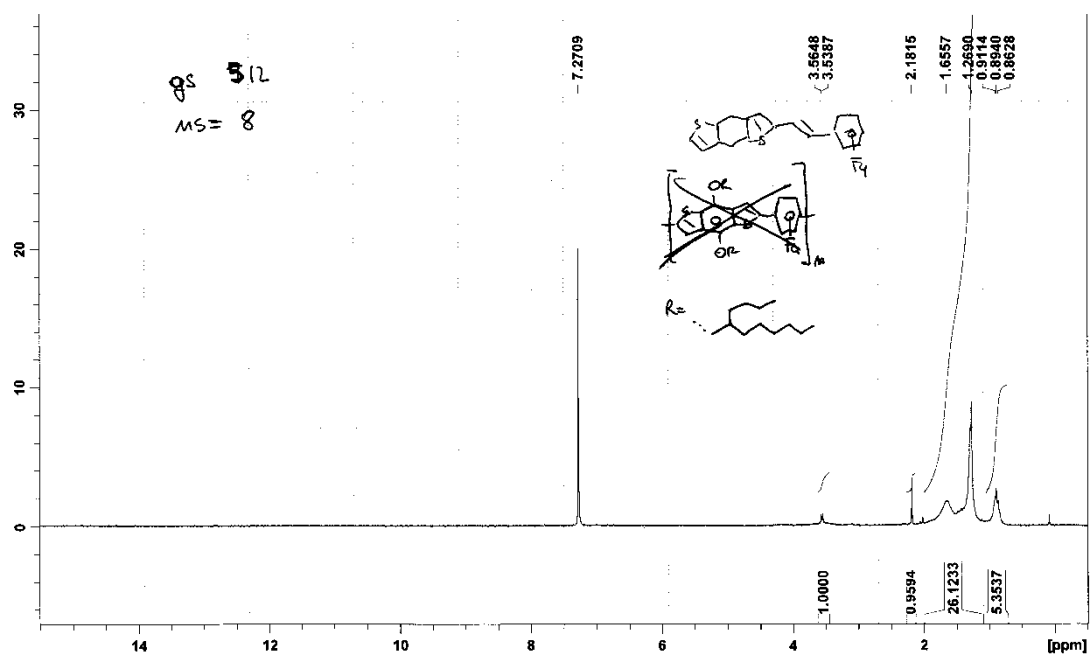




Polymer P3ain DMSO-d₆.

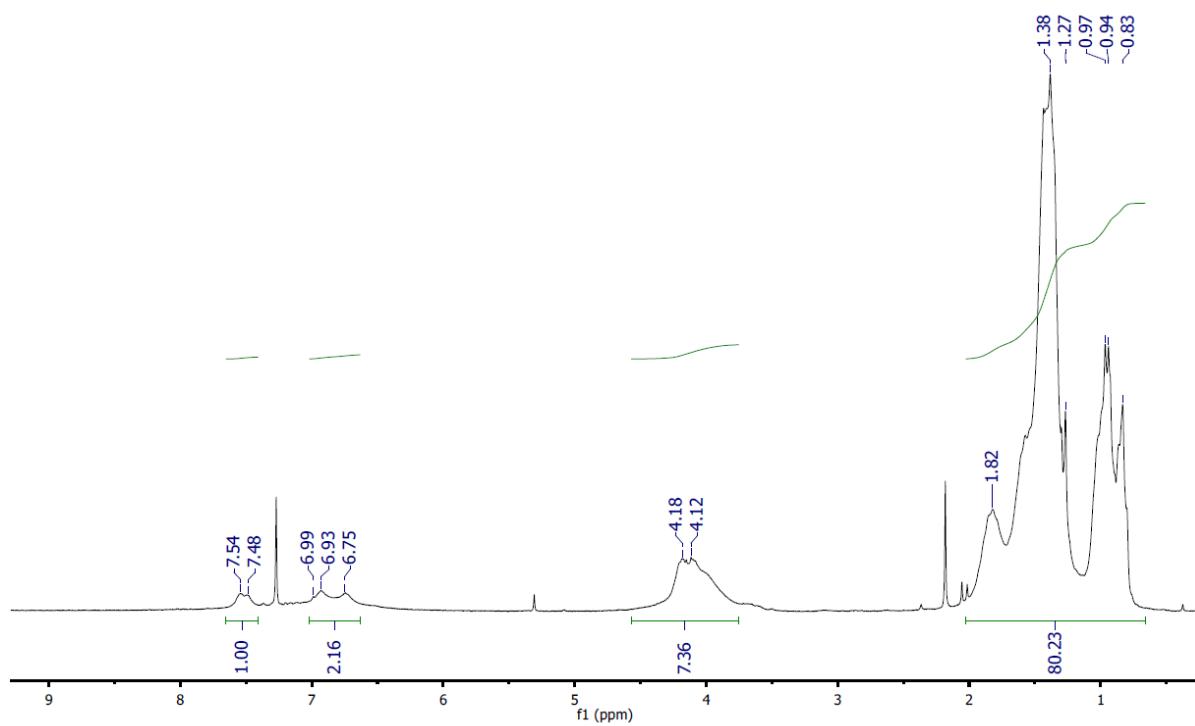


Polymer **P3b** (CDCl₃, 200 MHz)

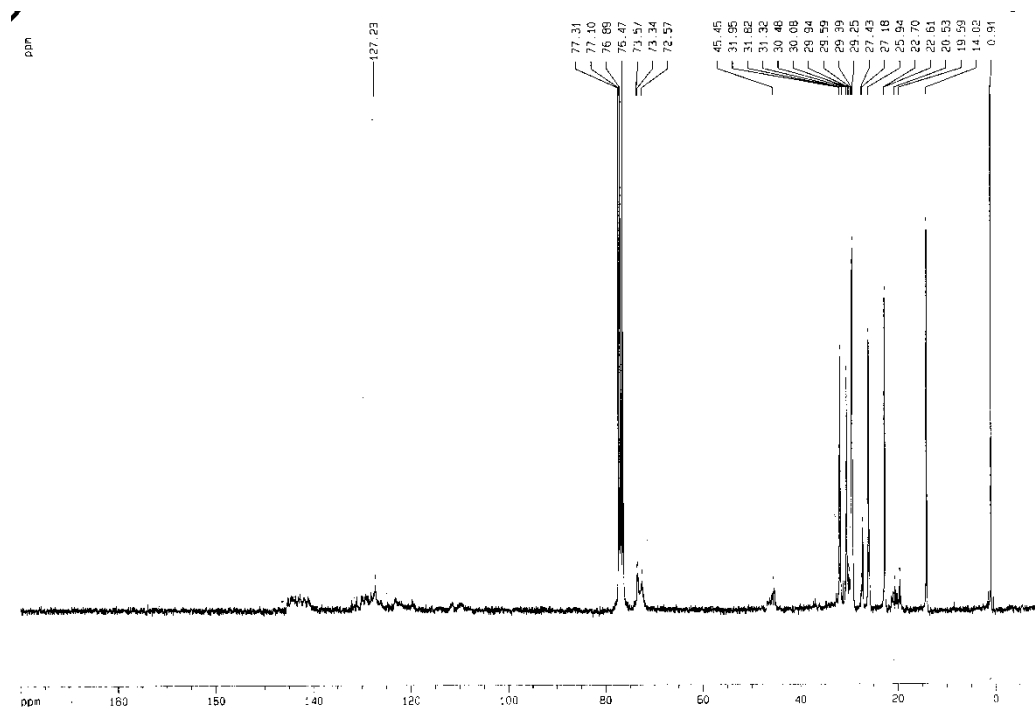


Polymer **P4a** (CDCl₃, 200 MHz)

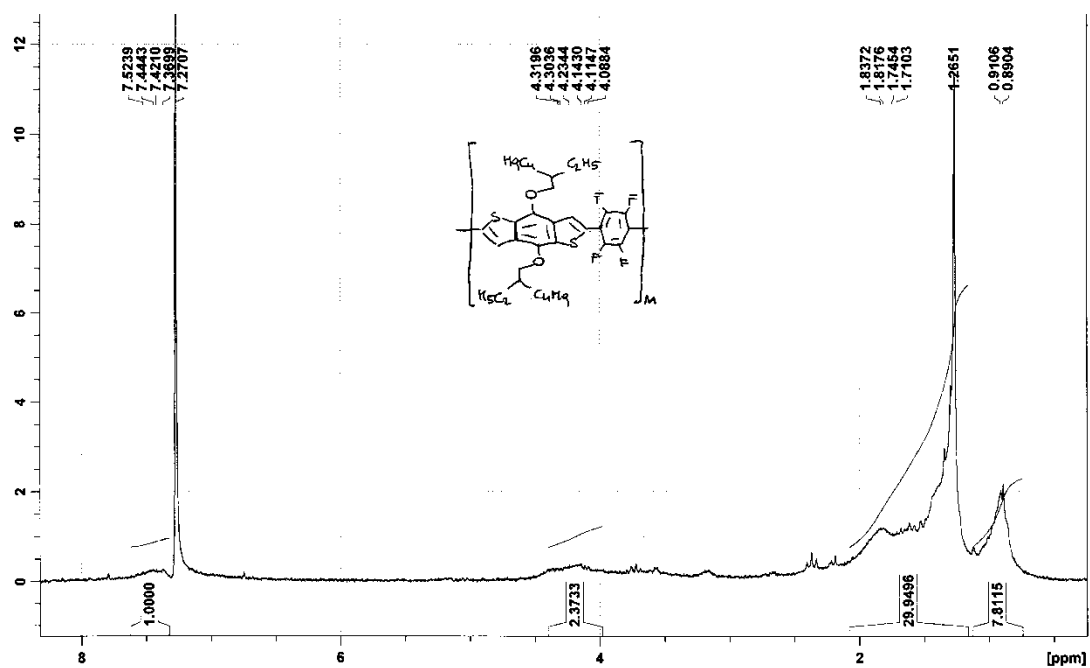
Andrea Nitti
AN103 polimero CDCl₃



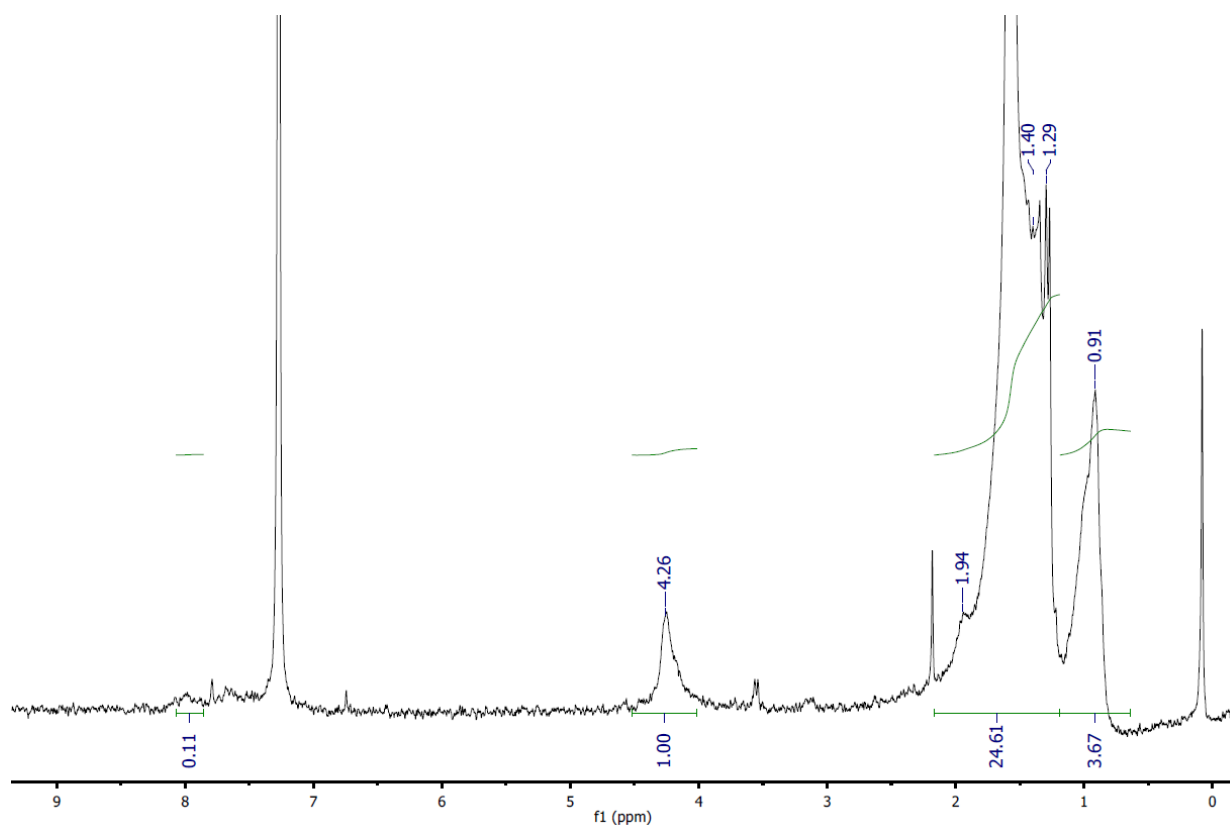
¹³C NMR (CDCl₃, 75 MHz)



Polymer **P4b** (CDCl₃, 200 MHz)

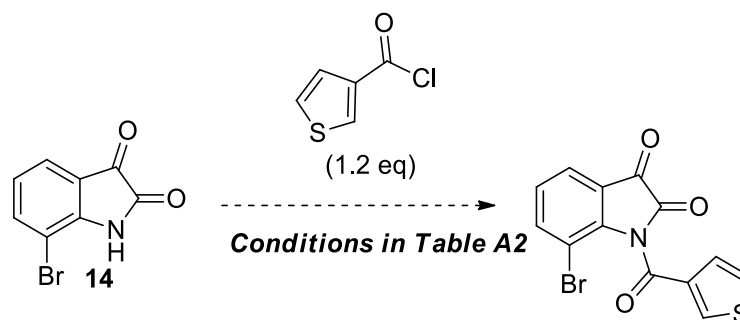


Polymer **P4cS** (CDCl₃, 200 MHz)



CONJUGATED THIOPHENE-FUSED ISATIN DYES THROUGH IN-TRAMOLECULAR DIRECT ARYLATION

Table A2. Conditions for the attempted acylation of isatin **14**



Entry	Method	Conv [%]
1	NaH (1.5eq), THF dry, 0°C-rt.	0
2	DMAP (0.2eq), triethylamine (1.1eq), THF dry.	0
3	DMAP (0.2eq), triethylamine (1.1eq), DCM dry.	0
4	Pyridine (2.1 eq), DCM dry.	0

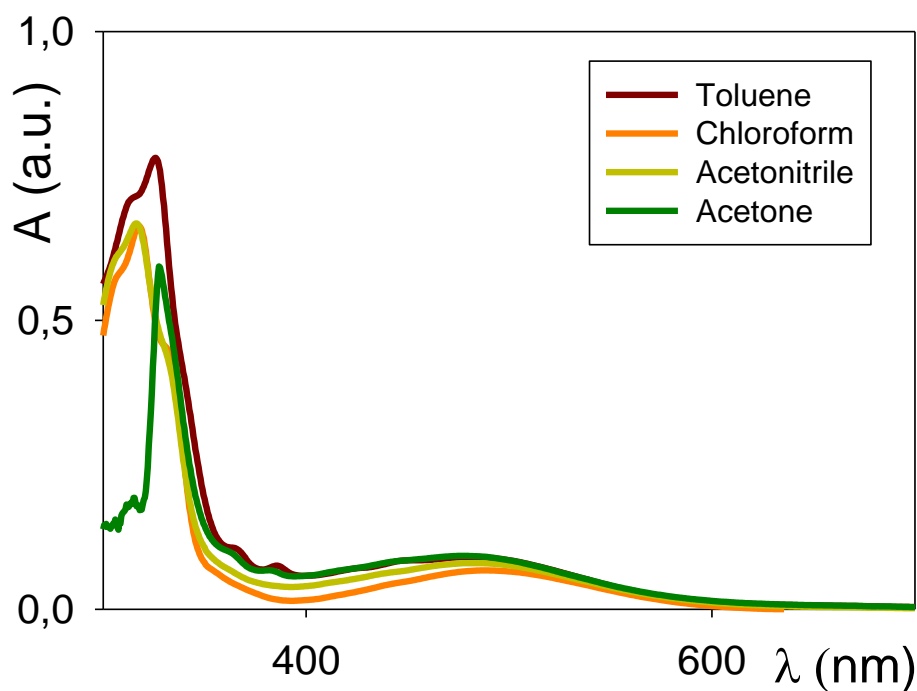


Figure A9. UV/Vis spectra of compounds **18** (ca. 5×10^{-6} M) in different solvents

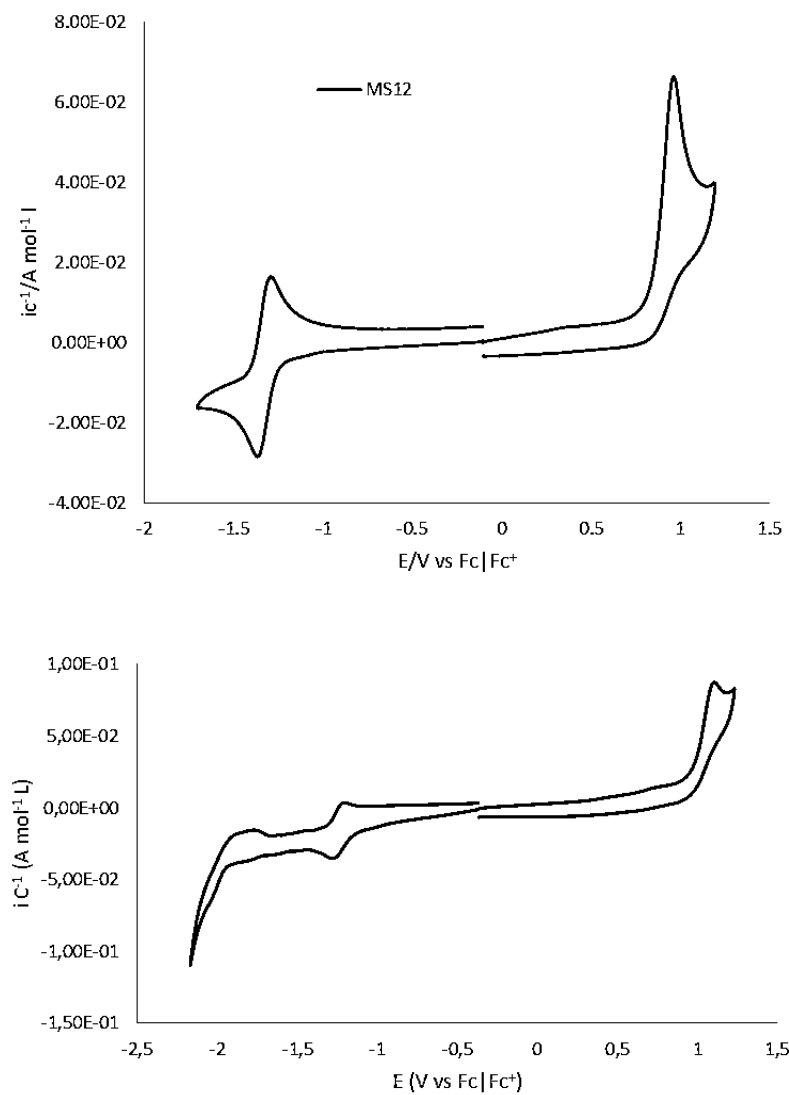


Figure A10. Cyclic Voltammetry of compound **18** (top) and **36** (bottom). For conditions, see General Experimental in the Experimental Section.

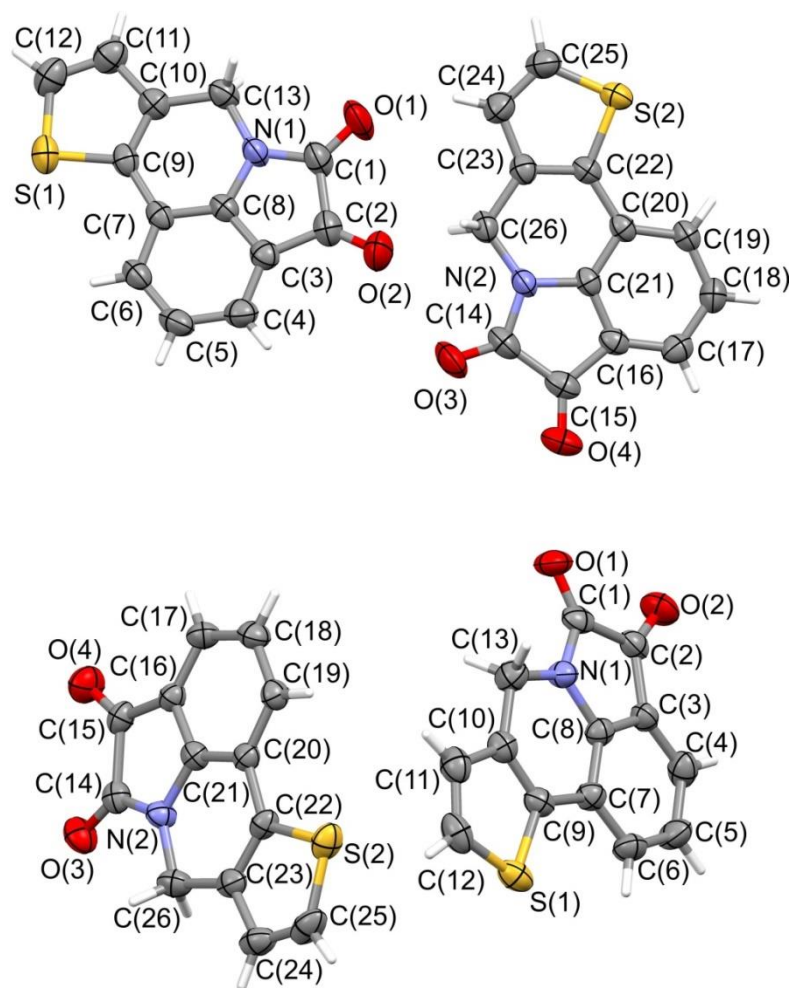


Figure A11. Plots showing thermal ellipsoids for the two independent molecules in the **18_1** crystal (above) and in the **18_2** crystal (below). Ellipsoids are drawn at the 50% probability level. Atom names are reported only for non-hydrogen atoms

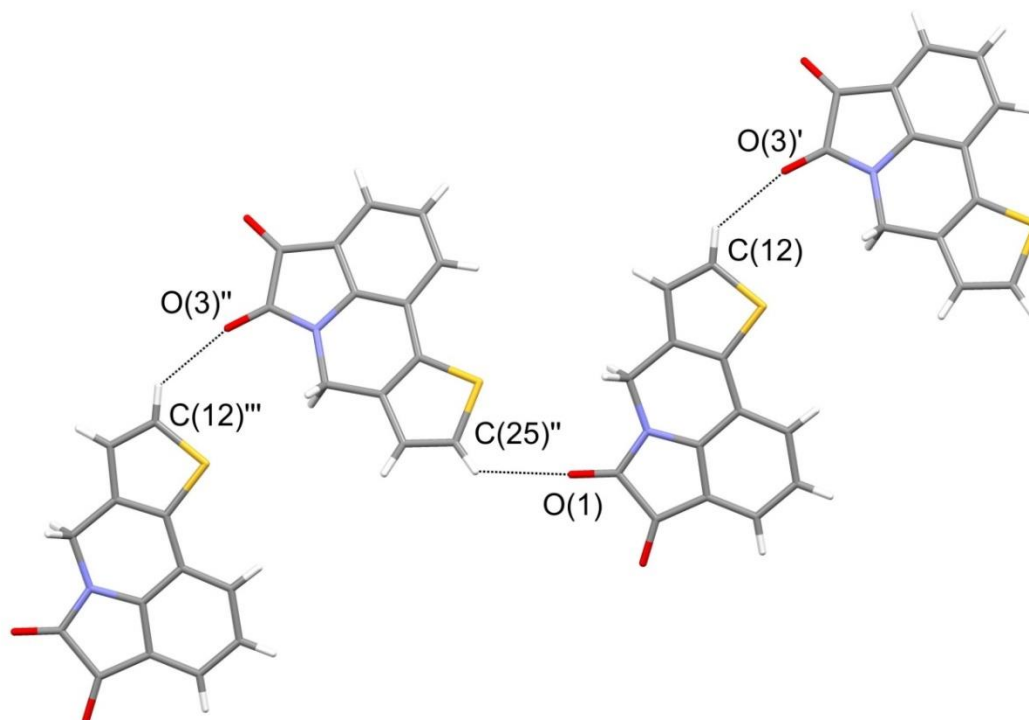


Figure A12. The C-H...O hydrogen bond motif occurring between couples of independent molecules in the **18_1** crystal. Complete H-bonds are shown only for the two central molecules. Features for the independent C-H...O interactions are: C(12)...O(3)' 3.24(1) Å, H(12)...O(3)' 2.51(1) Å, C(12)-H(12)...O(3)' 135.4(2)°; C(25)''...O(1) 3.22(1) Å, H(25)''...O(1) 2.57(1) Å, C(25)''-H(25)''...O(1) 127.8(2)°. Symmetry code: (') = 1-x, 1-y, 2-z; (") = 2-x, 1-y, 1-z; (") = 1+x, y, -1+z.

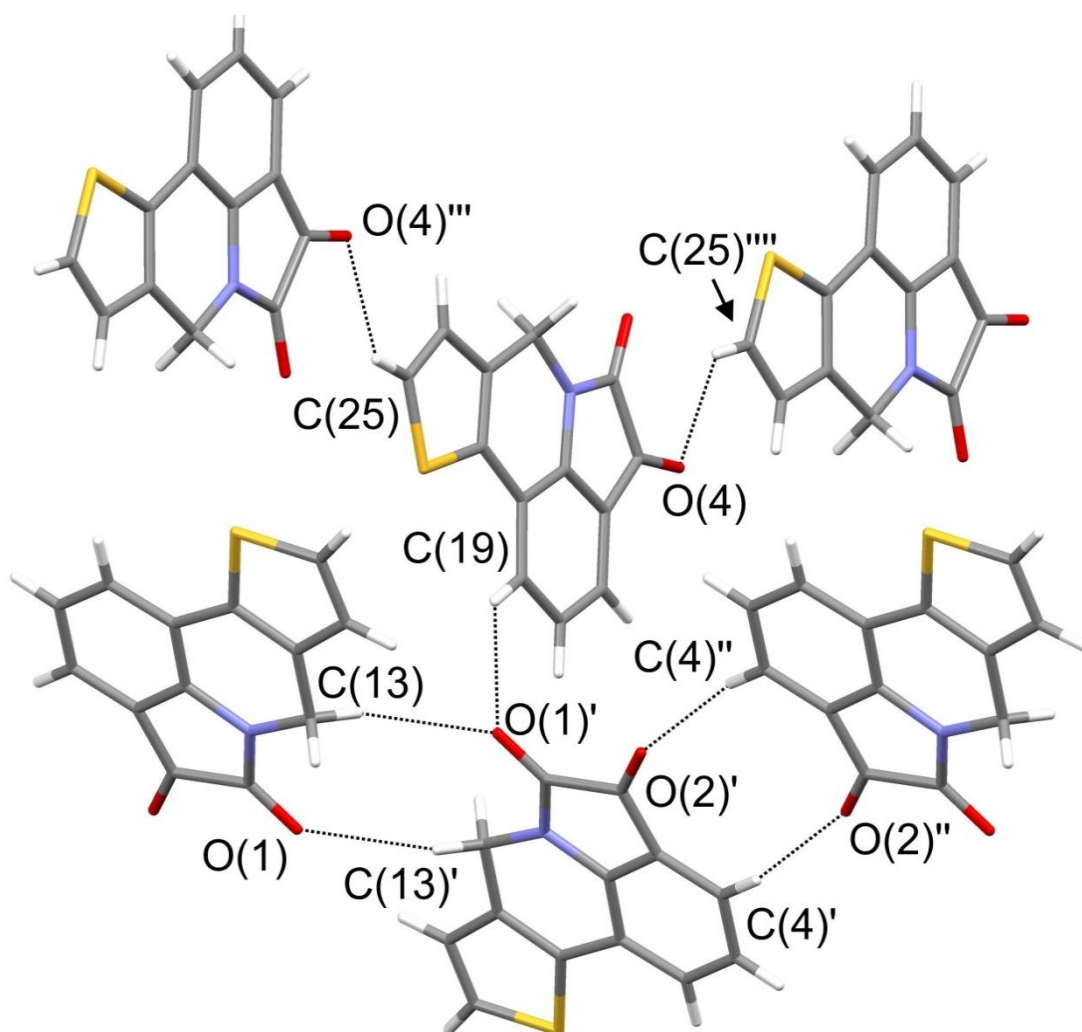


Figure A13. The C-H...O hydrogen bond motif in the **18_2** crystal. H-bonded chains made by symmetrically equivalent molecules are interconnected by additional C-H...O interactions between couples of independent molecules. Complete H-bonds are shown only for the two molecules in the middle. Features for the independent C-H...O interactions are: C(4)'...O(2)'' 3.46(1) Å, H(4)'...O(2)'' 2.55(1) Å, C(4)'-H(4)'\cdots O(2)'' 166.5(2)°; C(13)\cdots O(1)' 3.39(1) Å, H(13)\cdots O(1)' 2.54(1) Å, C(13)-H(13)\cdots O(1)' 147.1(2)°; C(19)\cdots O(1)' 3.27(1) Å, H(19)\cdots O(1)' 2.56(1) Å, C(19)-H(19)\cdots O(1)' 113.2(2)°; C(25)\cdots O(4)''' 3.14(1) Å, H(25)\cdots O(4)''' 2.43(1) Å, C(25)-H(25)\cdots O(4)''' 133.3(3)°. Symmetry code: (') = 1-x, -y, 1-z; (") = -1+x, y, 1+z; (')' = $^{-3/2+x, 1/2-y, -1/2+z}$; (''') = $^{3/2+x, 1/2-y, 1/2+z}$;

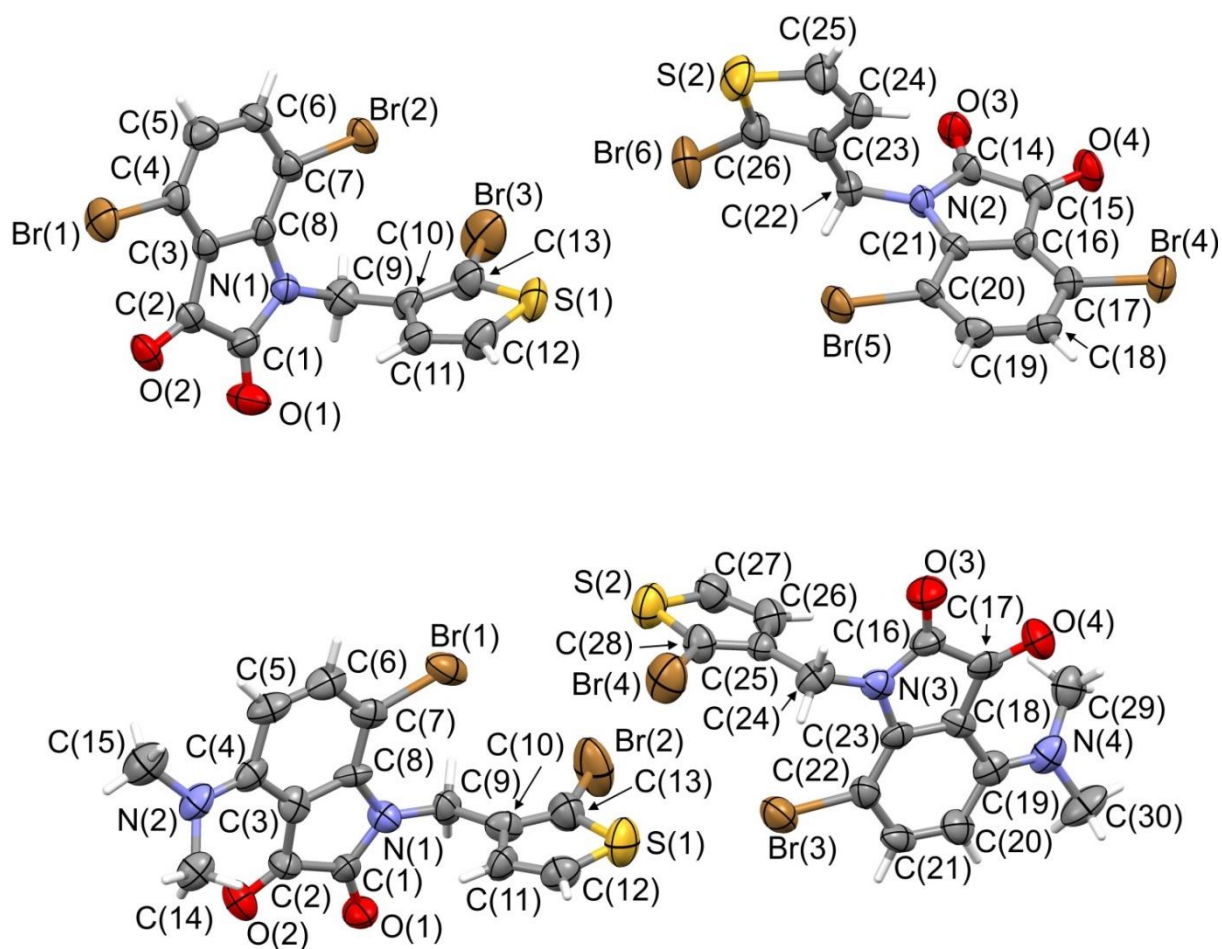


Figure A14. Plots showing thermal ellipsoids for the two similar but not equivalent molecules occurring in the crystals of **28** (above) and **30** (below) compounds (ellipsoids are drawn at the 50% probability level). For the crystal of **28**, the additional dichloromethane solvent molecule is not shown for clarity.

Table A3. Bond distances (Å) for the ring structures of the four crytralographically-independent molecules of compound 18 (two polymorphs 18_1 and 18_2). The corresponding distances for the two independent molecules of each crystal polymorph are reported on the same line.

18_1				18_2			
isatin				isatin			
C(1)-N(1)	1.361(3)	C(14)-N(2)	1.363(3)	C(1)-N(1)	1.362(4)	C(14)-N(2)	1.366(4)
C(1)-O(1)	1.208(3)	C(14)-O(3)	1.212(2)	C(1)-O(1)	1.210(4)	C(14)-O(3)	1.214(4)
C(2)-O(2)	1.208(3)	C(15)-O(4)	1.208(2)	C(2)-O(2)	1.206(4)	C(15)-O(4)	1.210(4)
C(1)-C(2)	1.571(3)	C(14)-C(15)	1.553(3)	C(1)-C(2)	1.564(5)	C(14)-C(15)	1.566(5)
C(2)-C(3)	1.462(3)	C(15)-C(16)	1.472(3)	C(2)-C(3)	1.467(5)	C(15)-C(16)	1.455(5)
C(3)-C(4)	1.387(3)	C(16)-C(17)	1.380(3)	C(3)-C(4)	1.384(5)	C(16)-C(17)	1.393(5)
C(3)-C(8)	1.382(3)	C(16)-C(21)	1.386(3)	C(3)-C(8)	1.387(5)	C(16)-C(21)	1.381(4)
C(4)-C(5)	1.387(3)	C(17)-C(18)	1.386(3)	C(4)-C(5)	1.376(5)	C(17)-C(18)	1.376(5)
C(5)-C(6)	1.384(3)	C(18)-C(19)	1.392(3)	C(5)-C(6)	1.393(5)	C(18)-C(19)	1.384(5)
C(6)-C(7)	1.393(3)	C(19)-C(20)	1.395(3)	C(6)-C(7)	1.389(5)	C(19)-C(20)	1.389(5)
C(7)-C(8)	1.385(3)	C(20)-C(21)	1.385(2)	C(7)-C(8)	1.378(5)	C(20)-C(21)	1.377(4)
C(8)-N(1)	1.407(2)	C(21)-N(2)	1.404(2)	C(8)-N(1)	1.410(4)	C(21)-N(2)	1.414(4)
thiophene				thiophene			
C(9)-S(1)	1.728(3)	C(22)-S(2)	1.722(2)	C(9)-S(1)	1.714(4)	C(22)-S(2)	1.717(3)
C(12)-S(1)	1.714(2)	C(25)-S(2)	1.711(2)	C(12)-S(1)	1.702(4)	C(25)-S(2)	1.704(4)
C(9)-C(10)	1.374(3)	C(22)-C(23)	1.373(3)	C(9)-C(10)	1.377(5)	C(22)-C(23)	1.376(5)
C(11)-C(12)	1.346(3)	C(24)-C(25)	1.347(3)	C(11)-C(12)	1.360(5)	C(24)-C(25)	1.340(5)
C(10)-C(11)	1.421(3)	C(23)-C(24)	1.419(3)	C(10)-C(11)	1.415(5)	C(23)-C(24)	1.420(5)
fused ring				fused ring			
C(7)-C(9)	1.449(3)	C(20)-C(22)	1.453(3)	C(7)-C(9)	1.459(5)	C(20)-C(22)	1.455(4)
C(10)-C(13)	1.501(3)	C(23)-C(26)	1.504(3)	C(10)-C(13)	1.495(5)	C(23)-C(26)	1.509(5)
C(13)-N(1)	1.464(3)	C(26)-N(2)	1.466(3)	C(13)-N(1)	1.459(4)	C(26)-N(2)	1.457(4)

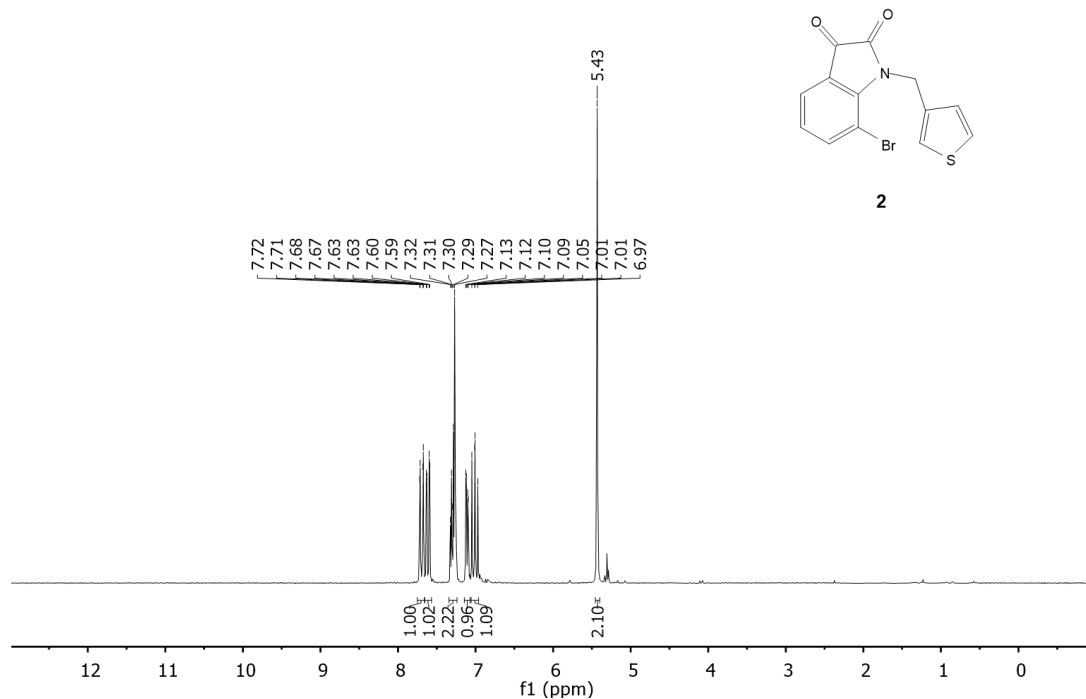
Table A4. Crystal data for investigated crystals

	18_1	18_2	28	30
Formula	$C_{26}H_{14}N_2O_4S_2$	$C_{26}H_{14}N_2O_4S_2$	$C_{27}H_{14}Br_6Cl_2N_2O_4S_2$	$C_{30}H_{24}Br_4N_4O_4S_2$
<i>M</i>	482.52	482.52	1044.82	888.26
Crystal system	triclinic	monoclinic	triclinic	monoclinic
Space group	<i>P</i> -1 (no. 2)	<i>P</i> 2 ₁ / <i>n</i> (no. 14)	<i>P</i> -1 (no. 2)	<i>P</i> 2 ₁ / <i>c</i> (no. 14)
<i>a</i> [Å]	7.331(2)	5.3775(6)	8.205(2)	23.534(4)
<i>b</i> [Å]	10.1068(15)	31.052(5)	14.884(4)	8.2908(12)
<i>c</i> [Å]	14.572(2)	12.3237(13)	14.978(4)	16.250(6)
α [°]	84.948(15)	90	62.98(2)	90
β [°]	83.20(3)	90.673(11)	86.64(3)	96.99(2)
γ [°]	79.94(14)	90	86.32(3)	90
<i>V</i> [Å ³]	1053.1(4)	2057.7(5)	1625.3(8)	3147.1(14)
<i>Z</i>	2	4	2	4
ρ_{calcd} [g cm ⁻³]	1.522	1.558	2.135	1.875
θ range [°]	2-26	2-26	2-26	2-25
Measured reflections	4490	4520	6941	6121
Unique reflections	4129	4065	6429	5532
<i>R</i> _{int}	0.019	0.035	0.042	0.1197
Strong data [<i>I</i> ₀ >2σ(<i>I</i> ₀)]	3347	2394	5045	3540
Refined parameters	307	307	397	401
<i>R</i> 1, <i>wR</i> 2 (strong data)	0.0403, 0.1018	0.0545, 0.1029	0.0761, 0.1819	0.1087, 0.2012
<i>R</i> 1, <i>wR</i> 2 (all data)	0.0530, 0.1096	0.1165, 0.1243	0.0999, 0.2077	0.1693, 0.2417
GoF	1.024	1.007	1.151	1.192
Max/min residuals [e Å ⁻³]	0.42/-0.30	0.26/-0.25	1.08/-1.22	0.70/-0.67

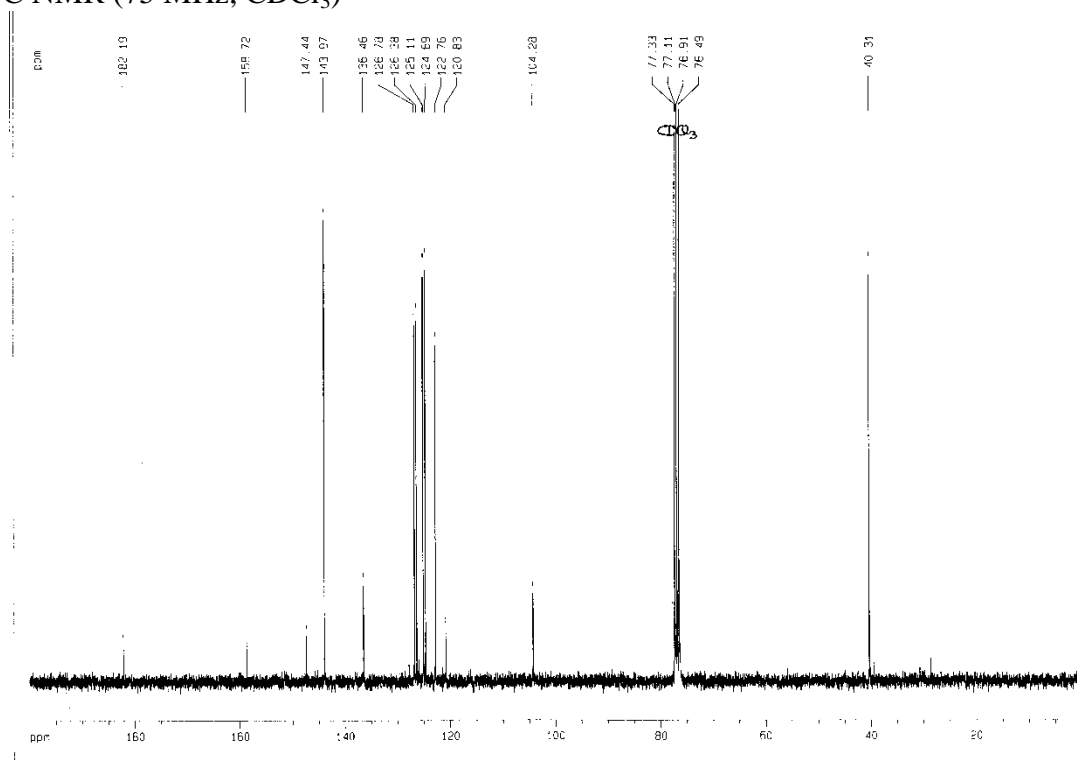
Copies of ^1H , ^{13}C NMR, ESI-MS and GC-MS spectra

Compound **15**

^1H NMR (200 MHz, CDCl_3)



^{13}C NMR (75 MHz, CDCl_3)



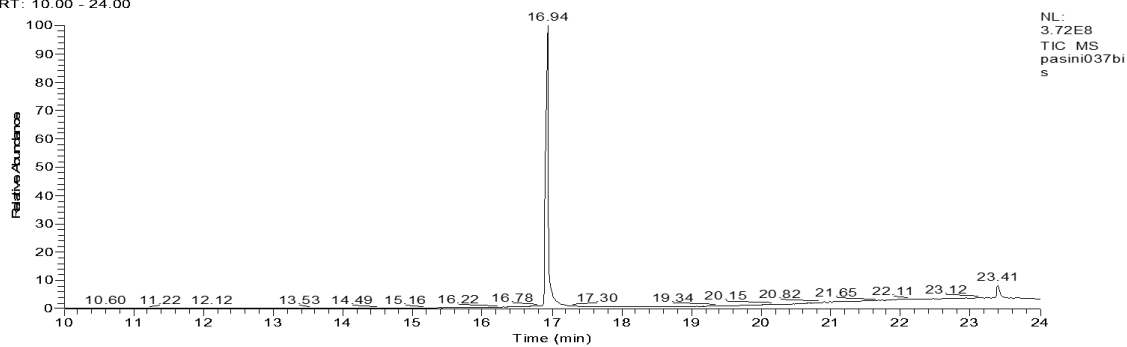
GC-MS

D:\LAVORICGS_2014\...pasini037bis

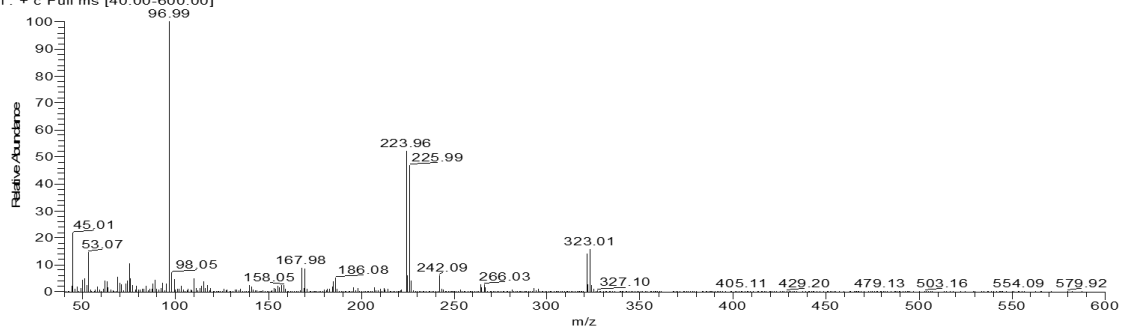
5/20/2014 12:14:42

AN70 conc

RT: 10.00 - 24.00

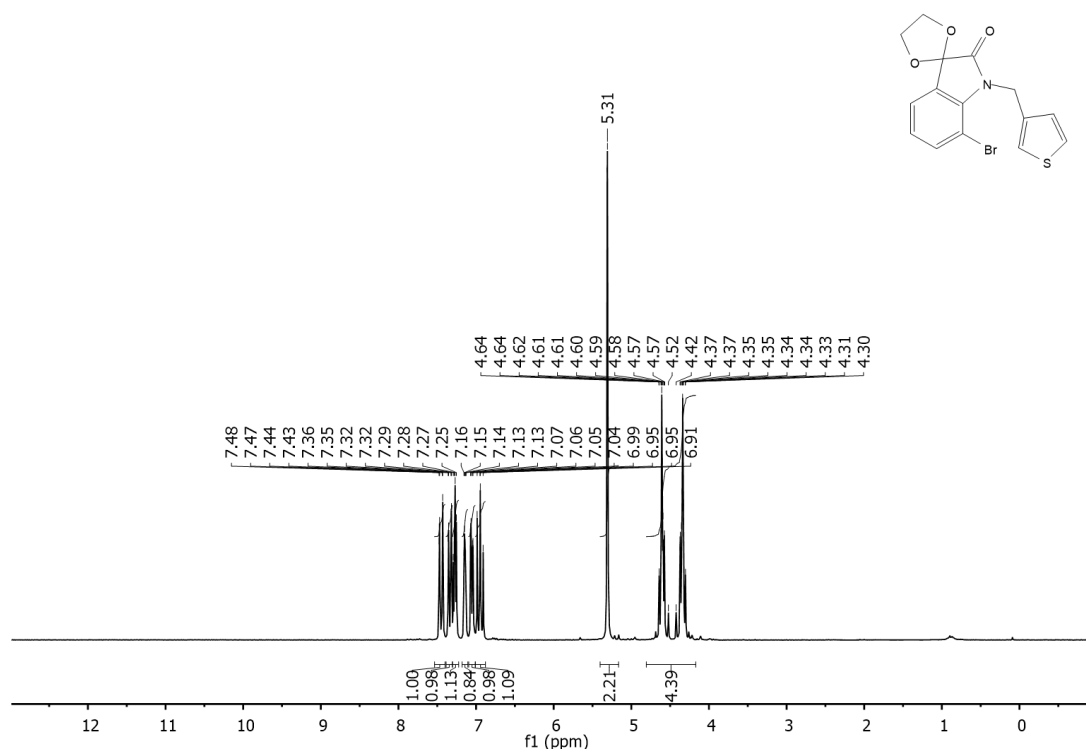


pasini037bis #1125 RT: 16.90 AV: 1 NL: 2.12E7
T: + c Full ms [40.00-600.00]

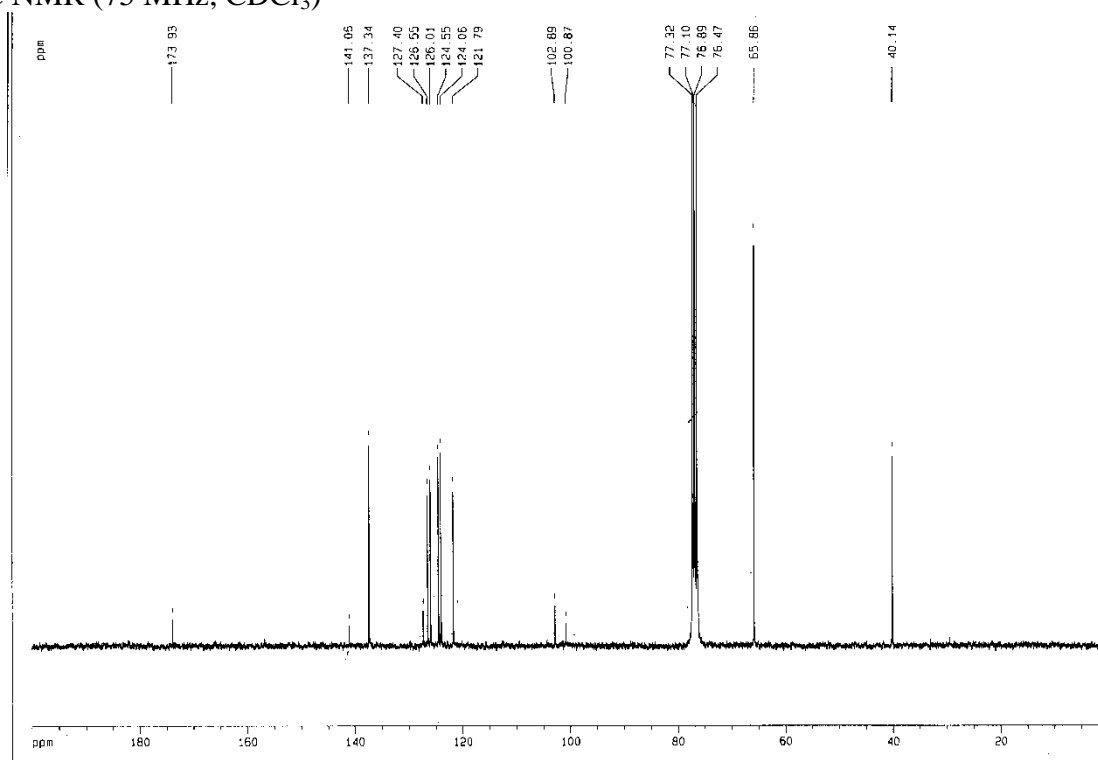


Compound 16

^1H NMR (200 MHz, CDCl_3)



^{13}C NMR (75 MHz, CDCl_3)



GCMS

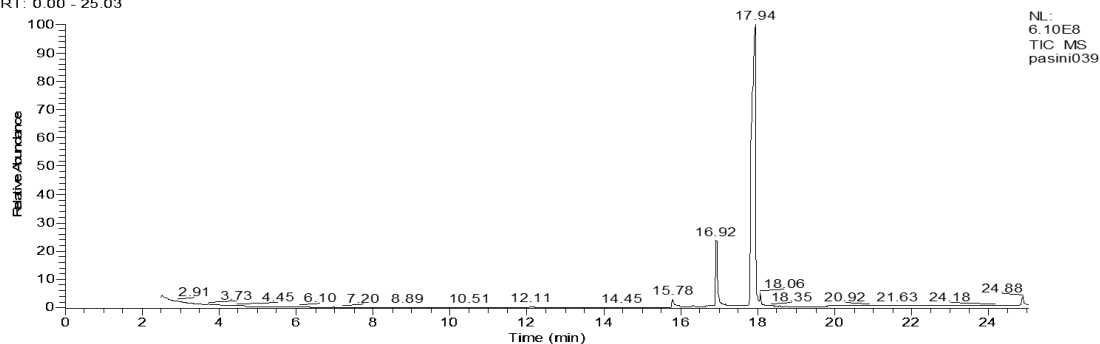
D:\LAVORICGS_2014\UNIPV\Fasini\pasini039

5/22/2014 10:55:17

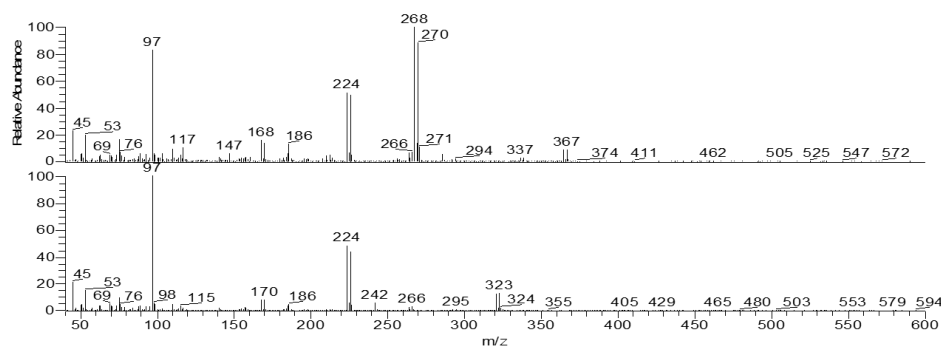
AN74conc

Sil

RT: 0.00 - 25.03



NL: 6.10E8
TIC MS
pasini039

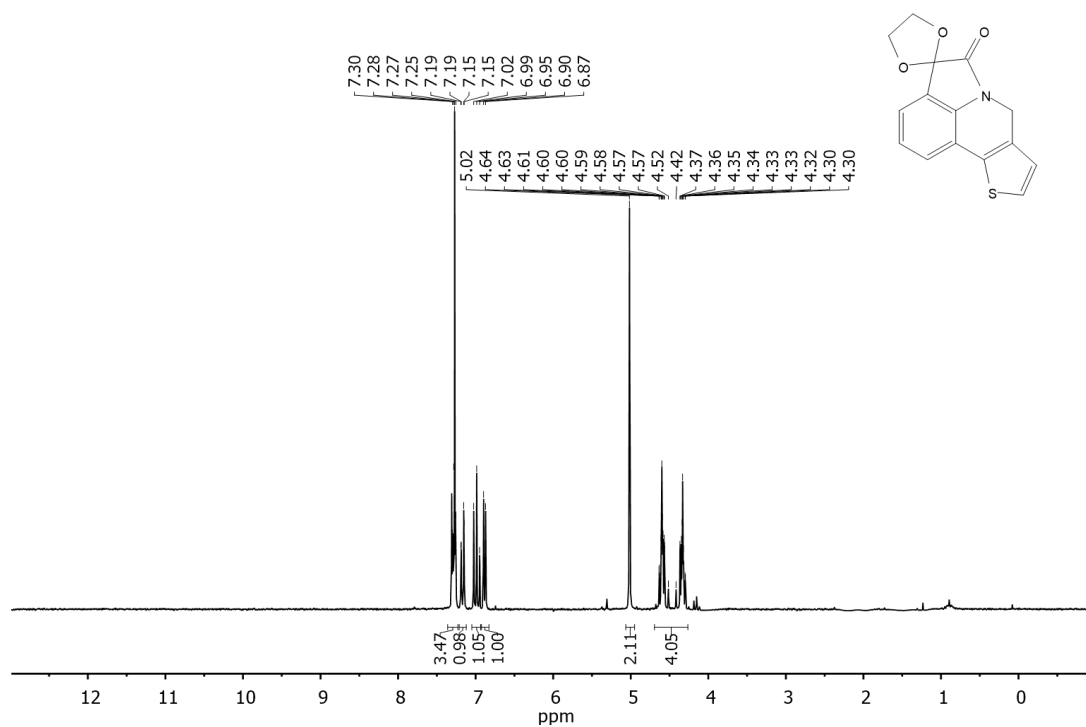


NL: 6.74E7
pasini039#1205 RT:
17.92 AV: 1 SB: 2 17.56
18.29 T: + c Full ms
[40.00-600.00]

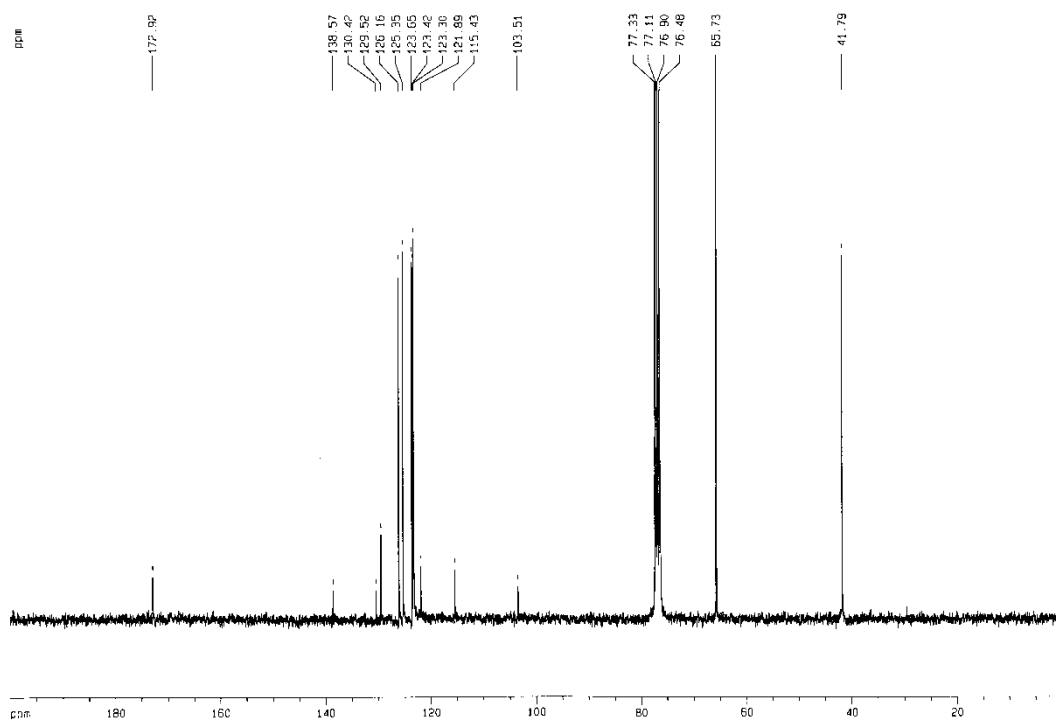
NL: 3.05E7
pasini039#1127 RT:
16.92 AV: 1 SB: 2 16.57
17.43 T: + c Full ms
[40.00-600.00]

Compound **17**

^1H NMR (200 MHz, CDCl_3)



^{13}C NMR (75 MHz, CDCl_3)



GCMS

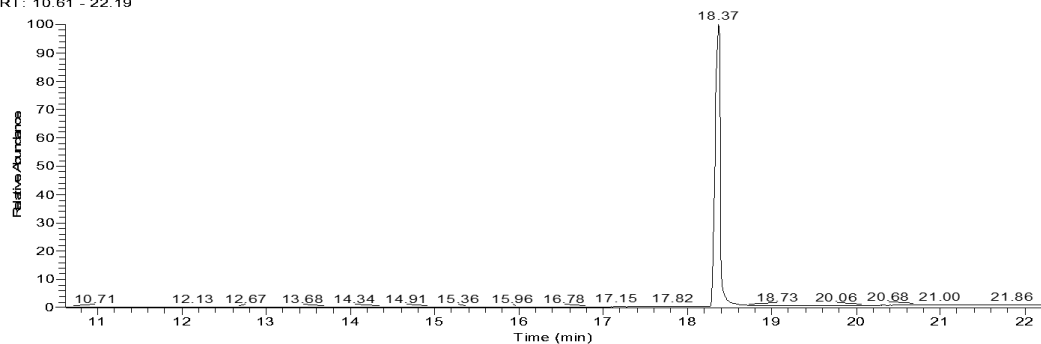
D:\LAVORICGS_2014\UNIPV\Pasini\pasini041

5/22/2014 11:55:52

AN75conc

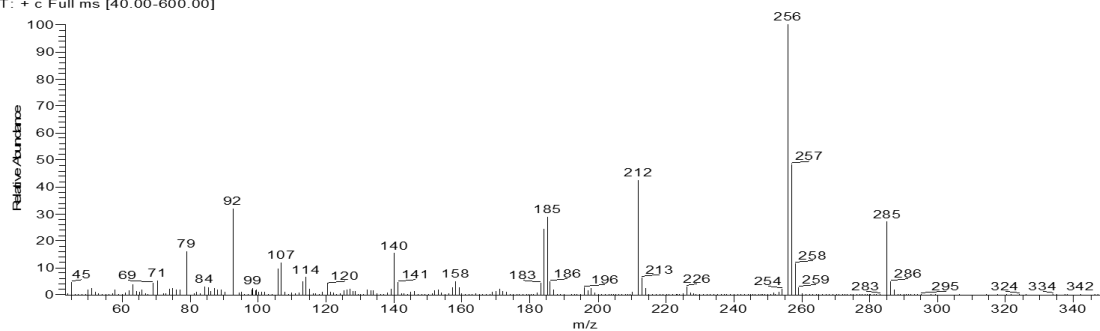
Sil

RT: 10.61 - 22.19



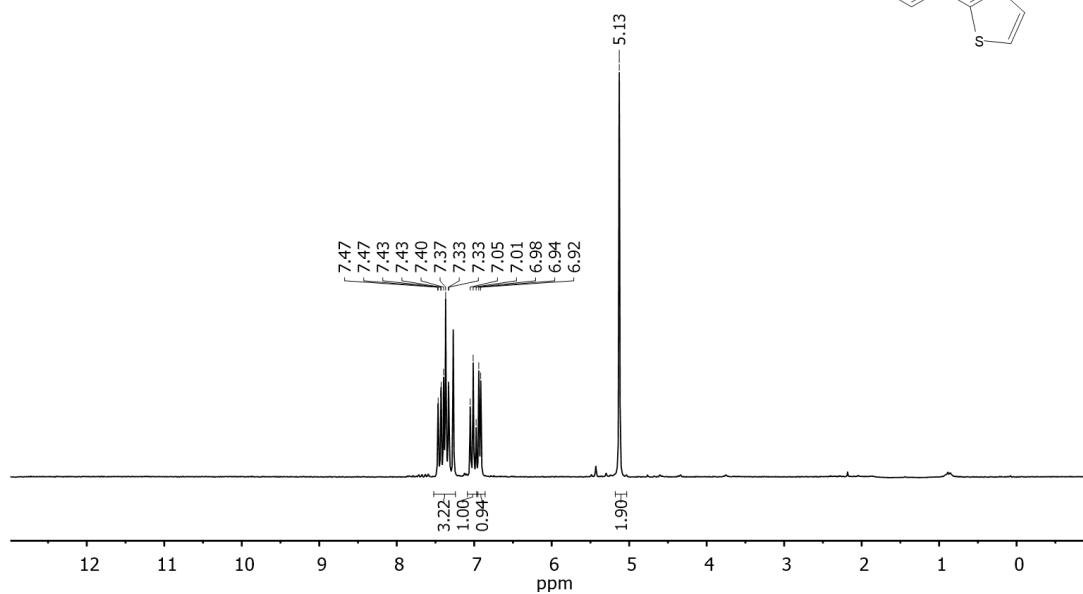
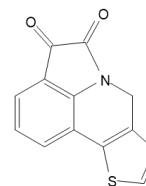
NL:
4.56E8
TIC MS
pasini041

pasini041 #1238 RT: 18.35 AV: 1 SB: 2 18.19, 18.97 NL: 6.76E7
T: + c Full ms [40.00-600.00]

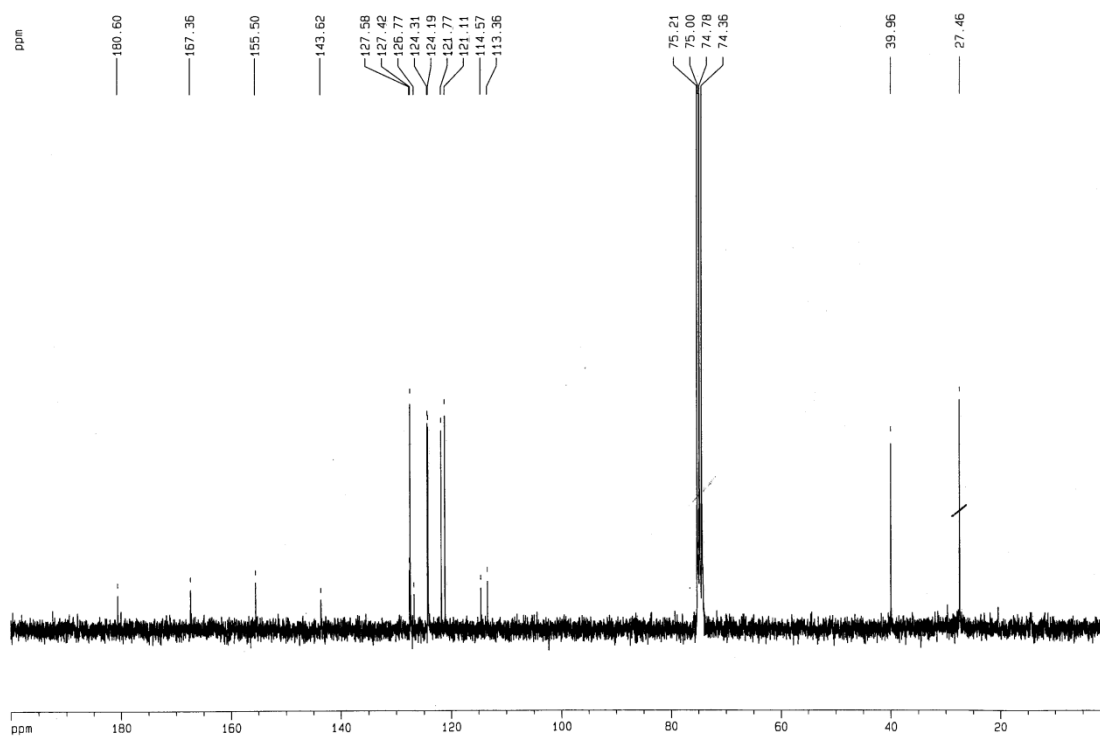


Compound 18

^1H NMR (200 MHz, CDCl_3)

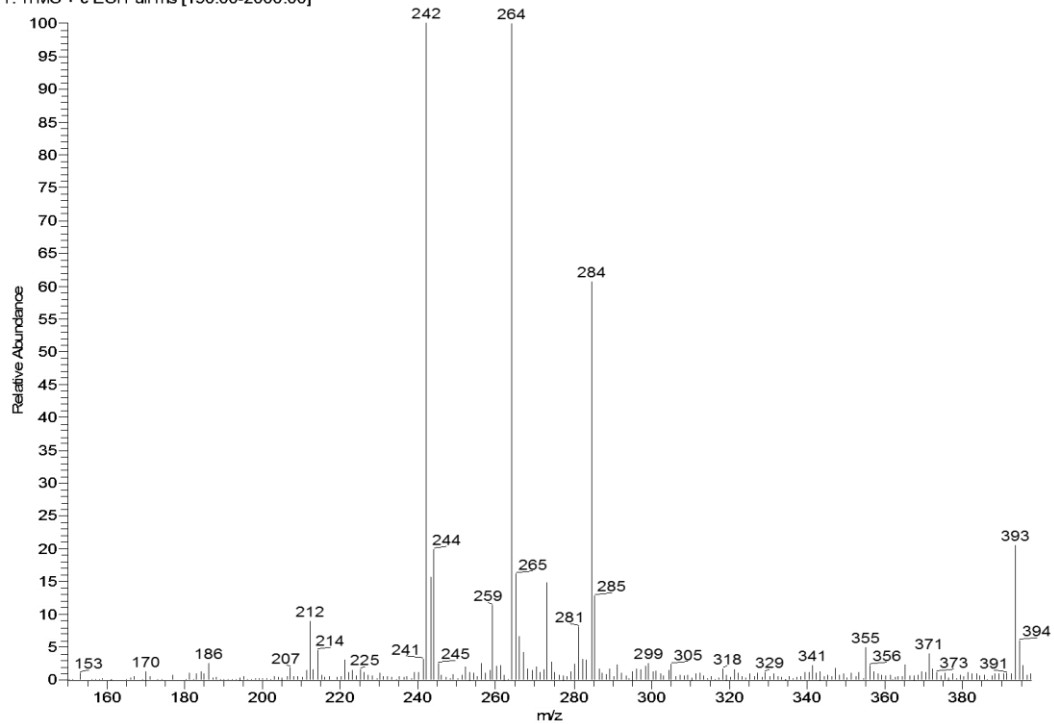


^{13}C NMR (75 MHz, CDCl_3)



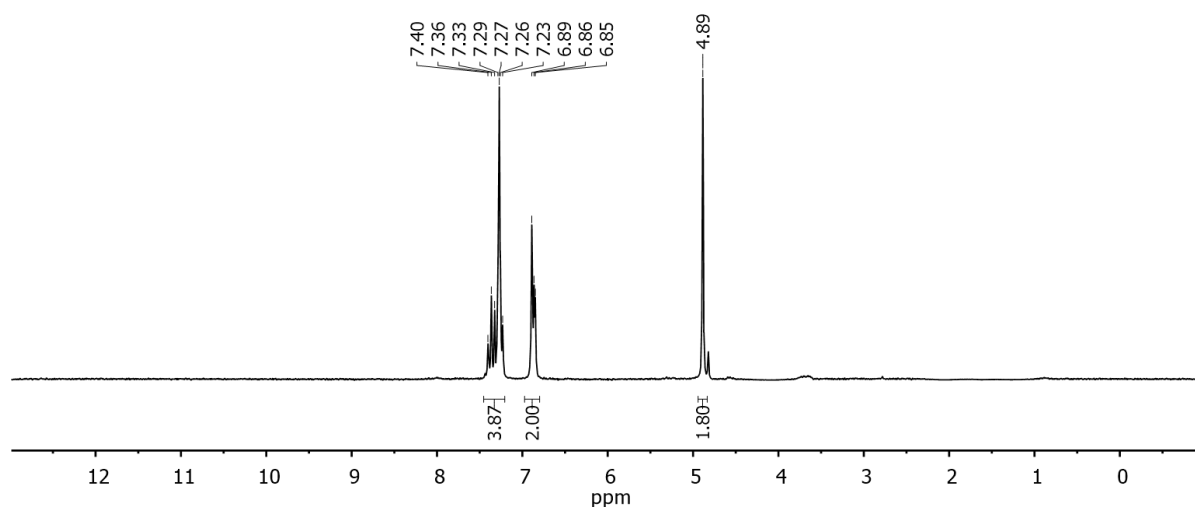
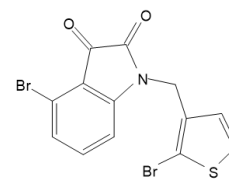
ESI-MS

MS12a #300-354 RT: 4.17-4.86 AV: 55 NL: 1.36E3
T: ITMS + c ESI Full ms [150.00-2000.00]

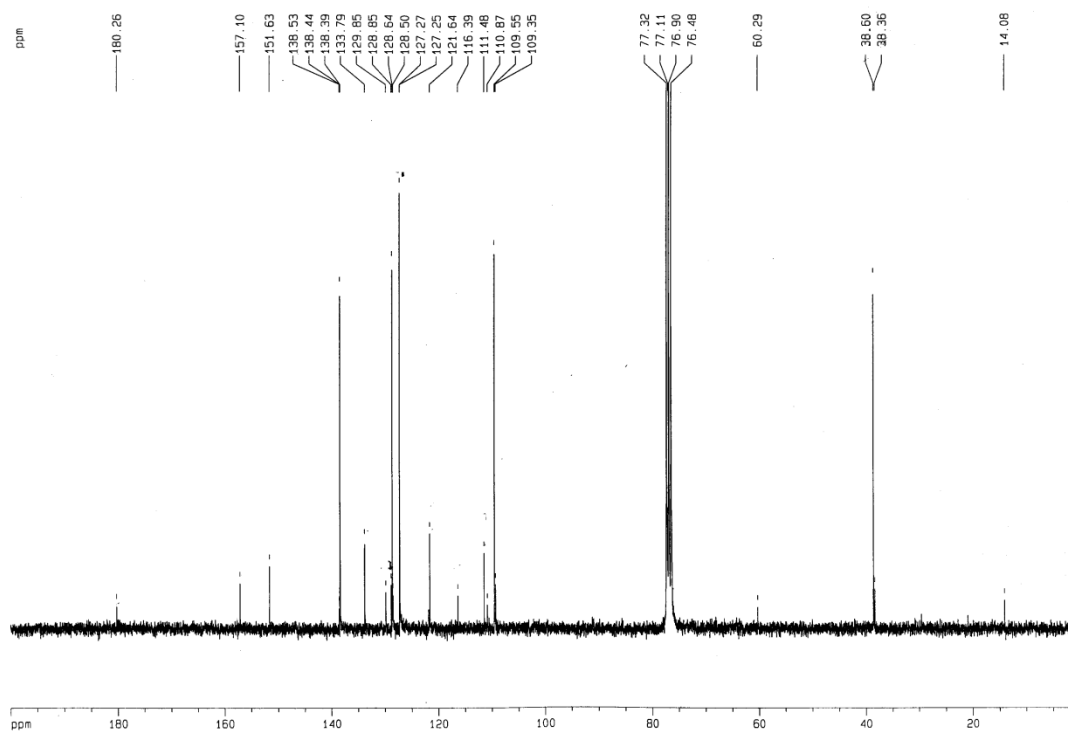


Compound **20**

^1H NMR (200 MHz, CDCl_3)

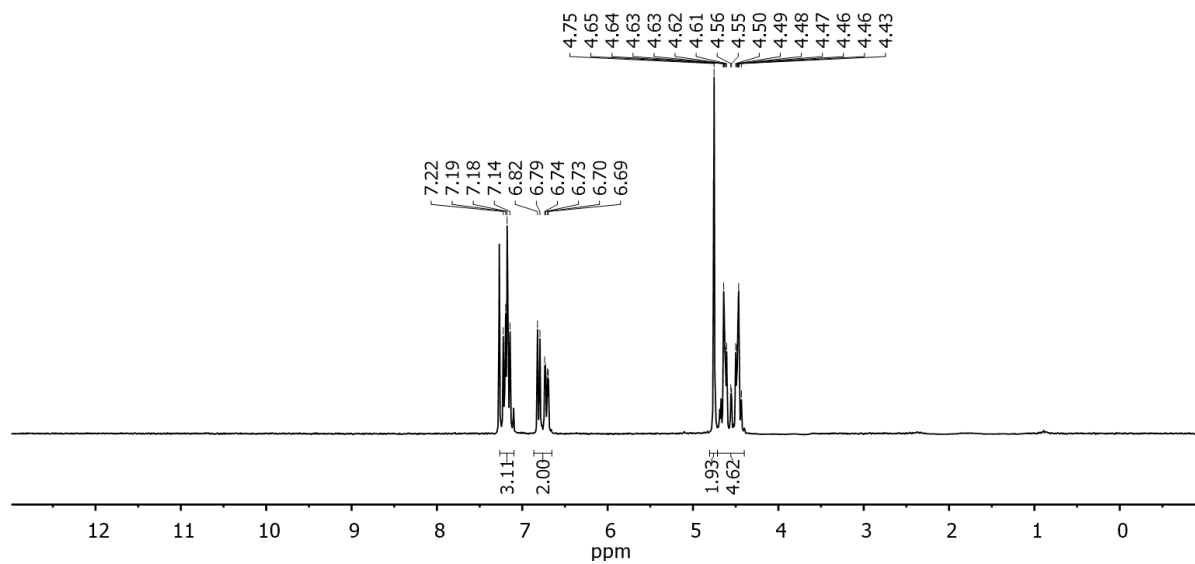
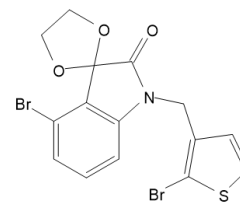


^{13}C NMR (75 MHz, CDCl_3)

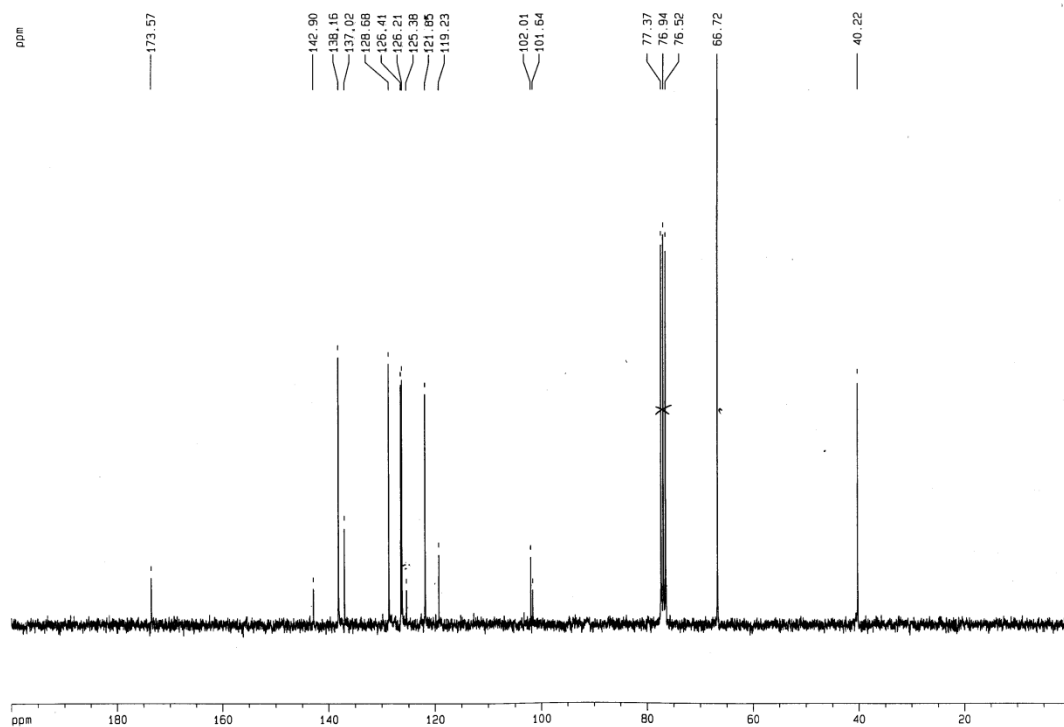


Compound 21

^1H NMR (200 MHz, CDCl_3)

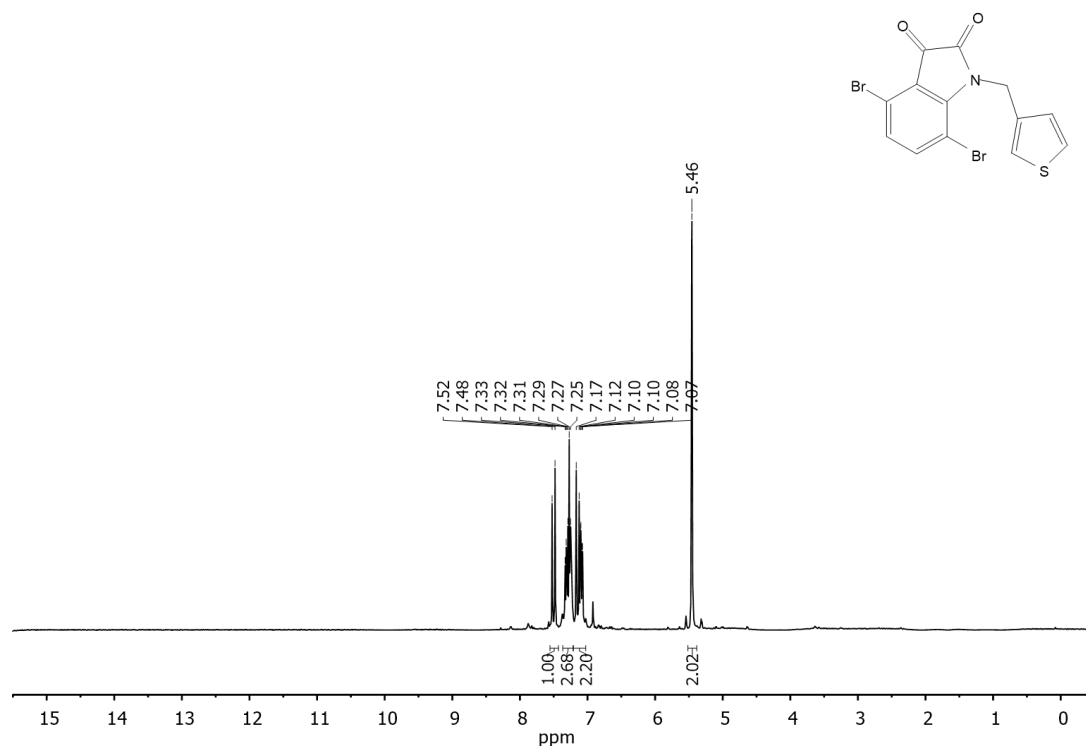


^{13}C NMR (75 MHz, CDCl_3)

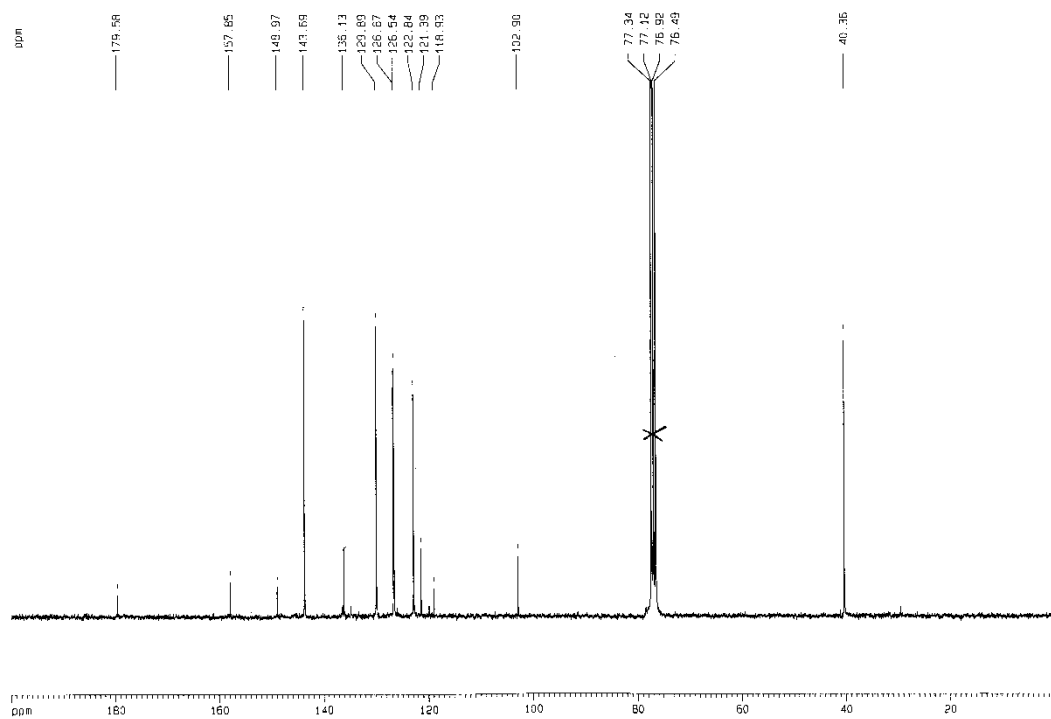


Compound 25

^1H NMR (200 MHz, CDCl_3)

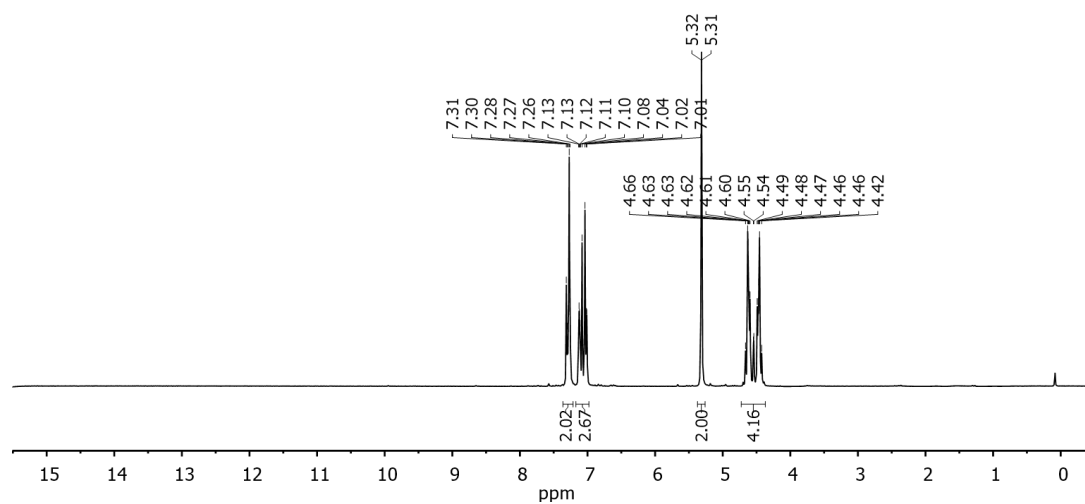
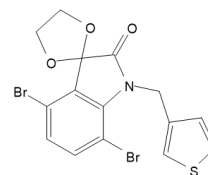


^{13}C NMR (75 MHz, CDCl_3)

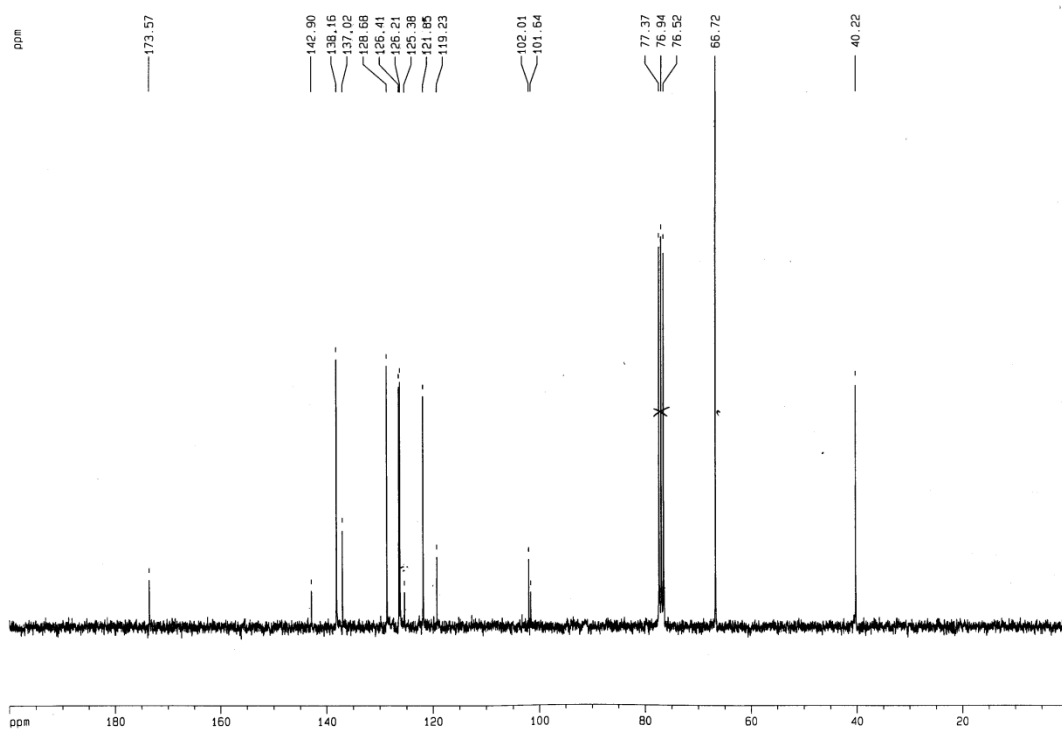


Compound 26

^1H NMR (200 MHz, CDCl_3)

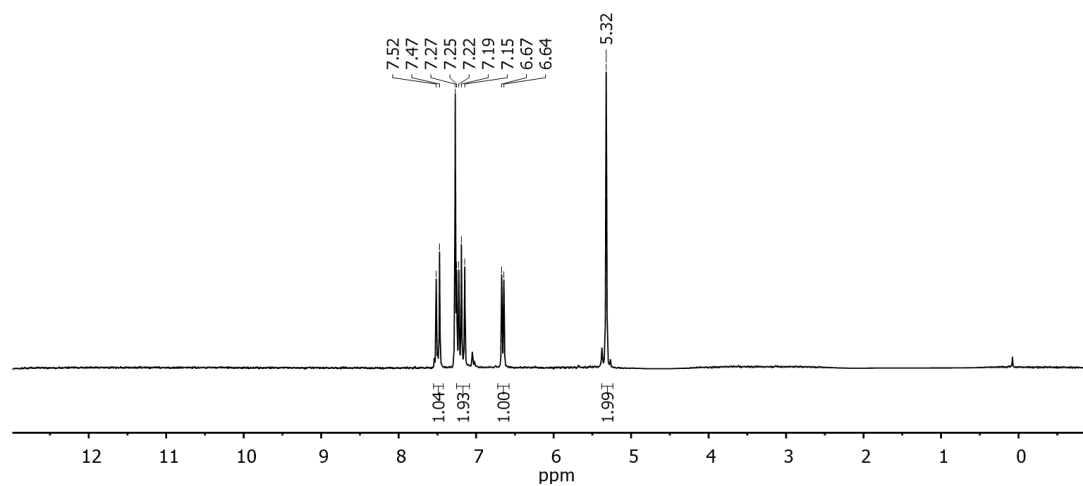
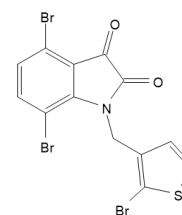


^{13}C NMR (75 MHz, CDCl_3)

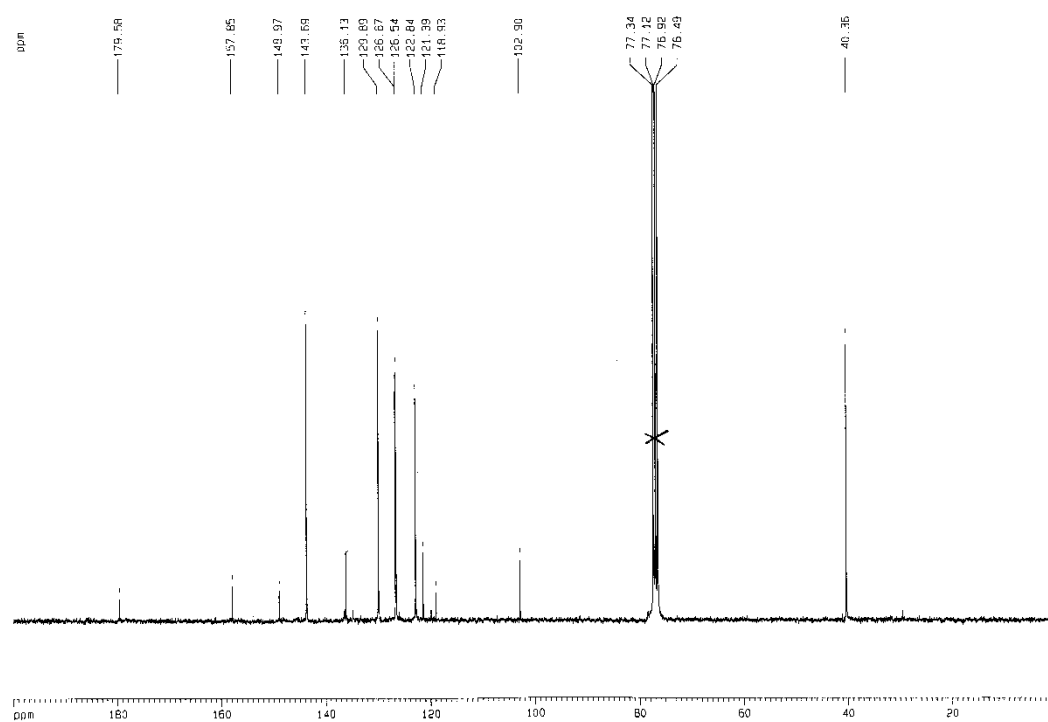


Compound **28**

^1H NMR (200 MHz, CDCl_3)

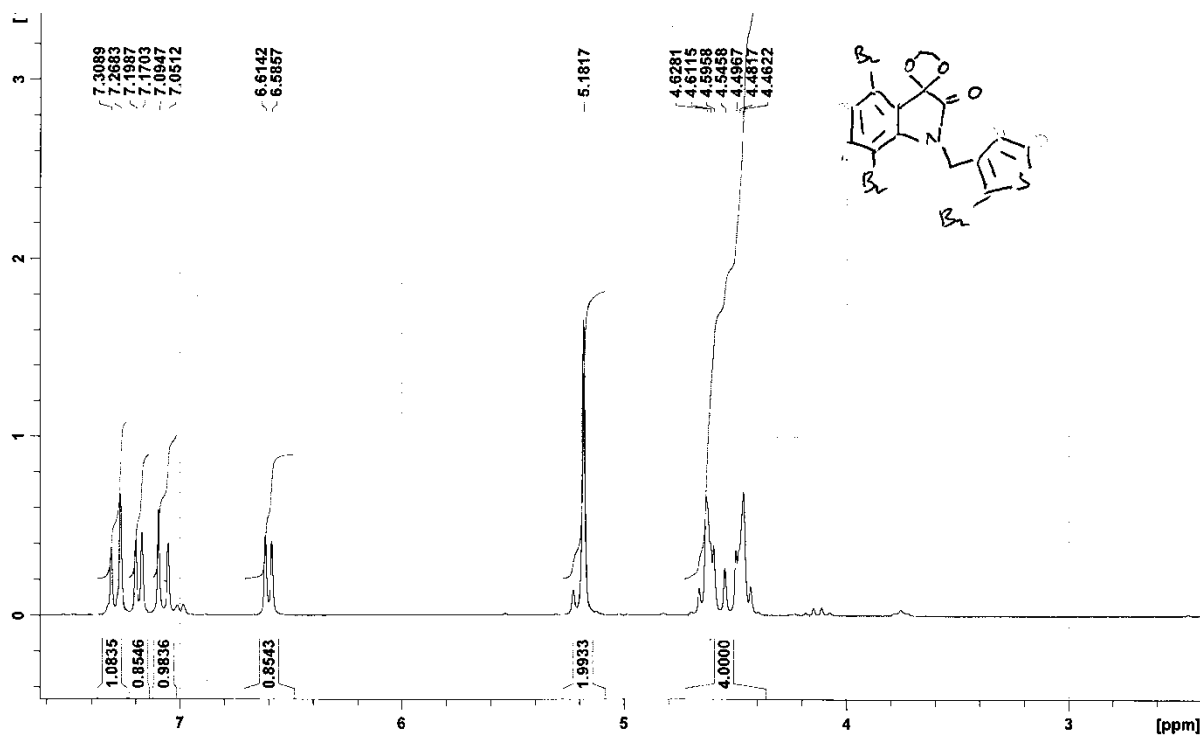


^{13}C NMR (75 MHz, CDCl_3)

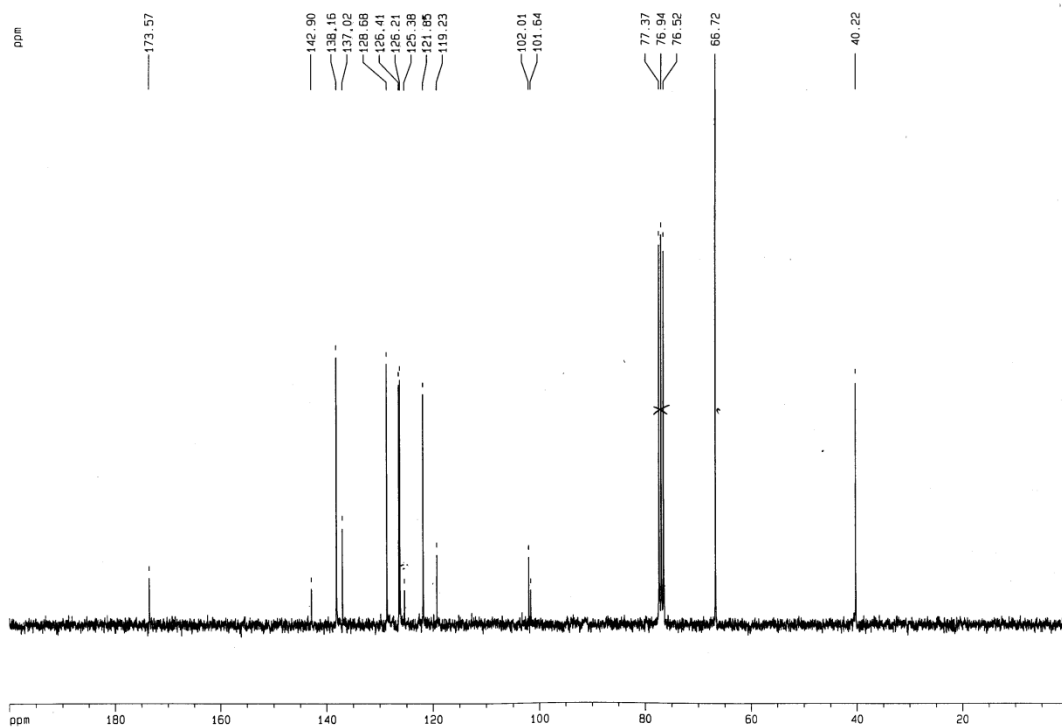


Compound 29

^1H NMR (200 MHz, CDCl_3)

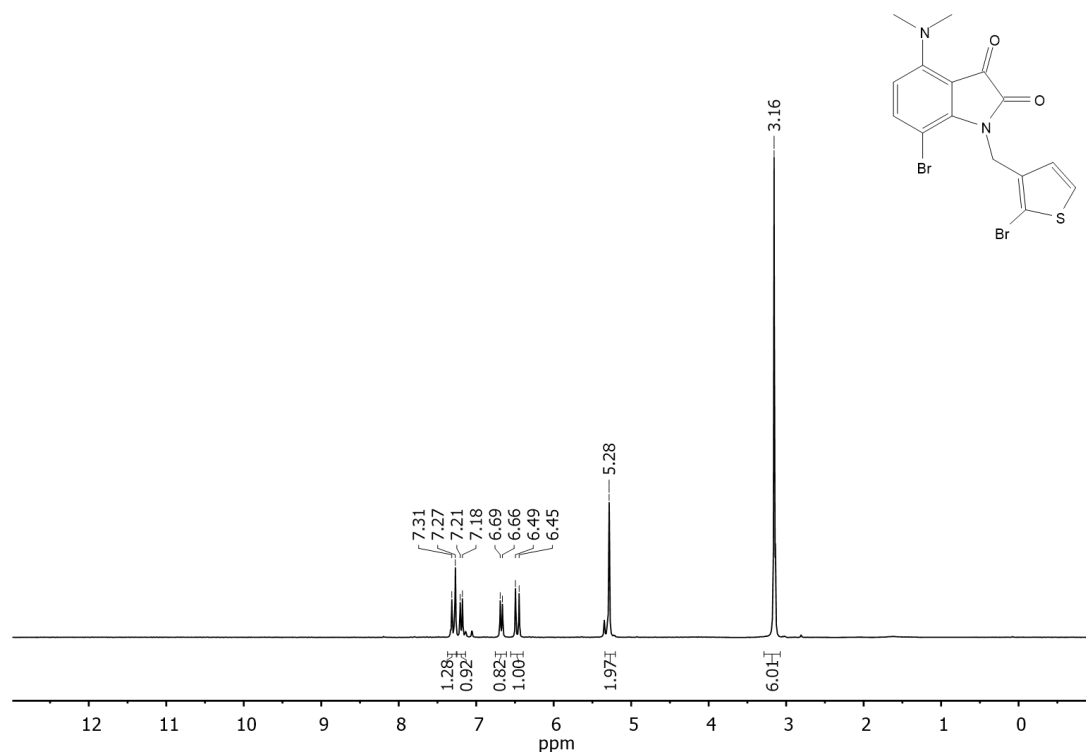


^{13}C NMR (75 MHz, CDCl_3)

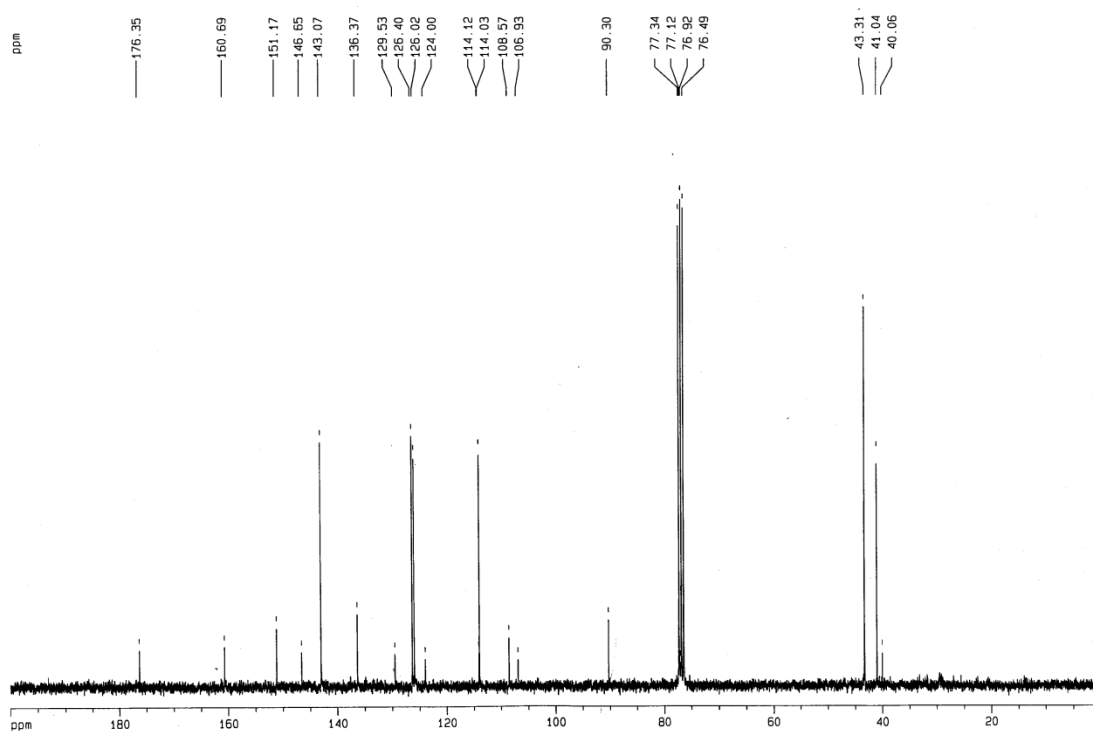


Compound **30**

^1H NMR (200 MHz, CDCl_3)

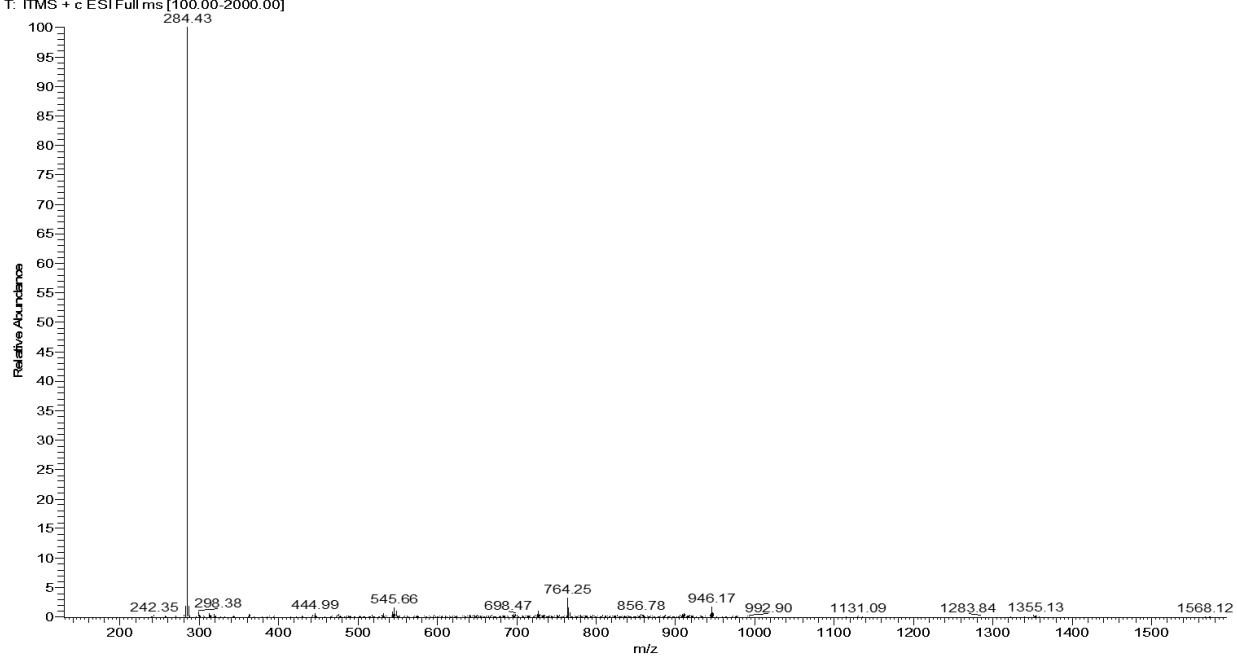


^{13}C NMR (75 MHz, CDCl_3)



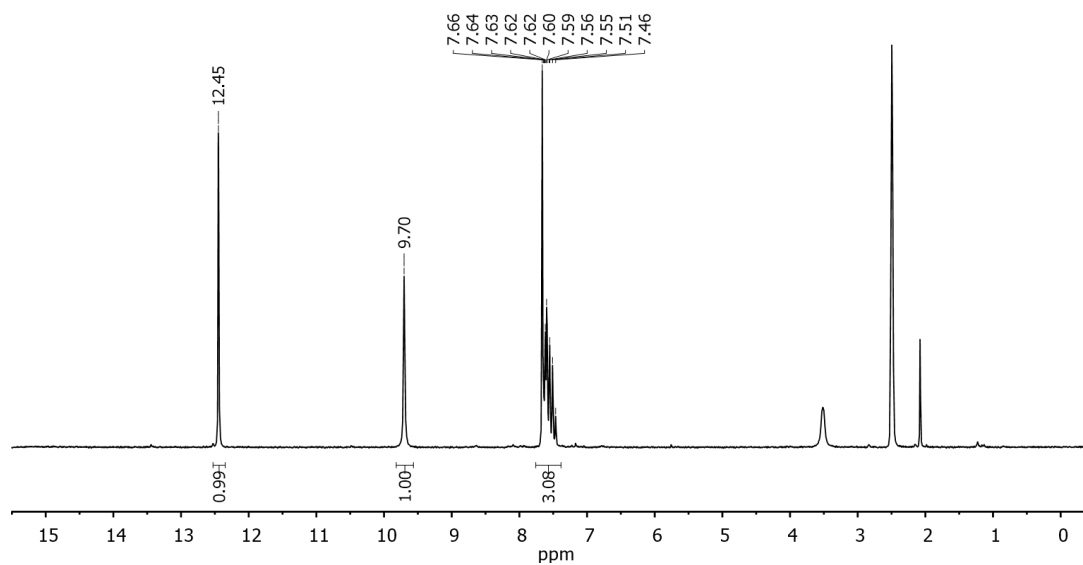
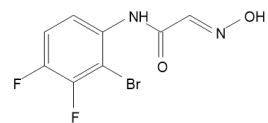
ESI-MS

NitiFIA04 #9 RT: 0.09 AV: 1 NL: 1.78E3
T: ITMS + c ESI Full ms [100.00-2000.00]

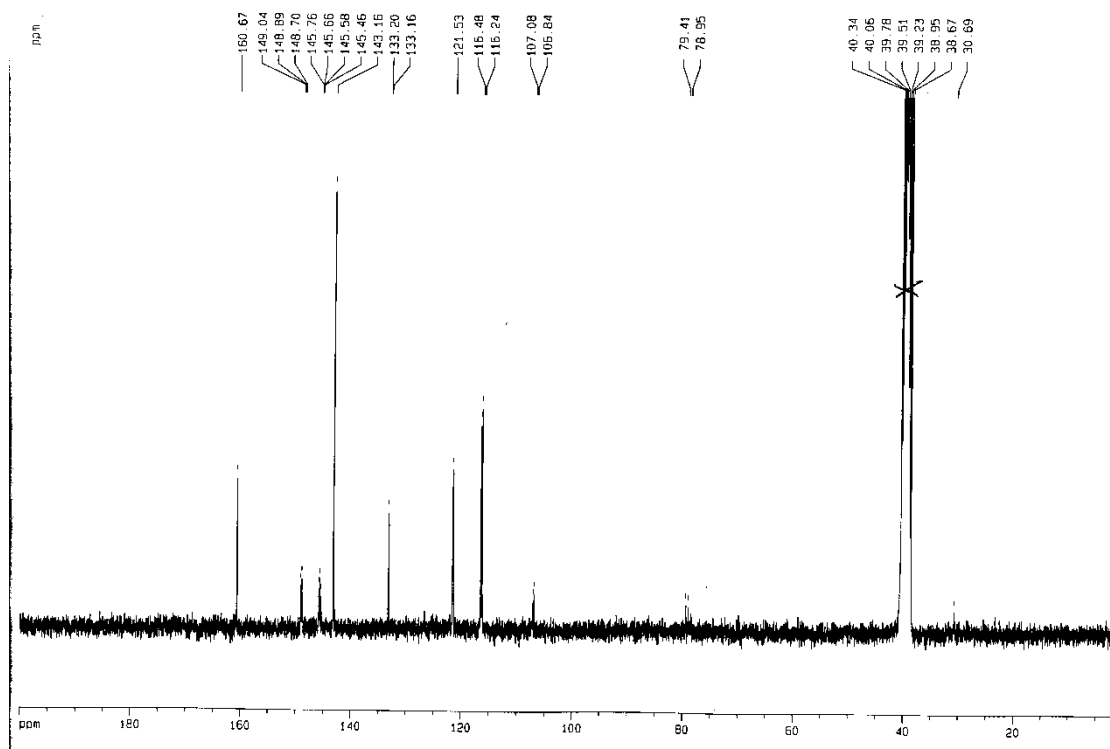


Compound 32

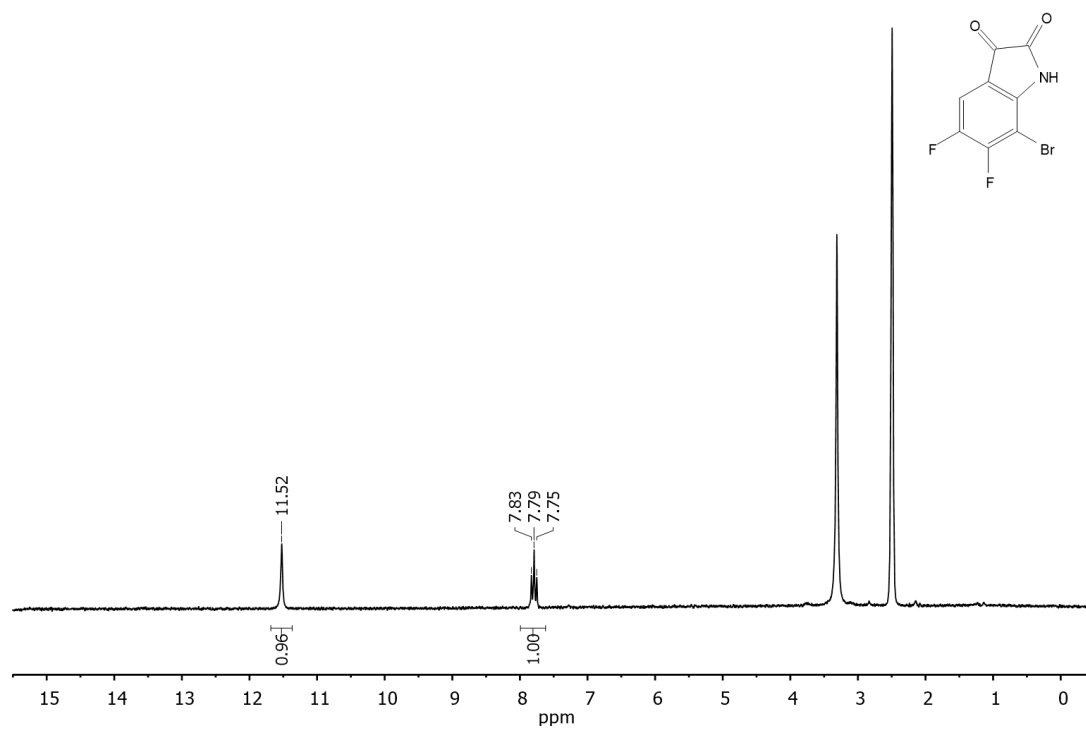
^1H NMR (200 MHz, d_6 -DMSO)



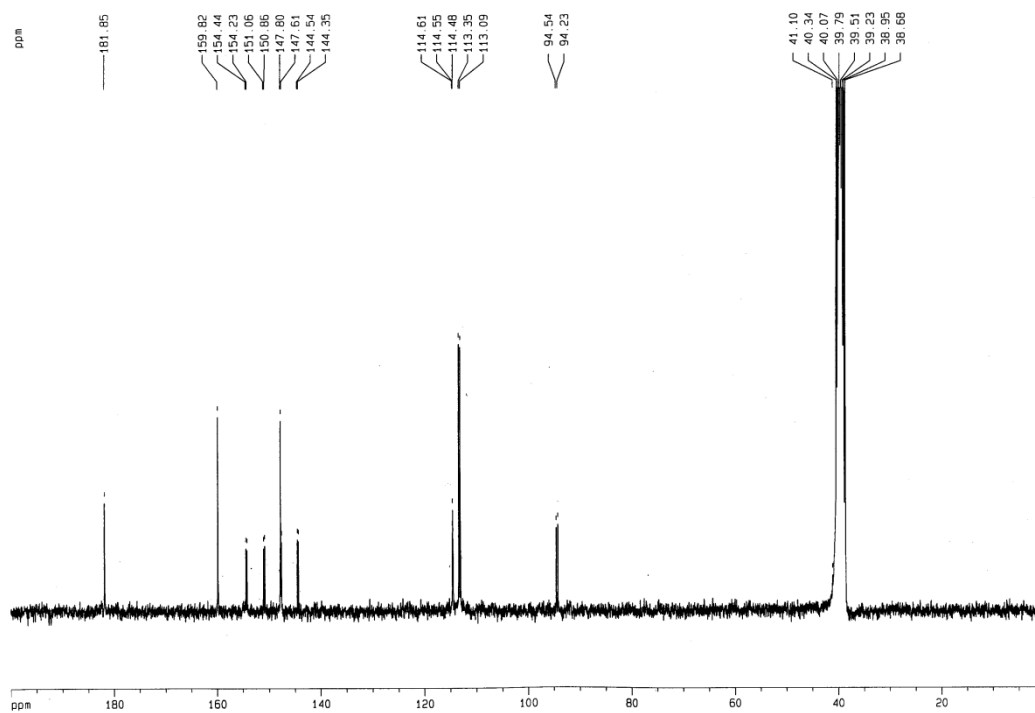
^{13}C NMR (75 MHz, d_6 -DMSO)



^1H NMR (200 MHz, d_6 -DMSO)



^{13}C NMR (75 MHz, d_6 -DMSO)



GCMS

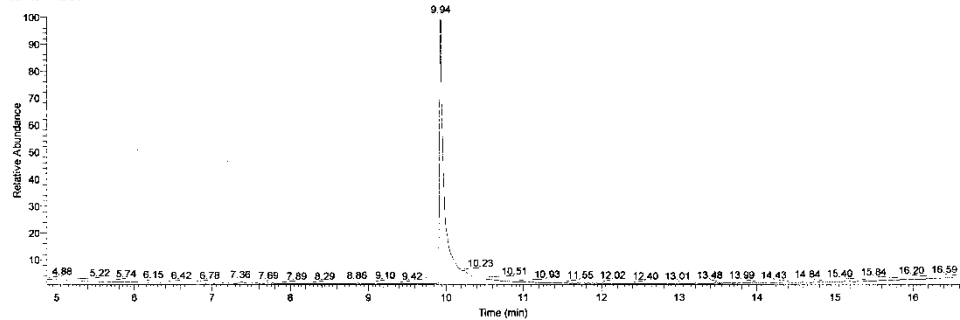
D:\DSQ2\1\UNIPV\Pasini\pasini087

10/16/2014 12:04:37 PM

AN146F38-56

Sil

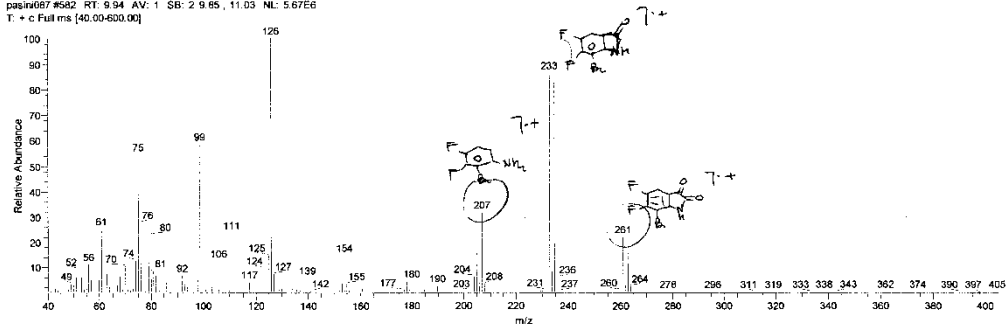
RT: 4.87 - 16.61



NL:
5.89E7
TIC MS
pasini087

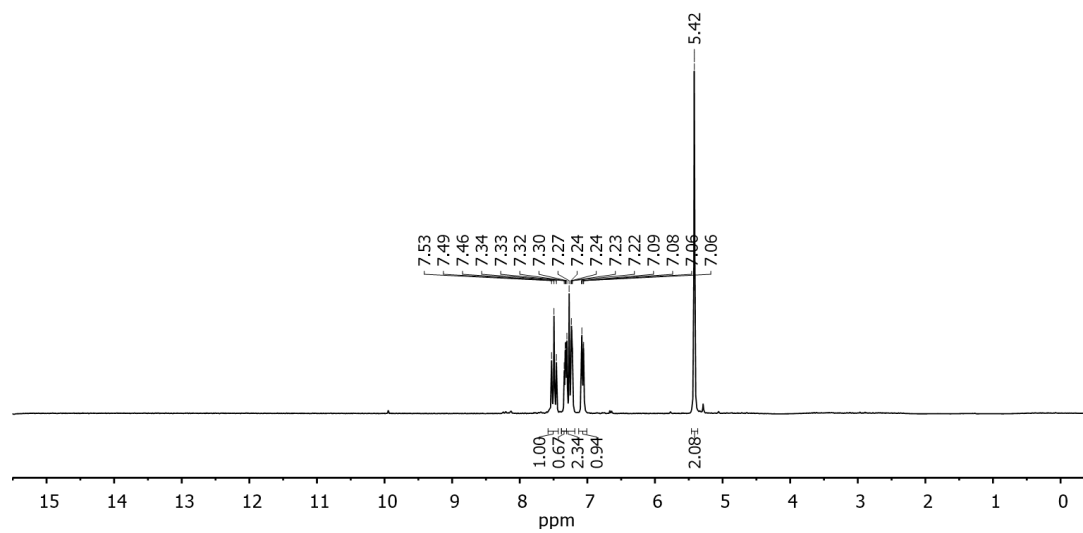
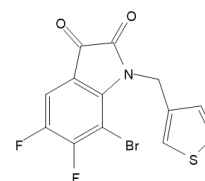
pasini087 #582 RT: 9.94 AV: 1 SB: 2 9.85, 11.03 NL: 5.67E6

T: + c Full ms [40.00-600.00]

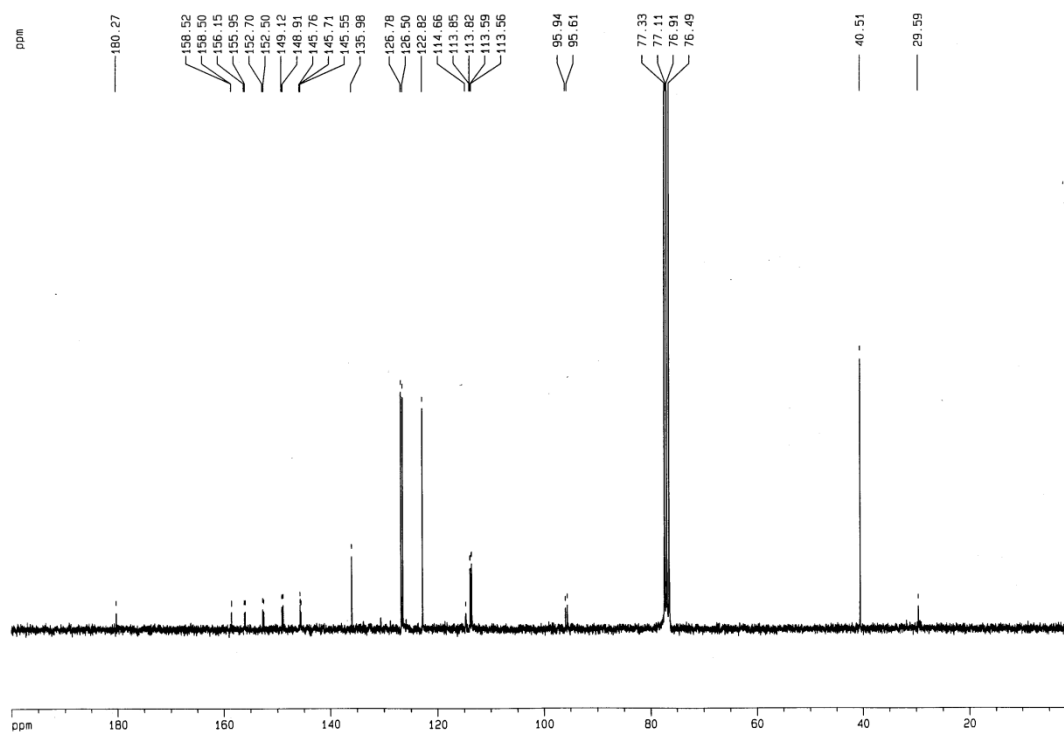


Compound **33**

^1H NMR (200 MHz, CDCl_3)

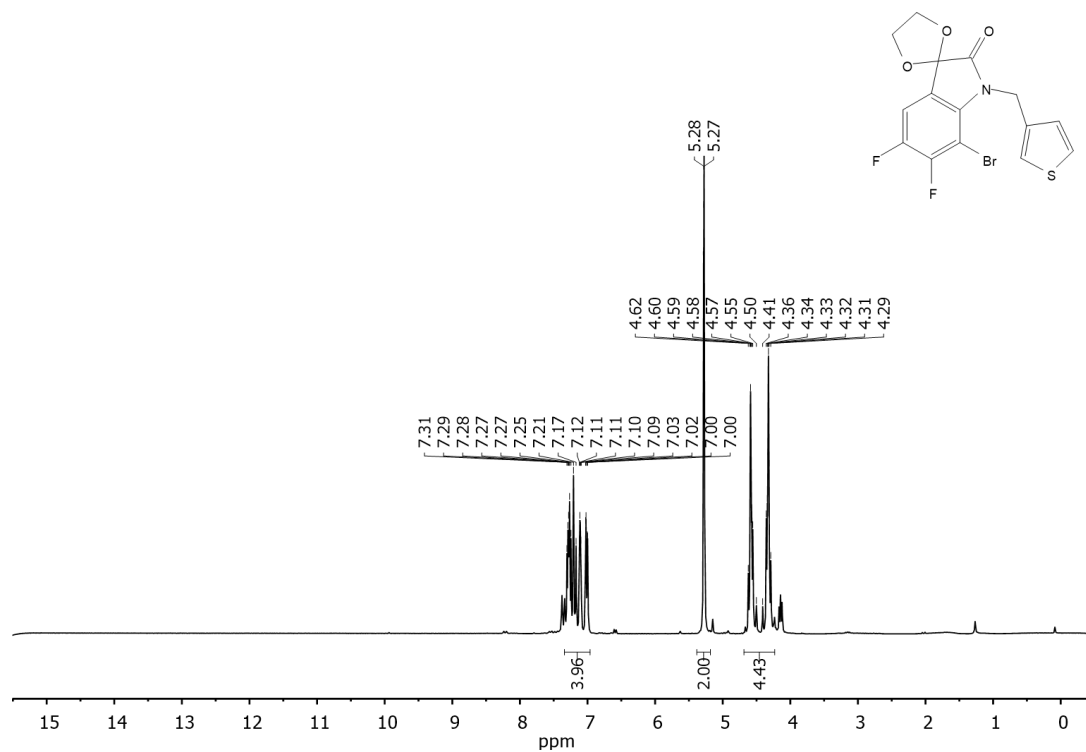


^{13}C NMR (75 MHz, CDCl_3)

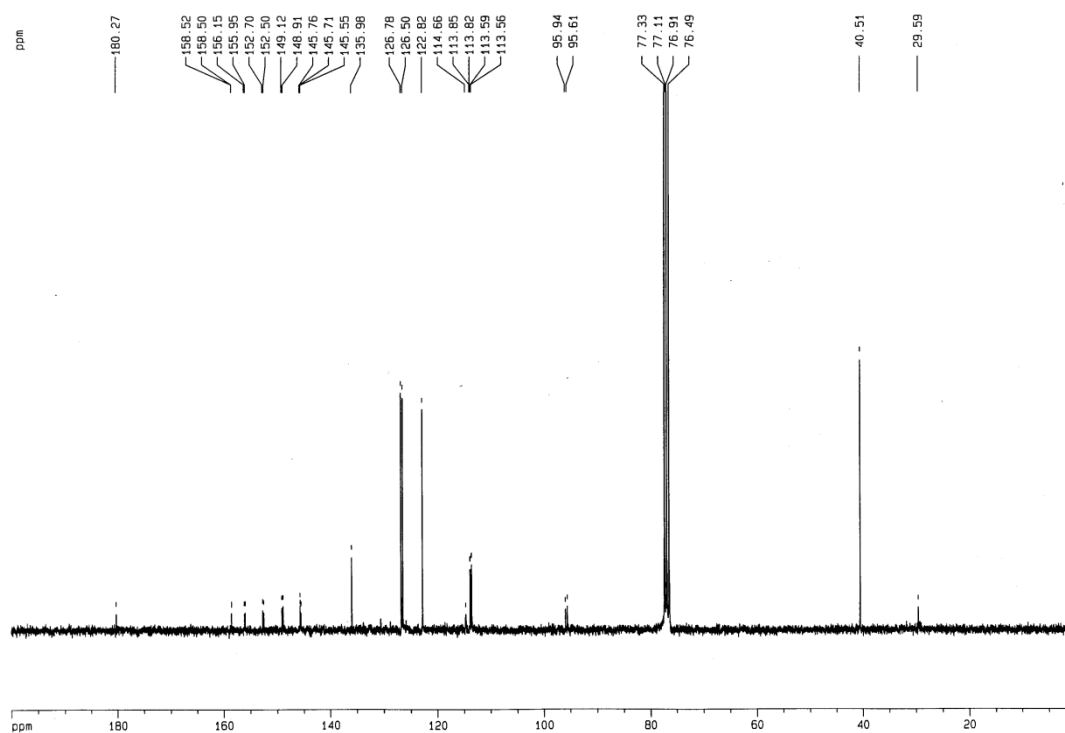


Compound **34**

^1H NMR (200 MHz, CDCl_3)

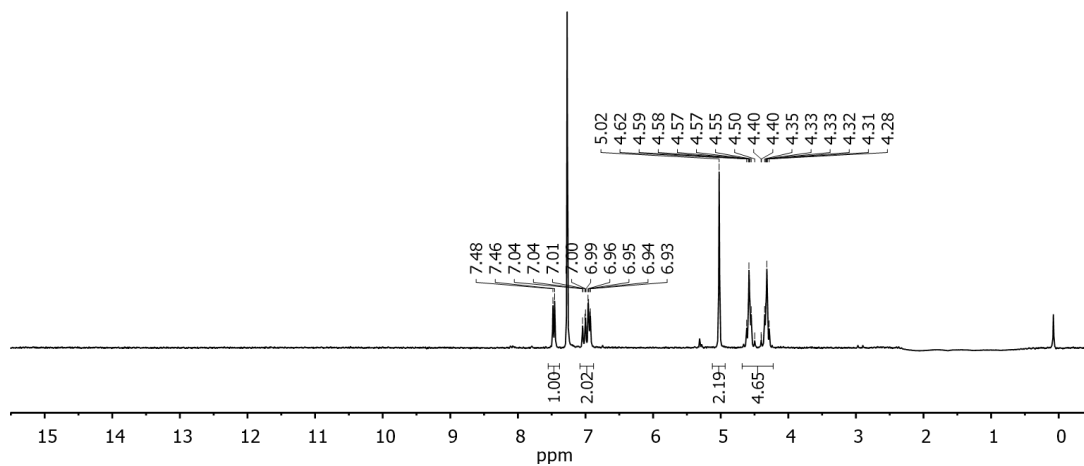
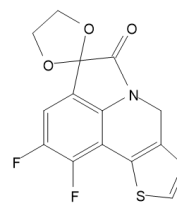


^{13}C NMR (75 MHz, CDCl_3)

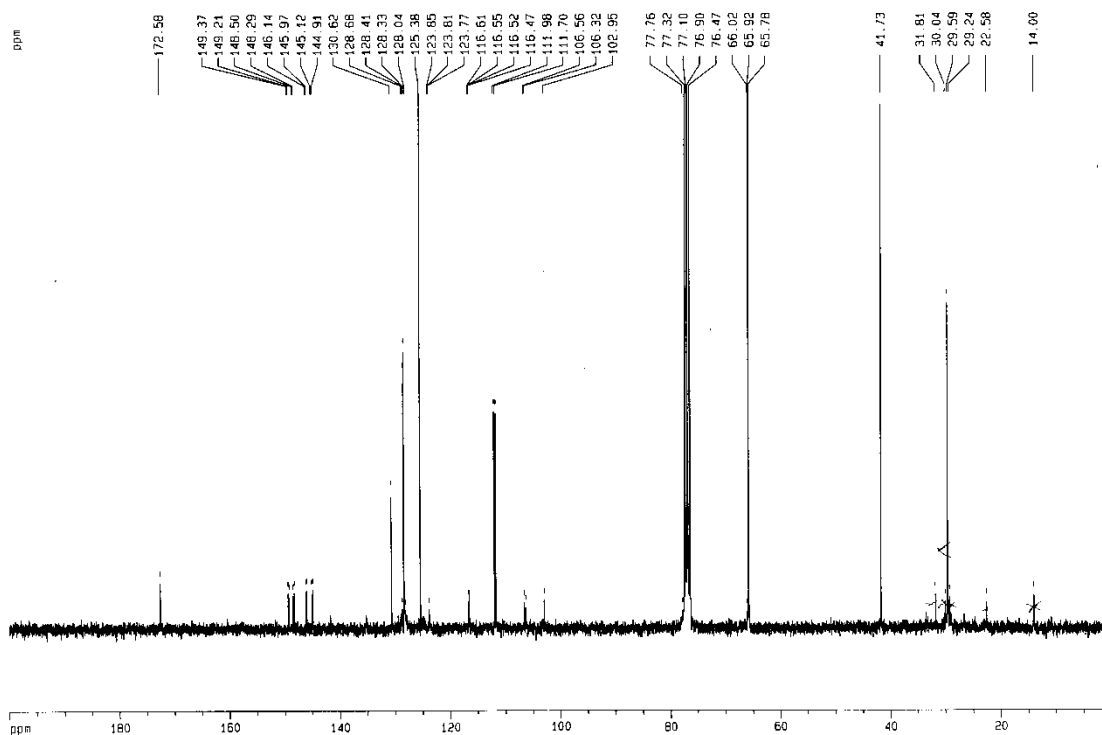


Compound 35

^1H NMR (200 MHz, CDCl_3)

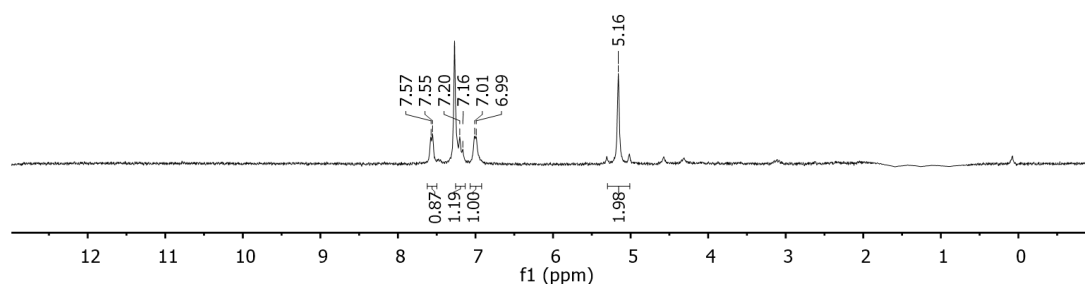
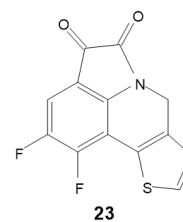


^{13}C NMR (75 MHz, CDCl_3)

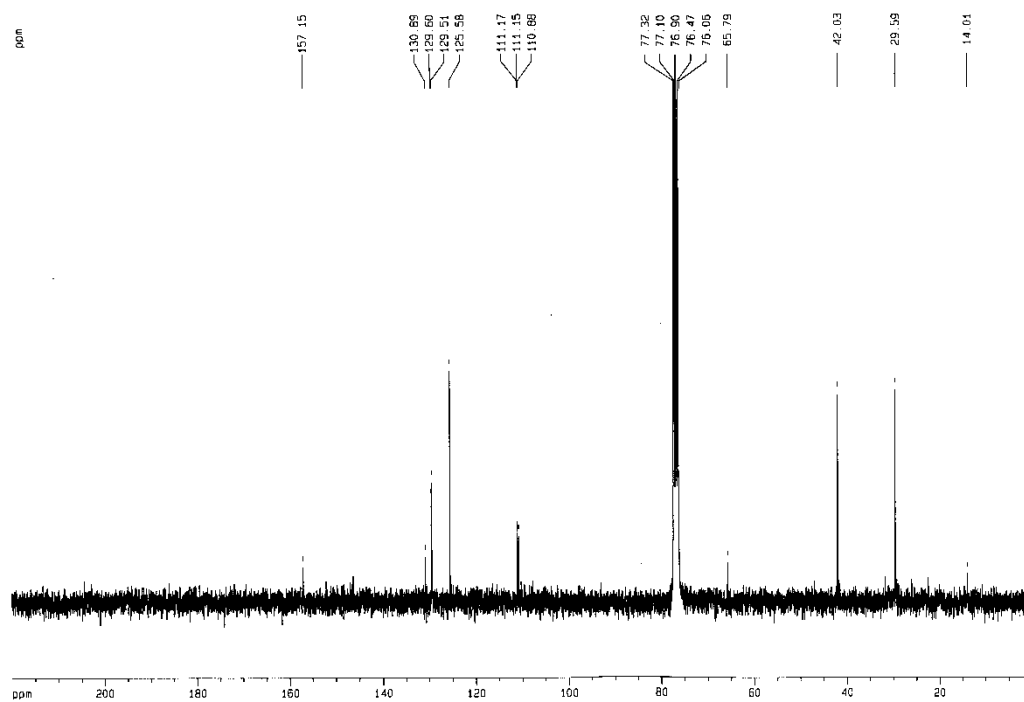


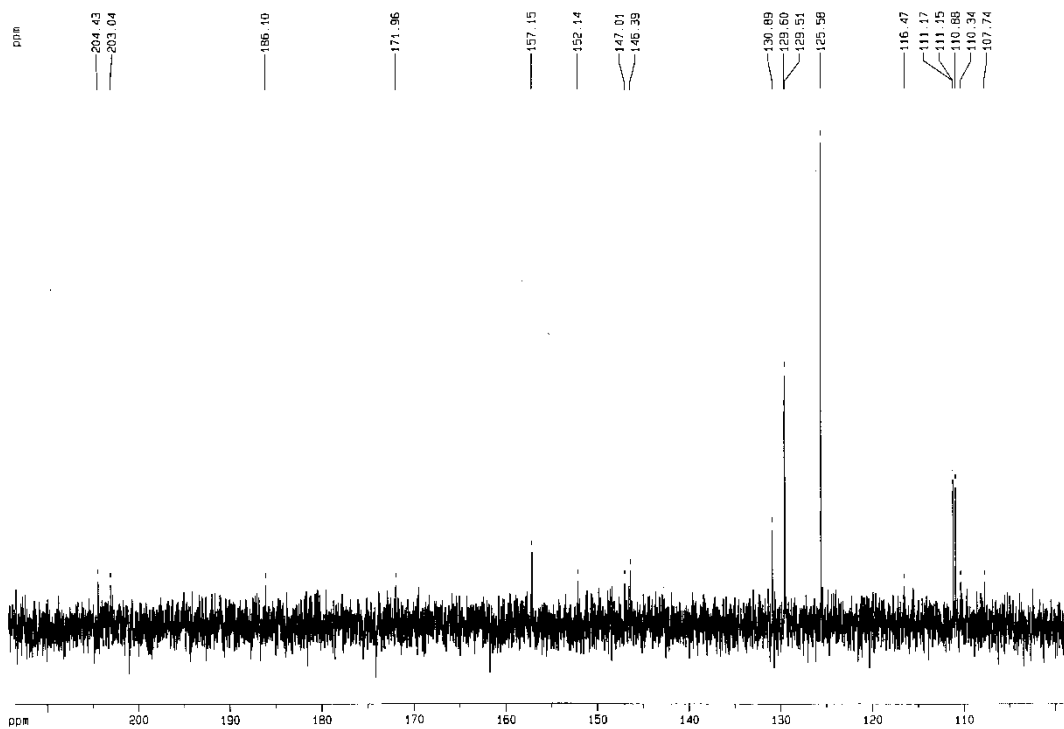
Compound **36**

^1H NMR (200 MHz, CDCl_3)



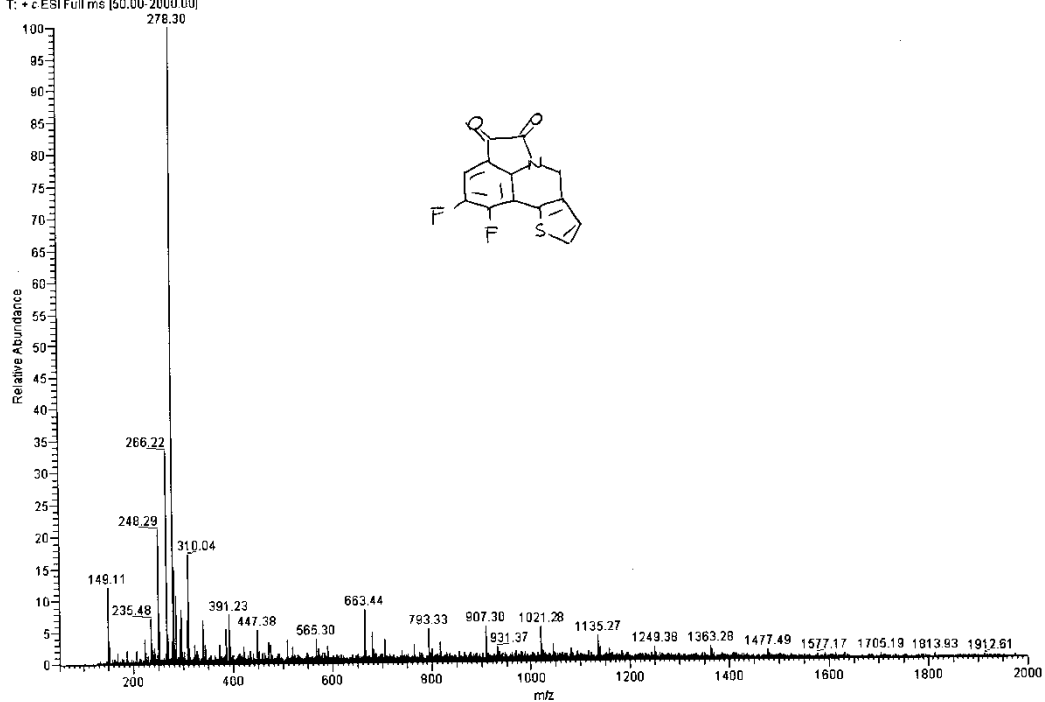
^{13}C NMR (75 MHz, CDCl_3)





ESI-MS

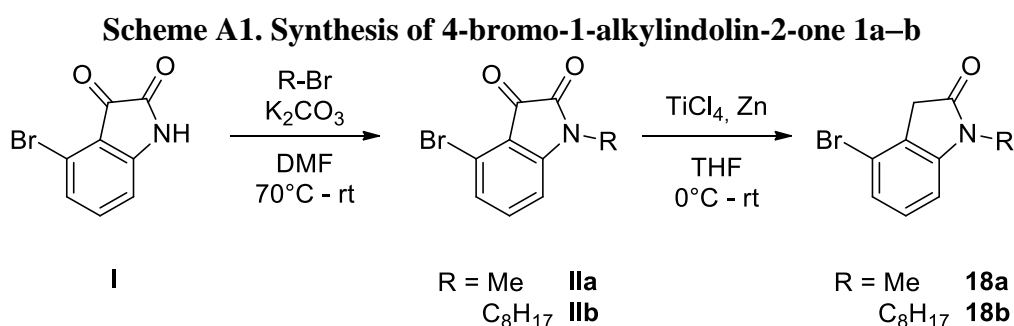
MS53#12-27 RT: 0.34-0.79 AV: 16 NL: 1.10E7
 T: +c ESI Full ms [50.00-2000.00]



ONE POT DIRECT ARYLATION AND CROSS-ALDOL CONDENSATION FOR THE RAPID CONSTRUCTION OF π -EXTENDED THIOPHENE AND FURAN-BASED SCAFFOLDS

Synthesis of Selected Compounds

In scheme A1, A2 and A3 the synthetic pathway for the starting materials used is shown.



Alkylated isatin **IIa–b** were synthesized using the following protocol reported in the literature.¹ Oxindole derivative **18a–b** were synthesized using a modified protocol reported in the literature.²

General Procedure for the Synthesis of Ia–b. Example for the synthesis of **Ia**. A flame-dried Schlenk flask was charged with 4-bromo-1H-indole-2,3-dione **I** (2.26 g, 10 mmol) and dry DMF (20 mL) under nitrogen. K_2CO_3 (1.38 g, 10 mmol) was added and the reaction mixture was stirred at 70 °C for 1 h. After this time iodomethane (1.24 mL, 20 mmol) was added *via* syringe and the reaction mixture was stirred at room temperature. After full conversion of the starting material (4h, TLC monitoring), the reaction mixture was quenched with water. The aqueous phase was extracted with ethyl acetate, the combined organic extracts were dried over anhydrous Na_2SO_4 and the organic solvent were removed *in vacuo*. Crude material was purified by flash chromatography (SiO_2 ; *n*-hexanes:ethyl acetate 7:3) to afford pure 4-bromo-1-methylindoline-2,3-dione **IIa** as red solid (2.35 g, 98%).

4-bromo-1-methylindoline-2,3-dione (IIa): obtained as a orange solid (2.35 g, 98%); ¹H NMR

(200 MHz, CDCl₃): δ 7.43 (t, J = 8.0 Hz, 1H), 7.34–7.18 (m, 1H), 6.85 (dd, J = 7.8, 0.9 Hz, 1H), 3.27 (s, 3H). ¹³C NMR (75 MHz, CDCl₃): δ 183.5, 151.6, 138.5, 125.4, 124.0, 117.6, 110.1, 26.4.

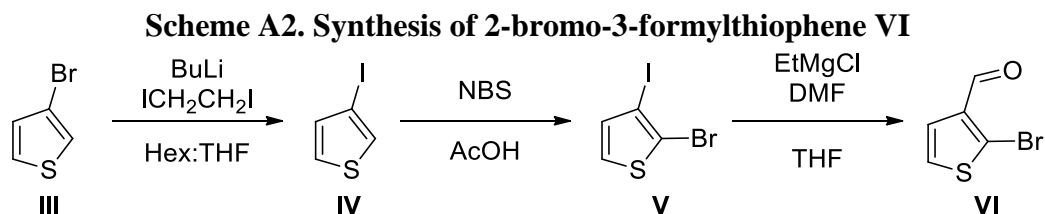
4-bromo-1-octylindoline-2,3-dione (**IIb**): obtained as a red solid (3.21 g, 95%); ¹H NMR (200 MHz, CDCl₃): δ 7.41 (t, J = 8.0 Hz, 1H), 7.33 – 7.17 (m, 1H), 6.85 (d, J = 7.8 Hz, 1H), 3.72 (t, J = 7.3 Hz, 2H), 1.78 – 1.55 (m, 2H), 1.49 – 1.16 (m, 10H), 0.99 – 0.76 (m, 3H). ¹³C NMR (75 MHz, CDCl₃): δ 180.8, 157.4, 152.9, 138.1, 128.1, 121.6, 116.3, 109.0, 44.3, 37.2, 30.4, 29.9, 29.4, 29.0, 28.5, 23.8, 22.9, 13.9, 10.4; GC-MS (EI): rt 16.92 min.; 337 [M]⁺.

General Procedure for the Synthesis of 18a–b. *Example for the synthesis of 18a.* TiCl₄ (3.3 mL, 30 mmol) was added to a stirred suspension of Zn powder (3.92 g, 60 mmol) in freshly distilled dry THF (80 mL) at rt under a dry N₂ atmosphere. After the addition, the mixture was refluxed for 2 h. The suspension with the low-valent titanium reagent thus formed was cooled to rt. A solution of 4-bromo-1-methylindoline-2,3-dione **IIa** (2.40 g, 10 mmol) in THF dry (20 mL) was added dropwise. The mixture was stirred at room temperature for about 1 h under N₂ (TLC monitoring). The reaction mixture was quenched with 3% HCl and extracted with DCM. The combined extracts were washed with water and dried over anhydrous Na₂SO₄. After evaporation of the solvent under reduced pressure, the crude product was purified by column chromatography (SiO₂; *n*-hexanes:ethyl acetate 6:4) to give the pure products **18a** as light yellow solid (1.12 g, 59%).

4-bromo-1-methylindoline-2-one (**18a**): obtained as a light yellow solid (1.12 g, 59%); ¹H NMR (200 MHz, CDCl₃): δ 7.23 – 7.09 (m, 2H), 6.88 – 6.62 (m, 1H), 3.49 (s, 2H), 3.21 (s, 3H). ¹³C NMR (75 MHz, CDCl₃): δ 173.7, 146.0, 129.4, 125.4, 125.3, 119.0, 106.8, 37.0, 26.5.

4-bromo-1-octylindoline-2-one (**18b**): obtained as a light yellow solid (1.12 g, 59%); ¹H NMR (200 MHz, CDCl₃): δ 7.16 (s, 2H), 6.77 (dd, J = 5.5, 3.2 Hz, 1H), 3.68 (t, J = 7.4 Hz, 2H),

3.48 (s, 2H), 1.80 – 1.53 (m, 2H), 1.49 – 1.17 (m, 10H), 1.02 – 0.68 (m, 3H). ^{13}C NMR (75 MHz, CDCl_3): δ 173.5, 145.5, 129.2, 125.5, 124.9, 107.0, 40.3, 37.0, 31.6, 29.1, 29.0, 27.3, 26.8, 22.5, 13.9.



Compound **VI** (which is however commercially available) was synthesized using the following protocol reported in literature (Scheme A2).³

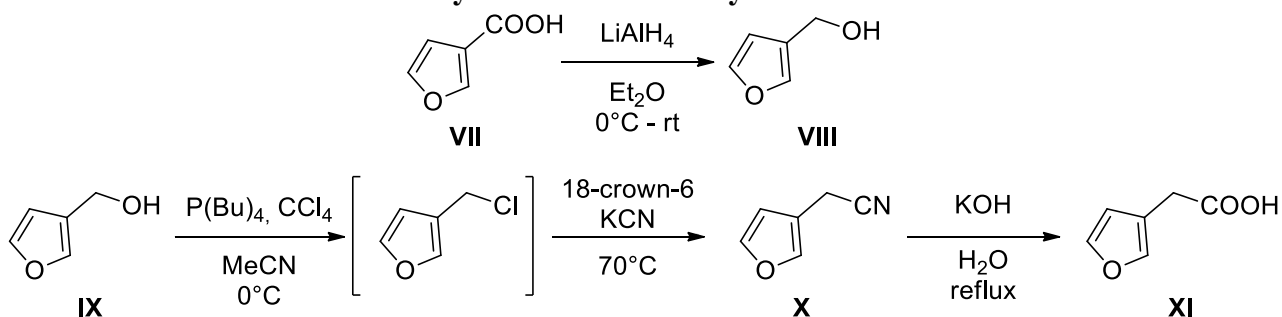
3-iodothiophene (IV). A 1.6 M solution of *n*-butyllithium in hexane (12.3 mL, 19.7 mmol) was added in one portion to a solution of 3-bromothiophene **III** (1.74 mL, 18.4 mmol) in hexane (27.6 mL) at temperature of -70°C under argon. Successively, a small amount of THF (2.7 mL), followed by hexane (9.3 mL), was added quickly. Then the mixture was stirred at 0°C for a short period of time and was cooled again to -70°C . After the addition of 1,2-diiodoethane (6.00 g, 21.3 mmol) at -70°C , the reaction mixture was warmed to room temperature and stirred there for 1 h. A sat. sodium thiosulfate solution was poured into the reaction mixture. The organic layer was diluted with ethyl acetate, washed with brine, and dried over anhydrous MgSO_4 . After removal of the solvent *in vacuo*, the residue was purified by flash chromatography (SiO_2 ; *n*-hexane) to afford **IV** as a yellow oil (3.32 g, 86%): ^1H NMR (400 MHz, CDCl_3): δ 7.41 (dd, $J = 3.0, 1.8$ Hz, 1H), 7.20 (dd, $J = 5.1, 3.0$ Hz, 1H), 7.10 (dd, $J = 5.1, 1.8$ Hz, 1H).

2-Bromo-3-iodothiophene (V). A mixture of **IV** (2.44 g, 11.6 mmol), *N*-bromosuccinimide (2.21 g, 12.4 mmol), and acetic acid (10 mL) was stirred at 100°C for 1 h under argon. The reaction mixture was diluted with water and sat. NaHCO_3 and was extracted with ethyl acetate. The extract was washed with brine and dried over anhydrous MgSO_4 . After removal of the solvent *in vacuo*, the residue was purified by flash chromatography (SiO_2 ; *n*-hexane) to

afford **V** as a colorless oil (2.47 g, 74%). $^1\text{H NMR}$ (400 MHz, CDCl_3): δ 7.23 (d, $J = 5.7$ Hz, 1H), 6.96 (d, $J = 5.7$ Hz, 1H).

2-Bromo-3-formylthiophene (VI). A solution of **V** (561 mg, 1.94 mmol) in THF (1.8 mL) was added dropwise into a 2.0 M solution of ethylmagnesium chloride in THF (1.9 mL, 3.8 mmol) at 0°C under argon atmosphere. The mixture was stirred at rt for a short period of time, and then freshly distilled DMF (0.27 mL, 3.5 mmol) was added dropwise at 0°C . After stirring at rt for 1 h, the reaction mixture was diluted with sat. NH_4Cl and was extracted with ethyl acetate. Evaporation of the solvent followed by flash chromatography (SiO_2 ; *n*-hexanes:ethyl acetate 8:2) gave a mixture of formylated products as a yellow oil (230 mg, 62%). The products were identified by $^1\text{H NMR}$ and GC-MS spectrometers. Pure product **VI** was obtained as pale pink crystals by crystallization with *n*-hexane for 2 weeks. $^1\text{H NMR}$ (400 MHz, CDCl_3): δ 9.94 (s, 1H), 7.36 (d, $J = 6.0$ Hz, 1H), 7.28 (d, $J = 6.0$ Hz, 1H).

Scheme A3. Synthesis of Furan-3-yl acetic acid XI



Compounds **VIII** and **XI** were synthesized using the following protocol reported in literature (Scheme A3).^{4,5}

3-Furanmethanol (VIII). A flame-dried Schlenk flask was charged with LiAlH_4 (0.38 g, 10 mmol) and freshly distilled Et_2O (5 mL) under nitrogen, then a solution of 3-furoic acid **VII** (1.12 g, 10 mmol) in freshly distilled Et_2O (5 mL) was added via *cannula* dropwise at 0°C . The reaction mixture was stirred at rt for 1 h (TLC monitoring), then was quenched adding slowly a solution 10% KOH aq and was extracted with diethyl ether. The extract was washed with 5% HCl aq., brine and dried over anhydrous Na_2SO_4 . 3-Furanmethanol **VIII** was ob-

tained after removal of the solvent *in vacuo*, as a colorless oil (1.32 g, 93%). ¹H NMR (400 MHz, CDCl₃): δ 7.40 (d, *J* = 2.0 Hz, 2H), 6.56 – 6.17 (m, 1H), 4.53 (s, 2H), 2.16 (s, 1H).

Furan-3-yl acetic acid (IX). 3-Furanmethanol **VIII** (4.00g, 40.80 mmol) was added to a solution of tri(*n*-butyl)phosphine (11.18 cm³, 44.88 mmol) and CCl₄ (4.33 cm³, 44.88 mmol) in dry CH₃CN (90 mL) at 0°C. The resulting reaction mixture was stirred for 1 hour and 18-crown-6 (2.50 g, 9.46 mmol) was added, followed by the careful addition of KCN (5.31 g, 81.50 mmol). The temperature was raised to 70°C and stirring continued for a further 12 h. Dilution with diethyl ether was followed by successive washes with water, 1 M citric acid and brine. The organic layer was collected, dried over anhydrous MgSO₄ and the solvent removed *in vacuo*. The crude product was purified by flash chromatography (SiO₂; *n*-hexane:diethyl ether, 10:1) affording the intermediate nitrile as a yellow crystalline solid (1.37 g, 31%). The nitrile (0.72 g, 6.72 mmol) was subsequently hydrolyzed by refluxing in an aqueous solution of KOH (10 mL, 2.5 M) for 5 hours. Following discoloration with charcoal, the organic layer was washed with dilute H₂SO₄, dried over anhydrous MgSO₄ and concentrated under reduced pressure affording a colorless residue. Upon addition of light petroleum ether the title compound was obtained as a colorless crystalline precipitate. ¹H NMR (200 MHz, CDCl₃): δ 7.40 (d, *J* = 1.4 Hz, 1H), 6.39 (t, *J* = 1.3 Hz, 2H) 3.52 (s, 2H). ¹³C NMR (75 MHz, CDCl₃): δ 177.4, 143.1, 140.6, 116.5, 111.3, 30.6.

Additional spectroscopic data for compound 46a

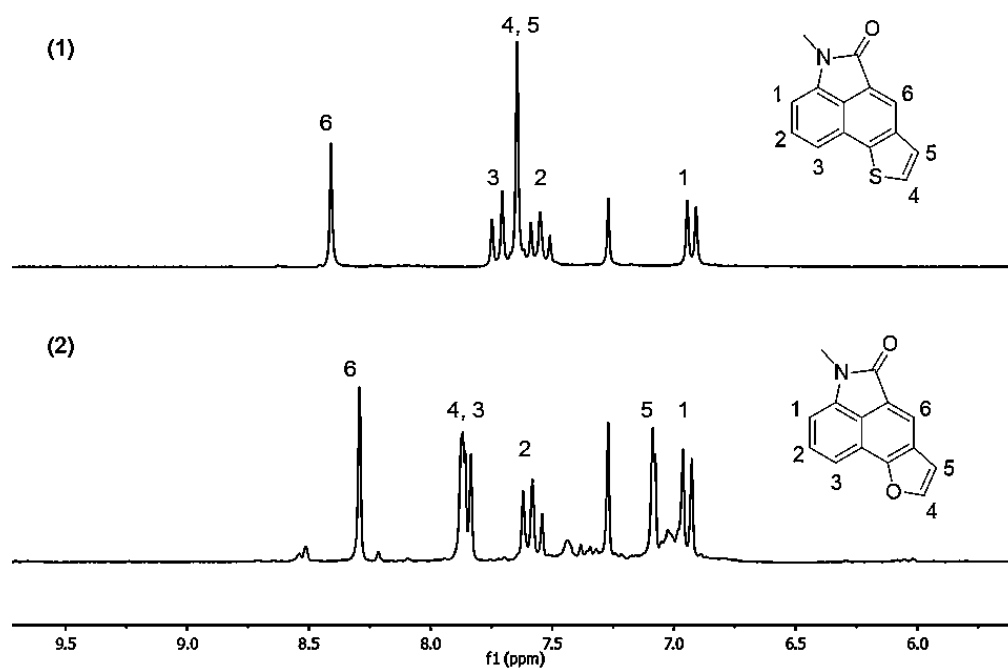


Figure A15. Stacked ^1H NMR (CDCl_3 , 200 MHz) of compounds **46a** (1) and **46c** (2).

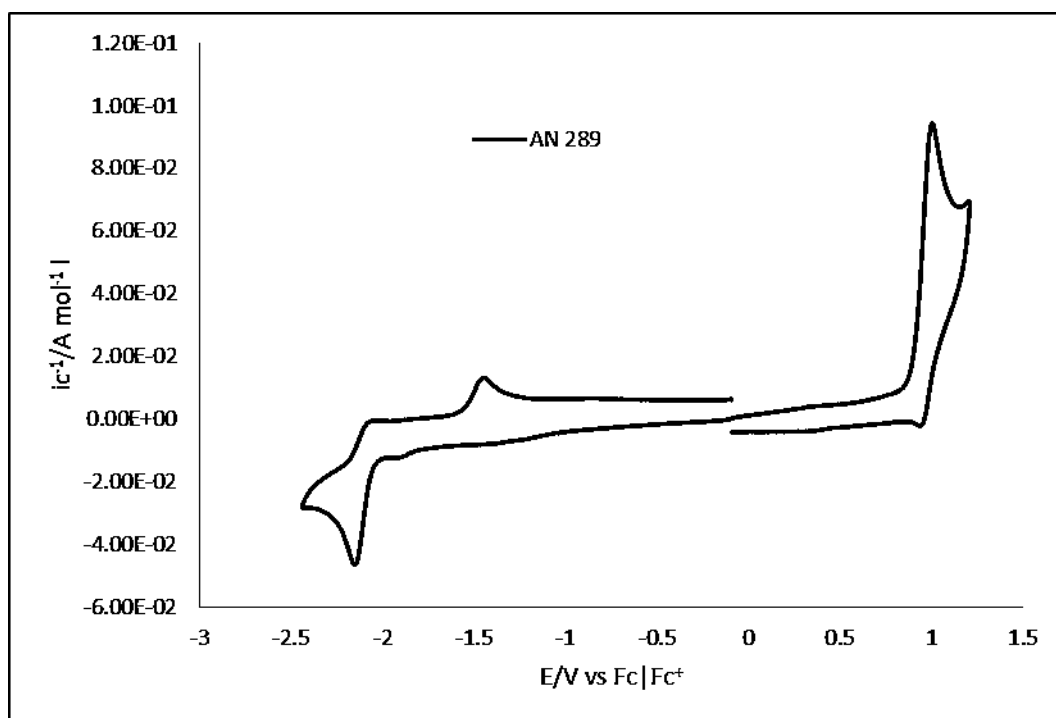


Figure A16. CV spectra of **46a** shown an irreversible oxidation and reduction peaks. Electrochemical polymerization was not observed. The energy gap obtained is 2.94 eV ($E_{\text{HOMO}} = -5.6$ eV, $E_{\text{LUMO}} = -2.75$ eV)

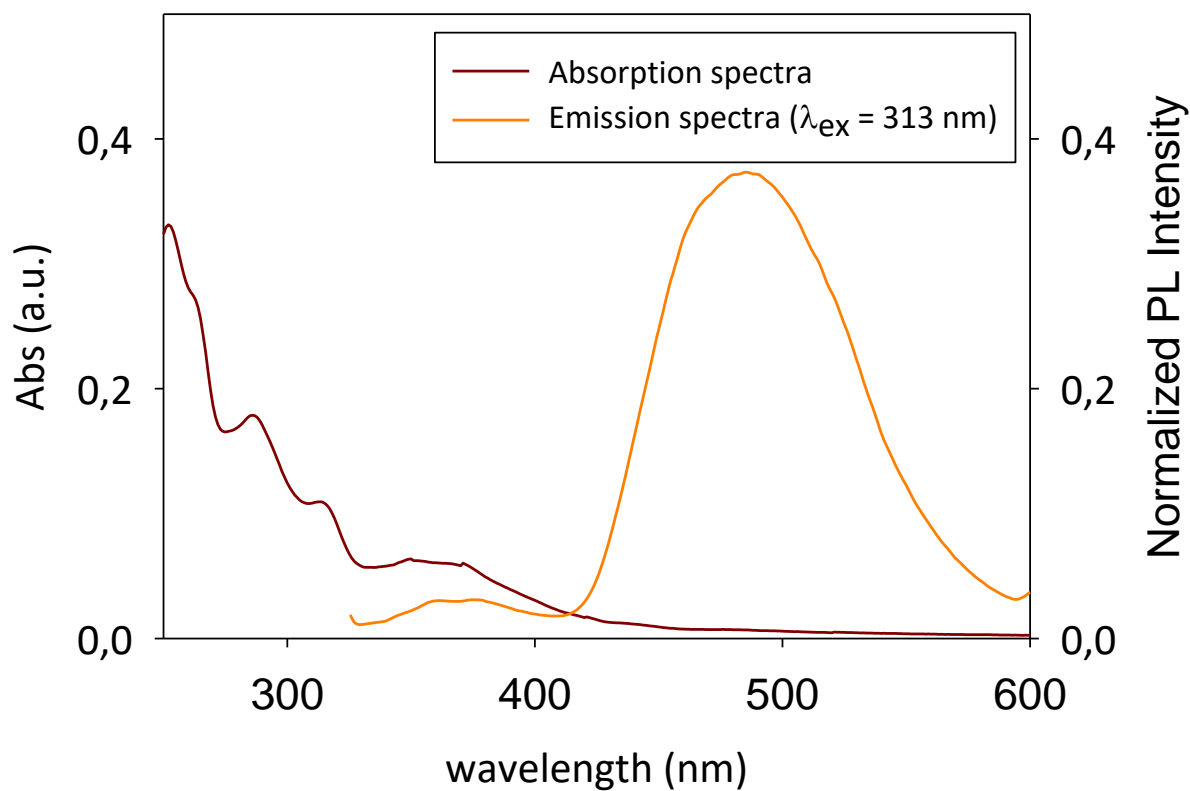
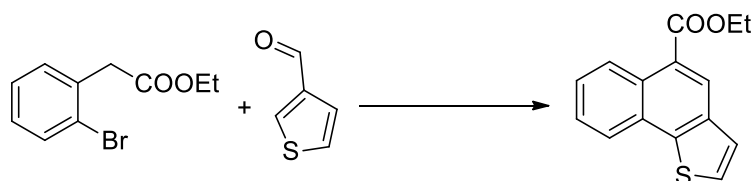


Figure A17. Absorption and emission spectra in CHCl_3 of **46a** (solution 10^{-5} M in CH_2Cl_2). **46a** does not absorb in the visible region while have a λ_{MAX} of emission in cyan region.

Additional experiments

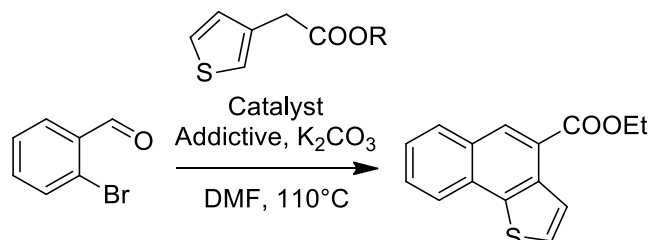
Table A5. Optimization of the synthesis of 49a



Entry	Catalyst	Base	Additive	Solv	T[°C]	Yield [%] ^a
1	Pd(OAc) ₂	KOAc	PPh ₃	DMF	150	0
3	Pd ₂ (dba) ₃	K ₂ CO ₃	-	DMF	150	0
3	Pd(OAc) ₂	K ₂ CO ₃	PPh ₃	DMF	150	0
4	Pd(OAc) ₂	K ₂ CO ₃	JhonPhos	DMF	150	0
5	Pd(OAc) ₂	K ₂ CO ₃	PPh ₃	Tol	150	0
6	Pd ₂ (dba) ₃	K ₂ CO ₃	-	Tol	150	0

General conditions: 1 mmol of ethyl 2-bromophenylacetate, 1.1 mmol of 3-formylthiophene, cat (5 mol%), phosphine (10 mol%), 2 mmol of base in 2 mL of solvent (50 mM in reagents). ^aIsolated yield after flash chromatography.

Table A6. Optimization of reaction conditions for the synthesis of 53 and 57

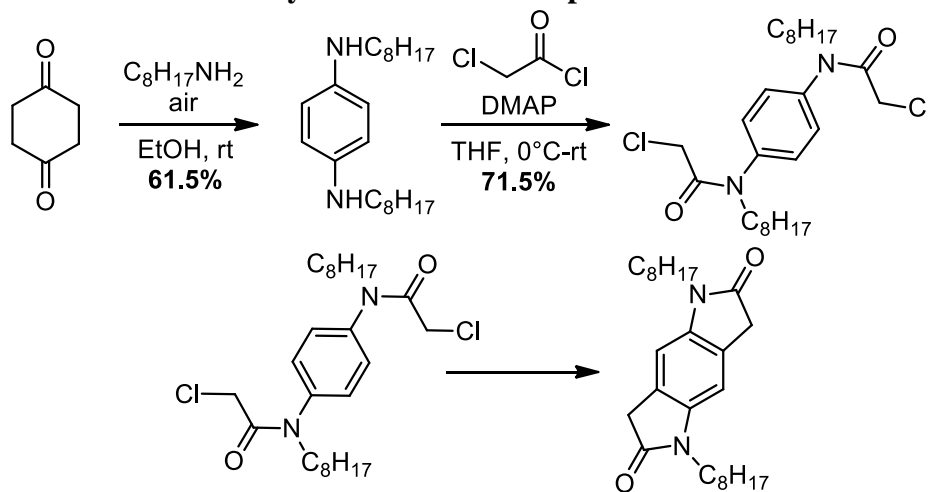


Entry	R	Catalyst	Add(4 mol%)	10:12 ^b	Yield[%] ^a
1 ^b	Et	Pd(PPh ₃) ₄	-	15:85	12
2	Et	PdCl ₂	-	0:100	-
3	Et	Pd(dppf)Cl ₂ ·DCM	-	0:100	-
4 ^b	Et	Pd(PPh ₃) ₂ Cl ₂	-	n.d.	19
5 ^b	Et	Pd(OAc) ₂	PPh ₃	65:35	35
7 ^b	Et	Pd(OAc) ₂	P ^t Bu ₃ ·HBF ₄	25:75	14
8 ^b	Et	Pd(OAc) ₂	dppp	53:47	21
9 ^b	Et	Pd(OAc) ₂	JhonPhos	50:50	31
10 ^b	Et	Pd(OAc) ₂	P(<i>o</i> -methoxyphenyl) ₃	62:38	30
11 ^{a,d}	H	Pd(OAc) ₂	PPh ₃	99:1	91
12 ^{a,c,d}	H	Pd(OAc) ₂	PPh ₃	99:1	91

^a Isolated yield after flash chromatography of **46**. ^b Cross-aldol product was isolated by column chromatography. Ratio in the crude reaction mixture was calculated using ¹H NMR. ^c Reaction conducted at 110°C. ^d The addition of EtBr at rt was conducted after 24h

Design of Thienobenzothienoisindoloindoleione-Based Compound via One Pot Cross-Aldol Condensation and Direct Arylation

Scheme A4. Synthesis of DIPID reported in literature⁶



Entry	Metod	Yield [%]
1	AlCl ₃ (7 eq), 190°C, 20 min	0
2	AlCl ₃ (7 eq), 190°C, 20 min	0
3	AlCl ₃ (7 eq), 190°C, 1h	0
4	AlCl ₃ (30 eq), 190°C, 20 min	0
5	AlCl ₃ (10 eq), NaCl (30 eq), 190°C, 1h	0
6	AlCl ₃ (10 eq), NaCl (30 eq), 120°C-190°C	0
7	AlCl ₃ (4 eq), DCE dry (0.1M), reflux	0
8	AlCl ₃ (4 eq), Heptane (0.1M), reflux	0
9	AlCl ₃ (4 eq), <i>o</i> -diclorobenzene (0.1M), reflux	0
10	AlCl ₃ (4 eq), Ethylen Glycol (0.1M), 190°C	0
11	Pd(OAc) ₂ , JHONPHOS, Et ₃ N, Tol dry, 80°C	0

Scheme A5. Experiment not achieved for the synthesis of benzodipyrrolidone⁷

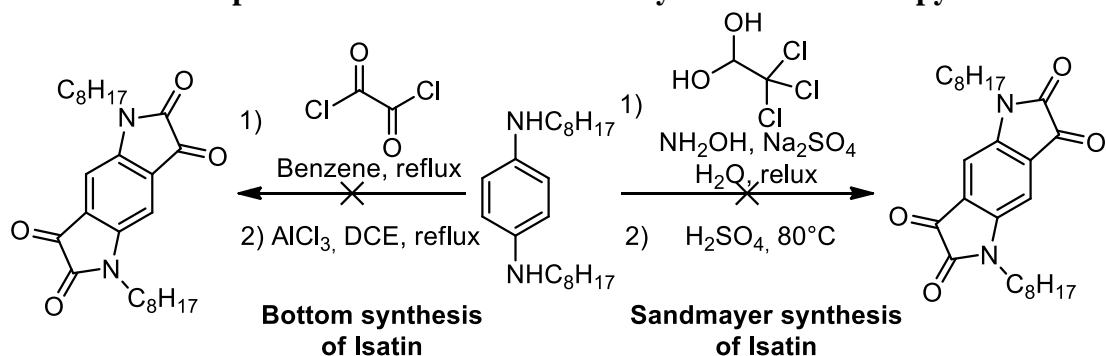
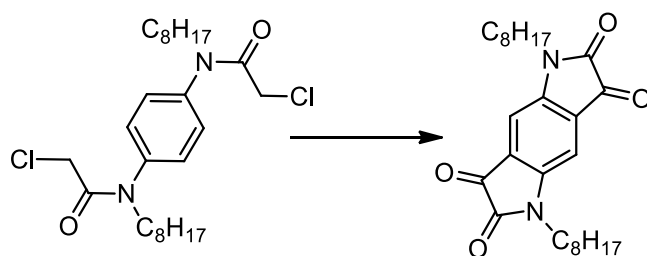
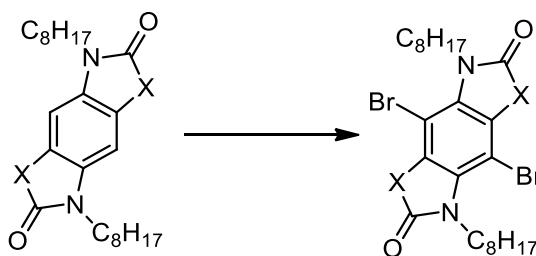


Table A6. Oxidative cyclization Cu-catalyzed for the synthesis of benzodipyrrolidone⁸



Entry	Metod	Yield [%]
1	CuI (5mol%), DMSO (0.1M), 100°C	9
2	CuI (5mol%), DMSO dry (0.1M), 100°C	14
3	CuI (10mol%), DMSO dry (0.1M), 100°C	13
5	CuI (5mol%), AcOH (2 eq), DMSO dry (0.1M), 100°C	11
4	CuBr (5mol%), DMSO dry (0.1M), 100°C	-

Table A7. Bromination trials on DIPID and benzodipyrrolidone



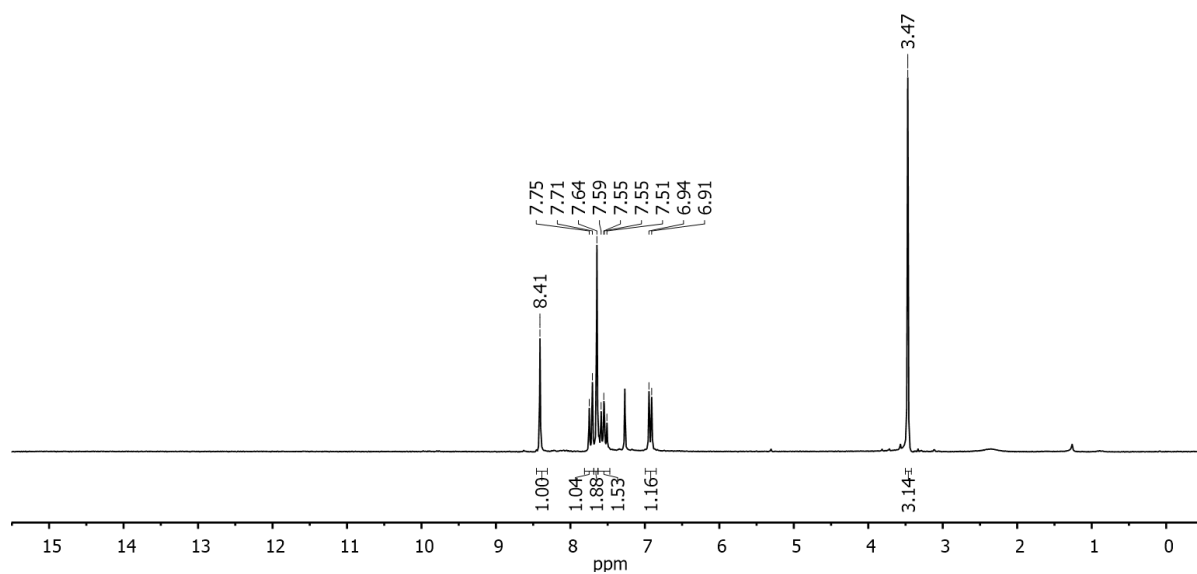
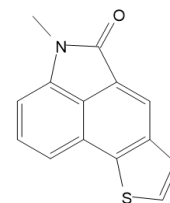
Entry	X	Metod	Yield [%]
1	CH ₂	Br ₂ , CHCl ₃ , rt	-
2	CH ₂	Br ₂ , DMF, rt	-
3	CO	Br ₂ , CHCl ₃ , rt	0
4	CO	Br ₂ , DMF, rt	0
5	CO	NBS, DMF:AcOH, rt	0

References

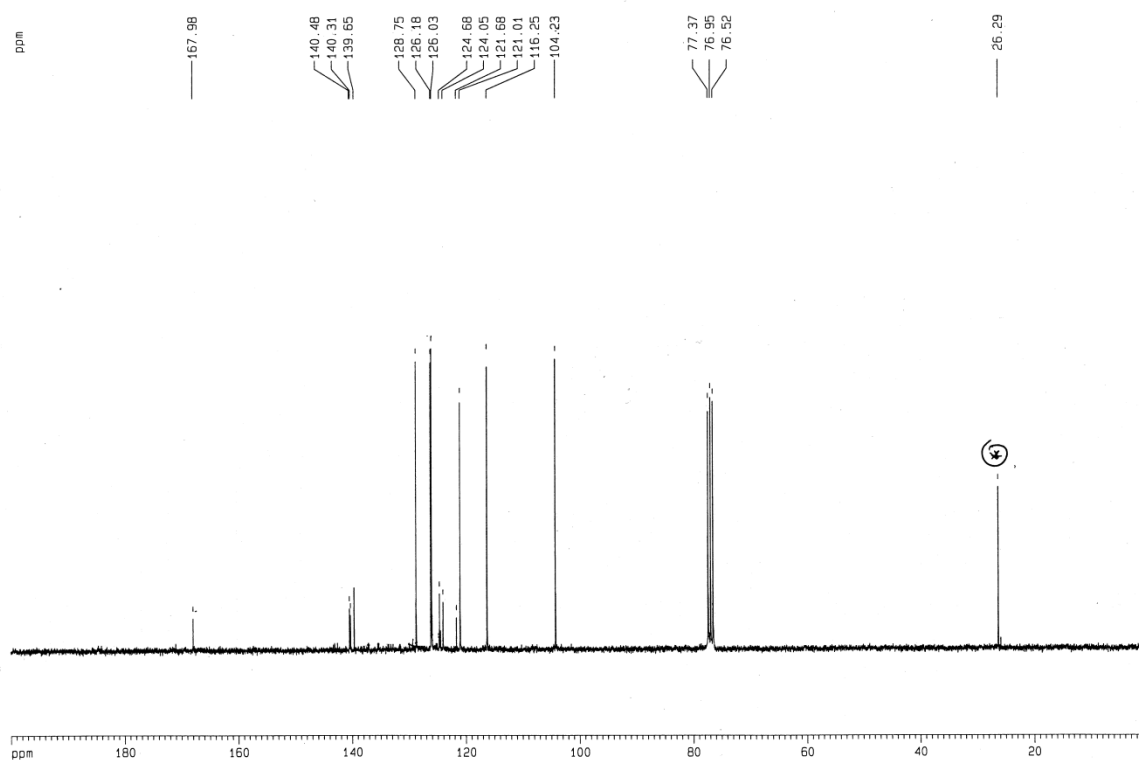
- (1). Xiaoyuan, L.; Jinhuan, S.; Zhoujun, L.; Yuanyuan, Z.; Zhenghao, D.; Shuai, Q.; Jiayi, W.; Li, L.; Zhiqiang, S.; Wenjin, Y. *Org. Lett.* **2016**, *18*, 956 – 959.
- (2). Wei, L.; Ming-Hua, H.; Xian, F.; Lei, F.; Cheng-Pao, C.; Zhi-Bin, H.; Da-Qing, S. *Tetrahedron Lett.* **2014**, *55*, 2238 – 2242.
- (3). Sonoda, M.; Kinoshita, S.; Luu, T.; Fukuda, H.; Miki, Koji; Umeda, R.; Tobe, Y. *Synth. Commun.* **2009**, *39*, 3315 – 3323.
- (4). Sherman, E.; Amstutz, E. D. *Austr. J. Chem.* **1989**, *42*, 2181 – 2190.
- (5). Kassianidis, E.; Pearson, R. J.; Philp, D. *Chem. Eur. J.* **2006**, *12*, 8798–8812.
- (6). W. Cui, F. Wudl, *Macromolecules* **2013**, *46*, 7232–7238.
- (7). Q. Gui, F. Dai, J. Liu, P. Chen, Z. Yang, X. Chen, Z. Tan, *Org. Biomol. Chem.* **2014**, *12*, 3349-3353.
- (8). N. Kaila, K. Janz, S. DeBernardo, P. W. Bedard, R. T. Camphausen, S. Tam, D. H. H. Tsao, J. C. Keith, C. Nickerson-Nutter, A. Shilling, R. Young-Sciame, Q. Wang, *J. Med. Chem.* **2007**, *50*, 21-39

Copies of ^1H and ^{13}C NMR spectra
Compound **46a**

^1H NMR (200 MHz, CDCl_3)

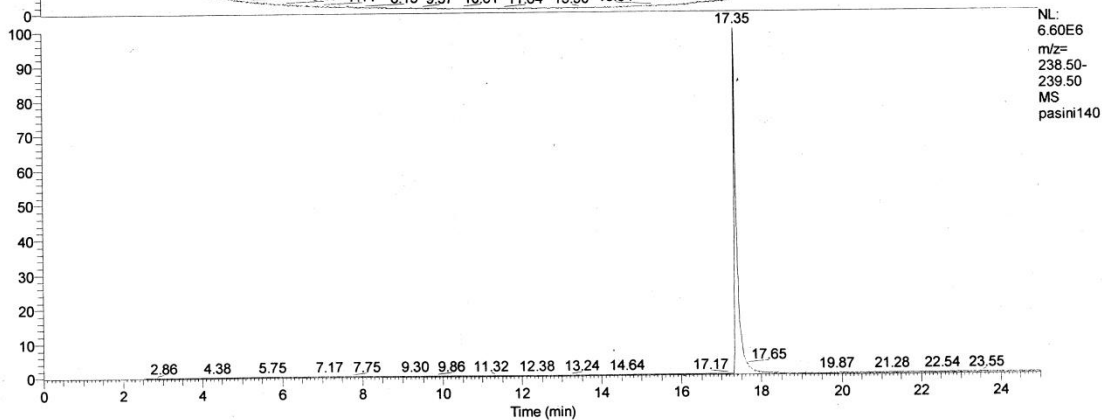
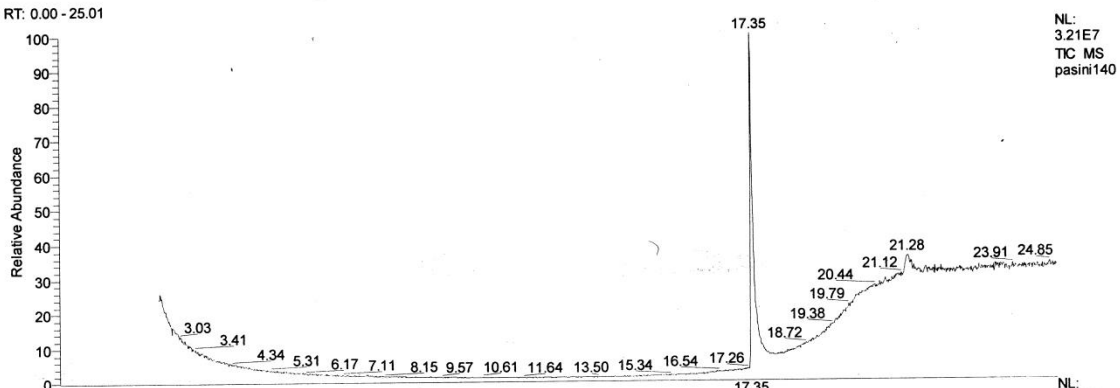


^{13}C NMR (75 MHz, CDCl_3)

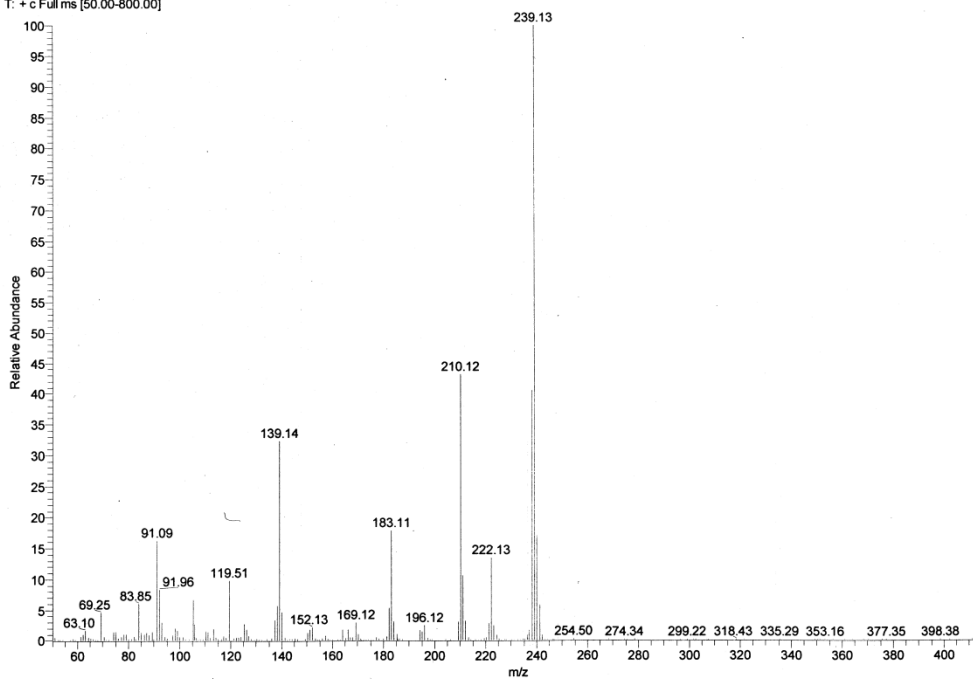


GC-MS

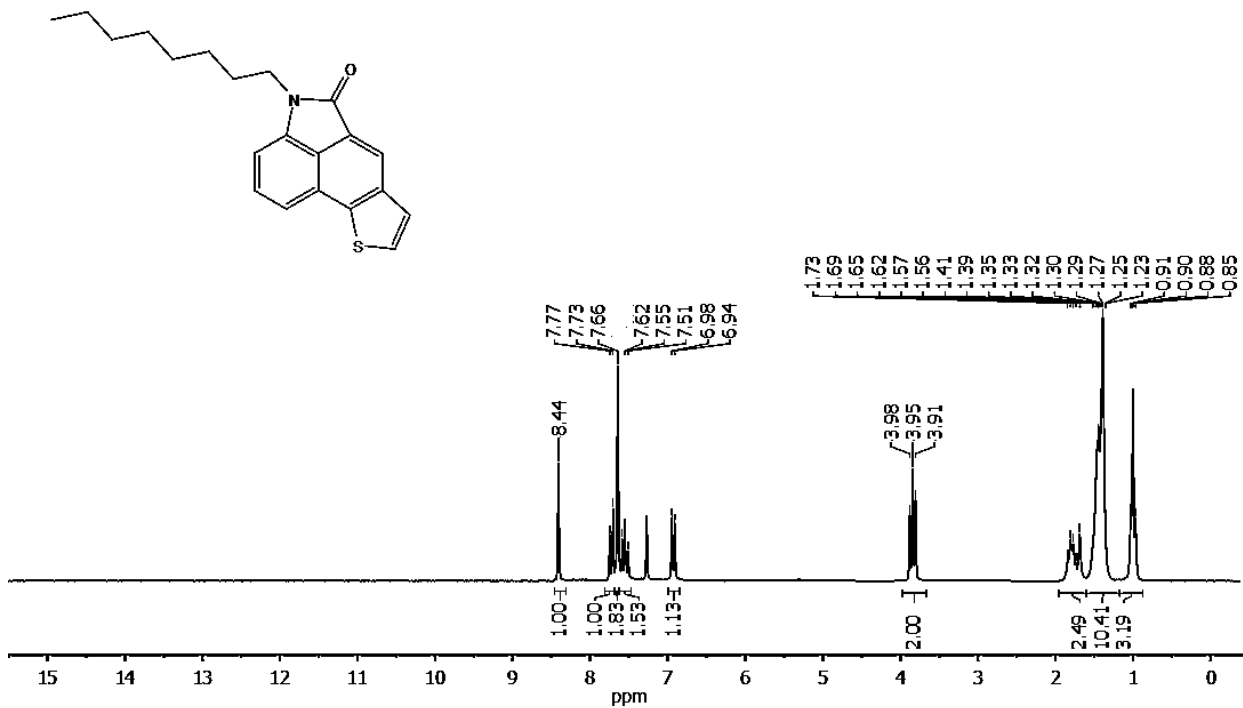
RT: 0.00 - 25.01



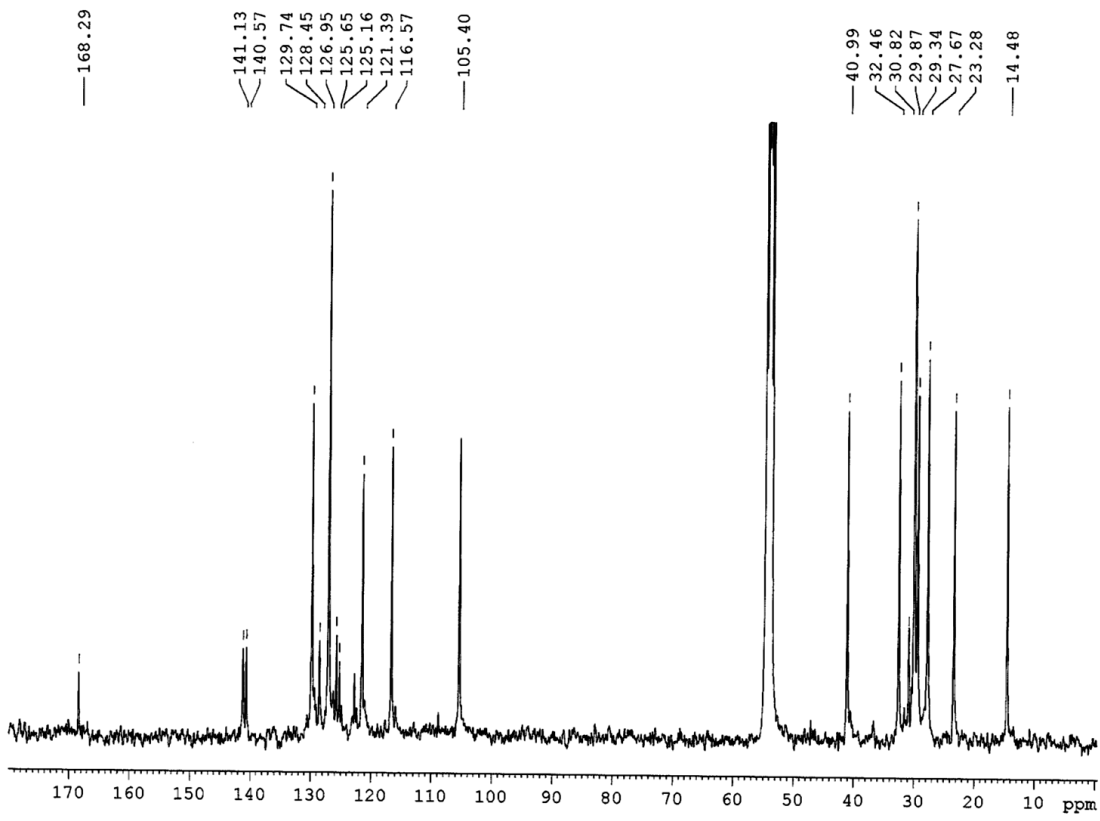
pasini140 #1157 RT: 17.34 AV: 1 SB: 344 14.80-17.02, 18.17-20.34 NL: 3.95E6
T: + c Full ms [50.00-800.00]



Compound **46b**
¹H NMR (200 MHz, CDCl₃)

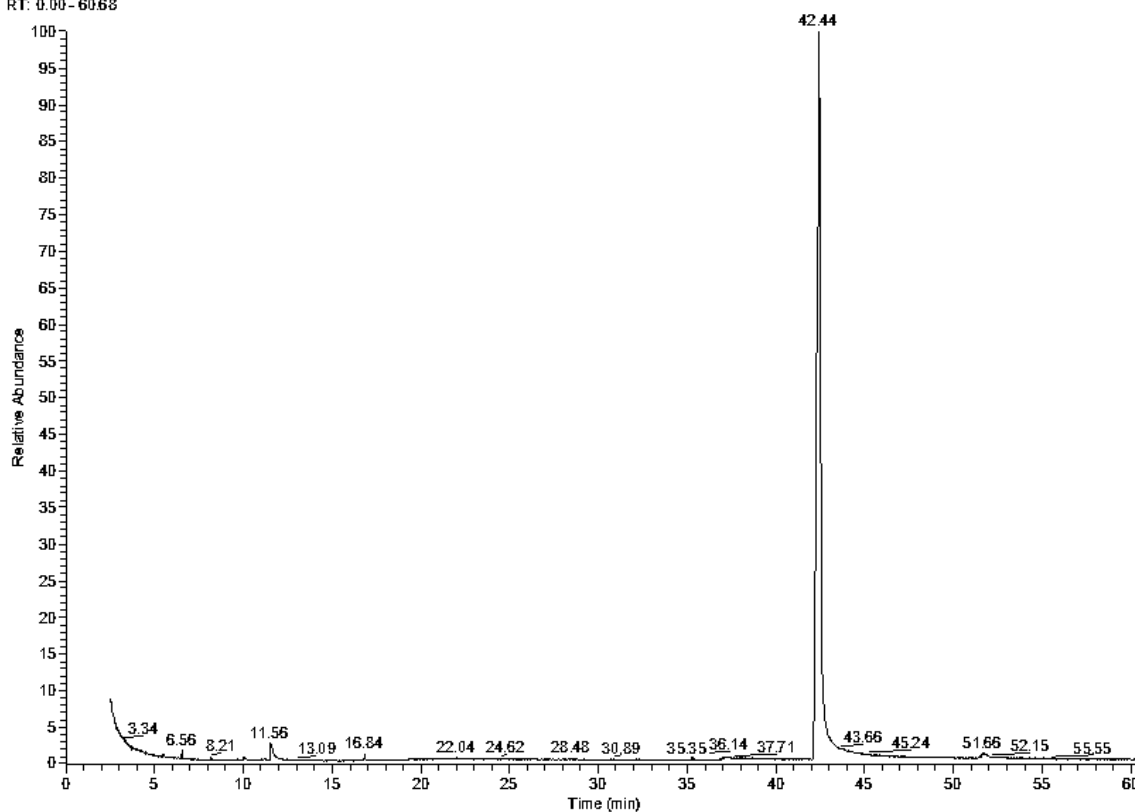


¹³C NMR (75 MHz, CD₂Cl₂)



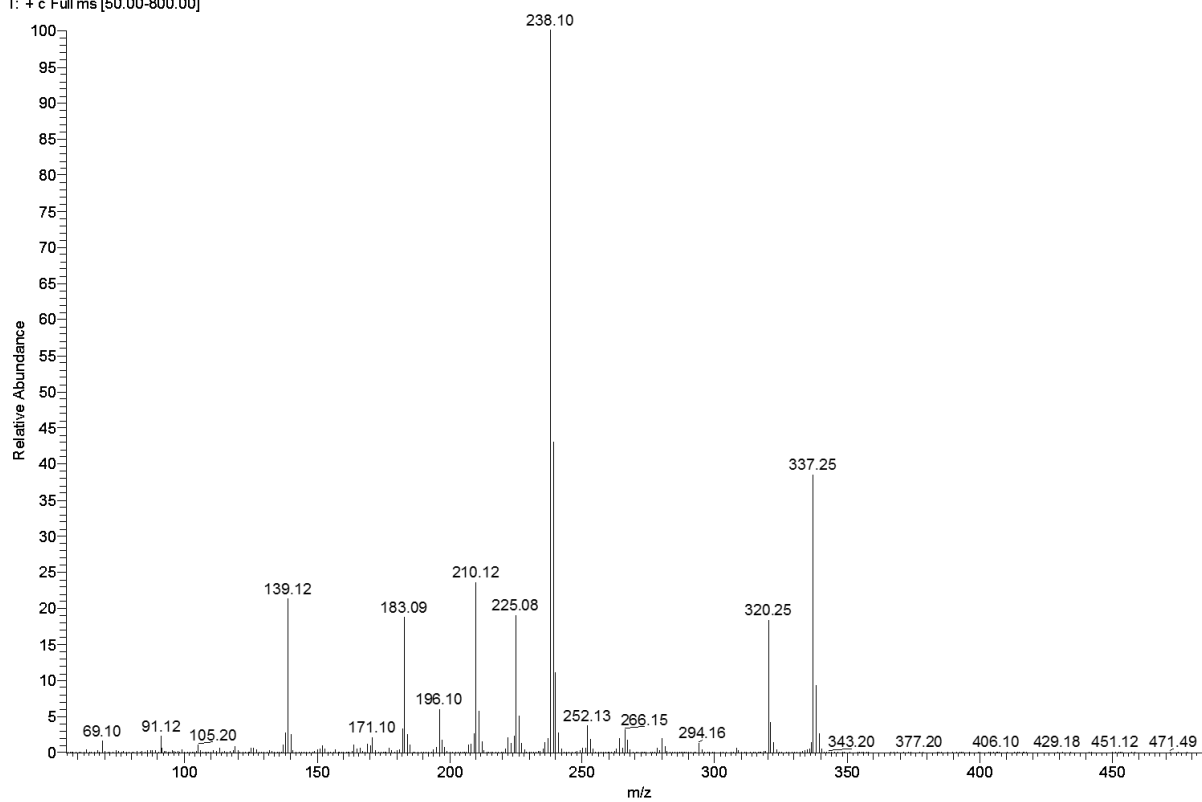
GC-MS

RT: 0.00-60.68



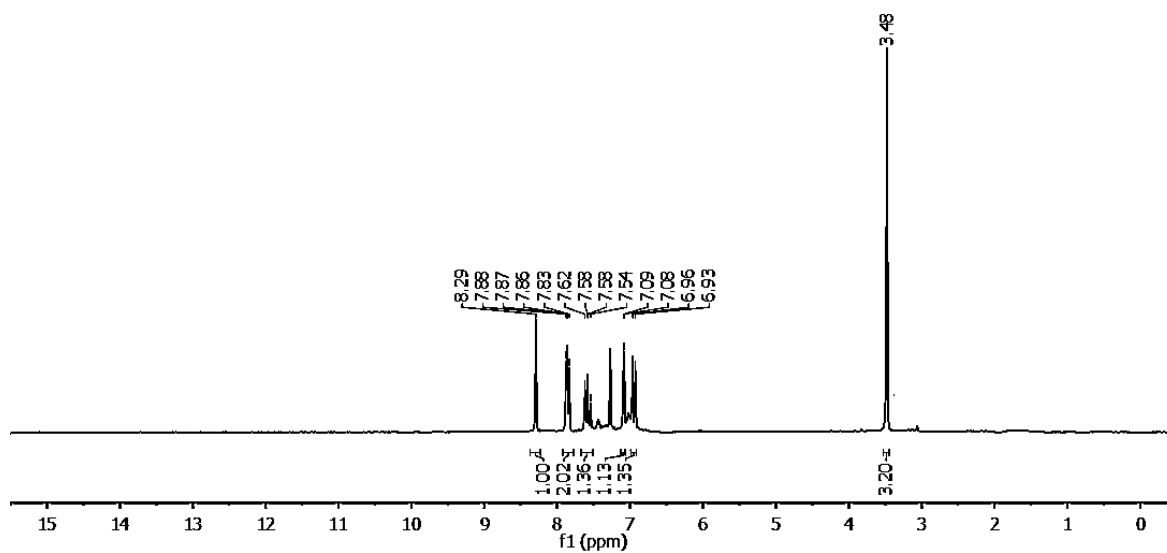
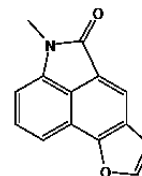
NL:
8.33E7
TIC MS
pasini126

pasini126 #3113 RT: 42.44 AV: 1 SB: 456 39.54-41.69, 44.19-47.87 NL: 1.93E7
T: + c Full ms [50.00-800.00]

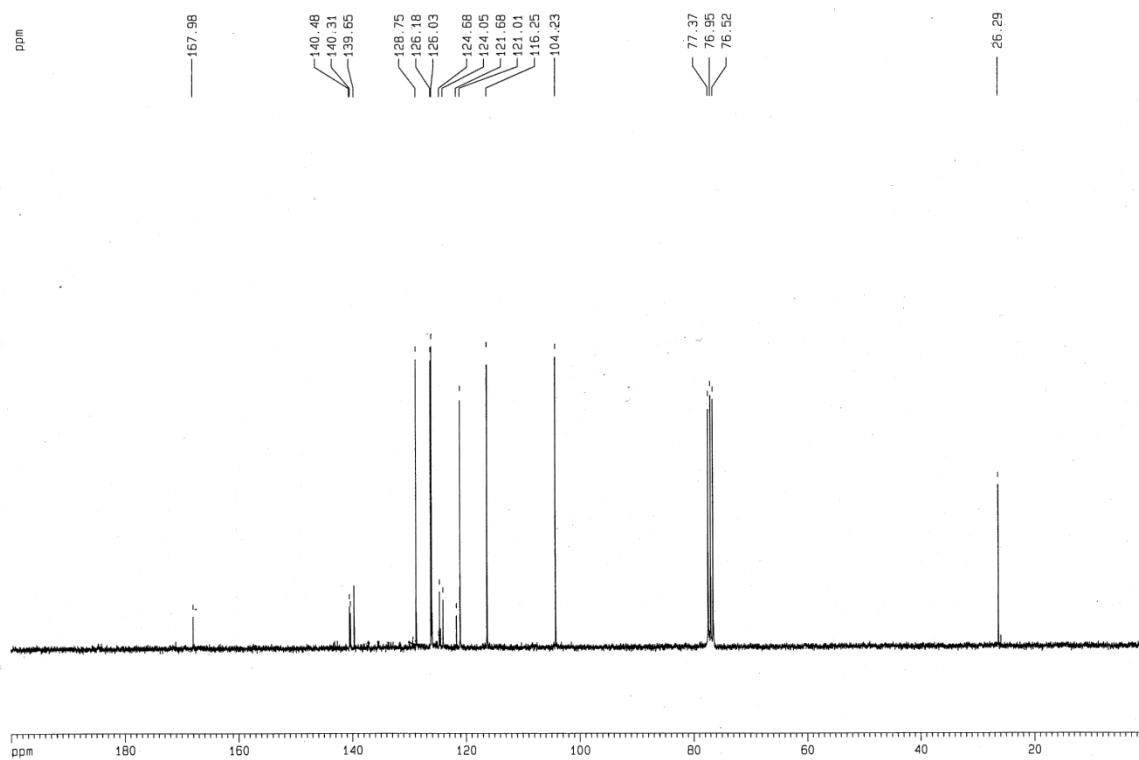


Compound **46c**

^1H NMR (200 MHz, CDCl_3)



^{13}C NMR (75 MHz, CDCl_3)



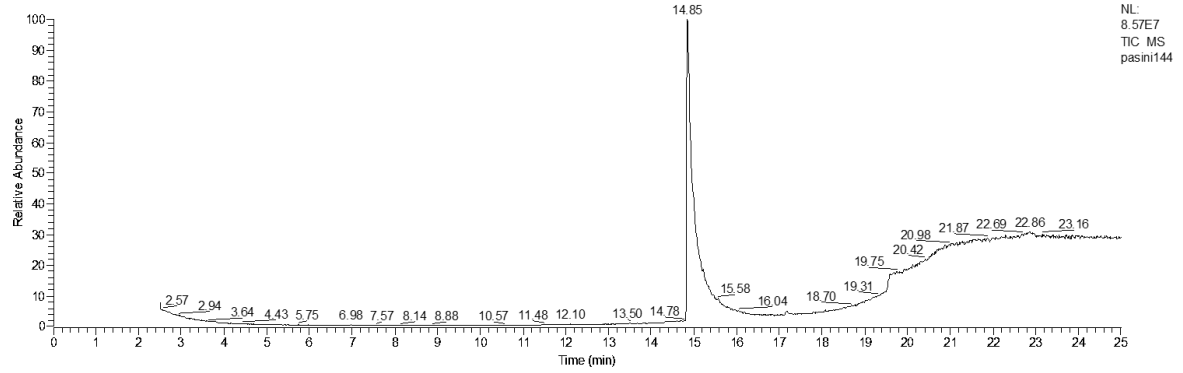
GC-MS

D:\LAVORICGS_2015\UNIPV\Pasini\pasini144
Sil

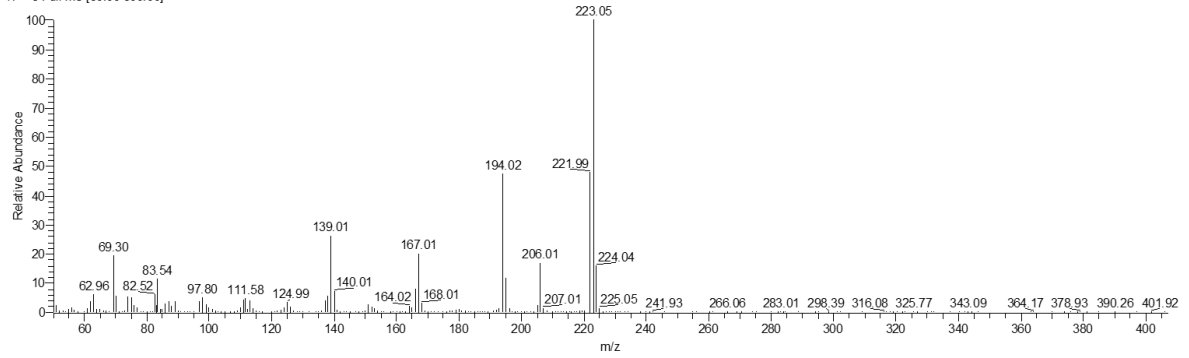
6/5/2015 11:34:07 AM

AN262F14-21

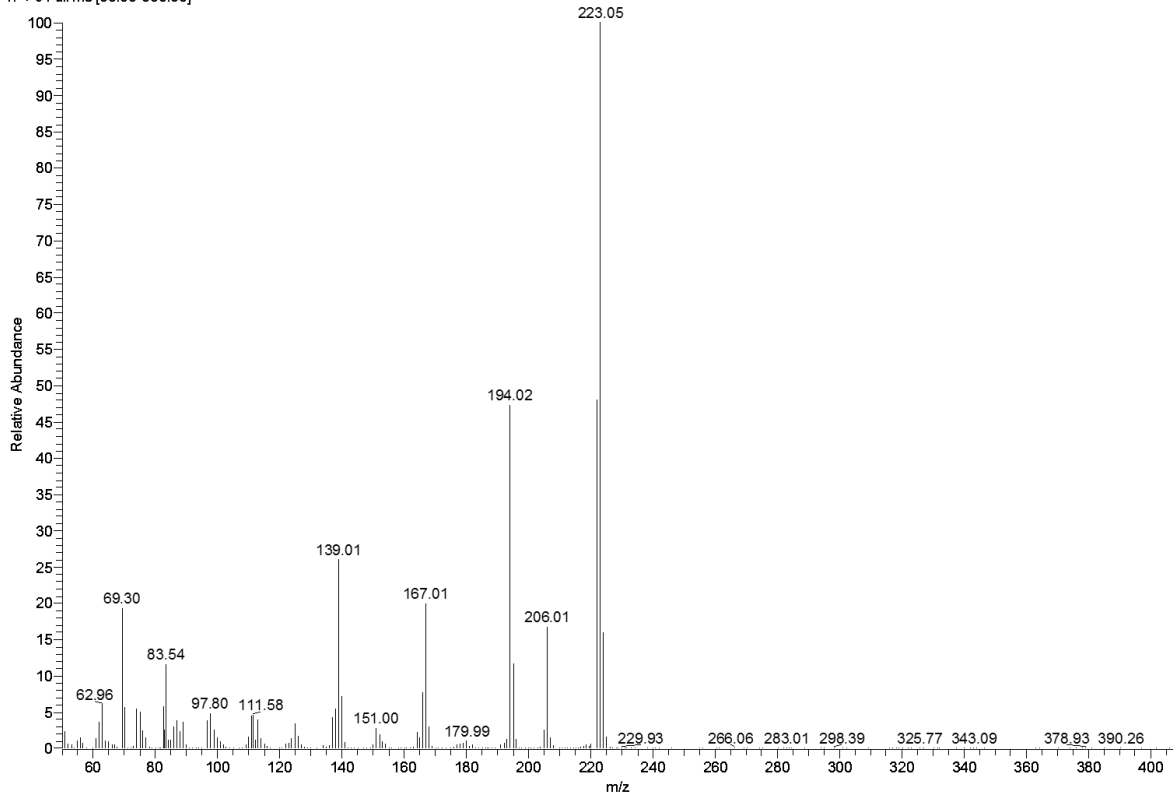
RT: 0.00 - 25.00



pasini144 #963 RT: 14.85 AV: 1 SB: 322 12.38-14.59, 16.90-18.80 NL: 1.73E7
T: + c Full ms [50.00-800.00]

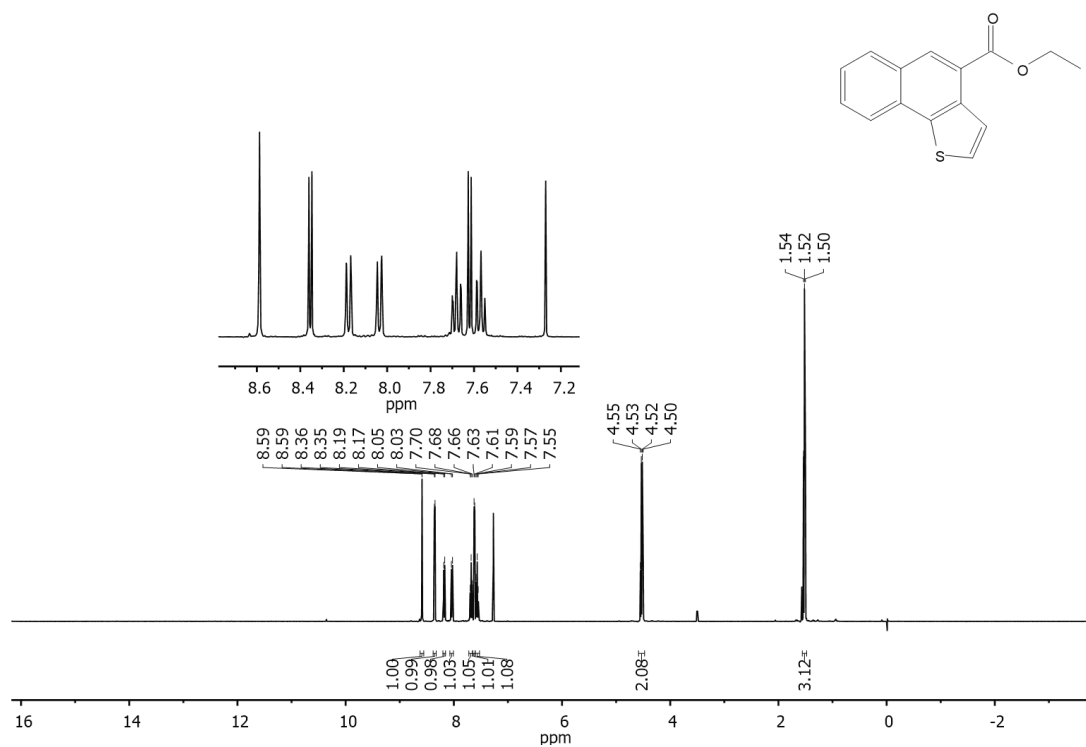


pasini144 #963 RT: 14.85 AV: 1 SB: 322 12.38-14.59, 16.90-18.80 NL: 1.73E7
T: + c Full ms [50.00-800.00]

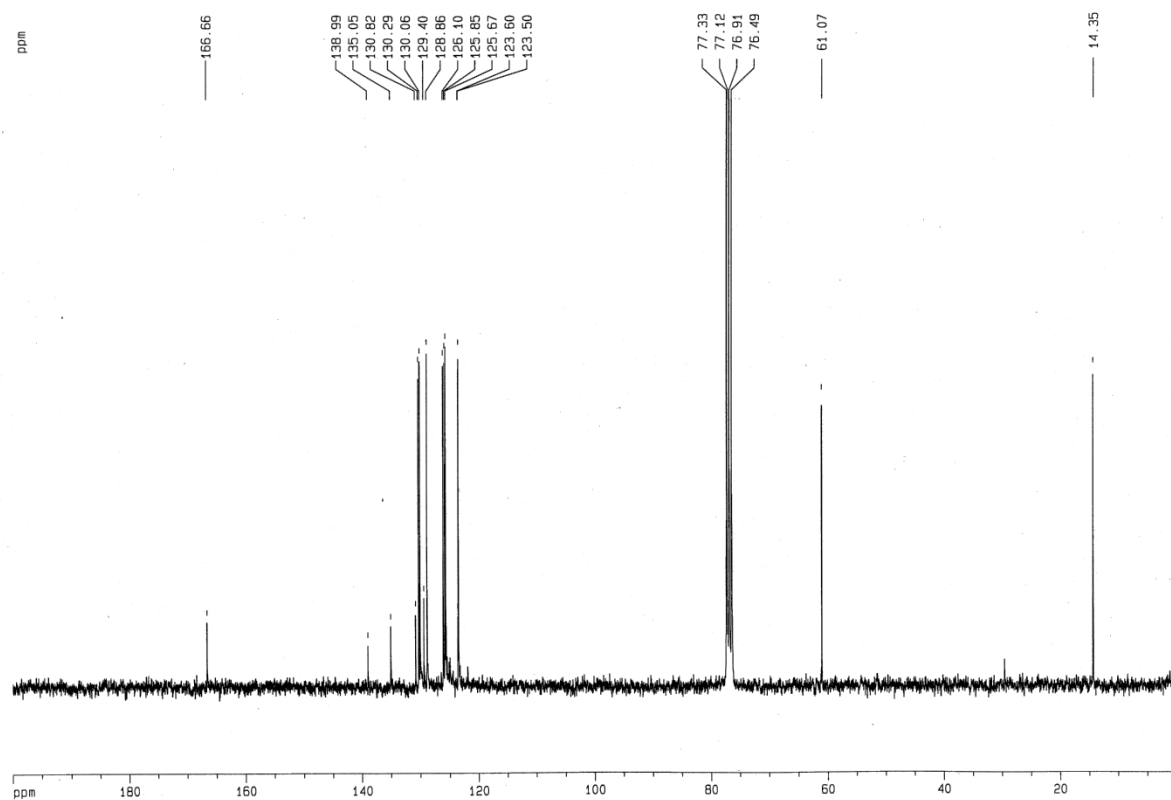


Compound 53

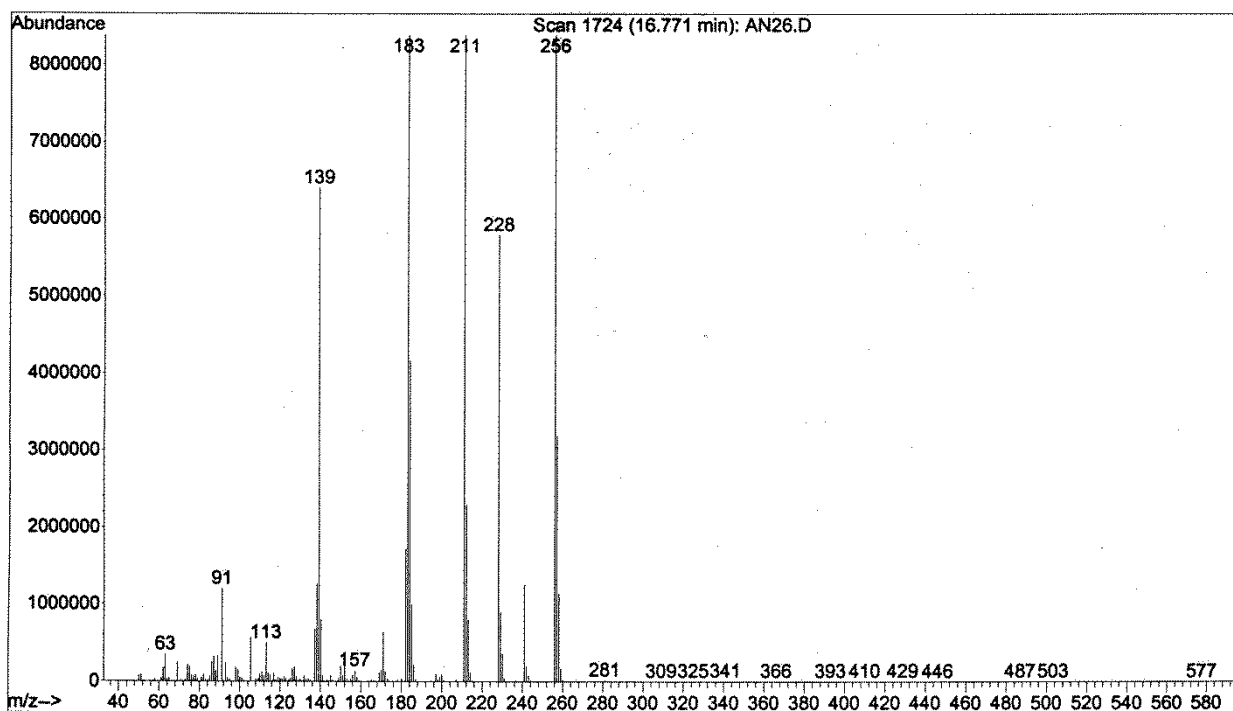
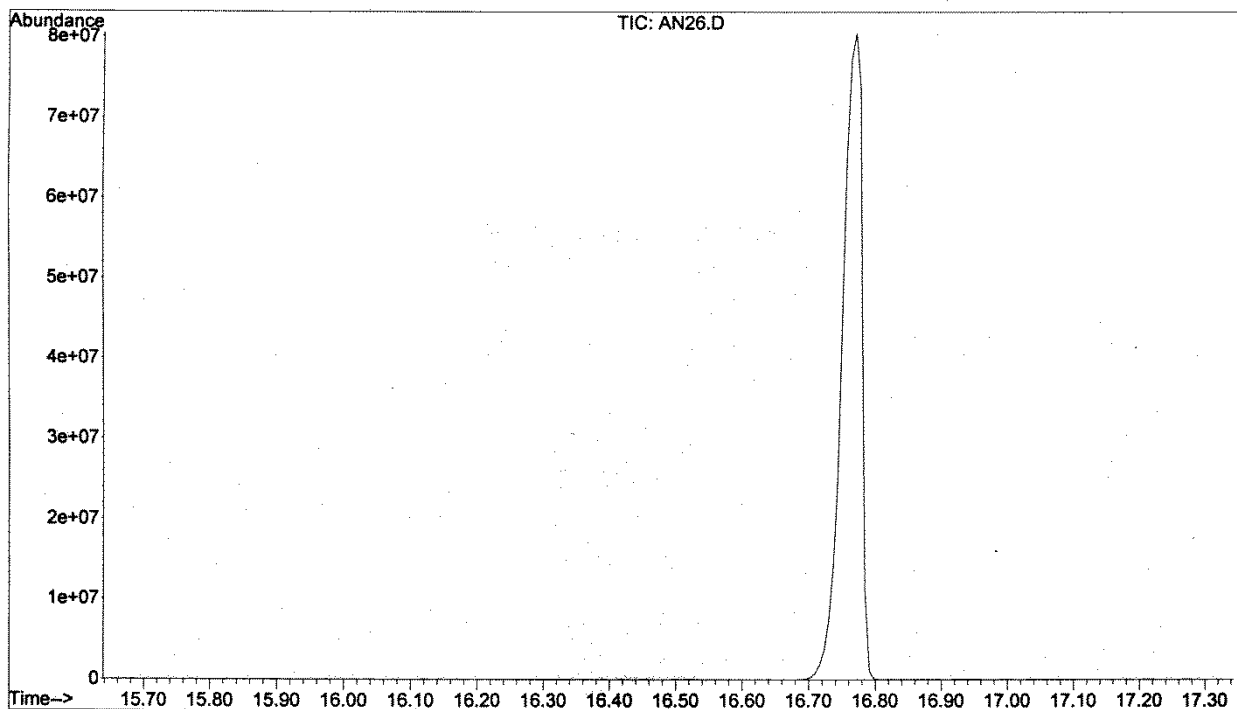
^1H NMR (400 MHz, CDCl_3)



^{13}C NMR (75 MHz, CDCl_3)

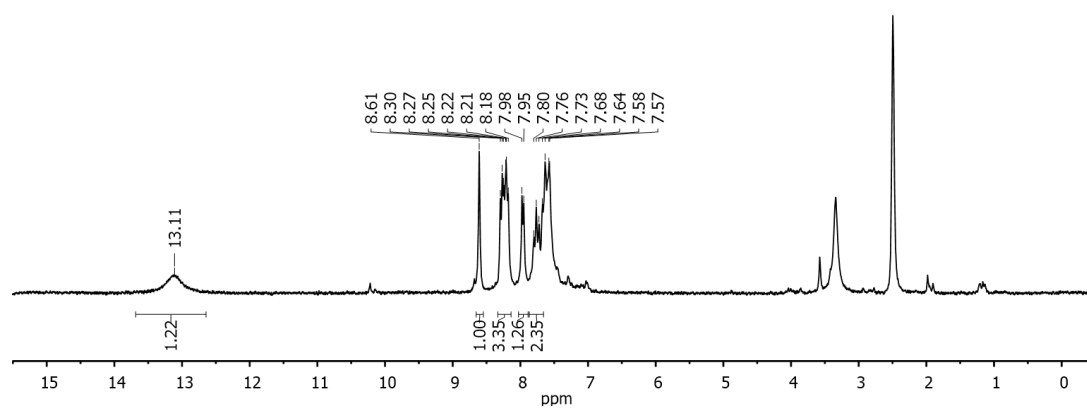
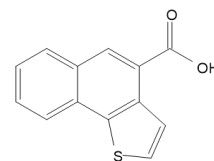


GC-MS

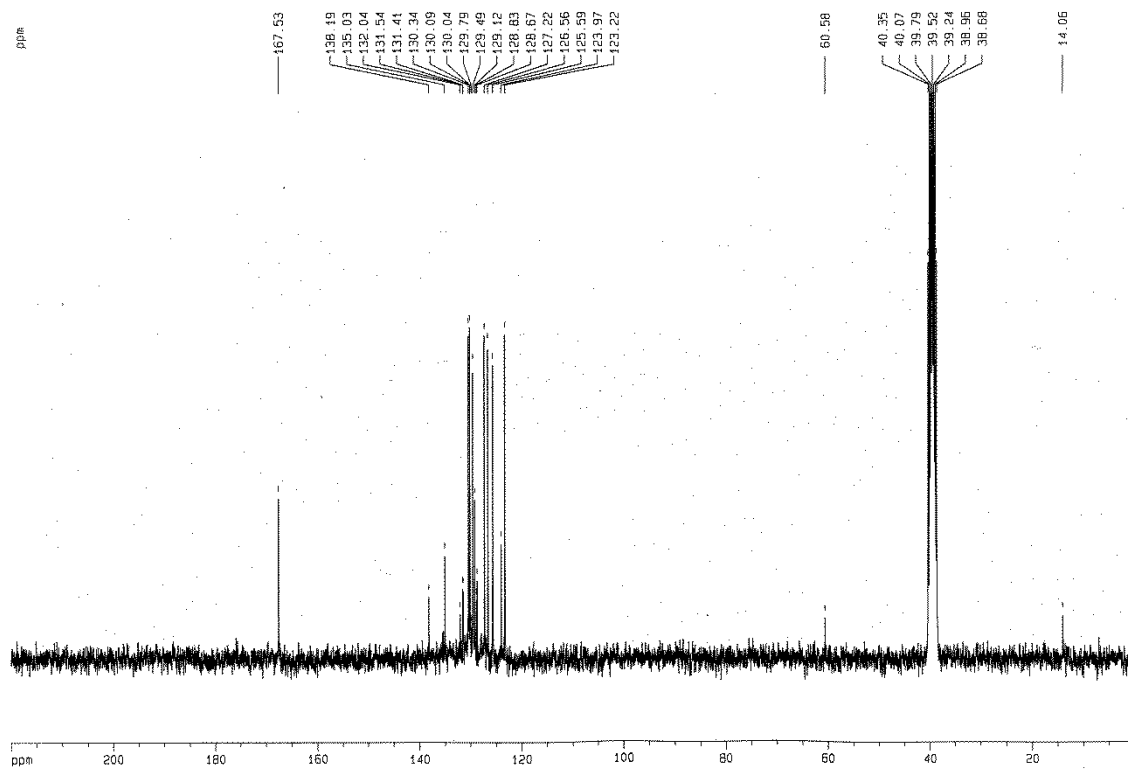


Compound 57

^1H NMR (200 MHz, $\text{DMSO}-d_6$)



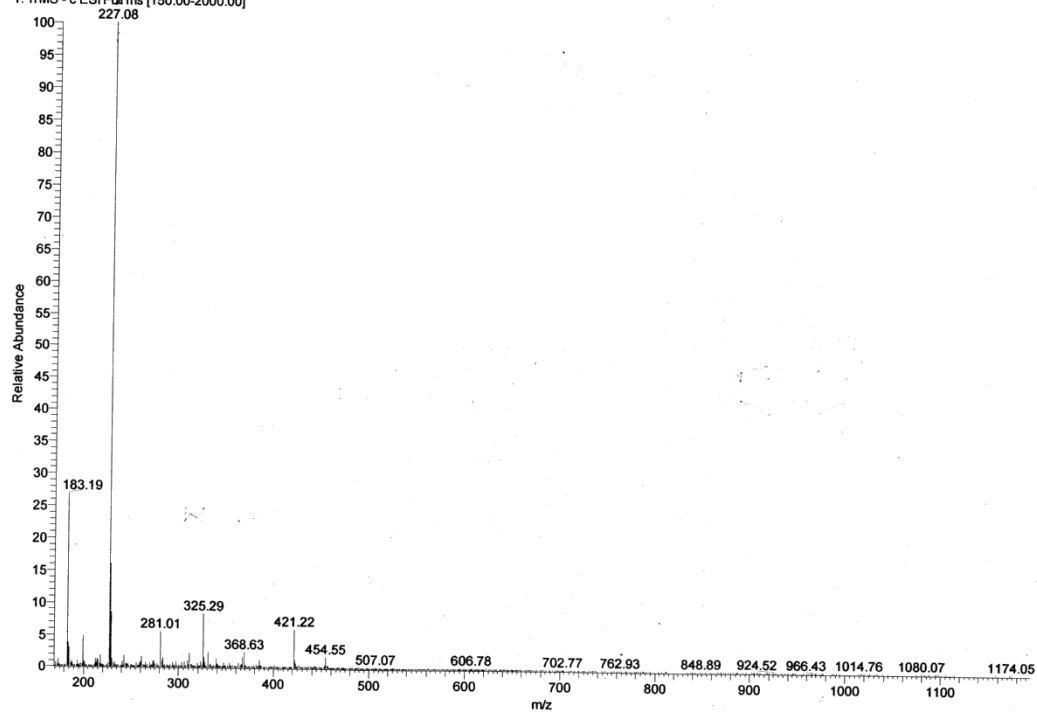
^{13}C NMR (75 MHz, $\text{DMSO}-d_6$)



ESI-MS

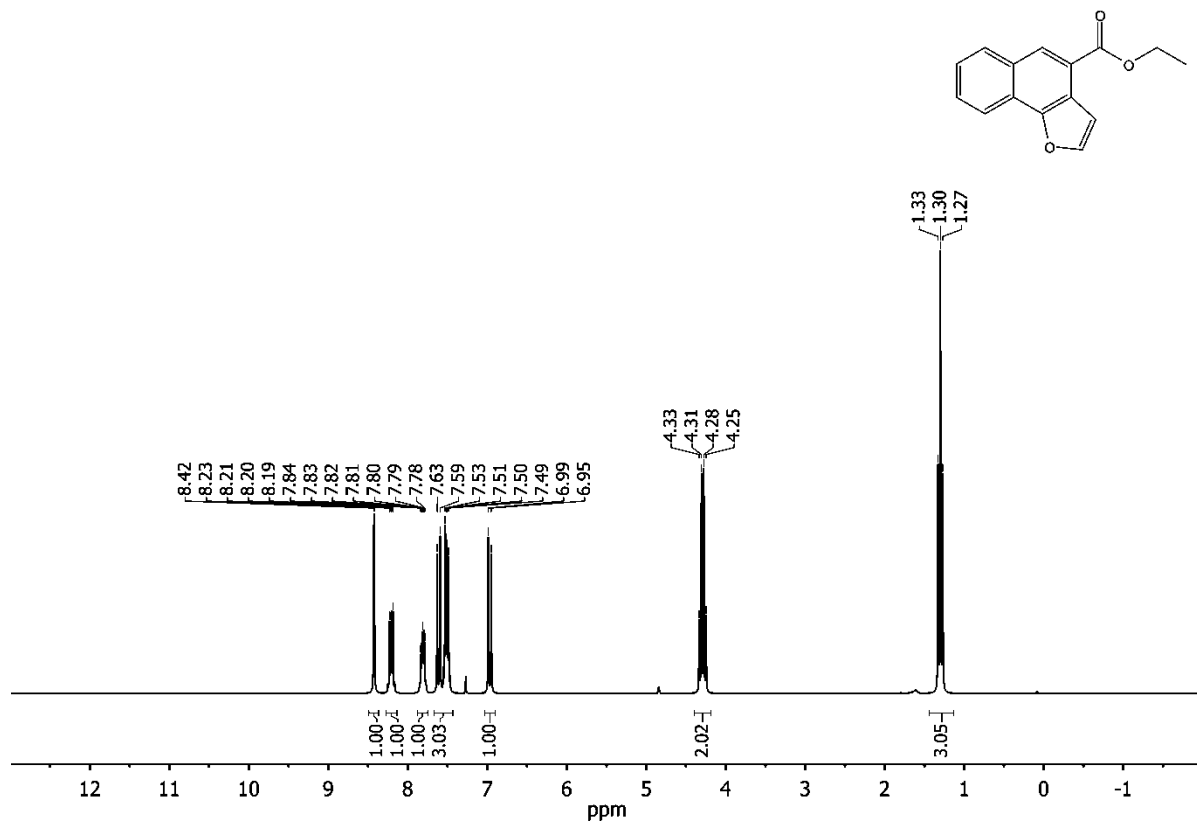
FIA-ESI Ioni negativi

NitroFIA05neg #6 RT: 0.05 AV: 1 NL: 1.37E4
T: ITMS - c ESI Full ms [150.00-2000.00]

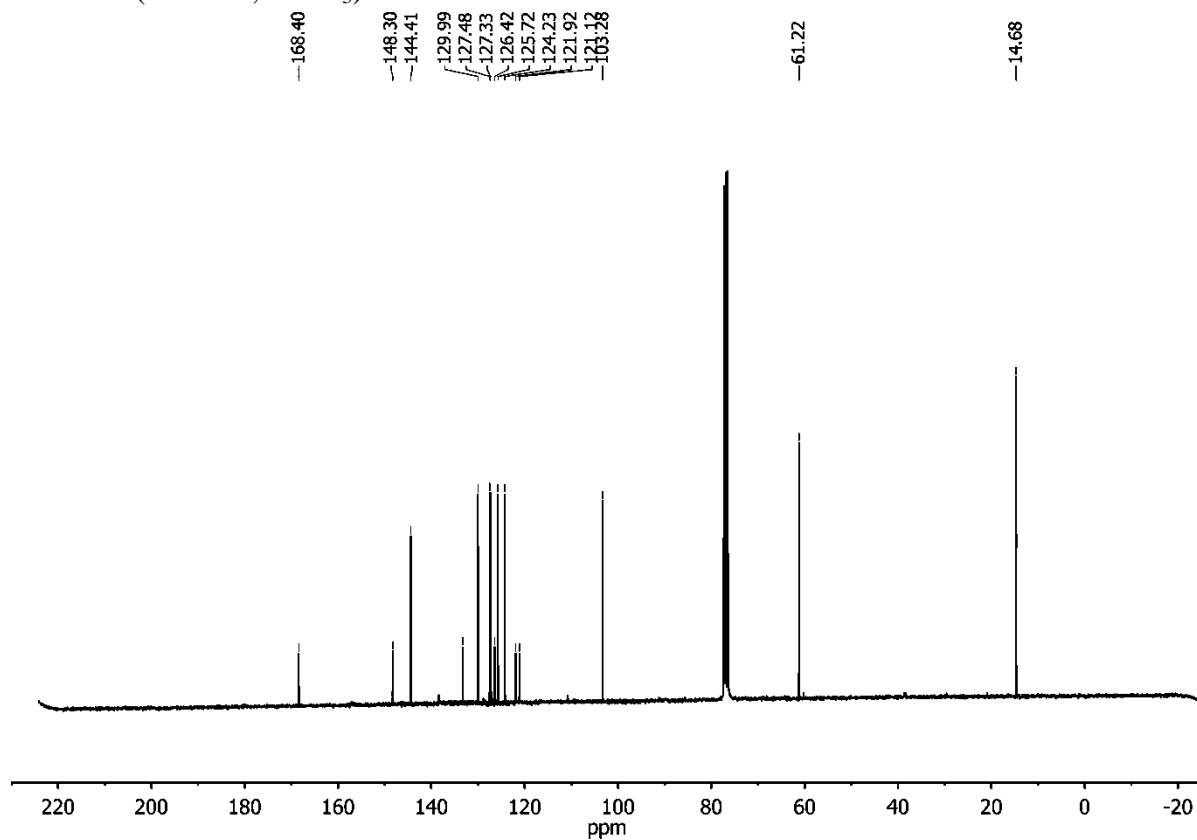


Compound **60**

^1H NMR (200 MHz, CDCl_3)

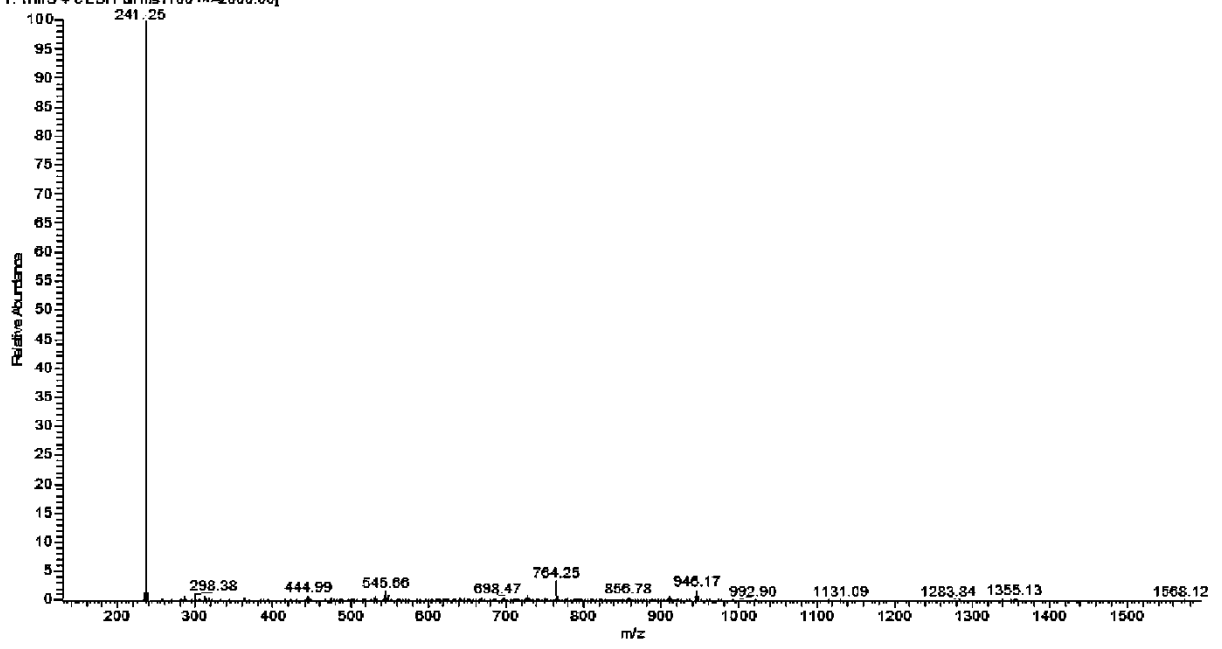


^{13}C NMR (75 MHz, CDCl_3)



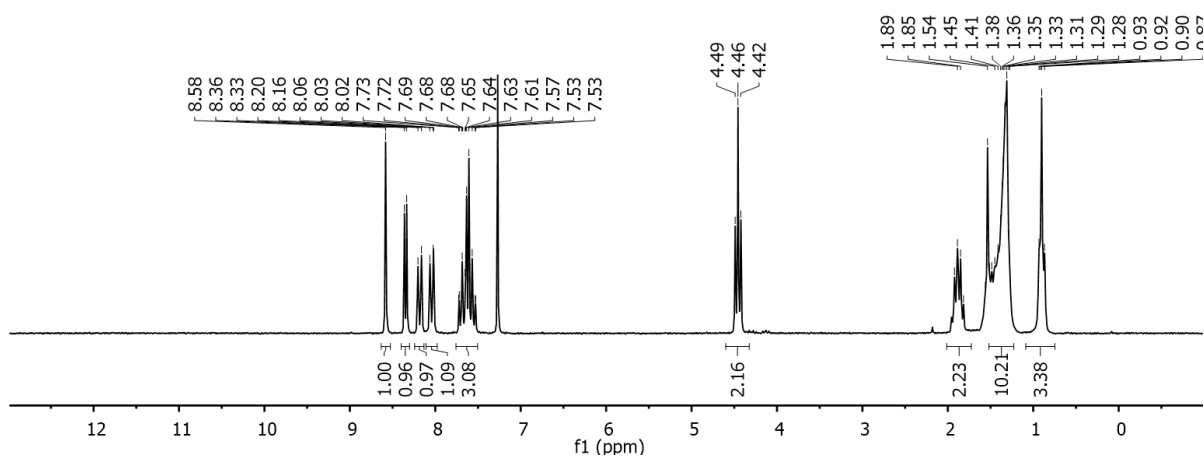
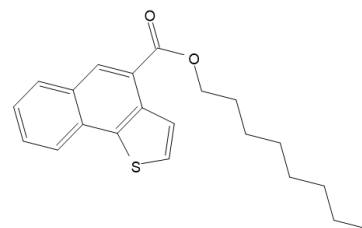
ESI-MS

NitiFIA RT: 0.09 AV: 1 NL: 1.78E3
T: [MMS + e ESI Full ms [100 00-2000.00]]



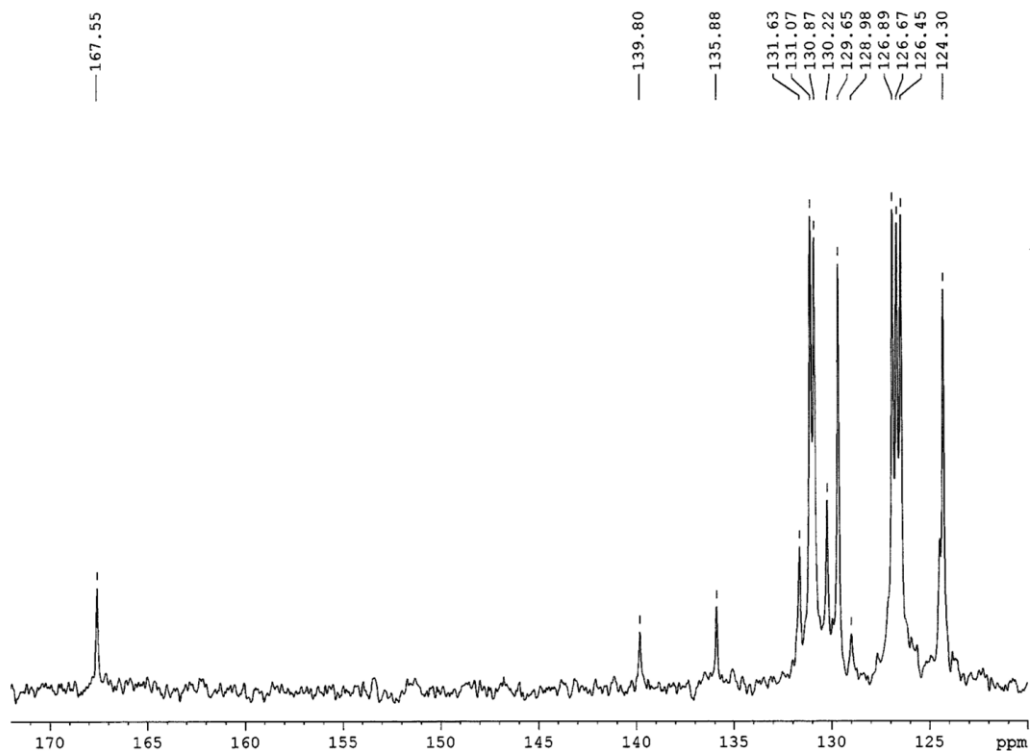
Compound **61a**

^1H NMR (200 MHz, CDCl_3)

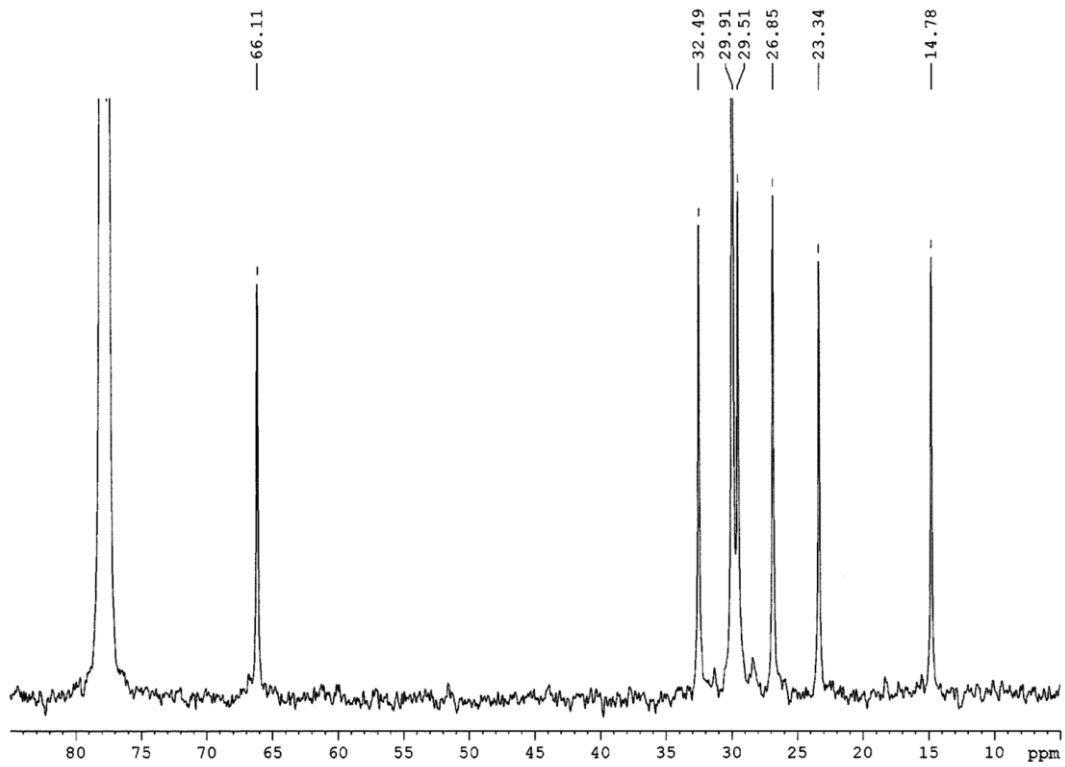


^{13}C NMR (75 MHz, CDCl_3)

MS 116 in CDCl_3 a 26°C con D1= 4 s. ^{13}C -NMR n. 6003



MS 116 in CDCl3 a 26°C con D1= 4 s. 13C-NMR n. 6003

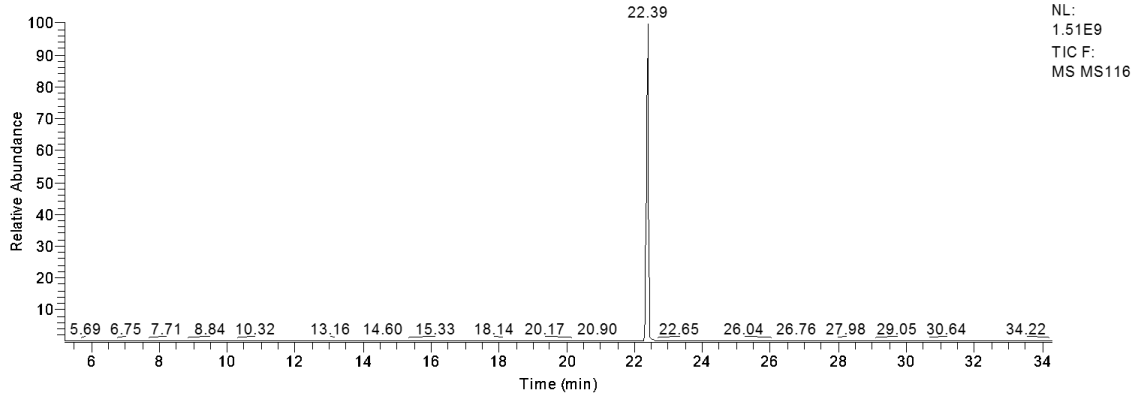


ESI-MS

C:\Xcalibur\data\BIANCHIG\2016\MS116
MS116.dcm
9/22/2016 4:54:04 PM

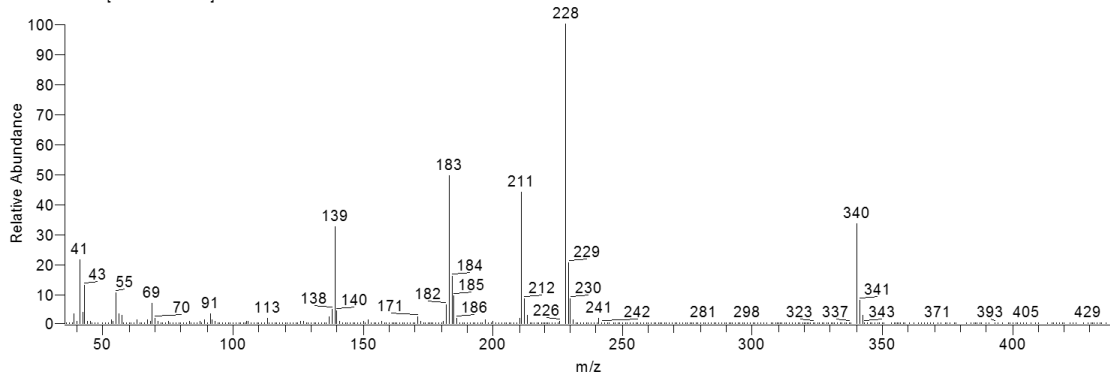
C:\Xcalibur\methods\80(2)\10-320SLESS.meth

RT: 5.20 - 34.26



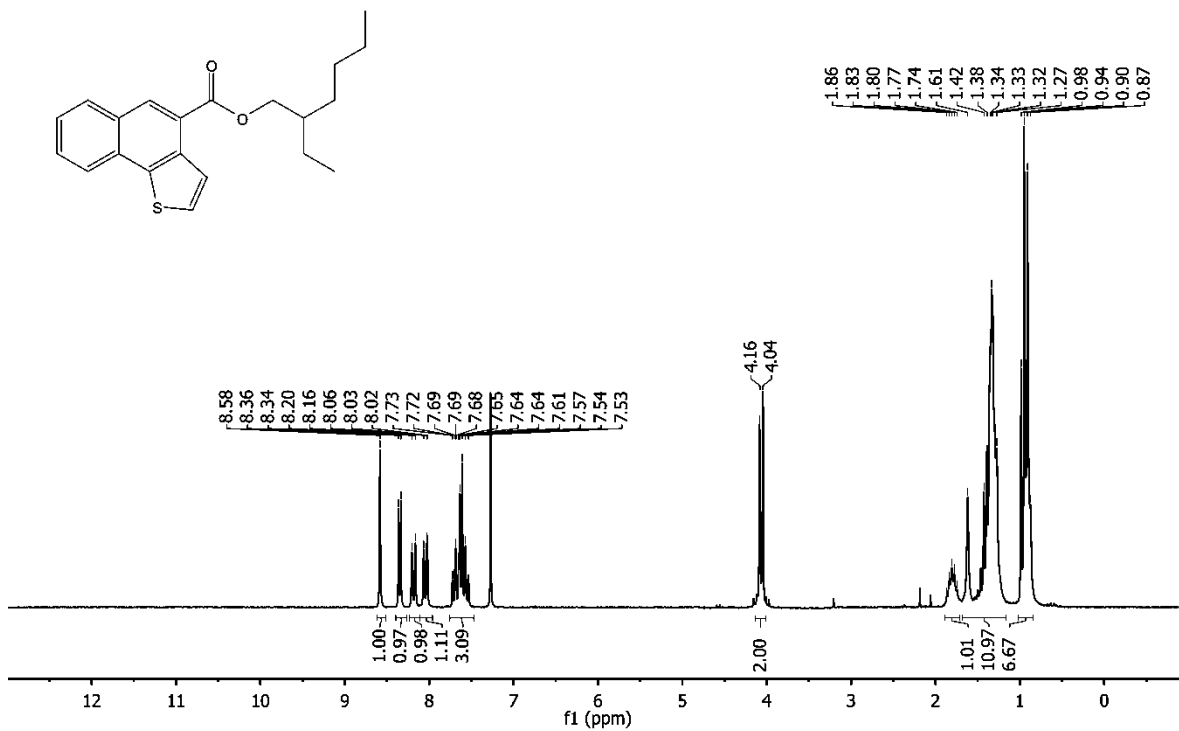
NL:
1.51E9
TIC F:
MS MS116

MS116 #904 RT: 22.35 AV: 1 SB: 72 10.68-12.05 NL: 1.78E8
T: + c Full ms [35.00-600.00]

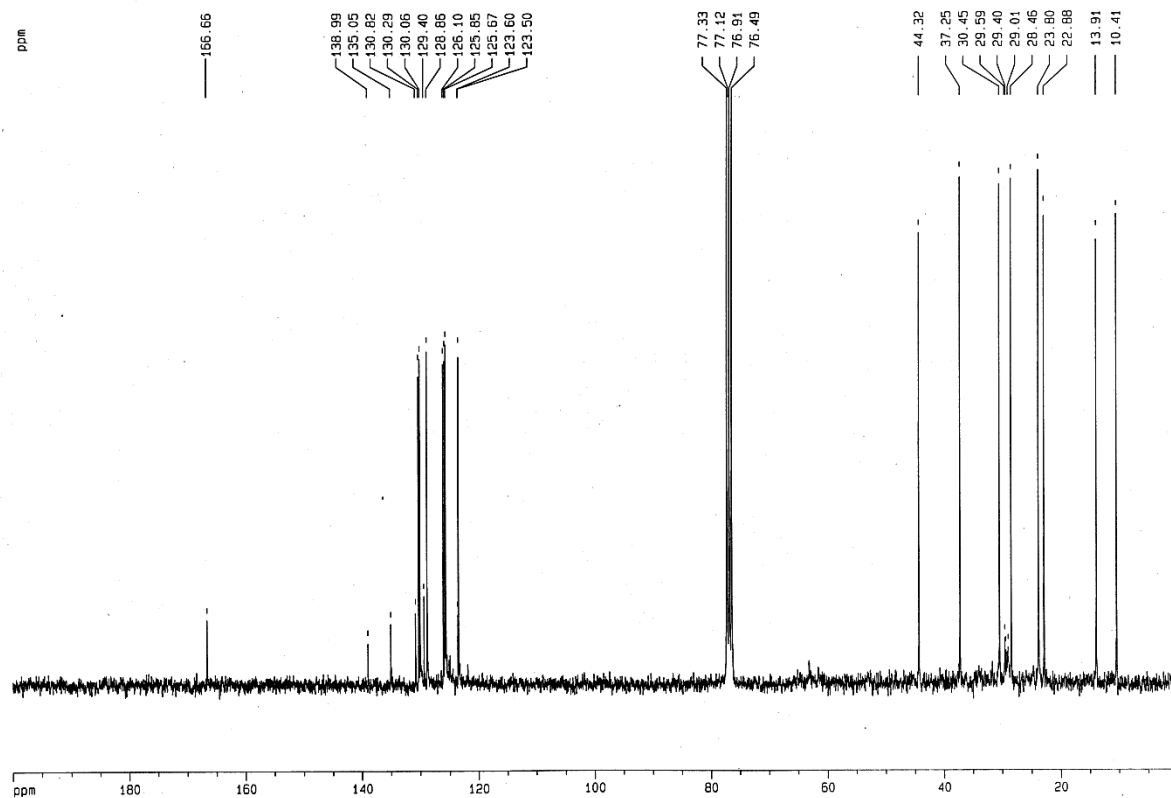


Compound **61b**

^1H NMR (400 MHz, CDCl_3)

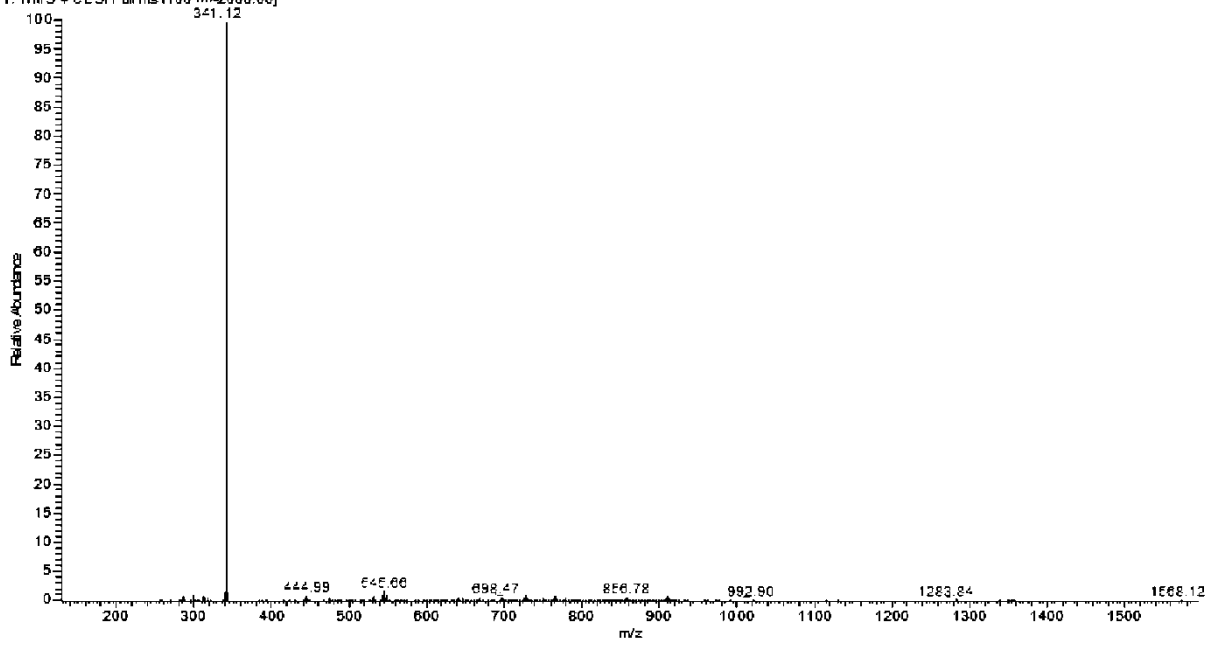


^{13}C NMR (75 MHz, CDCl_3)

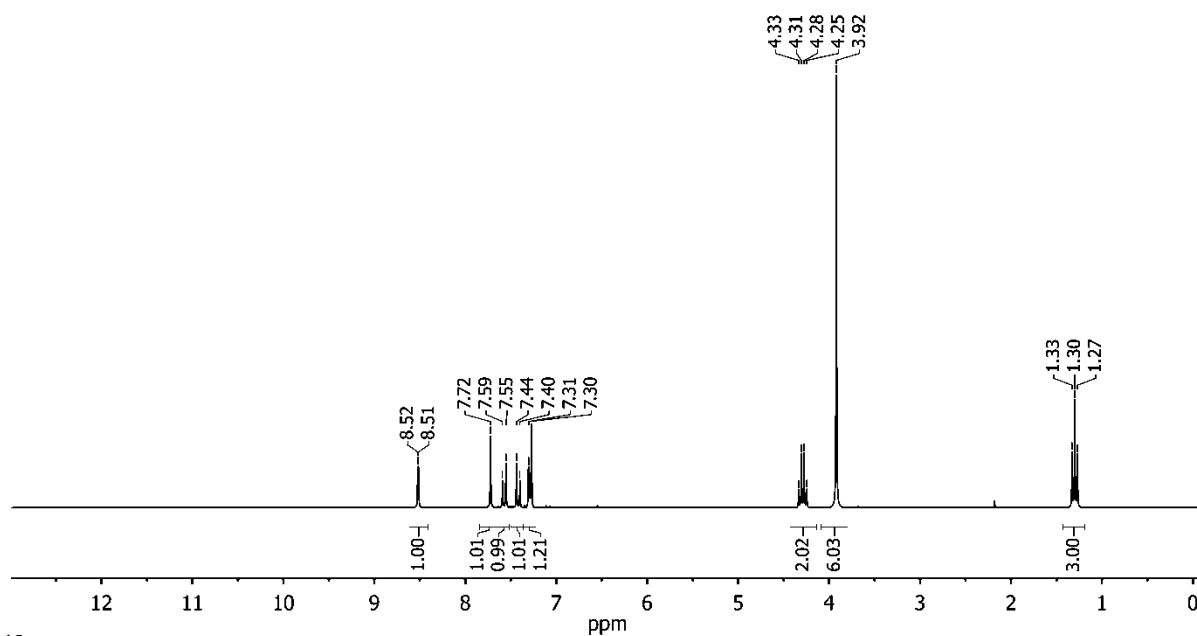


ESI-MS

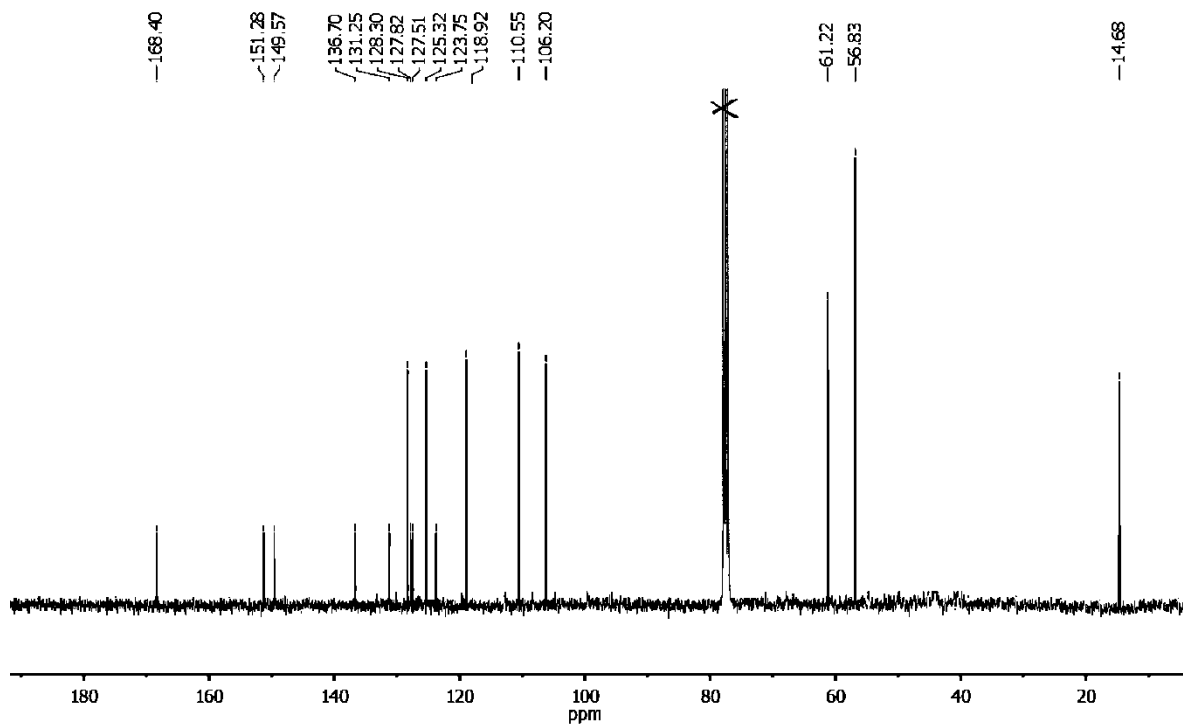
NitroFIA RT: 0.09 AV: 1 NL: 1.78E 3
T: ITMS + e ESI Full ms [100.00-2000.00]



Compound **62**
 ^1H NMR (400 MHz, CDCl_3)

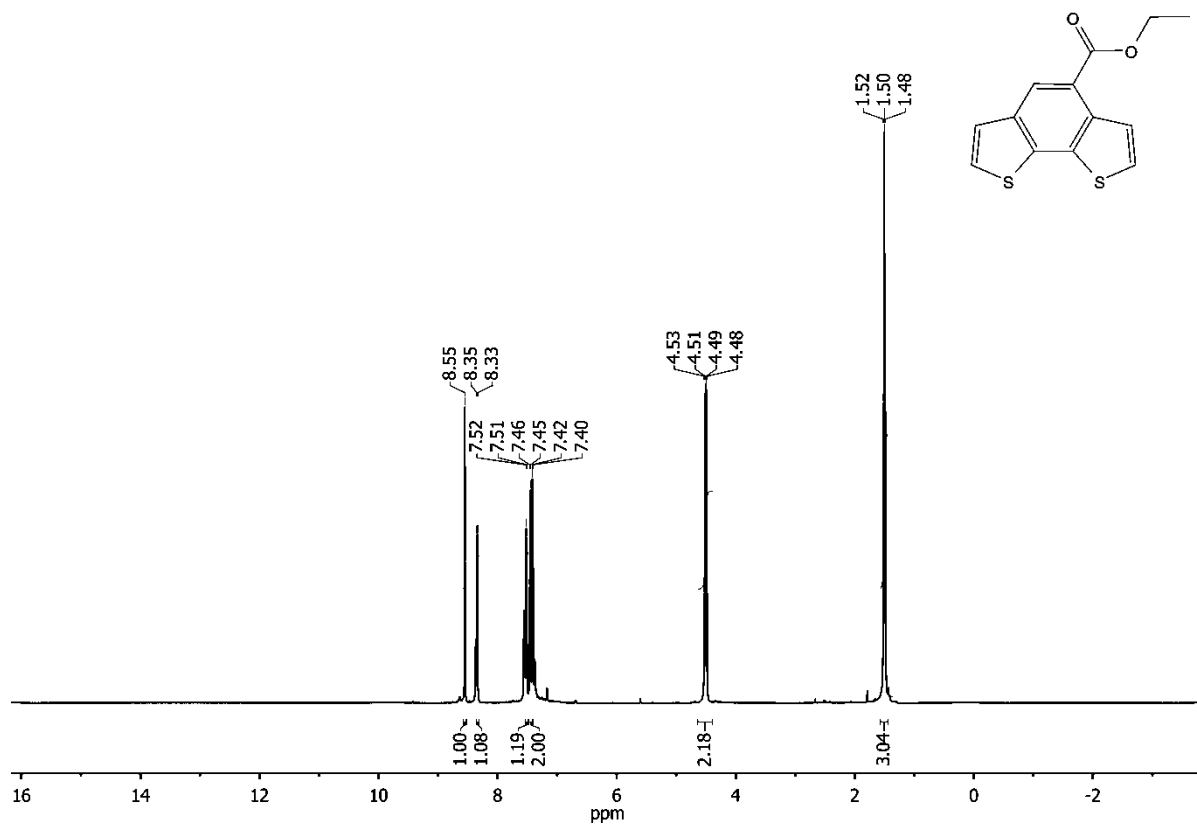


^{13}C NMR (75 MHz, CDCl_3)

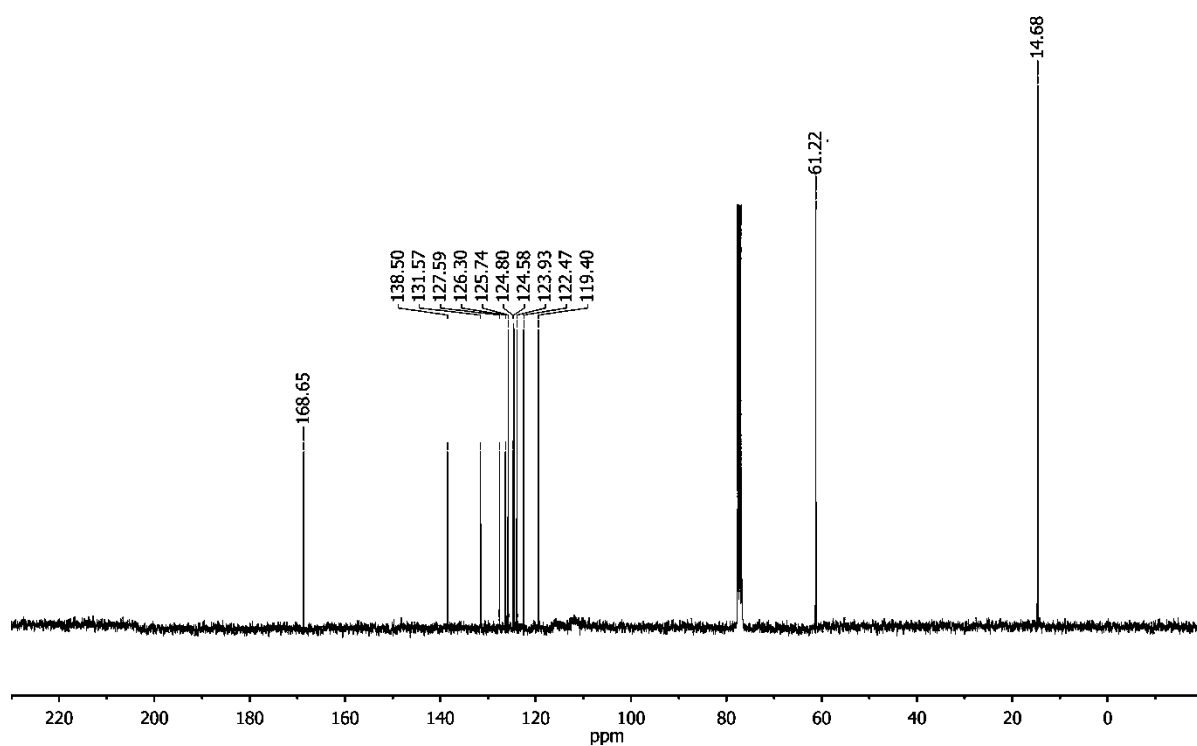


Compound **63**

^1H NMR (400 MHz, CDCl_3)

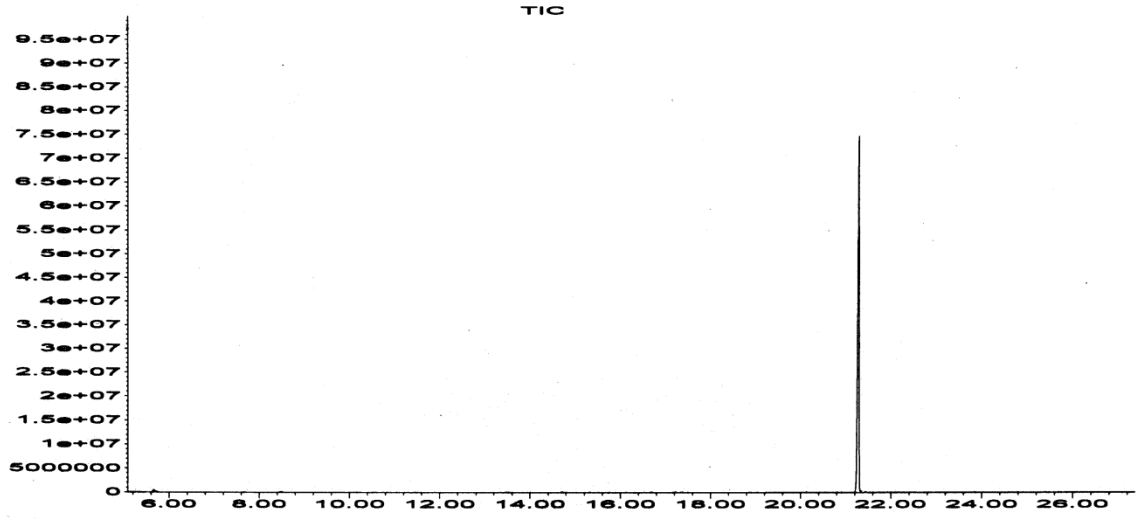


^{13}C NMR (75 MHz, CDCl_3)

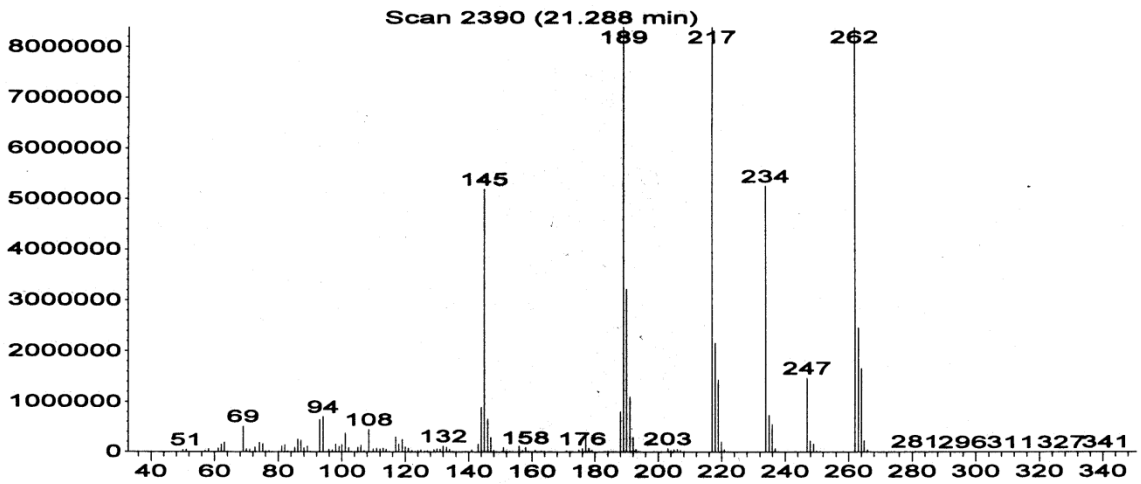


GC-MS

Abundance

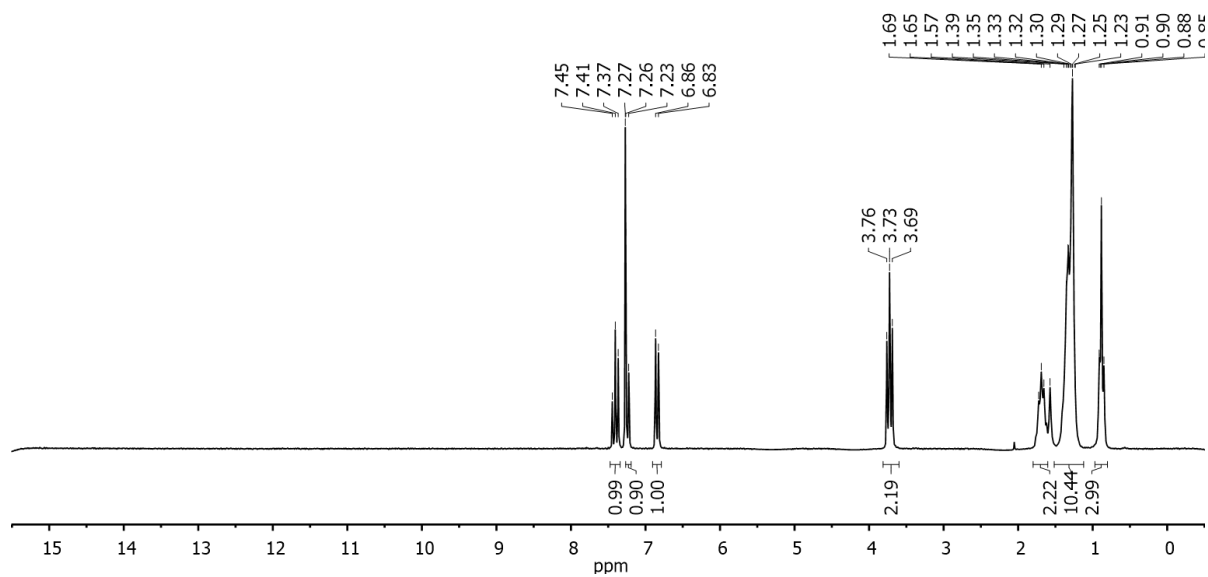
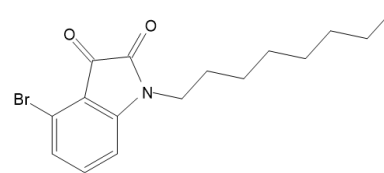


Time-->
Abundance

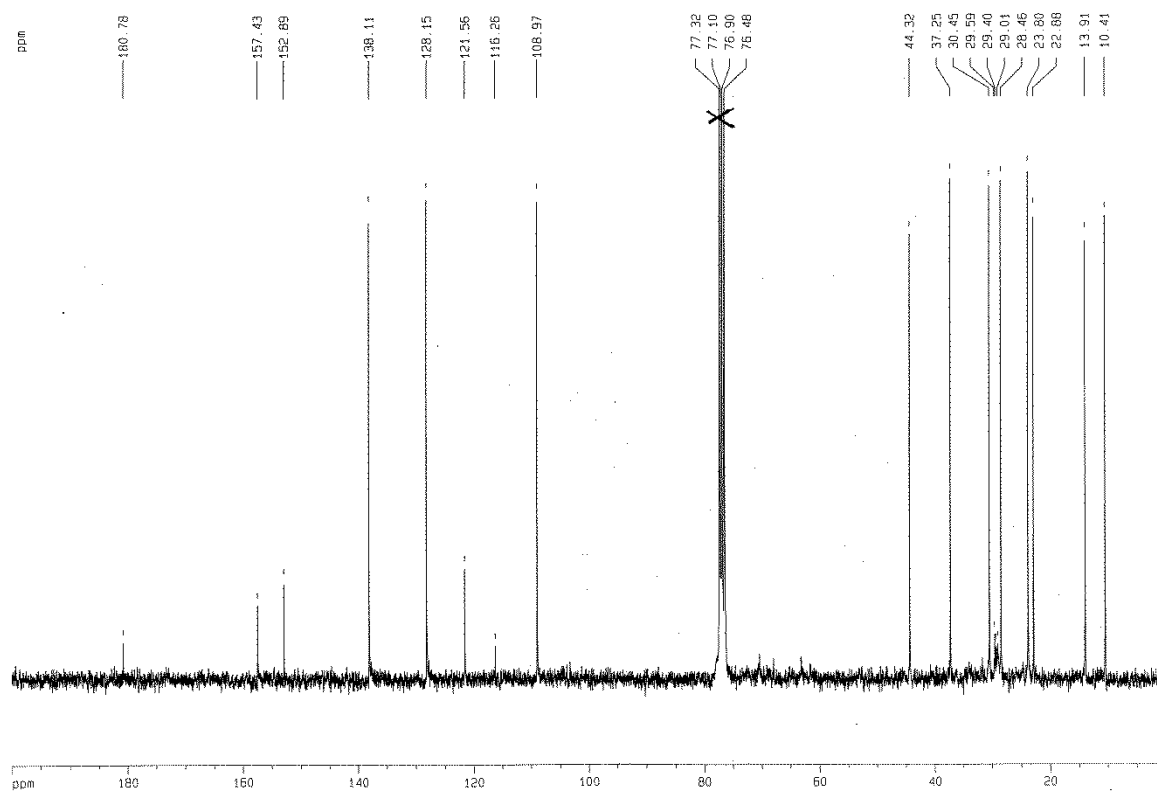


Compound **IIb**

^1H NMR (200 MHz, CDCl_3)



^{13}C NMR (75 MHz, CDCl_3)

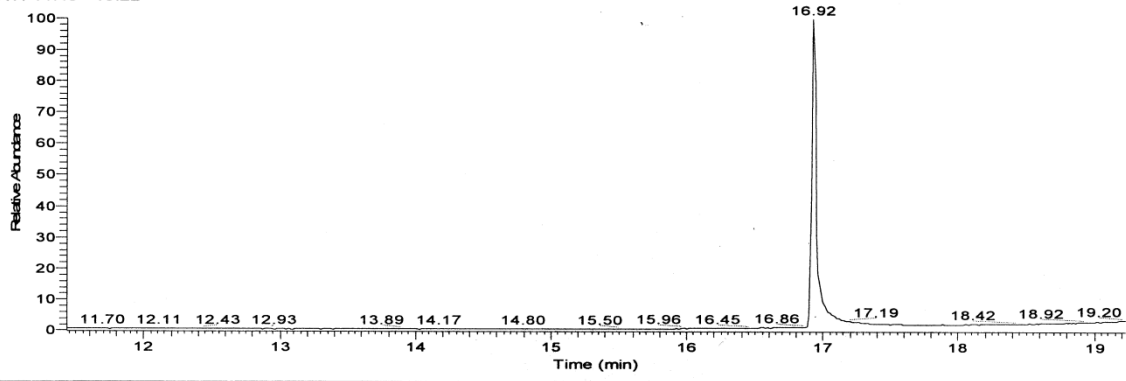


ESI-MS

5/22/2014 12:56:25

SII

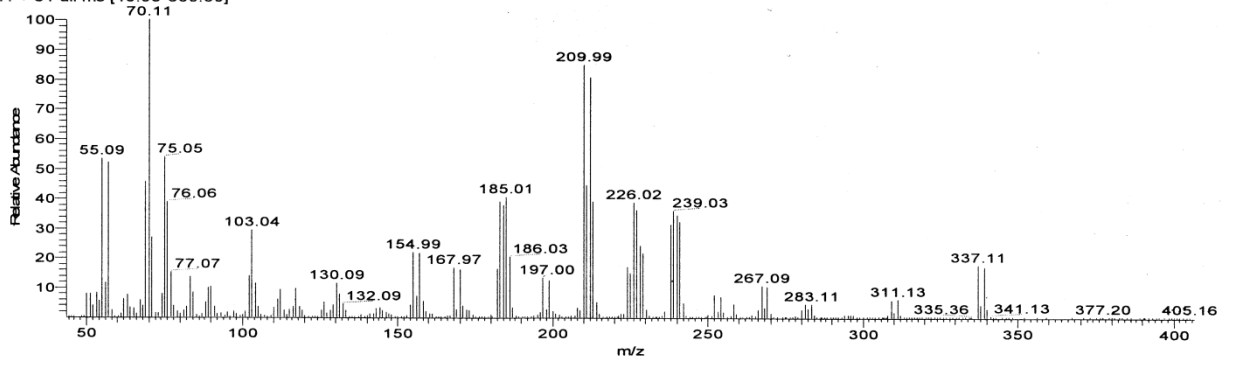
RT: 11.43 - 19.22



NL:
1.20E8
TIC MS
pasini043

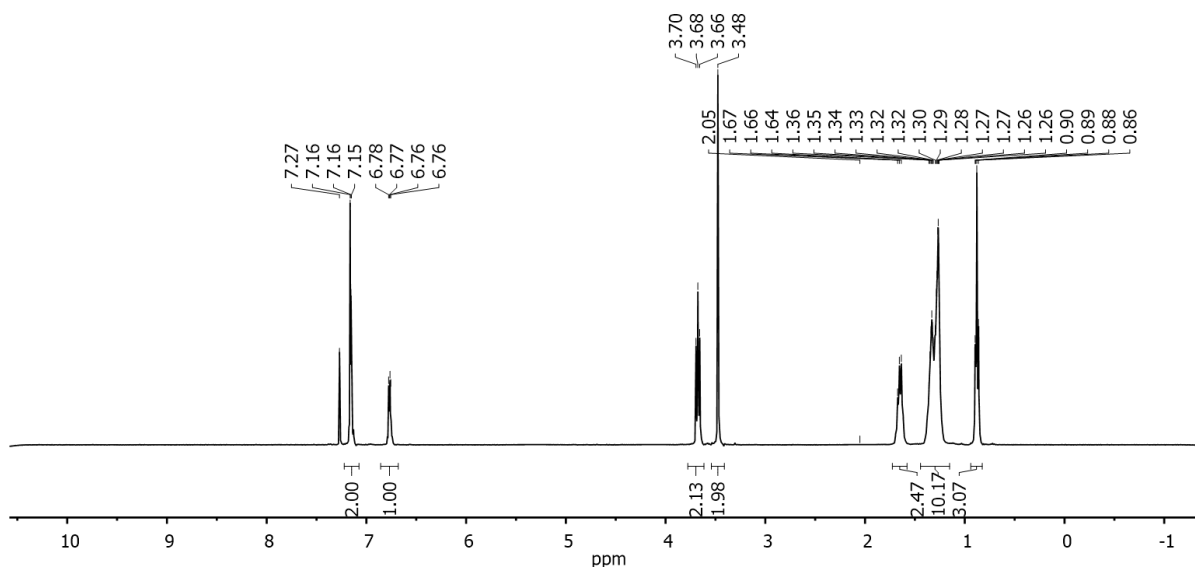
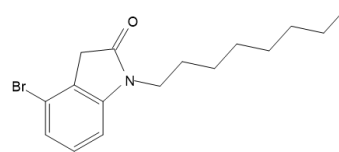
pasini043 #1127 RT: 16.92 AV: 1 SB: 2 16.81, 17.32 NL: 6.34E6

T: + c Full ms [40.00-600.00]

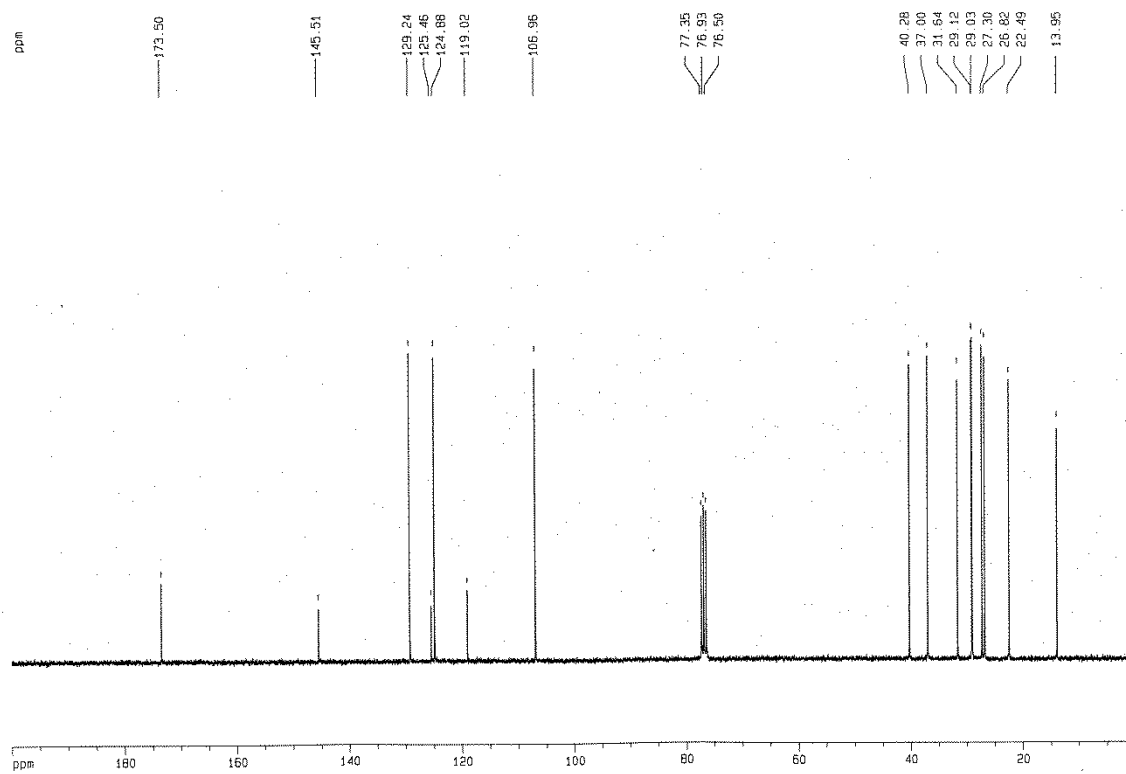


Compound **37b**

^1H NMR (200 MHz, CDCl_3)



^{13}C NMR (75 MHz, CDCl_3)

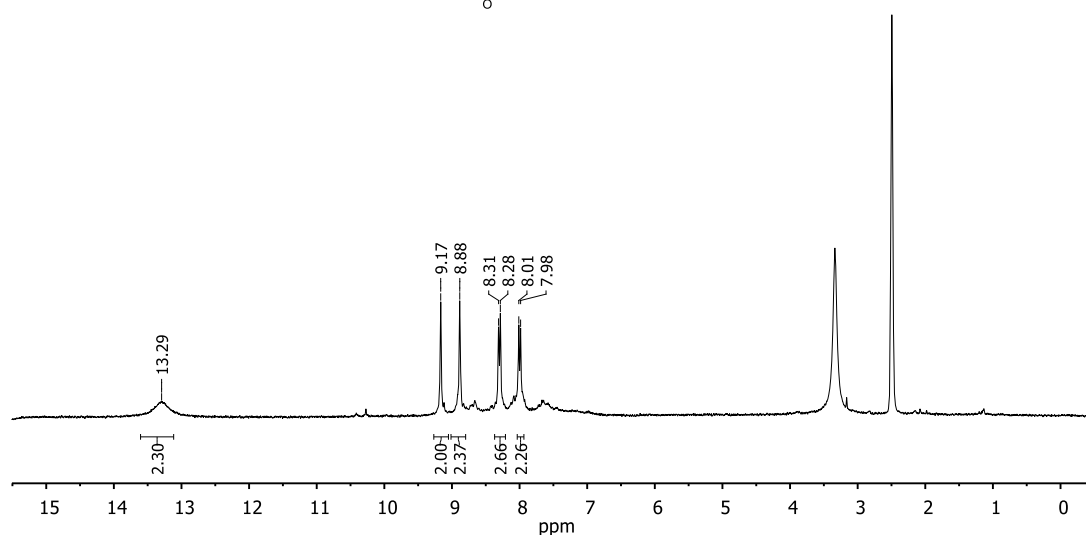
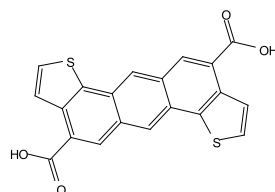


ANTHRADITHIOPHENE-BASED AND DIHYDROBENZODITHIOPHENE-BASED MONOMER FOR THE SYNTHESIS OF INNOVATIVE POLYMERS FOR PHOTOVOLTAIC APPLICATIONS

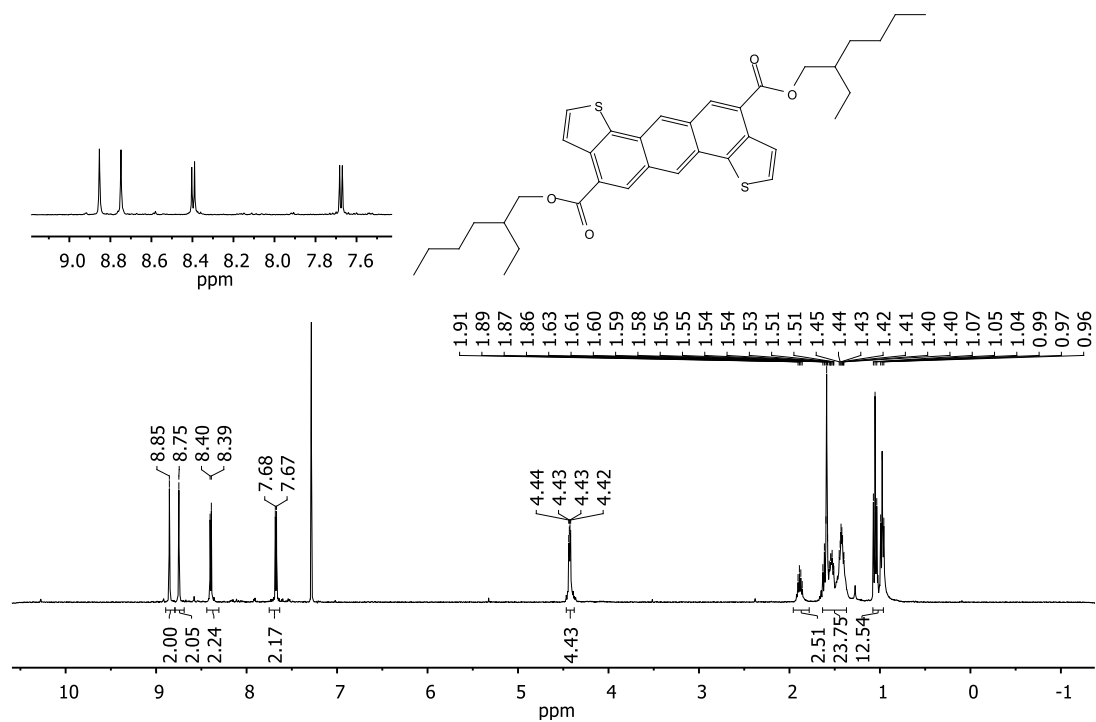
Copies of ^1H and ^{13}C NMR spectra

Compound **67**

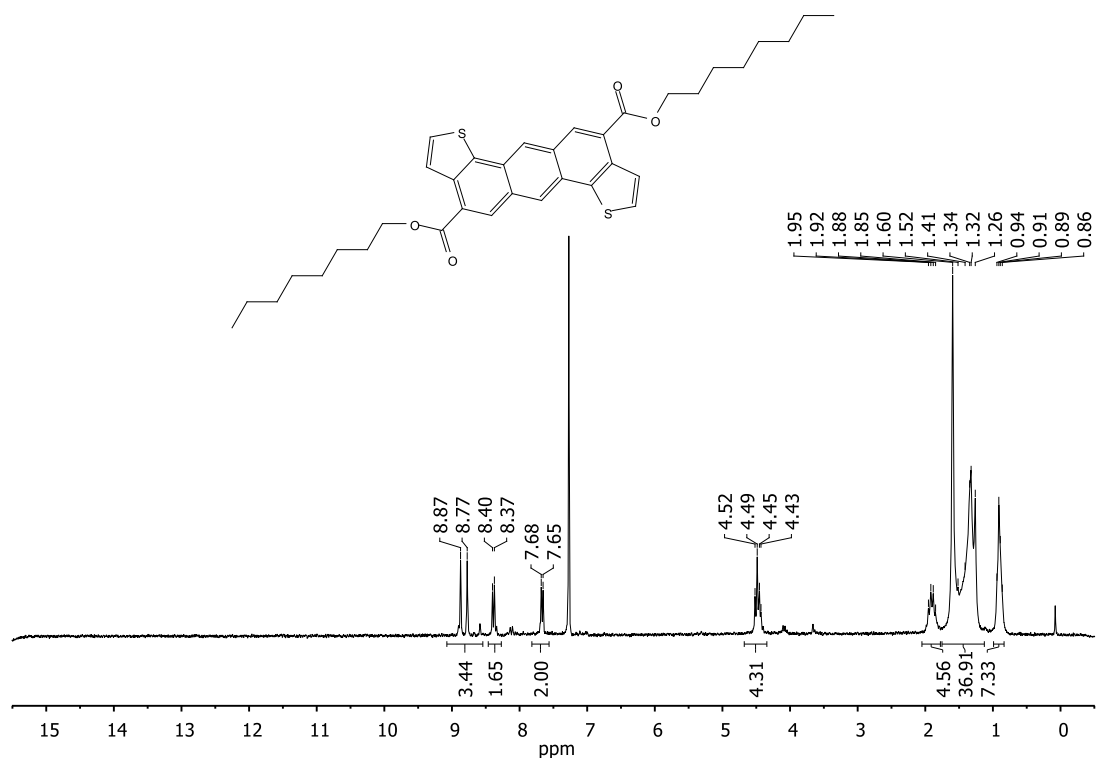
^1H NMR (200 MHz, DMSO- d_6)



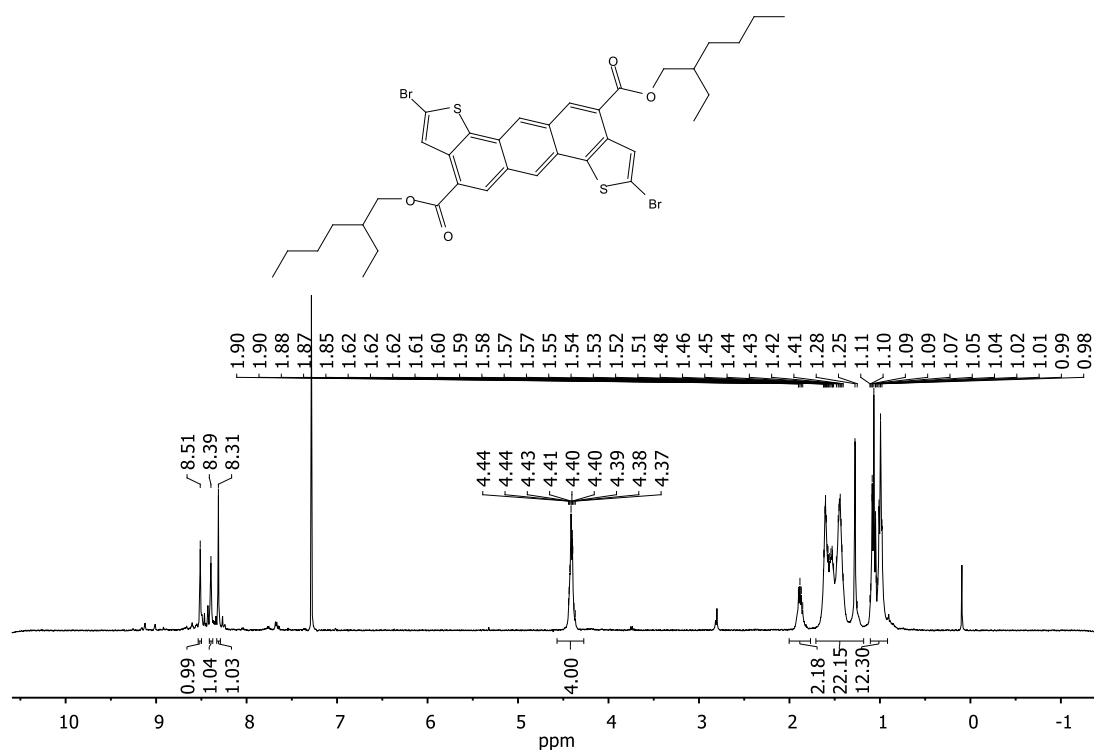
Compound **68a**
 ^1H NMR (200 MHz, CDCl_3)



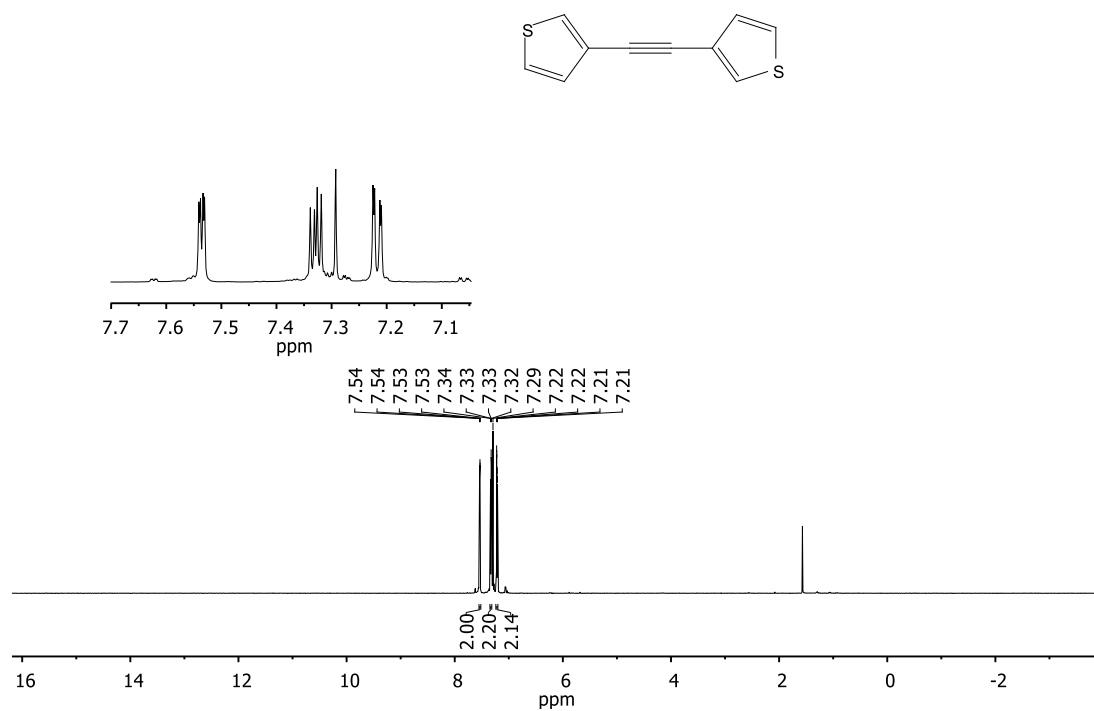
Compound **68b**
 ^1H NMR (200 MHz, CDCl_3)



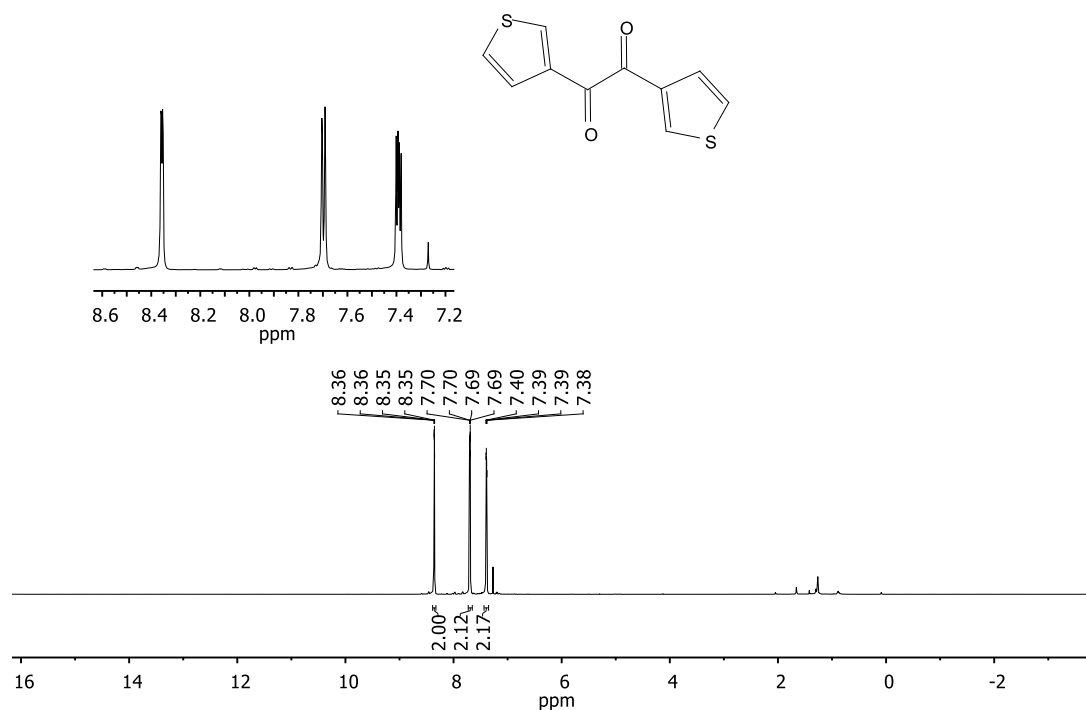
Compound **69**
 ^1H NMR (200 MHz, CDCl_3)



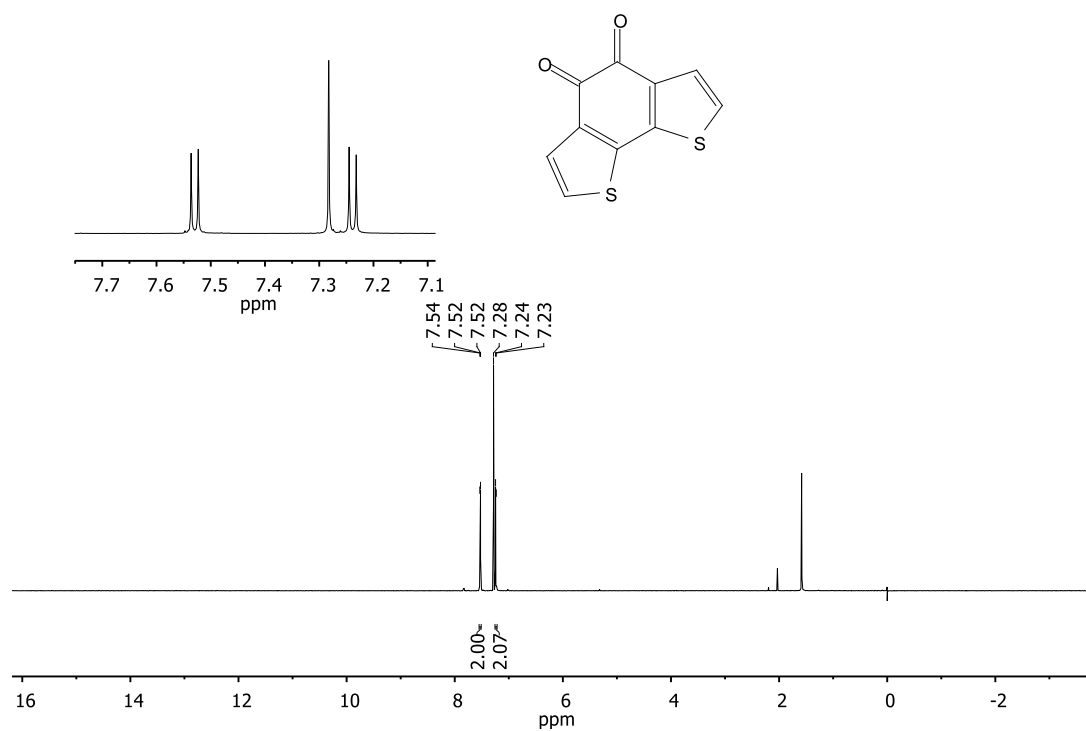
Compound **72**
 ^1H NMR (400 MHz, CDCl_3)



Compound **73**
¹H NMR (400 MHz, CDCl₃)



Compound **74**
¹H NMR (400 MHz, CDCl₃)



Compound **78a**
¹H NMR (400 MHz, DMSO-*d*₆)

